

EEG-Based **Brain-Computer Interfaces**

Cognitive Analysis and Control Applications



**Dipali Bansal
Rashima Mahajan**



EEG-BASED BRAIN-COMPUTER INTERFACES: COGNITIVE ANALYSIS AND CONTROL APPLICATIONS

EEG-BASED BRAIN-COMPUTER INTERFACES: COGNITIVE ANALYSIS AND CONTROL APPLICATIONS

DIPALI BANSAL

RASHIMA MAHAJAN



ACADEMIC PRESS

An imprint of Elsevier

Academic Press is an imprint of Elsevier
125 London Wall, London EC2Y 5AS, United Kingdom
525 B Street, Suite 1650, San Diego, CA 92101, United States
50 Hampshire Street, 5th Floor, Cambridge, MA 02139, United States
The Boulevard, Langford Lane, Kidlington, Oxford OX5 1GB, United Kingdom

© 2019 Elsevier Inc. All rights reserved.

No part of this publication may be reproduced or transmitted in any form or by any means, electronic or mechanical, including photocopying, recording, or any information storage and retrieval system, without permission in writing from the publisher. Details on how to seek permission, further information about the Publisher's permissions policies and our arrangements with organizations such as the Copyright Clearance Center and the Copyright Licensing Agency, can be found at our website: www.elsevier.com/permissions.

This book and the individual contributions contained in it are protected under copyright by the Publisher (other than as may be noted herein).

Notices

Knowledge and best practice in this field are constantly changing. As new research and experience broaden our understanding, changes in research methods, professional practices, or medical treatment may become necessary.

Practitioners and researchers must always rely on their own experience and knowledge in evaluating and using any information, methods, compounds, or experiments described herein. In using such information or methods they should be mindful of their own safety and the safety of others, including parties for whom they have a professional responsibility.

To the fullest extent of the law, neither the Publisher nor the authors, contributors, or editors, assume any liability for any injury and/or damage to persons or property as a matter of products liability, negligence or otherwise, or from any use or operation of any methods, products, instructions, or ideas contained in the material herein.

Library of Congress Cataloging-in-Publication Data

A catalog record for this book is available from the Library of Congress

British Library Cataloguing-in-Publication Data

A catalogue record for this book is available from the British Library

ISBN 978-0-12-814687-3

For information on all Academic Press publications visit our website at <https://www.elsevier.com/books-and-journals>



Working together
to grow libraries in
developing countries

www.elsevier.com • www.bookaid.org

Publisher: Mara Conner

Acquisition Editor: Chris Katsaropoulos

Editorial Project Manager: Peter Adamson

Production Project Manager: Surya Narayanan Jayachandran

Cover Designer: Greg Harris

Typeset by SPi Global, India

Preface

Neurotechnologists are progressively working on ways and means to merge minds with machines and are facilitating a plethora of interactive applications. The most important of these are the brain-computer interfaces (BCIs), which have the capabilities to promise alternate means of communication and control of external devices even in acute cases of disability. The implementation of external device control application platforms via interactive BCIs have become a progressive area of interest for researchers in recent years. Due to long-term usability, high temporal resolution, easy implementation, and low costs, the EEG has become the most acceptable neural signal for practical execution of BCIs. Human-brain interfacing has acquired a level of doing tasks and achieving functional targets that were unimaginable at some point of time. Research in this domain is expanding in every dimension, be it the vast breadth of EEG-based BCI control applications, depth of technology involved, and the usability it presents to the disabled and the general mass. Research publication in the domain of brain-controlled applications has covered not only medical needs but also has catered to the requirements of healthy users in their day-to-day life. The present emerging BCI research includes user friendly and wearable EEG headsets and EEG signal analysis techniques which have made possible to expand BCI application horizons toward automations, entertainment, emotion recognition, automated medical diagnostics, neuro-rehabilitation and much more. Overall, the related research and development opens the perspectives to offer an alternative means of interaction with external environment.

This book titled “EEG-Based Brain-Computer Interfaces: Cognitive Analysis and Control Applications” details the rationale behind working on BCI technologies, particularly based on brain patterns captured via the electroencephalogram (EEG). It also features EEG signal acquisition and various platforms for its analysis and provides a framework of eyeblink-based BCIs for control applications. The time and frequency domain analysis have been explored in detail to identify the occurrence of deliberate eye-blink from acquired EEG brain patterns as the basis for EEG-triggered control applications. It includes algorithms and scenarios to interface commercially available brain data acquisition unit (Emotive EEG Neuroheadset) with MATLAB for acquisition and control. The techniques deployed to extract relevant multidimensional feature sets for EEG signal analysis including event related potential (ERP), topographic scalp map, EEG sub-band power, and channel coherence are elucidated. This book demonstrates the approach to use EEG and develop more intuitive BCIs in real-time scenarios.

This book will benefit researchers working in the field of development of BCIs using biomedical signal processing, specifically automated control systems using physiological

signals (human neural responses) for the rehabilitation of physically challenged people. The readers will get real insight into implementation techniques of BCIs using cost-effective EEG acquisition units, signal processing, and feature extraction algorithms for control applications. The layout of the book has been structured to cover all aspects of BCIs using EEG and related pre- and post-processing techniques.

[Chapter 1](#) of this book aims at providing a rationale behind working on BCI technologies and provides segmentation and forecast for global BCI market. It also covers BCI classification, brain patterns, EEG-based basic acquisition system and eyeblink based BCI analysis and control applications. [Chapter 2](#) provides a comprehensive review of emerging research in BCI development techniques and perspectives of distinct BCI modalities, viz., electroencephalography (EEG), electrocorticography (ECoG), magnetoencephalography (MEG), magnetic resonance imaging (MRI), functional magnetic resonance imaging (fMRI). Acquisition methods, linear and nonlinear signal analysis and techniques followed to classify brain responses are covered at length. Efforts have been made to develop EEG-based inexpensive, portable and more intuitive brain computer interfaces for control applications. [Chapter 3](#) explores commercially available EEG headsets and its interface process to acquire real-time voluntary eyeblink-related brain signatures and create a robust database. Procedure to import acquired dataset into a compatible signal processing environment is also discussed. This chapter highlights a step-by-step development of EEG-based BCI for control application using eyeblink-specific neural signal acquisition. The processes and algorithms involved in cognitive analysis of acquired single eyeblink-related brain activity in time domain are detailed in [Chapter 4](#). Special emphasis is given on ERP analysis to identify activated cerebrum regions. The development of BCIs utilizing spectral features of acquired EEG signals is gaining importance these days. The processes and algorithms involved in cognitive analysis of acquired single eyeblink-related brain activity in frequency and spatial domain are detailed in [Chapter 5](#). Dominant EEG power subbands in response to eyeblink action are investigated and analyzed. [Chapter 6](#) reviews various existing control applications developed in MATLAB, Simulink & LabVIEW environment. It also explains the detailed step-by-step procedure of suggested voluntary eyeblink-based BCI for control applications. [Chapter 7](#) concludes with the major contributions made and future scope of work in this domain. It also recognizes the opportunities, challenges, and sustained efforts by the research community to extend the benefits and enhance quality of life.

Acknowledgments

We possess neither that eloquence of diction, that expression of imagination, nor that brilliance of metaphor to put in words what this project has meant to us. It has been the guidance and blessings of so many people that has made this book possible. This journey would be incomplete until we acknowledge every bit of contribution we have received during this phase.

As true believers, we start with thanking the Lord Almighty for giving us the strength and wisdom to write this book and for enlightening our path. We would also like to express our heartfelt gratitude to our family and friends who have been a true inspiration behind this journey of ours. They have helped us build the courage when courage seemed to fail, to regain faith when there seemed to be little cause for faith and create hope when hope became forlorn.

A bundle of thanks also go out to Manav Rachna, and our university for the backing and encouragement provided to us when it was needed the most.

And last but not the least, our thanks to the publishers who have helped us to make it possible to articulate our thoughts into this book.

**Dipali Bansal
Rashima Mahajan**

CHAPTER 1

Introduction

Dipali Bansal, Rashima Mahajan

Faculty of Engineering and Technology, Manav Rachna International Institute of Research and Studies, Faridabad, India

Contents

1.1 Rationale	1
1.1.1 BCI Success Stories	2
1.1.2 BCI Market Analysis	5
1.2 Technical Overview	6
1.2.1 Brain Anatomy	9
1.2.2 From Brain to Computer	11
1.2.3 Previous Work Related to Voluntary Eyeblink-Based BCI and Control	15
1.3 Objectives	16
References	17

1.1 RATIONALE

Computer is a manifestation of the human brain power.

It was a start of the long drive for my neighbor David and his family in a nice weather. It was a well thought out vacation driving out in the Sedan. All were excited and then touching 100 miles per hour was a song on a wide highway. And then came the crash. An overenthusiastic driver tried to overtake and ended up hitting the Sedan. All were safe ending with minor injuries. David paralyzed neck downwards.

A morning jog in the park. My student Roger just wanted to take a detour today through the downtown street being a weekend. Who knew that the greed of a young drug addict to get those extra bucks for his kick would end up with Roger being mugged with a heavy hit on the head. All senses intact but body immobile.

Above are two instances which would wreck a healthy individual's life including the near and dear ones. Both David and Roger were intellectuals excelling in their fields of work as financial consultant and technocrat. Highly functional brains but immobilized body due to incidents beyond their control. In this era, where ideas and knowledge are at premium, would it be appropriate to allow the individuals of the clan of David and Roger to lose their knowledge and life of oblivion.

Human brain power has manifested a device called computer to not only help human being in its endeavor to overcome its limitation but also surpass and achieve tasks much

beyond what is humanly possible. Brain and computer interface is an exciting field, which can help in taking this association of two entities namely brain and computer to its logical conclusion.

Brain and computer interface opens lot of vistas of collaboration where in the master-slave relationship can be transformed into a relationship between two intellectual entities. A classic example is the renowned scientist Stephen Hawking, an English theoretical physicist, and cosmologist. Contracted with motor neuron disease at a prime age of youth at 21, was given 2 years to live. In spite of the early onset and the gradual paralysis, he was still able to communicate through a cheek switch which is a speech generating device using cheek muscles that receives signal from his brain. He has been using lot of assistive technologies including brain-controlled interfaces to communicate with his computer. He has been awarded with many Honorary degrees, has written books and is considered a living legend in the field of physics since Einstein. His knowledge was a gift for the welfare of mankind.

Brain and computer interface is also helping people lead an independent life and go on with their daily routine-like life and making people independent. The brain-computer interface (BCI) is very practical for severely disabled people who can use the BCI systems to get things done at home, office, and even more. People can even be involved in their passion for music, play instruments, and also video games.

The possibilities are immense.

1.1.1 BCI Success Stories

Human brain is often called “The Final Frontier of Science” as it is one of the most complex structures in the known universe. It not only gives us sense of ourselves and our surroundings but also processes sensory data, makes humans think and emote, controls muscle movement, enables secretion of body fluids and hormones, supports breathe, maintains body temperature, regulates metabolic rate, and records the impressions of events throughout our life. The complexity of the brain arises from the innumerable nerve cells arranged in intricate manner coordinating with the entire human body through the nervous network. The experimental study conducted by the Mayo Foundation for Medical Education and Research reaffirms that while each part of the brain is responsible for certain task(s), the various parts of the brain coordinate to work together. Brain has intrigued philosophers and scientists from as early as 387 BCE when Plato suggested that mental processes are controlled through the brain. It undoubtedly is the root of human intelligence and does so even more than a machine can, it builds on and continuously improves whatever has been invented. Advancement in technologies especially over the past decades has enabled neuroscientists to understand how the brain functions and hence the diseases and abnormal behavior of the nervous system to an extent. Recent research and success stories related to brain and mind controlled applications are quoted below.

Researchers [Rao et al. \(2014\)](#) at the University of Washington demonstrated that it is possible to convey information taken out from one person's mind directly to another individual's mind and control desired hand motions of another person in less than a second. This has been made realistic through direct mind-to-mind communiqué over internet. This could help in creating a missing patch in the subject and making good a brain-damaged person. Another research led by Doo Yeon [Kim and Rudolph Tanzi \(2014\)](#) at Boston's Massachusetts General Hospital created "Alzheimer's in a dish." The research has the potential to accelerate new drug testing by creating a set of events on human brain cells by reproducing vital cell structures in a Petri dish. The work published in the journal *Nature* leads the way for other scientists to employ this unique approach to research superior methods for neurodegenerative disorders. In 2013, the Massachusetts Institute of Technology researchers planted false memories in a mouse by linking one memory with dissimilar memory and actually replacing negative memory with a positive one. The research was led by Susumu Tonegawa, Nobel Prize winner. This could help chronic patients come out of acute stress syndrome.

Fading memory or memory loss is a very common phenomenon faced by a majority of the population. The known reasons are aging, Alzheimer's, a brain stroke, or some unknown causes. Dr. Theodore Berger from the University of Southern California has toiled for 35 years and done exemplary work by finally devising memory enhancing implants. The memory neurons are part of the hippocampus, a deep and protected part of the brain. The input and output signals flow as an electrical signal from CA3 to CA1 hippocampus nodes, respectively. Initially, algorithms were written based on these signals in rats trained for a particular activity. The rats were drugged and tiny electrode implants programmed based on the algorithms recorded returned same results as if the rats had perfect memory. A similar thing was experimented successfully on monkeys. The success motivated though cautiously prompted Dr. Theodore to perform research with many epilepsy patients. The research returned 80% positive results in these patients with the implants giving similar memory predictions. The work is however just a beginning as the same has been applied for a single activity only. New and different set of algorithms needs to be defined for other activities. The similarity in such codes has to be studied for different individuals before using this as a probable step to aid memory in compromised cases. Lot more research needs to be done to understand the various input vs output signals and algorithms for different situations.

Initial efforts were made at the University of Chicago by [Tabot et al. \(2013\)](#) to develop a touch receptive robotic prosthetic hand controlled by brain signals, thus improving dexterity in motor functions of an arm. A two-way communication is required to restore touch sensation, that is, brain sends signal to limb and the limb sends back sensory signals to the brain by processing and reproducing brain patterns generated by external stimulation. In continuation to this, [Science Daily \(2017, April 25\)](#) reported that rehabilitation physicians from the Netherlands have given Johan Baggerman (2010), who lost his arm in a mishap with a click-on robotic arm, the first of its kind prosthetic

limb in the world. This prosthetic arm connects directly onto a metal rod in the bone itself and thus saves from a lot of inherent troubles of slipping off, skin problems, uneasy prosthetic socket, etc. This innovative arm can interact with user's nerves and allows him/her to control it using their mind and provides larger range of motion. Further to this, Clemente et al. (2017) have demonstrated recently that amputees implanted with osseointegrated prostheses which is attached directly to the skeleton, can resume tangible sensations to unfriendly environments. The subject can perceive and respond better to external stimuli by listening to the vibrations in the prosthetic limb. Touch-sensitive robotic limbs can further assist multifaceted assignments like surgical robots, rescue operations, manufacturing, and service industry (Oddo et al., 2017). Retinal prosthesis, another initiative in this area, is a ray of hope for millions of people worldwide who are blind or who experience blindness due to progressive retinal deterioration. Novel approach made by Castaldi et al. (2016) aims to reinstate destroyed retinal function by training the adult brain to see again. In yet another work, Luu et al. (2017) from the University of Houston have revealed recently that noninvasive electroencephalography (EEG)-based BCI technology can assist people relearn to walk after stroke or other spinal cord injuries. They have developed an interface with a virtual walking avatar that can control and improve gait.

It is evident that BCI finds paramount applications in medicine and assistive devices. However, being able to control brain signals has a plethora of exhilarating implications in entertainment and also in daily life. To quote an exciting event of April 2016, BCI technology helped the University of Florida participants to reach the finish line in a drone race where brain signals guided the drone. Think of a video game where your character did exactly as you wished and was in total command of your thoughts. A novel BCI application titled "Brain Composer," lets music composition through mind power. Pinegger et al. (2017) experienced an unusual musical tone generated using P300 brain wave, an adapted BCI and software for composing music. Our brain hierarchically processes image of the object that we gaze at and draws significant and complex features to predict what one is imagining or seeing. Horikawa and Kamitani (2017) of the Kyoto University have developed an algorithm to look into one's own imagination or dreams using functional magnetic resonance imaging (fMRI) signals and deep neural network AI. *Science Daily* (2013) reported that joint efforts were made by researchers at the University of Essex and NASA to control a virtual spaceship by thoughts alone. They came to the conclusion that BCI can hugely impact virtual reality (VR) and hands-free control applications through brain signal commands of two individuals combined together. Research article in *NeuroImage*, by Yang et al. (2016) from the Carnegie Mellon University illustrates that different languages when read or decoded generate similar brain patterns. Machine learning algorithm helps in establishing a relation between neural responses generated for a sentence meaning same both in English and Portuguese with a conclusion that BCI systems decipher thoughts and concepts independent of language barriers.

Logical, analytical, and emotive ability of human brain is something that makes humans distinct and notable compared with other animals even the primates.

Professor Matthew Rushworth and team from the Oxford University experimented on MRI images of 25 adult human volunteers and 25 macaque monkeys and found a unique feature in ventrolateral frontal cortex region of the human brain that links to superior cognitive abilities in a man (Neubert et al., 2014). The study gives us more reasons to explore what makes us HUMAN. One often wonders why some editorials go viral on social sites while some go unnoticed. Unconsciously our brain decides what is worth reading and sharing. Research based on fMRI data reveals interesting brain patterns associated with this and predicts the popularity of an article (Baek et al., 2017). There is no denying that advertisements have shaped consumer choice over times. The companies are trying almost everything under the sun, coming up with most innovative ways to reach the customers, where humor and/or an emotional pitch clicks the deal. One wonders how creative this outreach is looking at the short interaction of 30–60 s. The impact what this leaves on human beings was researched and published by Dooley (2011). Brain-fluence as it was coined, gives the linkage of the lasting and emotional connect left with customers. Neuro-engagement factor is another term used by “Sands Research” to combine and calculate the alterations in brain activity by analyzing effect of EEG, eye tracking, biometrics, and surveys. Facebook publicized in April 2017 that it is developing a noninvasive BCI for typing using brain signals. The motive was to allow five times faster typing speed simply controlled by one’s mind using optical imaging by scanning the brain multiple times within a second so as to translate thoughts into text. A lot is also being done to harness BCI to enhance smart living. The technology will eventually allow people to manage augmented reality (AR) and VR practices with their brainpower only.

However, the advancements till date are still a tip of the ice berg with the scientists progressing on few links of neurons and some particular neurons only. As per an estimate, there are 100 billion neurons and almost 1000 trillion links within the neurons. As per renowned neuroscientist Dr. Rafael Yuste, the extent of work is like understanding a television program by looking at a single pixel.

In the last few decades, research in neuroscience is progressing both on experimental cognitive psychology along with the latest techniques in brain imaging and BCI. The research which started more than a century back has picked up momentum now with a more holistic view including cognitive neuroscience, genetics, neurophysiology, cell biology, and even social sciences as briefed by Marcus (2009). An analytical survey highlighting BCI market on global front is presented in the following subsection.

1.1.2 BCI Market Analysis

Market for BCI technology-based applications has huge potential in health care sector, assistive devices, and entertainment industry as predicted by the “Allied Market Research” (2015) followed by the “Transparency Market Research” (2016).

Aging elders are the prime reasons for the progress in global BCI devices marketplace as they are prone to mental disorders like stroke, depression, Alzheimer’s, and Parkinson’s

disease. Revenue generated in the global BCI market was at US\$383.2 million in 2015; and is predicted to inflate at a compound annual growth rate (CAGR) of 14.9% during 2016–24 and go up to US\$1232.6 million by 2024. Modernization in BCI applications and associated market is seen to be largest in North America where the United States is the most significant contributor. Asia Pacific is also a potential market for BCI devices due to population explosion and people's ability to afford. The EEG-based BCI devices are anticipated to be in great demand in North America, Europe, and Asia Pacific. Fig. 1.1 clearly shows the global trend of BCI market. Of all available brain data acquisition systems, noninvasive technology shall be the most popular and would hold major market share during the forecast period. Maximum utilization of BCI shall be by the healthcare providers followed by communication and control segment. However, due to dearth of proficient personnel handling BCI systems, cyber threat and ethical concerns, the market is getting adversely affected, although experts believe that these matters will eventually get sorted. BCI manufacturers are in a race to develop varied application products. The key BCI manufactures in 2015 and 2016 were

- Advanced Brain Monitoring, Inc.
- Artinis Medical Systems B.V.
- ANT Neuro B.V.
- Blackrock Microsystems LLC
- Cadwell Laboratories Inc.
- Cortech Solutions, Inc.
- Elekta AB
- Emotiv Systems Inc.
- Guger Technologies OEG
- Mindmaze SA.
- Mind Solutions Inc.
- NeuroSky, Inc.
- Nihon Kohden Corporation
- NeuroPace Inc.
- OpenBCI
- Quantum Applied Science and Research, Inc.

Looking at the huge potential of BCI technologies and applications, it is imperative to understand the technical knowhow of the concept. The subsequent sections give the technical outline of brain anatomy, BCI technology, acquisition method, processing, and applications.

1.2 TECHNICAL OVERVIEW

The adult human brain weighs around three pound and is constituted of a neural network comprising of around 100 billion of neurons (nerve cells) out of 100 trillions of total brain cells (Brodal, 1992; Buckner et al., 2008). These neurons are interconnected together to

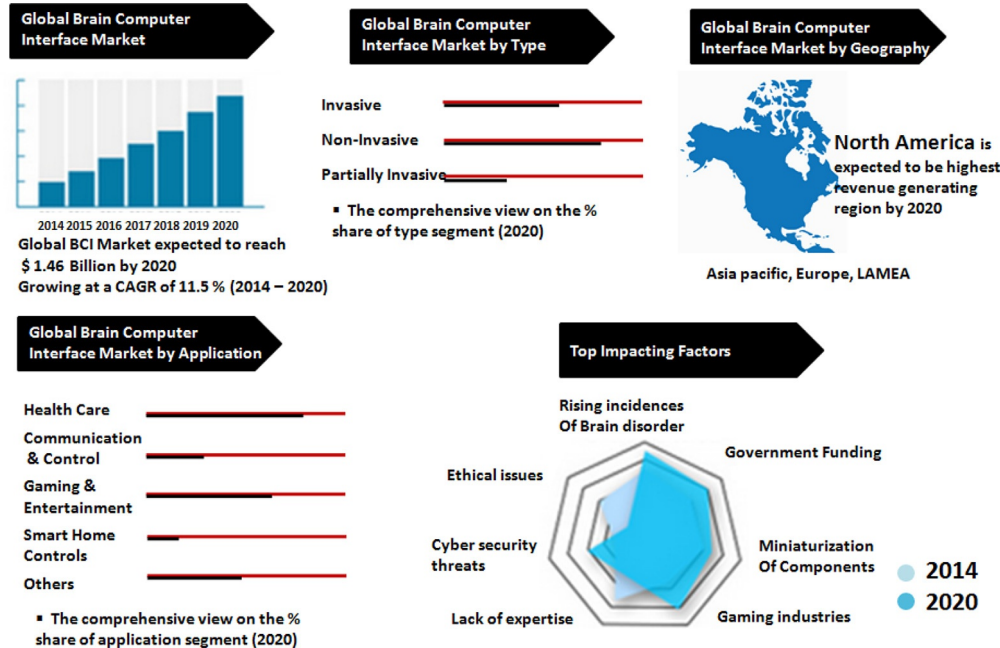


Fig. 1.1 Worldwide market of brain-computer interface: 2013–20. (Courtesy alliedmarketresearch.com.)

form information carrying and sharing neural network. The interconnections among neurons can be one-to-one, one-to-many, or many-to-many. The neurons carry information from brain to different body organs and vice versa. Therefore, the brain can be termed as a master organ that controls all human body systems/functions by receiving and interpreting signals from different body sensors (smell, hearing, taste, pain, and sight) through neurons. It controls our actions such as motor actions, thoughts, emotions, speech, etc. by receiving information through nerve fibers and generating respective control signals for distinct body parts. Nervous system along with respiratory system and digestive system are important functional blocks of human body. Human nervous system can be classified into the master control unit called the central nervous system (CNS) and peripheral nervous system (PNS) that sets up links to other body organs as depicted in Fig. 1.2.

Brain and spinal cord are the major elements of the CNS. It is known as “central” because the sensory information received through spinal and peripheral nerves (such as burn on a skin, seeing a scenic beauty, and cut on a skin) is primarily integrated and processed by the brain and subsequent action signals/impulses are sent back to actuators (muscles) through PNS to perform automatic or voluntary action. The CNS communicates with the whole body through PNS using a network of nerve cells known as neurons. The PNS quickly transfers sensory inputs collected from the body parts to the CNS and the moment CNS infers the data input, the PNS relays the precise instructions to the body. PNS brings in the signal and carries out the action whereas CNS interprets signals and redirects them. Cranial nerves are responsible for transmitting information as nerve impulses to and from the brain. Spinal nerves carry information from the spine. The PNS is primarily categorized as somatic and autonomic nervous system. The voluntary movement controls, movement of sensory data from sensory organs to CNS, and motor movement-related control signals to muscles are transmitted by the somatic nervous system. The autonomic nervous system, on the other hand, regulates involuntary vital

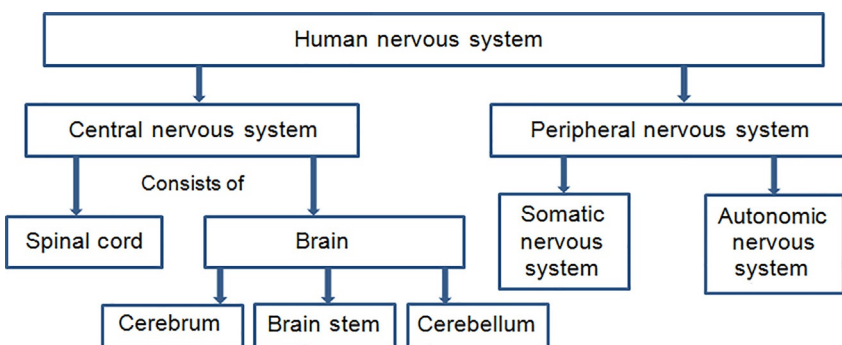


Fig. 1.2 Human nervous system.

processes like digestion, respiration, pupil movement and contraction, heart rate, secretion of hormones, etc., and thus, operates automatically without any conscious action. Detailed anatomy of the brain is presented in the subsequent section.

1.2.1 Brain Anatomy

The brain is encapsulated inside the skull that acts as a shield to prevent the brain from any injury. Anatomically, the brain is constituted of three basic parts including cerebral cortex (cerebrum), cerebellum, and brain stem. BCI applications involve the utilization of the largest part of brain, that is, cerebral cortex (called gray matter) located directly under the skull surface. The thickness of cerebral cortex is about 2–4 mm and is the outermost layer of neurons. It is separated into left and right cerebral hemispheres. Both the hemispheres are connected together through a thick bundle of about 500 million nerve fibers known as *colossal commissure*. It facilitates interhemispheric information exchange in the brain. The impulses generated by muscles to the left side of the human body are sensed by right hemisphere and are responsible for the left-side body movements. Right side of brain is random, creative, and intuitive and is responsible for imagination and emotions. Similarly, the movements related to the right side of body are controlled by left hemisphere which is logical, analytical, and rational and helps with reasoning and number skills.

Each of the hemisphere is further composed of four well-defined lobes viz., frontal, temporal, occipital, and parietal as depicted in Fig. 1.3. The most anterior lobe of brain, that is, frontal lobe is associated with cortical areas that deal with emotions, cognitive

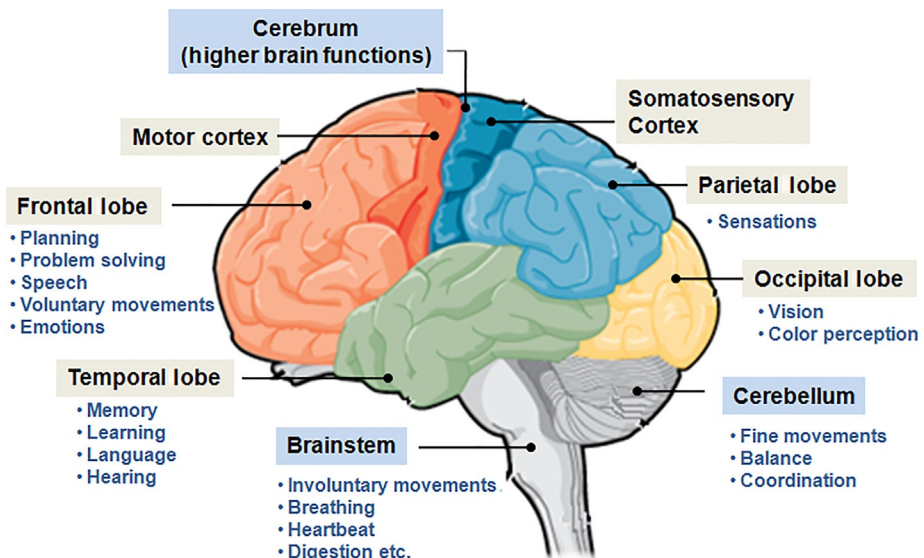


Fig. 1.3 Brain anatomy.

functions like reasoning, memory tasks, planning, voluntary muscle movement, etc. The parietal lobe is anterior to the occipital lobe and responds to stimulus related to sensation of pain, pressure, vibration, temperature, touch, etc. The extreme posterior lobe is occipital lobe which is accountable for vision-related stimuli and spatial detection and processing. It is comprised of primary and secondary visual area. The primary area receives preliminary visual information which is integrated and it is the task of secondary visual area to decode the incoming stimulus into meaningful information by relating it with past knowledge. Any injury to primary visual area may result in total blindness or appearance of blind spots in the visual input depending on the extent of the injury caused. On the other side, any injury to secondary visual area may not cause any effect on seeing visual stimuli, however, it would be difficult for the person to deduce any meaning from received visual function such as recalling somebody's name, words, etc. The temporal lobe is located anterior to occipital lobe and is associated with auditory stimuli processing. It is comprised of primary and secondary auditory area. At first, the auditory information is received by primary auditory area and a corresponding meaningful speech after processing is produced by secondary auditory area. Thus, four lobes of cerebrum are further comprised of certain areas, viz., primary and secondary visual area, posterior and anterior speech area, primary and secondary auditory area, primary and secondary motor area, and sensory areas. The major functions of cerebral cortex include processing of complex language, visual information, problem solving, motory movements, memory, reasoning, sensory, auditory information, etc. ([Kameswara et al. 2013](#)).

Cerebellum a crucial part of the brain is located at the back of the skull, above medulla oblongata and under the occipital and temporal lobes of cerebrum. It consists of hundred millions of neurons to process and carry information between cerebral cortex and body muscles. The function of cerebellum is to process the stimulus received from brain and PNS for coordination of distinct voluntary movements, posture adjustments to maintain body balance and equilibrium, and fine motor control. Any cerebellum damage may result in motor control and posture impairments. The cerebellum and cerebrum are connected together through pons. Midbrain, medulla oblongata, and pons collectively constitute the brain stem which is another important part of the brain. Lower part of brain stem is the medulla oblongata which connects the brain and spinal cord. It carries huge number of peripheral nerves to carry stimulus ([Gilbert et al., 2007](#); [Looney et al., 2014](#)).

An example has been shown in [Fig. 1.4](#) to explain the process followed by neurons to transfer visual information captured through eyes (sensory organ) to brain and then carry the processed information from brain to muscles for voluntary movement. Let visual information considered here is fire. The image of fire captured by eyes is transformed into sensory neurons. These set of neurons transport the signal to the primary visual area of occipital lobe. The signal is processed and decoded by secondary visual area of same lobe. The decoded information is transmitted to the motor cortex which transmits message to the motor neurons. The motor neurons carry the message through spinal cord and

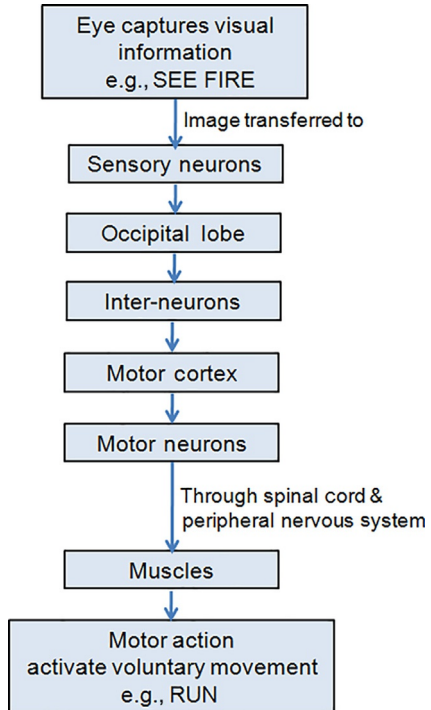


Fig. 1.4 Schematic diagram for visual information processing and control action.

PNS to the muscles for appropriate control action, for example, in this case to legs for running as a control action. The occipital lobe and motor cortex here constitute the CNS.

Analyzing brain structure and functionality to gauge human behavior and allow better living is undoubtedly a complex task but due to immense progress in robust acquisition units, computer technology, data analytics, machine learning, and imaging techniques it is becoming easier and interesting to explore man-machine interactions with the external world in real-time scenarios. Once a science fiction is now turning into reality and signals are reaching human brain that allows disabled people to see, hear, and feel again. It's not just about making life convenient for severely impaired, it has even more potential than that and so BCI may be considered as the most important technological step forward in the recent decades.

1.2.2 From Brain to Computer

The vision for BCI involves connecting mankind with the CNS with the intention of supplementing or restoring human cognition and better life. There are various approaches to trace and understand brain patterns. Different technologies used to record

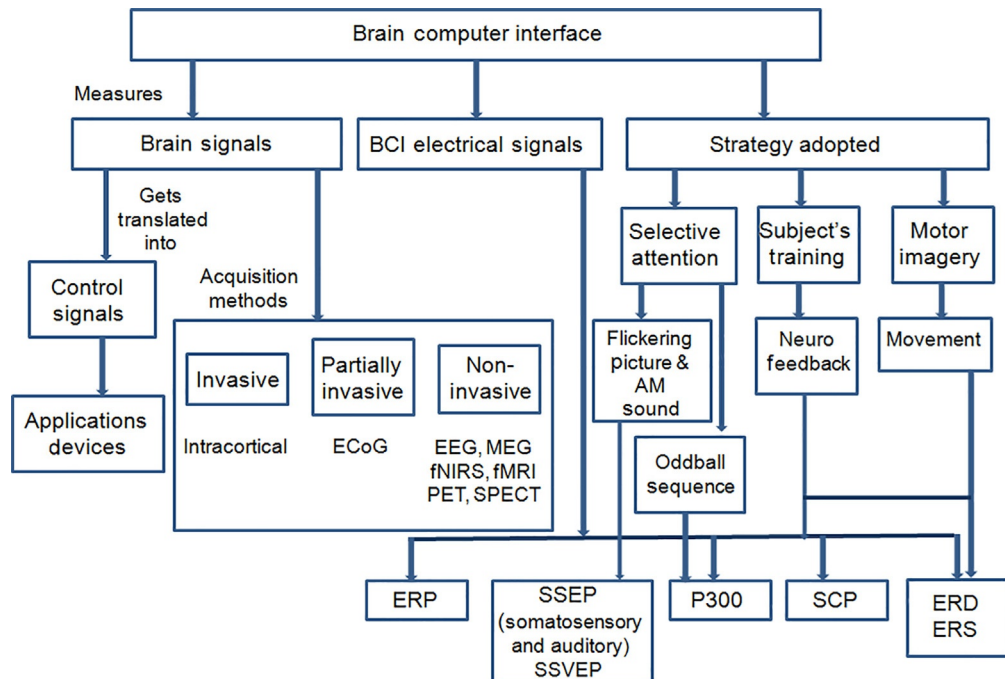


Fig. 1.5 Brain-computer interface perceptions.

brain activity can be broadly classified based on the signal acquisition site (invasive or noninvasive), controlled device, electrode type (electric, magnetic, or chemical), and based on the strategy adopted to comprehend brain patterns. [Lotte et al. \(2015\)](#) and [Graimann et al. \(2010\)](#) present a comprehensive review on BCI and its types as depicted in Fig. 1.5.

Invasive methods include intracortical electrodes and electrocorticography (ECoG) which are implanted for clinical diagnosis. Classification based on noninvasive signal acquisition methods is as under

- EEG records the electrical activity of brain
- magnetoencephalography (MEG)
- fMRI
- positron emission tomography (PET)
- single-photon emission computed tomography (SPECT)
- functional near-infrared spectroscopy (fNIRS) etc.

MEG has an excellent time and space resolution but is very expensive, stationary, sensitive to movements, and require intensive training. Likewise, fMRI has same limitations as MEG but demonstrates superb spatial resolution as it captures brain information from the site itself. EEG-based BCI systems are the most popular for understanding human

brain as it is user friendly and requires minimal training, is cost effective, light weight, and portable. Some quick EEG-related facts are listed as follows:

- Direct technique to measure and relate to subtle neural responses.
- High temporal resolution so is able to capture information during the time frame when cognitive process is active.
- Permits data collection in real-time settings anywhere.
- Has low spatial resolution is the disadvantage.
- Safe as it saves human subjects from exposure to high intensity magnetic fields/radiations ([iMotions Guide, 2016](#); [Niedermeyer and Lopes da Silva, 2012](#); [Sakkalis, 2011](#); [Kaiser, 2001](#)).

The prime subbands of the brainwave signals are beta (detectable over parietal and frontal lobes), alpha (noticeable in awake but eyes closed situation at occipital region), theta (found in children and sleeping adults), gamma, and delta (visible in infants and sleeping adults). Delta has the lowest frequency range (0–4 Hz) followed by theta (4–8 Hz), alpha (8–12 Hz), beta with a range between 12 and 31 Hz, and gamma is in the range beyond 31 Hz. The EEG subband activity is associated with neural activity and hence variations in cerebral blood flow (CBF) can be observed. Thus, by identifying these temporal and spectral variations and analyzing them, it is possible to characterize the correlated cognitive states as stated by [Iversen et al. \(2008\)](#) and [Wolpow et al. \(2000\)](#).

The commonly used brain activity patterns in EEG-based BCIs are

- Event-related potentials (ERPs) are electrophysiological response to a stimulus.
- Steady-state evoked potentials (SSEPs) are response to flickering stimulus.
- Steady-state visual evoked potentials (SSVEPs) are related to visual stimulation at specific frequencies.
- P300 wave do not link to the stimulus, but to a person's reaction to it.
- Event-related desynchronization (ERD)/event-related synchronization (ERS) is incidents reflecting sensorimotor brain activity amplitude decrease (ERD) or increase (ERS).
- *Slow cortical potential (SCP neurofeedback) is observed in the upper cortical layer of the brain. SCP is a slow event-related, direct-current variation in the EEG signal.*

Mostly, ERP is analyzed for control applications, but because they are very short events of 500 ms, a relatively large number of trials are averaged to attain resultant ERP as reported by [DeBoer et al. \(2006\)](#). To overcome this limitation, power spectral analysis can be utilized as an efficient tool to find the neural correlates during cognitive tasks finds [Jatupaiboon et al. \(2013\)](#). But, power spectral analysis is unable to conserve Fourier phase of signal which is vital information related to morphological variations in the captured EEG report [Karimifardand and Ahmadian \(2007\)](#). This may lead to misguided conclusions if variations in peak amplitude are not so prominent. This drawback of linear techniques has been addressed by [Martis et al. \(2013\)](#) to further develop higher-order spectra-based nonlinear feature extraction techniques and shall be extensively covered in the subsequent chapters.

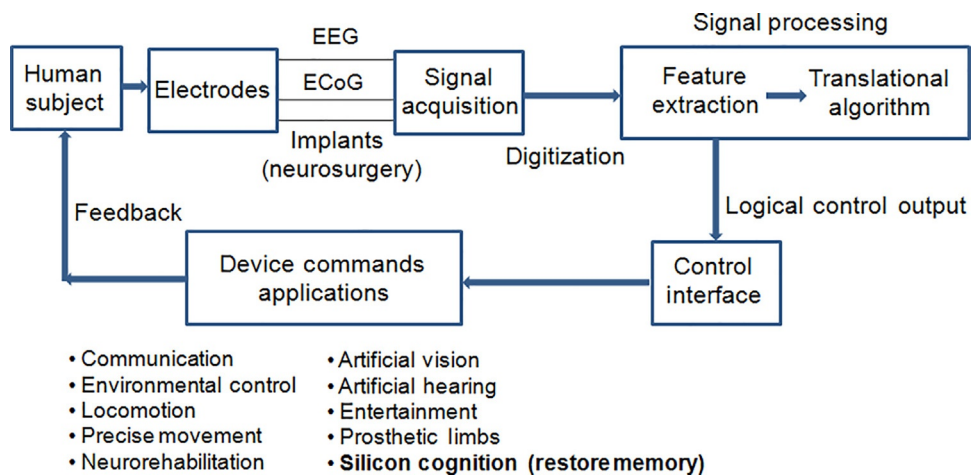


Fig. 1.6 Basic design of a BCI system.

Designing a BCI system needs a multidisciplinary approach combining computers, signal processing, electronics, neuroscience, and psychology. A generic BCI system consists of electrodes, signal acquisition system, signal processing unit, control interface, application device, and feedback unit as shown in Fig. 1.6.

Brain signals can be acquired using various sensors and acquisition units. This book will focus on commercially available units to obtain raw brain signal using EEG measurement techniques. Features of commercially available EEG acquisition devices viz. NeuroSky brainwave (single channel), emotive neuroheadset (14 channel), BioSemi Active-2 (280 channels), and Muse (4–6 channels) were surveyed by [Mahajan et al. \(2014\)](#). Most of the reported work involves the use of more complex headset units like Biosemi Active-2 with 280 scalp channels involving tedious instrumentation or only a single-channel device like NeuroSky covering only left frontal region of cerebral cortex to capture human neural responses. Emotive EEG neuroheadset is robust and user friendly and so has been selected to capture real-time EEG from human subjects to develop more interactive BCIs for control applications in this work. However, signal processing and computer-assisted algorithms are pertinent to draw meaningful information from subtle variations in acquired EEG. Signal processing unit comprises of preprocessing the input data using baseline removal and de-noising algorithms, feature extraction algorithm for understanding power spectrum of EEG data and classifiers. Command is then executed to control a specific task or device. A feedback unit is finally used to adapt to the requirement and to send real-time information to the user. BCI has evolved to become more robust and promising for a wide range of applications including communication and control, cognitive computing, artificial vision, artificial hearing, silicon cognition to restore memory, etc. to name a few. [Abdulkader et al. \(2015\)](#) have extensively compiled

various application domains of BCI highlighting the contribution toward preventive, diagnostic and rehabilitative medical applications, smart surroundings, neuromarketing, entertainment, security, and authentication. One control application is EEG-based BCI using voluntary eyeblink inputs in real time, which shall be the focus in the entire book. Literature in relation to this has been explored in the subsequent subsection.

1.2.3 Previous Work Related to Voluntary Eyeblink-Based BCI and Control

Way back in 1989, Fogarty and Stern, established that eyeblink is prompted by information processing inside the brain and suggested that blink latencies can be used as a trigger for a plethora of tasks. Eyeblink is considered as an artifact in the EEG signal, but research is at its peak to use them as control signals ([Krolak and Strumillo, 2012](#)). [Chambayil et al. \(2010\)](#) used eyeblink signal-related kurtosis coefficient data and signal strength to select the characters of a virtual keyboard. BCI has enabled eyeblink-based control of electric wheelchair as explained by Ning et al. in one of their paper published in [2012](#). Voluntary eyeblink electroculogram signal detected from acquired brain data is capable of controlling a wheelchair as reported. In another work, [Rihana et al. \(2013\)](#) acquired, detected, and classified eyeblink data from EEG signal using a portable unit and probabilistic neural network and suggested the use of this BCI in neuro-rehabilitation applications. Eyeblink intensity and human alertness level was used by [Stephygraph and Arunkumar \(2016\)](#) to develop a wireless mobile robotic model to navigate movements in four directions. A single-channel commercial acquisition unit was used to detect eyeblink data and discrete Fourier transform was used as a signal enhancement tool in this experiment. Eye movements based real-time control of video game characters using two temporal EEG sensors was demonstrated in [2015](#) by Belkacem et al. Wavelets were explored to identify eye movement instances and its time domain characteristics. A control interface with visual and auditory feedback presents a huge potential in real-time scenarios. One user was made to move a virtual wheelchair at the voluntary blink of an eye in one of the noninvasive BCI experiments using NeuroSky MindWave ([Schuh et al., 2016](#)). EEG-based headsets are capable of identifying concentration levels in an individual from the left prefrontal region of brain. Efforts are being made to provide a real-time solution to prevent accidents due to driving fatigue ([He et al., 2016](#)). A headband incorporated with Thinkgear EEG acquisition unit, accelerometer, gyroscope, and wireless transmission unit is used along with k -nearest neighbors (k -NN) algorithm to detect blink-based fatigue and generates alarm in this work. Another work illustrates control of a Quadcopter using brain concentration and voluntary eyeblink action ([Song et al., 2016](#)). Eyeblinking signals also find applications in authentication of biometric inputs. Enhanced signal processing algorithm and blink-based data are extracted using auto-regressive models ([Abo-Zahhad et al., 2015](#)). However, a lot needs to be explored in terms of developing improved signal processing

algorithms for identifying subtle eyeblink variations in human brain signal and its consequent utilization in real-time control applications. Objectives set in this book are an initiative in this direction.

1.3 OBJECTIVES

To appreciate real time acquired EEG signal for cognitive analysis and subsequent control applications to assist effective communication with the environment, the following objectives are set in this book:

- To acquire EEG-based real-time human neural response using 14-channel emotive headsets for voluntary eyeblink movements.
- To create a robust database for analysis and build up EEG-based BCI for control purposes using deliberate eyeblink movements. To save acquired data in .edf (European data format) or .csv (comma separated values) formats for future use.
- To import the acquired EEG signals into compatible and user friendly application software MATLAB using appropriate data read functions. This information is structured and contains signals from 14 scalp electrodes.
- To develop an efficient finite impulse response (FIR) band-pass filter structure for preprocessing the signal so that the required frequency band containing all the EEG subbands (delta, theta, alpha, beta, and gamma) are selected.
- To develop artifact removal and baseline removal algorithm and signal processing techniques to identify subtle changes in acquired human EEG wave.
- To identify and investigate the time domain parameters of EEG signal for voluntary movement using ERP analysis at different latencies. This gives a clear indication of the activated frontal brain region during deliberate eyeblink. Scalp maps shall also be plotted to show the potential distribution across frontal regions.
- To do cognitive analysis of EEG signal in frequency domain and identify dominant frequency sub bands using power spectrum. Channel spectral scalp maps shall also be plotted to draw inferences.
- To explore and implement a practical, economic, and socially acceptable EEG-based BCI for controlling hardware/software applications. The captured deliberate eyeblink-specific EEG variations to be used as a trigger to generate “active high” at the output of Arduino microcontroller interfaced with MATLAB. This high output signal at Arduino to control the working of interfaced application circuit/device.
- To test and verify the developed system using Arduino-Simulink interface. The final EEG signal processed and feature extracted MATLAB file (.mat) to be imported to Simulink and interfaced with Arduino digital block. The developed Simulink model to be deployed in Arduino microcontroller board for independent control application.

To meet with the set objectives, the book is divided into seven chapters and the focus shall be on making the reader understand the concept of EEG-based BCI and varied

control applications. [Chapter 2](#) shall extensively cover methods used in BCI for acquisition of brain patterns, the signal processing algorithms followed by details on various feature extraction and classification techniques. EEG-based BCI and control application area is also covered at length in this unit. [Chapter 3](#) explores commercially available EEG headsets and its interface process to acquire real-time voluntary eyeblink-related brain signatures and create a robust database. Procedure to import acquired dataset into a compatible signal processing environment shall also be explained. [Chapter 4](#) shall include cognitive analysis of EEG waves in time domain emphasizing on ERP analysis to identify activated cerebrum regions. Frequency domain cognitive investigation for analyzing dominant EEG power subbands in response to eyeblink action shall be covered in [Chapter 5](#). [Chapter 6](#) shall explore EEG-based BCI control applications using voluntary eyeblink. Other applications shall also be discussed in this unit followed by the last unit to conclude the major contributions made and future scope of work in this domain.

REFERENCES

- Abdulkader, S.N., Atia, A., Sami, M., Mostafa, M., 2015. Brain computer interfacing: applications and challenges. *Egypt. Informat. J.* (2), 213–230.
- Abo-Zahhad, M., Ahmed, S.M., Abbas, S.N., 2015. A new EEG acquisition protocol for biometric identification using eye blinking signals. *Int. J. Intell. Syst. Appl.* 06, 48–54. <https://doi.org/10.5815/ijisa.2015.06.05>.
- Allied Market Research, 2015. Brain computer Interface market by type (invasive, non-invasive and partially invasive) and application (communication and control, gaming and entertainment, smart home control and others)—global opportunity analysis and industry. Forecast, 2013–2020. <https://www.alliedmarketresearch.com/brain-computer-interfaces-market>. p. 104.
- Baek, E.C., Scholz, C., O'Donnell, M.B., Falk, E.B., 2017. The value of sharing information: a neural account of information transmission. *Psychol. Sci.* 28 (7), 851–861. <https://doi.org/10.1177/0956797617695073>.
- Belkacem, A.N., Saetia, S., Zintus-art, K., Shin, D., Kambara, H., Yoshimura, N., Berrached, N., Koike, Y., 2015. Real-time control of a video game using eye movements and two temporal EEG sensors. *Comput. Intell. Neurosci.* 2015, 653639 10 p. <https://doi.org/10.1155/2015/653639>
- Brodal, P., 1992. *The Central Nervous System: Structure and Function*. Oxford University Press, New York.
- Buckner, R., Andrews-Hanna, J., Schacter, D., 2008. The brain's default network: anatomy, function, and relevance to disease. *Ann. N. Y. Acad. Sci.* 1124, 1–38.
- Castaldi, E., Cicchini, G.M., Cinelli, L., Biagi, L., Rizzo, S., Morrone, M.C., 2016. Visual BOLD response in late blind subjects with Argus II retinal prosthesis. *PLoS Biol.* 14 (10), e1002569. <https://doi.org/10.1371/journal.pbio.1002569>.
- Chabayil, B., Singla, R., Jha, R., 2010. In: Virtual keyboard BCI using eye blinks in EEG, wireless and mobile computing, networking and communications (WiMob). IEEE 6th International Conference. <https://doi.org/10.1109/WIMOBI.2010.5645025>.
- Clemente, F., Hakansson, B., Cipriani, C., Wessberg, J., Kulbacka-Ortiz, K., Branemark, R., Fredén Jansson, K.-J., Ortiz-Catalan, M., 2017. Touch and hearing mediate osseoperception. *Sci. Rep.* 7, 45363. <https://doi.org/10.1038/srep45363>.
- DeBoer, T., Scott, L.S., Nelson, C.A., 2006. *Methods of Acquiring and Analyzing Infant EEG and Event-Related Potentials*. Psychology Press, London, pp. 5–38.
- Dooley, R., 2011. *Brainfluence: 100 Ways to Persuade and Convince Consumers With Neuromarketing*. Wiley, ISBN: 978-1-118-17594-1. 304 p.

- Fogarty, C., Stern, J.A., 1989. Eye movements and blinks: their relationship to higher cognitive processes. *Int. J. Psychophysiol.* 8 (1), 35–42.
- Gilbert, S., Dumontheil, I., Simons, J., Frith, C., Burgess, P., 2007. Wandering minds: the default network and stimulus-independent thought. *Sci. Mag.* 315 (5810), 393–395.
- Graimann, B., Allison, B., Pfurtscheller, G., 2010. Brain-computer interfaces: a gentle introduction. In: The Frontiers Collection. Springer-Verlag, Berlin, Heidelberg. https://doi.org/10.1007/978-3-642-02091-9_1.
- He, J., Zhang, Y., Zhang, C., Zhou, M., Han, Y., 2016. A noninvasive real-time solution for driving fatigue detection based on left prefrontal EEG and Eye blink. In: Ascoli, G., Hawrylycz, M., Ali, H., Khazanchi, D., Shi, Y. (Eds.), *Brain Informatics and Health*. In: BIH 2016. Lecture Notes in Computer Science, vol. 9919. Springer, Cham.
- Horikawa, T., Kamitani, Y., 2017. Generic decoding of seen and imagined objects using hierarchical visual features. *Nat. Commun.* 8, 15037. <https://doi.org/10.1038/ncomms15037>.
- iMotions Guide, 2016. EEG (Electroencephalography): The Complete Pocket Guide. <https://imotions.com/blog/eeg/>.
- Iversen, I.H., Ghanayim, N., Kübler, A., Neumann, N., Birbaumer, N., Kaiser, J., 2008. A brain-computer interface tool to assess cognitive functions in completely paralyzed patients with amyotrophic lateral sclerosis. *Clin. Neurophysiol.* 119, 2214–2223.
- Jatupaiboon, N., Panngum, S., Israsena, P., 2013. Real-time EEG-based happiness detection system. *Sci. World J.* 618649. 12 p.
- Kaiser, J., 2001. Self-initiation of EEG-based communication in paralyzed patients. *Clin. Neurophysiol.* 112, 551–554.
- Kameswara, T., Rajyalakshmi, M., Prasad, T., 2013. An exploration on brain computer interface and its recent trends. *Int. J. Adv. Res. Artif. Intell.* 1 (8), 17–22.
- Karimifardand, S.A., Ahmadian, A., 2007. In: A morphological heart arrhythmia classification using hermitian model of higher-order statistics. Proc. of the 29th Annual International Conference of the IEEE-EMBS, Lyon, France, pp. 3132–3135.
- Kim, D.Y., Tanzi, R.E., 2014. Massachusetts General Hospital/ Harvard Medical School, Alzheimer's-in-a-Dish: New Tool for Drug Discovery; Posted on December 9th, 2014 by Dr. Francis Collins. <https://directorsblog.nih.gov/2014/12/09/alzheimers-in-a-dish-new-tool-for-drug-discovery/>.
- Krolak, A., Strumillo, P., 2012. Eye-blink detection system for human-computer interaction. *Inf. Soc.* 11, 409–419.
- Looney, D., Kidmose, P., Mandic, P., 2014. Ear-EEG: user-centered and wearable BCI. *Brain-Comput. Interface Res. Biosyst. Biorobot.* 6, 41–50.
- Lotte, F., Bougrain, L., Clerc, M., 2015. *Electroencephalography (EEG)-Based Brain-Computer Interfaces*. In: *Wiley Encyclopedia of Electrical and Electronics Engineering*. Wiley, p. 44.
- Luu, T.P., Nakagome, S., He, Y., Contreras-Vidal, J.L., 2017. Real-time EEG-based brain-computer interface to a virtual avatar enhances cortical involvement in human treadmill walking. *Sci. Rep.* 7(1). <https://doi.org/10.1038/s41598-017-09187-0>.
- Mahajan, R., Bansal, D., Singh, S., 2014. A real time set up for retrieval of emotional states from human neural responses. *Int. J. Med. Health Pharm. Biomed. Eng.* 8 (3), 142–147.
- Marcus, E.R., 2009. A brief history of human brain mapping. *Trends Neuro. Sci.* 32 (2), 118–126.
- Martis, R.J., Acharya, U.R., Chakraborty, C., 2013. Cardiac decision making using higher order spectra. *Biomed. Signal Process. Contr.* 8 (2), 193–203.
- Neubert, F.-X., Mars, R.B., Thomas, A.G., Sallet, J., Rushworth, M.F.S., 2014. Comparison of human ventral frontal cortex areas for cognitive control and language with areas in monkey frontal cortex. *Neuron* 81 (3), 700. <https://doi.org/10.1016/j.neuron.2013.11.012>.
- Niedermeyer, E., Lopes da Silva, F., 2012. *Electroencephalography: Basic Principles, Clinical Applications, and Related Fields*, fifth ed. Lippincott Williams & Wilkins (Kindle Edition).
- Ning, B., Li, M.-J., Liu, T., Shen, H.-M., Hu, L., Fu, X., 2012. Human brain control of electric wheelchair with eye-blink electroculogram signal. In: Su, C.-Y., Rakheja, S., Liu, H. (Eds.), *Intelligent Robotics and Applications. ICIRA 2012, Part I, LNAI. 7506*. Springer-Verlag, Berlin, Heidelberg, pp. 579–588.
- Oddo, C.M., Mazzoni, A., Spanne, A., Enander, J.M.D., Mogensen, H., Bengtsson, F., Camboni, D., Micera, S., Jörntell, H., 2017. Artificial spatiotemporal touch inputs reveal complementary decoding in neocortical neurons. *Sci. Rep.* 8, 45898. <https://doi.org/10.1038/srep45898>.

- Pinegger, A., Hiebel, H., Wriessnegger, S.C., Müller-Putz, G.R., 2017. Composing only by thought: novel application of the P300 brain-computer interface. *PLoS One* 12 (9), e0181584.
- Rao, R.P.N., Stocco, A., Bryan, M., Sarma, D., Youngquist, T.M., Wu, J., Prat, C.S., 2014. A direct brain-to-brain interface in humans. *PLoS One* 9 (11), e111332.
- Rihana, S., Damien, P., Moujaess, T., 2013. EEG-eye blink detection system for brain computer interface. In: Pons, J., Torricelli, D., Pajaro, M. (Eds.), *Converging Clinical and Engineering Research on Neurorehabilitation, Biosystems & Biorobotics*. In: vol. 1. Springer, Berlin, Heidelberg.
- Sakkalis, V., 2011. Review of advanced techniques for the estimation of brain connectivity measured with EEG/MEG. *Comput. Biol. Med.* 41 (12), 1110–1117.
- Schuh, A., Campos, M.D.B., Bez, M., Mossmann, J.B., 2016. In: Antona, M., Stephanidis, C. (Eds.), Usability evaluation of a wheelchair virtual simulator controlled by a brain-computer interface: lessons learned to the design process. *UAHCI 2016, Part II, LNCS 9738*. Springer International Publishing, pp. 92–101.
- Science Daily, 2013. Control a Virtual Spacecraft by Thought Alone. University of Essex. www.sciencedaily.com/releases/2013/02/130205101735.htm.
- Science Daily, 2017. Click-On Arm Prosthesis Controlled by Patient's Thoughts. Radboud University Nijmegen Medical Centre. www.sciencedaily.com/releases/2017/04/170425093016.htm.
- Song, X., Mann, K., Allison, E., Gieder, C., 2016. In: A quadcopter controlled by brain concentration and eye blink. Conference: 2016 IEEE Signal Processing in Medicine and Biology Symposium (SPMB). <https://doi.org/10.1109/SPMB.2016.7846875>.
- Stephygraph, L.R., Arunkumar, N., 2016. In: Suresh, L., Panigrahi, B. (Eds.), Brain-actuated wireless mobile robot control through an adaptive human-machine interface. *Proceedings of the International Conference on Soft Computing Systems. Advances in Intelligent Systems and Computing*. In: vol. 397. Springer, New Delhi.
- Tabot, G.A., Dammann, J.F., Berg, J.A., Tenore, F.V., Boback, J.L., Vogelstein, R.J., Bensmaia, S.J., 2013. Restoring the sense of touch with a prosthetic hand through a brain interface. *Proc. Natl. Acad. Sci. USA*. <https://doi.org/10.1073/pnas.1221113110>.
- Transparency Market Research, 2016. Brain computer interface market (type— invasive BCI, partially invasive BCI, and non-invasive BCI; technology—electroencephalography (EEG), electrocorticography (ECOG), near infrared spectroscopy (NIRS), functional magnetic resonance imaging (fMRI), and magnetoencephalography (MEG); application—health care, gaming and entertainment, communication, defence and aerospace, and home automation)—global industry analysis, size, share, growth, trends and forecast. pp. 2016–2024. <https://www.transparencymarketresearch.com/brain-computer-interface-market.html> p. 109.
- Wolpaw, J.R., McFarland, D.J., Vaughan, T.M., 2000. Brain-computer interface research at the Wadsworth Center. *IEEE Trans. Rehabil. Eng.* 8, 222–226.
- Yang, Y., Wang, J., Bailer, C., Cherkassky, V., Just, M.A., 2016. Commonality of neural representations of sentences across languages: Predicting brain activation during Portuguese sentence comprehension using an English-based model of brain function. *NeuroImage*. <https://doi.org/10.1016/j.neuroimage.2016.10.029>.

CHAPTER 2

EEG-Based Brain-Computer Interfacing (BCI)

Dipali Bansal, Rashima Mahajan

Faculty of Engineering and Technology, Manav Rachna International Institute of Research and Studies, Faridabad, India

Contents

2.1	Introduction	22
2.1.1	EEG-Based BCI Architecture	23
2.2	Techniques in BCI	27
2.2.1	Invasive and Partially-Invasive BCI Techniques	28
2.2.2	Noninvasive BCI Techniques	29
2.3	Data Acquisition	33
2.3.1	Brain Electric Potential	33
2.3.2	EEG Electrode Positioning	35
2.3.3	EEG Electrodes	36
2.3.4	EEG Signals and Rhythms	37
2.3.5	Preamplification, Filtering and Analog-to-Digital Conversion	37
2.4	Preprocessing	38
2.4.1	EEG Artifacts	38
2.4.2	EEG Artifact Rejection	40
2.5	Feature Extraction	47
2.5.1	EEG Signal Representation in Time Domain	48
2.5.2	EEG Signal Representation in Frequency Domain	51
2.5.3	EEG Signal Representation in Time-Frequency Domain	53
2.5.4	EEG Signal Representation in Spatial Domain	54
2.6	Classification	54
2.6.1	Linear Classifiers	55
2.6.2	Nonlinear Classifiers	56
2.6.3	BCI Performance	56
2.7	BCI Applications	57
2.7.1	BCI: Clinical Applications	58
2.7.2	BCI: Nonclinical Applications	62
2.8	Conclusion	63
	References	64
	Further Reading	71

2.1 INTRODUCTION

Recent advancements in the field of cognitive neuroscience have led to the development of more interactive brain-computer interfaces. It involves the direct interface between human brain and computer system to develop various control and medical applications to restore a quality life among differently abled subjects. Brain-computer interfacing (BCI) systems have been evolved to provide tremendous applications including neuro-prosthetics (robotic arms/hands), hands free mind controlling applications without any muscle interventions through interpretation of thoughts/feelings by identifying distinct human neural patterns. These applications are not only developed to provide aid to medically challenged people with severe motor disabilities, but also may provide assistance to healthy users too in their routine and occupational work. BCI technology has been proven to be a blessing for patients suffering from neuromuscular disabilities. Brain-computer interfaces acquire the human neural responses and involve processing of captured brain signals to translate these responses into operative control actions and commands. The whole process involves the integration of a set of operations, viz., brain signal acquisition, preprocessing of acquired dataset, feature extraction, and classification followed by development of control interface. Thus, BCI research is multidisciplinary in approach as it combines the application of many fields including human brain physiology, cognitive neuroscience, electronic instrumentation, signal transmission, signal processing, pattern recognition, machine learning, etc. The brain-computer interfaces are designed to extract and quantify temporal and morphological features from recorded brain signals and it determines the subject's intentions. The extracted feature set is utilized to generate operative device control signals and it accomplishes the subject's intent. The system developed must be able to quickly acquire as well as process the neural responses to develop efficient application-oriented BCIs.

This chapter provides an introduction to the various concepts of BCI followed by a comprehensive method of BCI development using electroencephalography (EEG) signals. It involves the description of acquisition techniques to capture brain activity using different invasive, noninvasive or partially invasive modalities, timing of brain activity while acquisition (synchronous or asynchronous), and type of application to be developed (medical or control). The human brain network is constituted of billions of neurons. The signals/information from neurons to different body parts and vice versa is carried through spinal cord. The perspectives of distinct neuroimaging modalities to capture high-quality human neural data from these distinct brain regions have been explained. Development of neural-driven BCI involves the acquisition of either electrophysiological or hemodynamic brain signals from distinct regions of cerebrum cortex through scalp electrodes. The first set of electrophysiological responses involves the recording of EEG, electrocorticography (ECoG), and magnetoencephalography (MEG). However, the other set of hemodynamic responses involves the recording of

magnetic resonance imaging (MRI), functional magnetic resonance imaging (fMRI), position emission tomography (PET), single-photon emission computed tomography (SPECT), and functional near-infrared spectroscopy (fNIRS) to capture brain signals from central nervous system (CNS). These well-characterized neuroimaging modalities provide a lot of neurophysiological information. However, BCI developments involving modern noninvasive and inexpensive bioinstrumentation technology are gaining a lot of importance in the clinical monitoring and emerging control applications for rehabilitation. This is due to the absence of any surgical procedure and ease of usage. Significant breakthroughs and widespread applications have been able to demonstrate the major advancements achieved in BCI research. However, existing BCI technology is still concerned about architecture/hardware complexity, portability, expensive instrumentation and limited functionality available with proprietary software of neuro acquisition units, and extraction of the best informative feature set for the successful implementation of rehabilitative control applications. Development of an efficient BCI control application module based on real-time human brain activity primarily involves the development of cognitive brain-state-specific signal dataset from healthy subjects. The BCI hardware involved in dataset acquisition must possess the features such as portability, sustainability (with low maintenance cost), robustness, reliability, and compatibility with assistive technology software in distinct developing environments to develop a user-friendly, intuitive, manageable, and affordable BCI system by translating acquired cognitive brain states into neuro-operative commands for control applications.

One of the most commonly noninvasive neuroimaging modality used for BCI is electroencephalogram (EEG). Focus is on exploring the ability of EEG to capture vital electrophysiological neural responses portraying cognitive activity of human subjects to develop brain-computer interfaces. The candidature of EEG as a preferred neuroimaging tool has been discussed in detail due to its noninvasive nature, high temporal resolution, availability of portable EEG recording devices, and nonexposure to high-intensity magnetic fields. The field of cognitive analysis of human neural activity via EEG is an effective way of implementing cognitive brain-computer interface applications such as robotic arm, wheel chair movement (locomotion), imaginary motor tasks, voluntary motor actions, hands free neuro gaming, development of social applications to capture human feelings/emotions, development of communication interface among partially disabled subjects and external world/devices, control of appliances through mind (environment control), etc. ([Wadeson and Nijholt, 2015](#)). The focus in this chapter shall be on EEG-based BCI architecture and design.

2.1.1 EEG-Based BCI Architecture

Brain-computer interfaces potentially link the human cognitive neural responses to outside physical world in order to translate the subject's intentions/thoughts into real-time

device control signals. To achieve the desired function, a BCI system has entities including acquisition device to acquire electrophysiological activity patterns from human subject, interfaced computer to perform signal processing for feature extraction and subsequent feature translation, and generate output in terms of operative device commands for selected BCI applications. These elements and their subsequent interactions are governed by an effective controlling protocol. This protocol governs the corresponding operation instances (onset, offset, and operation timing), description/selection of signal preprocessing and postprocessing procedures, type of device output commands followed by parameters to analyze the overall performance of a designed BCI application. Such brain-computer interfaces have proven to be an efficient and unique communication control system for patients suffering from severe motor disorders. [Fig. 2.1](#) summarizes the whole architecture of EEG-based BCI.

2.1.1.1 Signal Acquisition

It includes the recording of electrophysiological or hemodynamic responses corresponding to the subject's brain activity. The neural signals are recorded using surgical (invasive) or nonsurgical (noninvasive) BCI neuroimaging modalities. This book shall focus on EEG as a selected neuroimaging modality. Different types of sensors can be employed to acquire the raw brain signals and shall be explored in detail in the subsequent sections. The acquired brain responses are preamplified to enhance the signal level and filtered to remove power-line interference and other undesirable electrical noise components. This shall be followed by their conversion to digital format using analog-to-digital converters. Once acquired, the brain signals are amplified, digitized, and transmitted to the interfaced computer for further signal processing.

2.1.1.2 Preprocessing

It involves the development of algorithmic procedures for normalization, baseline removal, de-noising, and artifacts removal [electromyography (EMG): electrical activity of motor neurons and electrooculography (EoG): electric potentials due to eye movements] from recorded EEG brain data. The aim is to enhance the information content in the acquired raw brain data. It is the step to extract the required useful information content from recorded neural responses and involves the representation of acquired signals using compact mathematical functions and operations. Main focus is on design and development of efficient signal acquisition and accurate signal processing system to prevent a loss of any relevant data and information. The filtration of acquired neural data is often employed followed by signal transformation during preprocessing stage. The ultimate intention is to enhance signal-to-noise ratio (SNR) of recorded brain signals. This contributes toward the efficient characterization of input brain patterns.

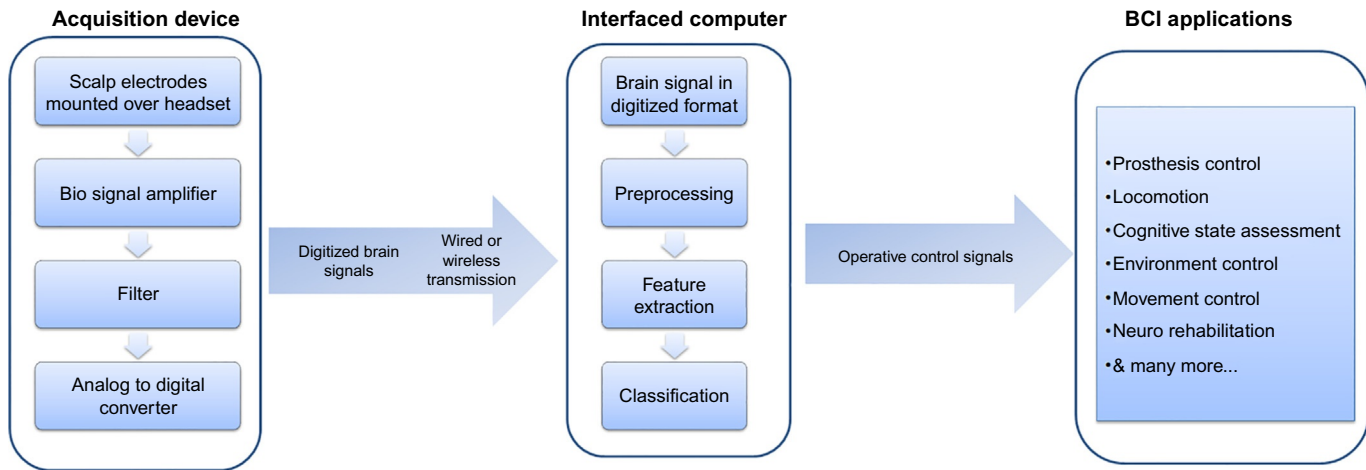


Fig. 2.1 EEG-based BCI architecture.

2.1.1.3 Feature Extraction

This stage involves construction of the most discriminative and informative compact feature set from preprocessed brain signals. A low-dimensional feature vector comprising of linear and nonlinear features is extracted to capture and characterize the variations (temporal and morphological variations) in acquired neural responses corresponding to specific neural activity. The feature extraction algorithm must use both linear and non-linear signal analysis techniques to build a feature vector consisting of both time domain and frequency domain features ([Bi et al., 2013](#)). Each brain signal is described/quantified by a few relevant values known as “features.” These extracted features must contribute toward the minimization of the intra-class feature variances while maximizing the variances among different class features. This stage contributes toward generation of the discriminative characteristics of brain signal thereby decreasing the size of information required to classify the neural activity.

2.1.1.4 Classification

Classification involves the utilization of extracted feature set from preprocessed neural signals and assigns a defined class or category to acquired brain patterns ([Abdulkader et al., 2015](#)). This class mapping is done by exploiting the differences and similarities in the brain signal features. An assigned class identifies the type of corresponding captured neural activity pattern (e.g., single eyeblink, double eyeblink, left-hand movement, right-hand movement). This stage translates the extracted feature set into operative device control signals.

2.1.1.5 Translation Into Operative Control Signals

Once the user’s intentions are identified on the basis of extracted feature set and a classification stage, appropriate control signals are generated. The feature translation algorithms are developed and applied on resulting classified features to convert them into output device commands. Therefore, this stage involves the assignment of commands/control signals to the type of identified class associated with performed neural activities. The control signals are used to operate the external interfaced device, for example, a recognized single eyeblink pattern could be translated into the control signal/command “switch ON the device” and a double eyeblink pattern into “switch OFF the device.” These commands are used to control the designed BCI application. The feature translation algorithm must be dynamic enough to adapt or learn the spontaneous variations in features to have accurate and efficient device control application.

Further, the device control operation provides feedback to the subject to make him aware of the identified/classified neural responses. This may assist or guide the user to modulate or refine respective neural activity and have better control over the designed application BCI. However, the success of designed brain-computer interface depends upon the interaction of user and BCI system to adapt to the variations. There must be

good correlation between user's intent and the features used by BCI to characterize the brain activity. The features must be extracted and selected in order to control and operate designed BCI application (such as movement control, device control, locomotion, neuromodulation, artificial vision, and artificial hearing) efficiently and correctly. The performance of developed BCIs can be evaluated using performance parameters such as information transfer rate (ITR), classification accuracy to distinct tasks/states, and reduction in number of commands to operate a device or using an application via human neural responses (Navarro et al., 2011).

The following sections include discussion of the current progress and a roadmap going forward in EEG-based BCI development including various techniques in BCI, data acquisition types, preprocessing, feature extraction, classification, and application development.

2.2 TECHNIQUES IN BCI

Brain-computer interface technology allows differently abled individuals to communicate with outer world (human and assistive devices) by translating human neural responses into corresponding operative commands for respective neurofeedback and control applications. BCI applications utilize brain signals and the nervous system. Bio-potential recordings done by monitoring electrophysiological responses or hemodynamic responses are vital clinical tools for both BCIs development and medical use (Shibasaki, 2008). The electrophysiological responses result from the acquisition of ionic currents which flow due to the exchange of information carrying neurons. These are measured by capturing EEG, ECoG, MEG, and intracortical neuron recordings. The electrophysiological activity is captured from neuronal oscillations across the active brain regions. In case of hemodynamic responses, the active regions are identified by capturing and analyzing the level of oxyhaemoglobin across active brain region. It is a process in which glucose and oxygen from blood are released at much higher rates across active brain regions. The variations in the local ratio of oxyhaemoglobin to de-oxyhaemoglobin are measured to quantify the level of associated brain activity. The neuroimaging modalities used to capture these blood-oxygen-level-dependent (BOLD) changes are fMRI, fNIRS, SPECT, and PET recordings (Laureys et al., 2009). These methods are not directly related to neuronal activity across active brain regions. To construct BCI systems, the electrophysiological and hemodynamic neural responses are captured directly from cerebral cortex either in an invasive, partially invasive, or noninvasive manner. This classification depends on the positioning of sensors to acquire brain signals from neuron cells, that is, whether the brain activity is recorded from the surface (noninvasive) of the cerebrum or from the cortical tissues (invasive) under the scalp. The acquired brain activities can be synchronous or asynchronous depending on the mode of operation whether it is computer driven or user driven. The subsequent subsections are detailing the various techniques used for BCI development.

2.2.1 Invasive and Partially-Invasive BCI Techniques

Invasive and partially invasive BCI signal acquisition techniques involve the neurosurgical implantation of microelectrodes either inside the cerebral cortex or over the surface of cerebrum beneath the scalp, respectively ([Abdulkader et al., 2015](#)). The most widely used partially invasive and the invasive modality used in BCI research is ECoG (measures neuronal activity on the cortical surface) and intracortical neuron recording (measures the neural activity inside the motor cortex), respectively. These neuroimaging modalities possess very high temporal and spatial resolution which leads to high SNR of recorded brain signals. The high SNR helps to preserve the diagnostic details in acquired neural responses and thus possess many advantages in medical and neuroprosthesis control applications ([Konrad and Shanks, 2010](#)). These invasive/partially invasive techniques are preferred where high-resolution neural signals are the primary requirement for the development of neuroprosthetics with high efficiency to restore useful life among severely paralyzed patients ([Lebedev and Nicolelis, 2006](#)).

However, involvement of surgical procedures during implantation may lead to certain risks involving scar tissue, protection from infection, and denial of body to adapt to new object leading to severe medical complications. The lack of flexibility is also a major concern as once implanted, the position of electrodes can't be shifted to monitor neural responses in other brain regions. Only a small brain area can be monitored. A need is there to use nanotechnology to develop implantable nano-electrodes that can be placed in large arrays across distinct brain regions to capture detailed spatial information. The partially invasive BCI techniques possess bit less spatial/temporal resolution and reduced risk of forming scar tissue ([Lebedev and Nicolelis, 2006](#); [Wolpaw, 2003](#)). The subsections further discuss the types of invasive neuroimaging modalities.

2.2.1.1 Electrocorticography (ECoG)

ECoG acquires neural responses by recording electrical activity of neurons from the cortex surface after microelectrode grid implantation. The resultant signals possess higher temporal-spatial resolution, signal amplitude, and spectral bandwidth as compared with noninvasive EEG signals ([Jinyin et al., 2011](#)) since signals are captured from more close and localized regions of active brain. Being a high-amplitude signal, it is less noisy and muscle motion artifact free. Certain studies were conducted on animals and it has been concluded that these under scalp penetrated electrodes could acquire stable ECoG signals for months without any recalibration ([Chao et al., 2010](#); [Margalit et al., 2003](#); [Yuen et al., 1987](#)). Once brain signals are acquired, the linear and nonlinear features of ECoG are extracted to classify the neural responses corresponding to distinct motor, imaginary or voluntary actions. Because of higher spectral bandwidth of ECoG, it includes higher frequency component up to 200 Hz. The gamma band activity and event-related potentials (ERPs) are most widely used to characterize the variations in captured human neural responses. Various BCI applications have been developed in the past using ECoG signal

acquisition. A group of researchers has utilized ERPs (Levine et al., 1999) and analysis of alpha, beta, or gamma subbands (Crone et al., 1998; Miller et al., 2007) successfully to classify distinct voluntary-involuntary motor actions, cursor control (Schalk et al., 2007) or to control a prosthetic hand by analyzing P300 ERPs.

2.2.1.2 *Intracortical Neuron Recording*

Intracortical neuron recording involves acquisition of electrical activity of neurons via single or array of electrodes implanted inside the cortex, that is, very close to the signal source. This highly invasive method is capable of providing neural signals possessing very high temporal and spatial resolution. However, it may suffer from a neuron death or inclusion of significant noise component due to increased cerebral tissue resistance encountered during signal communication from deep-implanted electrode to recording device (Polikov et al., 2005). The intracortical neuron parameters such as single-unit activity (SUA) acquired from single neuron, multiunit activity (MUA) acquired from multiple neurons indicate spiking activity, and local field potentials (LFPs) obtained by applying low-pass filter (<300 Hz) to acquired neuron activity, are most widely used to capture and characterize variations in acquired neuron recordings (Waldert et al., 2009). A number of control applications using motor cortical control responses obtained by implanted electrodes have been developed including cursor movement control by a neurodegenerative disorder patient and robotic arm (Muller and Kubler, 2007).

2.2.2 Noninvasive BCI Techniques

Noninvasive BCI signal acquisition techniques involve measurement of brain activity using external sensors placed over the scalp. These techniques do not require any neurosurgical procedures to implant sensors inside the cortex and thus involve minimal risk, and are relatively more convenient and safe. However, the amplitude of electrical activity of neurons may get attenuated while their transmission from different layers of brain from cortex to skull and finally to scalp. This may lead to loss in diagnostic information. The various noninvasive neuroimaging modalities used in BCI research include EEG, MEG, fMRI, fNIRS, PET, SPECT, etc.

2.2.2.1 *Magnetoencephalography (MEG)*

MEG is a noninvasive neural acquisition method to capture the resultant magnetic activity produced by naturally occurring electrical activity of neurons in the human brain. The magnetic fields are produced by means of magnetic induction phenomenon due to flow of intracellular currents (Babiloni et al., 2009). The architecture of neural cells (dendrites) producing these currents, the neighboring cells, and the degree of group synchronization among these cells contribute significantly in the levels of net current generated. The levels must be high enough to be efficiently detected and measured outside the head. The mechanism of active ion channeling and electrical potential difference between the apical and basal dendrites contribute toward the primary currents with large amplitudes.

The source of primary currents in dendrite potential is due to fairly synchronized postsynaptic potentials (both inhibitory and excitatory). The temporal durations (typically from few tens to hundreds of milliseconds) and amplitudes of action potentials get overlapped to generate resultant postsynaptic potentials. The similar postsynaptic potentials add up locally and generate net intracellular currents. These currents are also termed as primary currents and are the major source of magnetic activity. This magnetic activity is captured by the arrays of magnetometers in MEG. The flow of primary currents induces secondary currents that flow through different brain tissues and eventually reach at the scalp surface. These currents are detected from the scalp surface by placing electrodes to record MEG.

Magnetic signals in MEG are recorded by using a sensitive superconducting quantum interference device (SQUID). These devices possess the capability to capture minute magnetic variations produced by neural oscillations in brain. The magnetic fields captured by MEG are less distorted than electric fields captured by EEG electrodes. This is due to the property of magnetic fields to travel freely through brain tissues whereas electric fields suffer distortion while their travel through brain tissues to skull and scalp (Babiloni et al., 2009). The MEG signals could interfere with magnetic fields from external sources such as earth's magnetic field. To prevent this interference, laboratory settings providing effective attenuation and shielding from such induced electromagnetic interferences due to external sources are required.

MEG is a nonportable device and with ideal laboratory settings, the MEG captures neural activity with higher spatiotemporal resolution than EEG. This could lead to characterization of these signals with more compact and efficient feature set. This would in turn reduce the training time and thus increase the BCI communication speed (Mellinger et al., 2007). The high spatiotemporal property of MEG enhances the capability of BCI to localize activated regions inside the brain (Wang et al., 2010). This is due to the usage of large number of sensors that enhance spatial resolution. Further, the MEGs can also capture the neural information in the frequency range above 40 Hz whereas EEG is capable to capture <40 Hz. This encourages the need to explore the development of MEG-based brain-computer interfaces. In spite of these advantages of MEG and its close relationship with EEG, it is still not a preferred brain imaging modality for BCI design. The reason is its nonportable, expensive, and bulky acquisition machine. Further, MEG signal analysis techniques are focused on characterization of stimulus-induced neural responses rather than motor neural responses. The signal processing algorithms developed to remove MEG scanner artifacts and extract required information from raw MEG signals are still at initial stages and are not widely accepted.

2.2.2.2 Functional Magnetic Resonance Imaging

fMRI is another noninvasive brain imaging method that works on the principle of detection of variations in local cerebral blood flow and oxygen levels in blood flow using electromagnetic fields. This brain mapping technique maps neural activities to the activated

brain regions and thus provides source localization. The whole process follows the principle that the involvement of any brain region for specific activity is associated with increased blood flow in region of interest (ROI). Thus, fMRI is used to measure oxygen levels in blood flow across activated brain regions. It is a kind of hemodynamic response measured using blood oxygen level-dependent (BOLD) contrast during activations of neurons in brain (Lee et al., 2009). The variations in deoxyhemoglobin concentrations across brain tissues are obtained by intensities of BOLD contrast during specific brain activity. The BOLD activity is first extracted from one or more brain ROIs followed by average activity computation among all ROIs or any other relevant relation by defining and applying appropriate mathematical functions.

The fMRI responses are recorded using MRI scanners with electrical field strength in the range of 3–7 T. It provides high spatial resolution (in the range of millimeters) by acquiring neuronal variations from deep localized active brain regions that are otherwise difficult to be captured by other brain imaging modalities. However, temporal resolution of fMRI is very low of about 1–2 s. It also deals with the issue of physiological delay of 3–6 s (Weiskopf et al., 2004). This leads to unsuitability of fMRI-BCIs for high-speed BCI communications required almost in all nonclinical applications. Also, the expensive, nonportable, and bulky MRI scanners are highly susceptible to electromagnetic interference and motion artifacts.

2.2.2.3 Functional Near-Infrared Spectroscopy (fNIRS)

The fNIRS is a noninvasive brain signal acquisition tool based on optical spectroscopy that employs near-infrared light to measure variations in localized cerebral metabolism while performing specific brain activity. The light in near-infrared range can penetrate the brain skull up to a depth of around 1–3 cm under its cerebrum surface to measure blood flow (Taga et al., 2007). It acquires brain signals with low temporal and high spatial resolution, however, it is less effective as compared with the other brain imaging modalities based on electromagnetic signals. The fNIRS measuring device is comparatively less expensive and portable, however, has less brain imaging capabilities. This optical imaging technique is not capable of penetration to inner cortical regions. It also suffers from a problem of propagation delay in reception of hemodynamic responses corresponding to specific neural activity. The motion artifacts due to head movements and obstruction due to hair may further deteriorate the signal quality and hence the performance of designed BCI (Coyle et al., 2007).

2.2.2.4 Electroencephalography (EEG)

EEG described by a German psychiatrist Berger H. Uber in 1929, involves the recording of electrical neural impulses by placing electrodes over different scalp regions of cerebrum. On the basis of experimental results, he suggested that the frequency of brain wave

recordings via EEG reflects the corresponding brain activity in the cerebrum cortex. An electrical potential (microvolts) vs. time recordings are acquired by nonpolarized and thus interference-free electrodes. Once acquired, the signals are amplified and digitized to store and perform subsequent analysis using computers. The electrodes act as an interface between scalp and EEG recording circuitry and transform the ionic current generated by communication of millions of neurons to the electrical current. The number of electrodes may vary among available commercial EEG units; however, they are positioned over the scalp in such a manner that it should efficiently capture neural responses from all the regions of cerebrum, viz., frontal, temporal, parietal, and occipital. Electrodes mounted electro-headcaps are often used to acquire multichannel EEG recordings with large number of electrodes.

Electroencephalogram is a preferred noninvasive neurodiagnostic tool to measure neural activity with high temporal resolution, that is, its ability to detect neural variations within a stipulated time interval is very high ([Sakkalis, 2011](#)). However, it suffers lack of performance in terms of spatial resolution and SNR since amplitude of brain signals get deteriorated during their transmission from internal cortical regions of brain to scalp regions. The signal amplitude is dependent upon the distance of source generating neural electrical impulses from the recording electrodes, intensity of impulses, and spatial orientation of source with respect to recording electrodes. A number of solutions have been suggested in the literature to address the above limitations. It includes increasing the number of sensors/electrodes up to 256 electrodes, thus, covering the wide cerebrum regions (frontal, temporal, parietal, and occipital) by limiting the distance between successive pair of electrodes from 10% to 20% of the scalp diameter ([Bi et al., 2013](#)). Literature reveals that the high-frequency potential variations captured from scalp regions in the vicinity of placed electrodes and from cortical tissues oriented at an angle of 90 degrees, contribute maximum toward the recorded brain signals. Thus, electrical activity of neurons is highly localized and is captured from large groups of synchronized and activated neurons. BCI researches are also working to reduce the number of required electrodes to capture brain activity while maintaining a high SNR.

A variety of BCIs measure and record electrical activity of neurons using sensors placed over the scalp regions. Furthermore, ECoG and intracortical recordings rely on implanting the microelectrode arrays under the cerebrum and inside the cortical regions of brain, respectively. The magneto-encephalography acquires magnetic fields corresponding to specific neural activity. While fMRI records the small variations in oxygen levels of blood due to related brain activity. Similarly, fNIRS measures the hemodynamic optical response to assess functional activity in the cortex area of brain. All these neuroimaging modalities have been implemented successfully by the researchers to develop BCIs. However, ECoG and intracortical recordings are invasive methods of signal acquisition and use implanted electrodes. The reliability, safety in surgical procedures, consistent performance, and convenience are major concerns with these techniques.

The MEG and fMRI are associated with very high magnetic fields and suffer with high cost and nonportability of large acquisition devices. Further, the brain signals are acquired with low temporal resolution. These limitations make these techniques impractical for high-performance major BCI control applications as compared with EEG, a noninvasive neuroimaging modality that possesses high temporal resolution. The detailed summary of electrophysiological and hemodynamic brain responses along with their respective features is tabulated in [Table 2.1](#).

2.3 DATA ACQUISITION

Brain signal acquisition is critical to set up brain-computer communication. EEG-based BCIs consist of an acquisition device as a headset or a cap mounted with electrodes. The internal circuitry of acquisition unit comprises of electrodes, bio-signal amplifier, and analog-to-digital converter. The electrodes capture brain signals corresponding to specific brain activity based on selective thoughts/attention, motor actions, motor imagery, etc. The recorded signals are transmitted from EEG scalp electrodes to the next stage, a bio-signal amplifier to raise the amplitude of the acquired neural signals. Once amplified, signals are passed to analog-to-digital converter that transforms neural responses from analog-to-digital domain. These digitized brain signals are transmitted to interfaced computer using wired or wireless mode of communication. This computer processes the received brain data and generates control signals to run specific BCI application.

2.3.1 Brain Electric Potential

Any specific neural activity in cerebral cortex causes variations in electric fields over the surface of skull. The resultant varying electric fields generated by millions of neighboring neurons are recorded by EEG electrodes placed over four regions of cerebrum, viz., frontal, temporal, parietal, and occipital. The variations in electric potential are dependent on two factors: first is the timely synchronization between post-synaptic excitation of the dendrites in neurons of the cerebral cortex and the second is the orientation of these neurons with respect to the cortical surface. The neurons oriented at the right angles with respect to the cortical surface contribute maximum to resultant surface potential than the rest. The simultaneous excitation of neurons is measured as EEG signals. These signals are of very small amplitude (10–100 μV approximately) in the frequency range of 1–100 Hz. Only large clusters of active neurons are able to generate recordable electrical potentials over the scalp. The resultant electric current travels through several neuronal layers, skull, and skin to be finally captured by scalp electrodes. The EEG, therefore, has the potential to locate the electrical potentials over the regions of neural activation and their subsequent strength ([Teplan, 2002](#)) and is effectively employed in BCI designing. Two conventions are followed to measure neuroelectric potential using EEG:

Table 2.1 Summary of electrophysiological and hemodynamic brain responses

Features	Brain responses					
	Electrophysiological responses				Hemodynamic responses	
	Intracortical neuron recording	ECoG	EEG	MEG	fMRI	fNIRS
Acquisition technique	Invasive (electrodes are implanted within cortical tissues)	Partially invasive (electrodes are implanted over the surface of cortex)	Noninvasive (electrodes are placed over the scalp)	Noninvasive	Noninvasive	Noninvasive
Temporal resolution	Very high	High	High	Medium	Low	Low
Spatial resolution	Very high	High	Low	Medium	High	High
Signal type	Electrical	Electrical	Electrical	Magnetic	Metabolic	Metabolic
Portability	Portable	Portable	Portable	Nonportable	Nonportable	Portable
Associated risks	Surgery required (risk of infection)	Surgery required (risk of infection)	No risk	High magnetic field	High magnetic field	NA

- Bipolar measurement: A technique of measuring potential difference between two active electrodes.
- Reference-point measurement: A technique of measuring potential difference between an active electrode and an electrically inactive reference electrode positioned over the earlobe. This method is less prone to the artifacts and thus less distortion in signals.

2.3.2 EEG Electrode Positioning

The EEG records are acquired by positioning EEG electrodes over the brain scalp by following standardized 10–20 electrode system ([Jasper, 1958](#)) as depicted in [Fig. 2.2](#). According to this system, two reference points are used over the scalp to place electrodes or to determine electrode location. The one reference point known as Nasion is marked at the intersection of top vertical position of the nose below forehead and horizontal alignment of the eyes. Inion, the second reference point is located at small bony lump between the skull and the neck (base of the skull). As per 10–20 electrode system, electrodes are located by making the transverse and median planes at intervals of 10% and 20%. The electrode locations are marked by letters and numbers that specify the different regions of cerebrum. The letters identify the brain lobe (frontal, temporal, parietal, and occipital) and the brain hemisphere is identified by a number. The right hemisphere electrodes are represented by even numbers and left hemisphere electrodes are represented by odd numbers. The letter “F” represents the frontal lobe, “P” represents the parietal lobe,

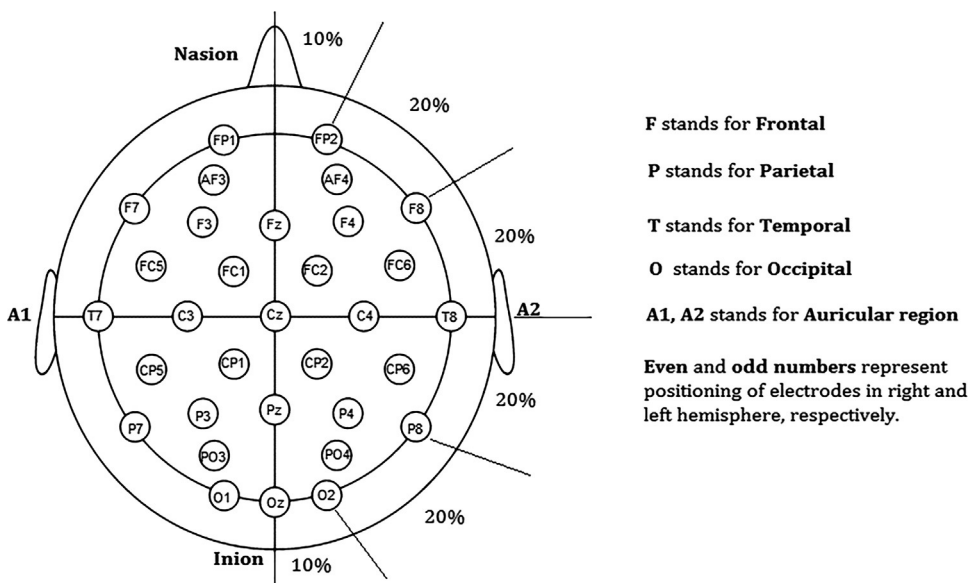


Fig. 2.2 Electrode positioning over scalp using 10–20 electrode system.

“T” represents the temporal lobe, “O” represents the occipital lobe, “C” represents the central region, “A” represents the auricular (ear lobe) region, and a small letter “z” represents the midline electrodes. Once the location of electrodes is understood, the next major task is to record EEG responses. The EEG signals are acquired as the difference in potential between active scalp electrodes and reference scalp electrodes with respect to time.

2.3.3 EEG Electrodes

The EEG electrodes can be broadly classified into needle and surface electrodes. The needle electrodes involve placement of needles under the skin and are attached to wired/wireless leads to record EEG. The more convenient and comfortable electrodes are surface electrodes that consist of conductive plate of tin, silver, lead, or gold-plated fine silver metal coated with silver chloride (AgCl) and are mounted over a headcap like device. These circular-shaped flat or cup-shaped thin metal surface electrodes have diameter in the range of 4–10 mm. The cup-shaped electrodes have hole in the center filled with an electrolyte solution to develop metal-electrolyte interface. Adhesive wet electrodes adhere to the skin very well, however, may cause discomfort to the subject. A conductive gel or electrolyte solution is used to ensure a low-impedance electrical contact at the electrode-scalp interface. These must be dried after use to protect from moisture. These electrodes could be reusable disk electrodes or disposable gel less or pre-gelled type. The reusable electrodes are positioned over the scalp using a conducting gel applied between electrodes and scalp. These disks are made up of tin, gold, or silver and are fitted in washable elastic headbands/headsets/headcaps. The electrode consists of a metal conductor with a lead of insulated wire gauge. Their cost is moderate to high. On the other hand, the disposable electrodes consist of silver/silver chloride and have adhesive pad around them. These low-cost electrodes are the best suited for EEG recordings from scalp regions without hair, otherwise the pad could stick to hair and no recording will be obtained.

Researchers are also exploring the usability of dry and noncontact EEG electrodes in BCI development. Dry electrodes do not require an electrolyte to operate and are made up of simple stainless steel thin discs or micro-fabricated silicon structures. It may cause increase in the skin-electrode impedance during initial electrode placement. However, this usually gets reduced after a few minutes because of moisture built up due to sweat. The usefulness and performance of signal acquisition device are usually evaluated in terms of comfort/utility at the system level and bio-signal quality in terms of noise and subject’s motion sensitivity (Chi et al., 2010). A recent study has been implemented to capture EEG signals of subjects using gel-free dry electrodes, while writing an average of error-free 8.76 letters in a minute. It has been observed that a high-speed brain-computer interface communication at a bit rate >100 bits per minute can be achieved using dry electrodes (Spüler, 2017).

2.3.4 EEG Signals and Rhythms

The EEG signals can be broadly recorded in three ways viz., routine EEG; sleep EEG; and ambulatory EEG. Routine EEGs are the simplest one and are recorded by placing electrodes on a scalp as per the requirement. EEG recordings taken along with the heart rate, respiration, oxygen saturation, airflow, and limbic movements constitute the sleep EEGs. The ambulatory EEGs are captured throughout the day and night using portable EEG acquisition units.

According to Berger H. Uber (1929), the specific brain activity in the cerebrum is related to corresponding frequency of EEG wave. The EEG signals are comprised of five frequency subbands and are referred to as delta (0–4 Hz), theta (4–8 Hz), alpha (8–12 Hz), beta (12–30 Hz), and gamma (>30 Hz) rhythms, respectively. Delta rhythms are the lowest frequency EEG waves and gamma is the fastest activity followed by beta. Another type of EEG rhythm is “mu” rhythm with frequency of near around 10 Hz and minute amplitude of near about 50 μ V approximately. Although these rhythms have frequency range similar to alpha rhythm still “mu” rhythm is physiologically different from alpha waves. The “mu” waves are strongly correlated with motor activities and are dominant in motor cortex region of cerebral cortex (Pfurtscheller et al., 2006a,b). The gamma rhythms are less frequently used for EEG signal analysis because of their low amplitudes and are more susceptible to peripheral electrical activities such as EMG or electrooculography (Müller et al., 1996). However, high-frequency gamma rhythms may offer high ITRs and spatial specificity (Darvas et al., 2010). Therefore, are gaining more attention in designing high-speed brain-computer interfaces.

2.3.5 Preamplification, Filtering and Analog-to-Digital Conversion

The EEG signals acquired by electrodes need to be amplified to increase the signal strength of neural responses. As discussed in the preceding sections, the EEG acquisition unit includes bio-signal amplifier, filter, and analog to digital converter apart from scalp electrodes. This stage involves the preamplification (to have adequate signal amplitude), analog filtering (to reject noise and interference), and analog to digital conversion of amplified and filtered EEG responses. The neural activity signals acquired through scalp electrodes are very low-amplitude signals of the order of microvolts. This amplitude depends on the following parameters:

- intensity of neural oscillations generated from the source
- spatial orientation of neurons with respect to scalp electrodes
- distance between source of electrical impulses from acquisition electrodes
- electrical properties of brain tissues between source of neural activity and recording electrodes

The bio-signal amplification stage provides signal amplification while maintaining high SNR. The power-line interference signals of 50/60 Hz can be rejected by integrating

low-pass filters with cutoff below 50/60Hz. A notch filter rejecting a narrow band around 50/60Hz can also be implemented to keep high-frequency EEG subbands also; however, it may introduce phase distortion. A high-pass filter may also be implemented to reject low-frequency bioelectric flowing potentials (exist in the frequency range of <0.4 Hz) due to breathing. The filtered signals are sampled at fixed sampling interval (more than twice of the largest frequency component of interest). Each sample is finally converted into digital equivalent by using high-resolution analog-to-digital converter. This digitized EEG signal is transmitted to interfaced computer for subsequent signal processing.

2.4 PREPROCESSING

Once the EEG signals are acquired, these are preprocessed to de-noise the recorded EEGs to enhance the required information specific brain activity patterns from raw EEG records. Apart from electrical neuronal activity, some peripheral electrical and muscular activities are also picked up during neural signal acquisition. These undesirable temporal and spatial variations originated from noncerebral regions contaminate the acquired neural responses and are known as artifacts. The presence of artifacts may deteriorate the performance of designed BCI system. Therefore, the identification and rejection of artifacts are very crucial before further signal processing. Classification of EEG artifacts and its rejection process is discussed in subsections further.

2.4.1 EEG Artifacts

EEG artifacts can be broadly classified as physiological (caused by peripheral electrical and muscular activities) and nonphysiological (caused by interference due to electromagnetic sources) artifacts as depicted in [Fig. 2.3](#).

2.4.1.1 Physiological Artifacts

EEG signals captured from specific brain regions are very much susceptible to artifacts caused by bioelectrical activities such as EoG activity (caused by unintentional eye movement or eyeblink), electromyographic (EMG) activity (muscle movements/contractions in the vicinity of EEG recording site), electrocardiograph (ECG) artifacts, pulse artifacts, etc.

- The movements of eyes (horizontal and vertical) may shift the generated electric fields and generate electric potentials similar to rotating electric dipoles. The eyeblinks generate electrical potentials due to charge variations. The voluntary eyeblinking generates very high-amplitude brain patterns as high potential difference is generated between positively charged cornea and negatively charged retina ([Iwasaki et al., 2005](#)). These *eye movement and blinking artifacts* are the most prominent over frontal lobes of cerebrum ([Fatourechi et al., 2007](#)).

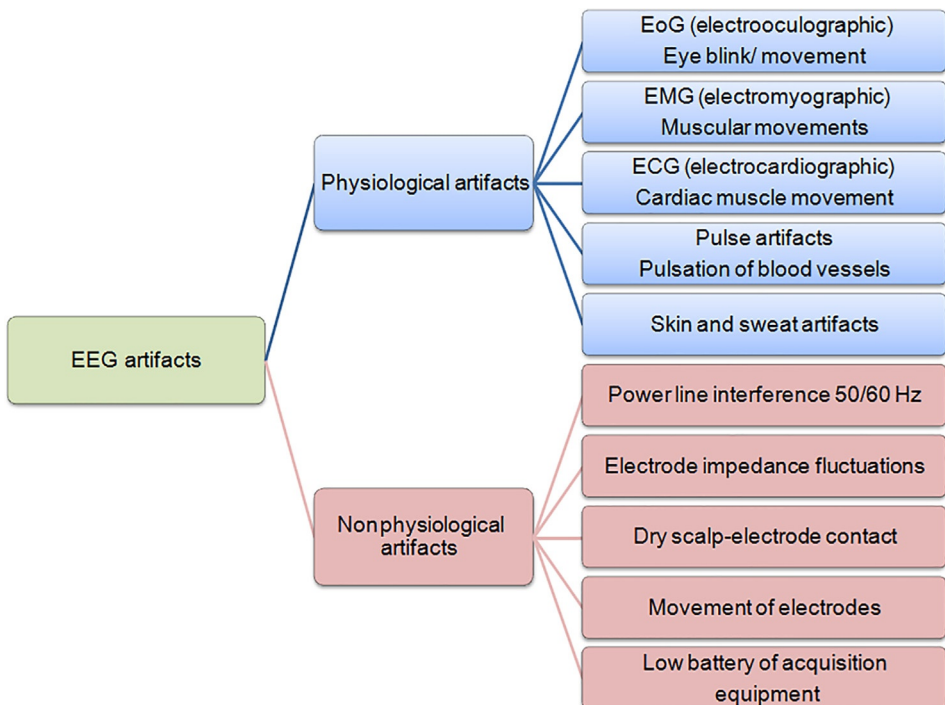


Fig. 2.3 EEG artifacts.

- The contraction and expansion of atria and ventricles introduce strong muscular dipoles throughout the human body and are called *ECG artifacts*. These rhythmic activities interfere with brain activity and may have amplitudes as high as 10 times the magnitude of EEG waves. However, ECG artifacts can be easily detected due to their fixed wave pattern consisting of P-QRS-T complex.
- The other type of artifacts known as *pulse artifacts* occurs when a recording electrode is placed over the pulsating blood vessel. This kind of artifact shows a uniform wave pattern, therefore, can be easily identified and rejected from acquired EEG.
- Further, the movement of muscles close to the scalp such as face muscles, neck muscles, jaw clenching, muscular movement of head, and body movements cause *muscle movement artifacts* to arise across temporal and frontal scalp regions ([Keren et al., 2010](#)).
- The changes in skin potential may also lead to the appearance of low-frequency (0.2–1 Hz) irregular patterns in EEG known as *skin and sweat artifacts*. The process of sweating may also cause additional synchronous potential variations across different scalp electrodes due to electrical activity of skin and sweat glands.

2.4.1.2 Nonphysiological Artifacts

Recorded EEG signals are mainly contaminated by external electromagnetic sources such as power-line interference 50/60 Hz, variations in electrode impedances, cable movements, low battery of acquisition unit, etc.

- The power-line interference 50/60 Hz is caused by 50/60 Hz alternating current sources such as electric devices, main power lines, if there is improper shielding from AC sources and improper grounding.
- The high-frequency waves (radio/microwaves) also give rise to artifacts over 10 kHz. These waves interfere with low-frequency EEG patterns when they are translated to low-frequency waves during demodulation.
- The rubbing of feet, shoes against the floor, rubbing of hands against each other may produce large interfering electrical potentials due to exceptional rise in a ground current between user and EEG recording electrode device.
- The faulty electrodes, dry scalp electrode contact, noncontact biopotential sensors, movement of reference, or cable connector faults cause occurrence of sharp positive or negative potential variations in EEG brain patterns.
- The relative movement of EEG electrodes with respect to head and resultant friction between electrodes and scalp surface contributes toward EEG signal artifacts. A transversal movement of electrodes causes variations in coupling impedance of skin-electrode interface. This may generate vibrations and thus require careful mitigation to avoid such mechanical deflections. A lateral movement of electrodes may induce friction and thus give rise to triboelectric charges (frequent charges introduced due to electrification of frictional contacts between scalp and electrodes) on the electrode surface. These artifacts are the most prominent when electrodes with poor resistive contacts are used.
- Apart from these external sources, certain internal sources may also attribute toward the generation of shot, flicker, or thermal noises which cause variations in acquired brain potentials.

2.4.2 EEG Artifact Rejection

The detection of EEG artifacts involves analysis of acquired brain signals carefully over specific time instants and applying amplitude thresholds to identify the artifacts. For example, the muscle artifacts are of shorter duration as compared with EEG patterns but are random in nature in time and amplitude both. These artifacts can be identified and removed by performing a group average of these random variations followed by low-pass filtering. Some externally controlled artifacts such as skin and sweat artifacts can be eliminated and controlled by temperature control in laboratory settings and subject's skin preparation prior to electrode placement over scalp. The effect of electrode movement artifacts can be reduced by introducing more sophisticated acquisition units with more comfort and controlled size and weight of mounted EEG electrodes.

However, the identification of artifacts is very critical to further preprocess the acquired brain signals in order to extract relevant brain activity information. The detection of artifacts can be done by analyzing acquired EEGs carefully over specific time course and applying amplitude threshold algorithms. It is followed by subsequent filtering and segmentation of EEG data to reject the portion of corrupted data. This filtering and segmentation operation is known as EEG epoching. The aim is to isolate and maximize the relevant information carrying EEG samples associated with specific brain activity over specific time duration for a frequency range. The whole process involves the averaging and thus helps in simplifying the subsequent stages of feature extraction and classification. The significant EEG activity usually lies in the range of 0.2–40 Hz. Four types of filters can be implemented depending upon the required frequency response, viz., low pass (passes a set of frequencies below cut-off frequency), high pass (passes a set of frequencies above cut-off frequency), band pass (passes a desired band of frequencies), and band stop (restricts a defined band of frequencies). Therefore, a band-pass filtering process aids in rejecting the noise signals outside the required frequency range. The segmentation of filtered data involves the division of continuous EEG data into time-locked sliding windows for further processing. The baseline drift associated with EEG recordings is also removed in this stage. This is performed to obtain quasistationary EEG segments of small duration. Further, the secondary artifact removal involves the implementation of appropriate temporal and spatial filters particularly for rejection of large amplitude (generally exceeding 1 mV) artifacts and EEG signal amplitude variations exceeding 200 μ V. The distinct categories of temporal and spatial filters used for preprocessing are depicted in Fig. 2.4.

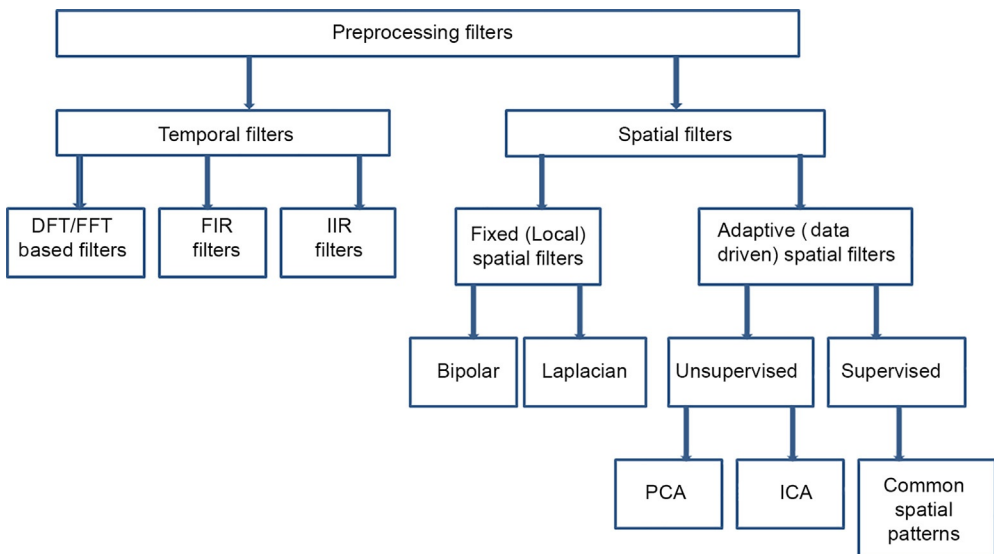


Fig. 2.4 Categorization of preprocessing filters.

2.4.2.1 Artifact Rejection Using Temporal Filtering

Brain signals are preprocessed by implementing temporal filters to select the specific EEG sub frequency bands carrying the neuro signals of interest. For example, a brain-computer interface capturing the EEG motor rhythms is generally designed to capture *mu* and *beta* rhythms located in the 8–30 Hz frequency range. Thus, a band-pass temporal filter needs to be implemented to select the desired band of frequencies. Temporal filters are also implemented to reject the artifacts arising from power-line interference and scalp electrode polarization. Three techniques are used to implement the temporal filters:

- discrete Fourier transforms (DFTs)/fast Fourier transform (FFT)
- finite impulse response (FIR) filters
- infinite impulse response filters (IIR), respectively

The DFT can be used successfully to filter long-duration brain signals by removing all the DFT coefficients that do not correspond to frequencies of interest. The flowchart in Fig. 2.5 depicts the step-by-step procedure. At first, the DFT on input EEG signal $s(n)$ is performed. The DFT $S(f)$ of an input EEG signal $s(n)$ is calculated as a sum of N samples at different frequencies f . The filtering operation is performed by removing unwanted filter coefficients. The resultant filtered EEG signal is obtained by applying inverse DFT to transform the signal again into time domain. A fast computation technique FFT can also be implemented to perform required filtering (Birvinskas et al., 2013).

The process of temporal filtering can also be performed by implementing FIR and IIR filters. The nonrecursive FIR filters utilize last M input samples of recorded EEG signal $s(n)$ to provide a filtered EEG signal $s(n)_{FIR}$ as follows:

$$s(n)_{FIR} = \sum_{k=0}^{M-1} a_k s(n-k) \quad (2.1)$$

where $\{a_k\}$ represents filter coefficients.

In a similar way, the recursive IIR filters can be implemented by utilizing the last N output samples in addition to last M input samples of a raw EEG signal as follows:

$$s(n)_{IIR} = \sum_{k=0}^{M-1} a_k s(n-k) + \sum_{k=1}^{N-1} b_k s(n-k)_{IIR} \quad (2.2)$$

where $\{a_k\}$ and $\{b_k\}$ represent filter coefficients.

IIR filters are capable of performing filtering operation with comparatively less number of filter coefficients than required for FIR filters (Smith, 1999).

2.4.2.2 Artifact Rejection Using Spatial Filtering

The desirable characteristic of any spatial filtering technique is dimensionality reduction while retaining the relevant information necessary for signal classification. This is achieved by removing redundancy among neighboring channel information. The spatial

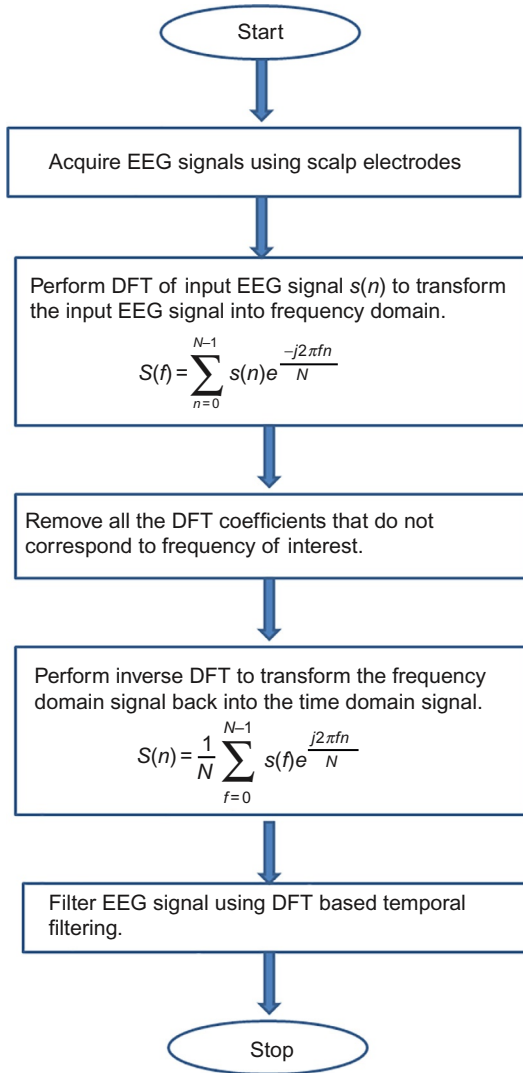


Fig. 2.5 Temporal filtering using DFT.

filters are implemented to extract the EEG components carrying the most relevant information present in the acquired EEG response. At first, the electrodes providing the intended information related to specific neurophysiological activity of interest are selected. The rest of the electrodes are assumed to produce noise or peripheral activity. The EEG signals at selected electrodes are weighted to implement spatial filtering operation. As has been documented earlier, the frontal electrodes are commonly used to acquire eye movement/blinking-related variations in brain signals. To reject these

artifacts, the independent high-amplitude variations from these frontal channels are isolated and discarded from the acquired dataset. Thus, spatial filters promote localized brain activity and suppresses spatial activity.

The spatial filtering makes use of a small set of channels that are defined as a weighted linear combination of all the original EEG channels. The resultant filtered EEG signals can be defined as

$$\hat{S} = \sum_i W_i S_i = WS \quad (2.3)$$

where \hat{S} is the spatially filtered EEG signal, S_i is the EEG signal acquired by channel i , W_i is the weight assigned to the channel i , and S is a matrix of EEG signals acquired from all scalp channels.

It is clear that the spatial filtering contributes toward the dimensionality reduction by providing less number of spatially filtered EEG signals (only more relevant) than original set of EEG signals from all channels. Further, a smearing effect of the underlying brain region plays a significant role in captured EEG signal quality. According to this effect, the signals originating from different internal brain regions may interfere with each other and may produce blurred images of original EEG signals. The spatial filtering operation may help in recovering the relevant neural information spread across different EEG channels. The importance of efficient spatial filter selection and its implementation to increase the SNR of acquired EEG responses and thus, improve the accuracy and speed of EEG-based BCIs has been explained well by [McFarland et al. \(1997\)](#).

The spatial filters can be broadly categorized among fixed and adaptive spatial filters ([Fig. 2.4](#)) depending on the manner of assigning a weight to respective EEG channels. The fixed spatial filters are implemented by fixing the weights manually in advance. This is done by analyzing the trends of acquired neurophysiological responses to locally reduce the background noise and interference due to smearing effect ([McFarland et al., 1997](#)). However, the adaptive spatial filtering involves an automatic optimization of weights according to the acquired EEG responses designated as training samples.

The fixed spatial filters can be implemented as bipolar or Laplacian filters ([Fig. 2.4](#)). A bipolar spatial filter over any selected channel is implemented by computing difference between two neighboring EEG channel electrode. The function to obtain bipolar spatial filter can be defined as

$$\hat{S}_i = S_j - S_k \quad (2.4)$$

where \hat{S}_i is the potential at i th channel after filtering; S_j and S_k are the potentials at j th and k th channel, respectively; and (j, k) are the neighboring channels of channel i . For example, a bipolar filter over channel AF3 would be defined as per Eq. (2.5) and shown in [Fig. 2.6](#):

$$AF3_{bipolar} = FP1 - F3 \quad (2.5)$$

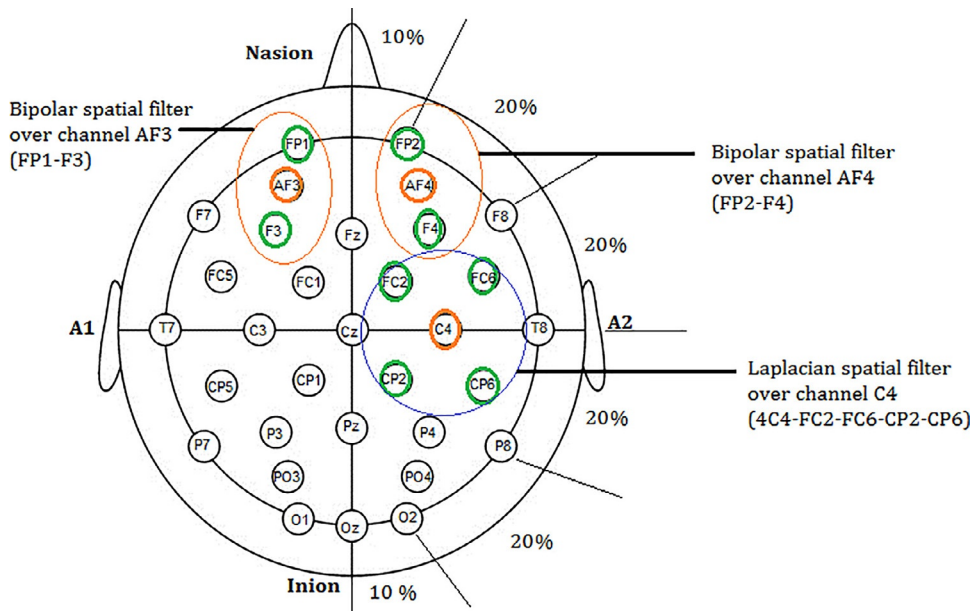


Fig. 2.6 Bipolar and Laplacian spatial filter implementation.

On the other hand, a Laplacian filter would be implemented by computing difference between four times the EEG signal at selected central electrode and signal at four electrodes in the periphery. The function to obtain spatial Laplacian filter is given as

$$\hat{S}_i = 4S_i - \sum_{j=1}^4 S_j \quad (2.6)$$

where \hat{S}_i and S_i represent the i th channel potential after and before spatial filtering, respectively. A set of four neighboring channels of channel I is represented by four values of j . For example, a Laplacian filter over electrode C4 would be defined as per Eq. (2.7) and shown in Fig. 2.6:

$$C4_{\text{laplacian}} = 4*C4 - FC2 - FC6 - CP2 - CP6 \quad (2.7)$$

Here, the channel C4 is selected as central channel and spatial filtering will be the result of weighted combination of C4 and its four peripheral channels FC2, FC6, CP2, and CP6, respectively.

Other than fixed spatial filters, there exists adaptive spatial filters which involve an automatic assignment of weights (rather than fixed as in case of fixed spatial filters) to each scalp channel data according to the incoming training samples. The spatial filters can be optimized while incorporating either supervised learning (with class labeled EEG training dataset) or unsupervised learning (without class labeled EEG training dataset).

The implementation of unsupervised spatial filtering involves two techniques; principal component analysis (PCA) which is based on sorting the variance among input EEG signals and independent component analysis (ICA) that computes statistically independent components to filter out incoming data (Kachenoura et al., 2008; Tangermann et al., 2009).

PCA involves the sorting of most relevant signal components among the input EEG dataset based on their decreasing variance in such a way that the very first principal component possesses the highest value of variance. It implies that the first principal component accumulates maximum activity followed by second, third, and so on. This sorting allows the separation of neural responses into different components. A set of data is obtained with first few the most significant components showing most of the signal dynamics and thus removing the remaining less significant components. This in turn enhances the SNR by rejecting noise components and reduces the dimensionality of input EEG dataset. Therefore, PCA can be successfully implemented to first identify and then reject artifact components and thus, reduce the feature vector dimensionality (Boye et al., 2008).

Apart from PCA, there is another technique of separating statistically independent components from a set of linearly/nonlinearly mixed EEG responses and is known as ICA. It possesses the capability to identify the artifacts embedded in acquired EEG dataset coming from multiple cognitive/control activities of brain. This separation makes use of the fact that the different artifacts are usually statistically independent of each other. It is well suited to reject/attenuate ocular artifacts in EEG dataset (Flexer et al., 2005; Gao et al., 2010) and the effect of peripheral EMG activity (Fatourechi et al., 2007).

On the other hand, common spatial pattern (CSP) algorithms are based on supervised learning. These transform the multichannel EEG dataset into a sub domain by highlighting the variations among different classes and minimizing the similarities. CSP algorithms are mostly applied when the acquired brain signals belong to a two-class system. This type of spatial filtering technique provides a filtered EEG signal with maximum variance for one class and minimum for the other one (Ramoser et al., 2000). The variance between two classes is captured in terms of discriminative band power of respective classes. The CSP-based spatial filtering is implemented by maximizing the following function:

$$CSP(w) = \frac{wS_1S_1^Tw^T}{wS_2S_2^Tw^T} = \frac{wC_1w^T}{wC_2w^T} \quad (2.8)$$

where T represents transpose; S_i represents the training matrix consisting of band-pass filtered signals belonging to class i (in this matrix rows represent channels and columns represent samples); and C_i represents average spatial covariance matrix of each trial belonging to class i .

Now, wS_i represents spatially filtered EEG signal belonging to class i and $w S_i S_i^T w^T$ represents the variance computed from the above spatially filtered EEG signals of class i . The maximum of function $CSP(w)$ provides the spatially filtered EEG signals with maximum band power difference among distinct classes (Blankertz et al., 2008).

The CSP-based spatial filters have number of advantages including their computational efficiency, easy implementation, versatility to work with event-related desynchronization (ERD) and event-related synchronization (ERS)-based BCIs, and high classification performances based on captured spatial information. However, it is not able to capture spectral details of input EEG dataset and have shown nonrobustness toward most of the nonstationary and random noise-related variations in input EEG data. Further, CSPs are also highly prone to over-fitting during training process when less number of training samples are used (Grosse-Wentrup and Buss, 2008). The classification accuracy of synchronous BCIs improves with the use of CSP-based filters as signals are allowed to be sent only during defined periods of time. However, this increase is not attained in asynchronous BCIs because of nonstationary nature of EEG signals (Mousavi et al., 2011).

Therefore, the classification performance of designed BCI increases with the features extracted from spatially filtered (fixed or adaptive) EEG signals as compared with those obtained from original raw EEGs (McFarland et al., 1997). Further, the classification performance was found to be the best using supervised adaptive spatial filters with the method of common spatial filters. However, the performance of fixed Laplacian spatial filter and unsupervised adaptive filter using ICA was found to be comparable when applied on EEG data corresponding to motor imagery task (Naeem et al., 2006).

2.5 FEATURE EXTRACTION

Feature extraction is the process to describe the recorded and preprocessed EEG signals using a compact and relevant signal values known as features. These features are represented as a feature vector. The algorithms for feature extraction are developed to transform multichannel EEG dataset into a significant and reduced dimension feature vector. This further facilitates the subsequent pattern recognition and classification of acquired brain patterns to develop operative command signals for designed BCI applications. EEG signals possess nonlinearity, non-Gaussianity, and nonstationarity. Therefore, nonlinear frequential features along with linear temporal features of EEG are extracted to study its rhythmic activity in distinct EEG subbands. Therefore, the acquired EEG neural patterns are characterized by a set of amplitude- and frequency-related features. Broadly, four different domains are used to represent these types (nonlinear, nonGaussian, and nonstationary) of signals as depicted in Fig. 2.7:

- EEG signal representation in time domain
- EEG signal representation in frequency domain
- EEG signal representation in time-frequency domain (hybrid techniques)
- EEG signal representation in spatial domain

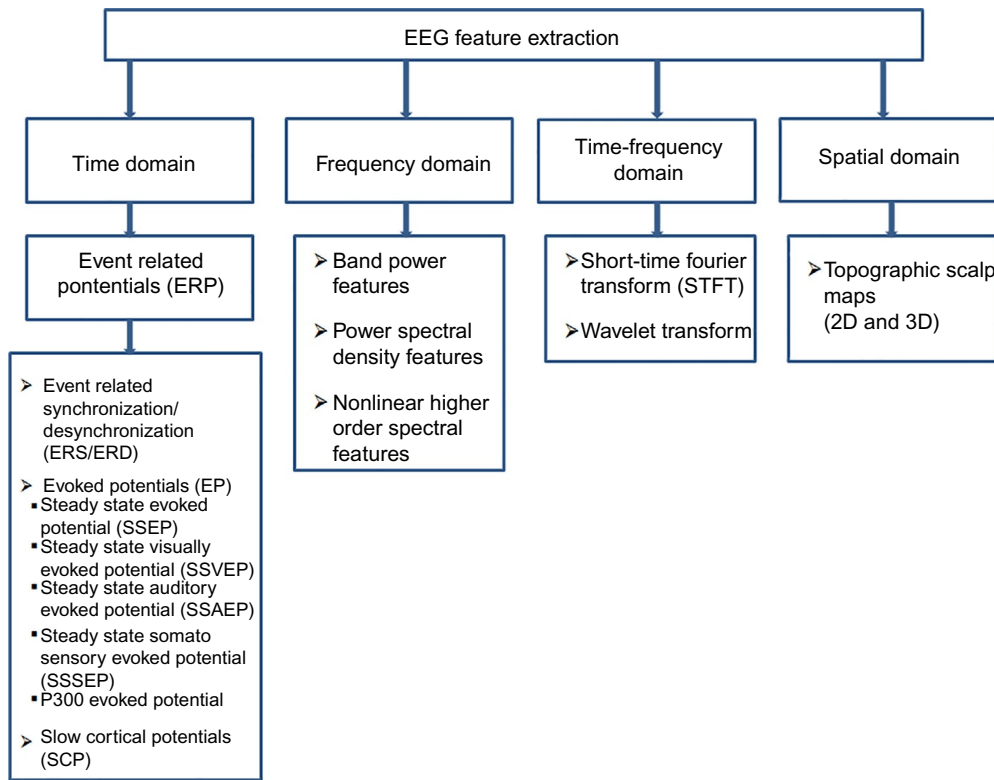


Fig. 2.7 EEG Feature extraction domains.

2.5.1 EEG Signal Representation in Time Domain

The EEG signals are represented in time domain when acquired by scalp electrodes, amplified and produced by acquisition units. In time domain analysis, the temporal variations of the neurophysiological signal are captured as features to describe EEG signals with precise time signatures. These types of features include peak-related and time duration-related information extracted from acquired EEG potentials and subsequently provide analysis related to signal variation with respect to time. The most important and widely used feature to characterize the brain signals in time domain is ERPs. These techniques are based on extraction of epochs (trials of small portions of signals) for further brain activity analysis. The most significant and relevant epochs are picked up by applying cross-trial averaging (a statistical procedure) to suppress the nonphase consistent background oscillations across the trials.

The ERPs represent time-locked EEG responses that occur while capturing the specific sensory, cognitive, motor, or some stimulated brain activity. These small potentials are used to study psychophysiological correlates of neural activities. As the event-based

activity is recorded when any external stimulation is provided or cognitive activity is performed, the resultant correlated brain potentials are called ERPs. These tiny amplitude potentials (range $<1 \mu\text{V}$ to several microvolts) are barely noticeable. However, the ERPs become clearly noticeable after performing averaging of these individual potentials. The ERPs may be categorized as follows:

- ERS/ERD
- Evoked potentials
 - Steady-state evoked potential (SSEP)
 - Steady-state visually evoked potential (SSVEP)
 - Steady-state auditory evoked potential (SSAEP)
 - Steady-state somatosensory evoked potential (SSSEP)
 - P300 evoked potentials
- Slow cortical potentials (SCPs)

2.5.1.1 Event-Related Synchronization/Desynchronization (ERS/ERD)

A type of ERP commonly used in motor imagery and voluntary movement-related BCIs is ERS and ERD. The increased neuronal synchronization among brain cells causes increase in EEG signal power/amplitude in specific EEG frequency band and is termed as ERS. However, ERD represents a decrease in EEG signal power/amplitude in specific EEG frequency subband due to inhibited neural synchronization. Any voluntary movement (eye, limb, hand, etc.), preparation of movement, or even the imagination of any movement leads to variation in neural activity across the primary and secondary motor cortex. These oscillatory variations in brain activity are known as sensorimotor rhythms (SMRs) recorded from motor cortex. The brain activity is categorized in distinct frequency bands as delta, theta, alpha, beta, and gamma activity. The gamma activity is difficult to detect with noninvasive neuroimaging modalities in which electrodes are placed over the scalp. However, gamma activity is often used as the analysis parameter in invasive BCIs. The amount of variations in these brain activities captured from motor areas is characterized in terms of ERS and ERD patterns. The ERS patterns specify the increase in oscillatory neural activity in specific EEG frequency subband (delta, theta, alpha, beta, and gamma). On the other hand, the decrease is characterized by ERD patterns. Therefore, by developing and analyzing ERS/ERD patterns across the involved cortical regions, the motor actions or motor imagery tasks can be identified and classified. However, to develop the well-discriminative ERD/ERS patterns, the involved cortical regions must be large enough. This requires prominent variations in the resulting brain activity as compared with the background EEG. For example, the hand, tongue, and foot-related cortical areas are having different topographic specifications and are large enough to produce prominent ERS/ERD brain patterns ([Schlögl et al., 2005](#)). The BCIs involving these motor actions and motor imagery movements do not require any external stimuli to perform a required associated task.

2.5.1.2 Evoked Potentials

The brain activity is recorded from the nervous system in terms of evoked potentials when any stimulation (visual, auditory, sensory, etc.) is presented to a subject. These evoked potentials are labeled as exogenous or endogenous. The exogenous BCIs are designed to capture neuronal activity elicited due to application of certain external stimuli such as auditory or visual (Kleber and Birbaumer, 2005). These systems require only one EEG channel to quickly set up and record the resultant control signals without the need of any intense training. However, endogenous BCIs are independent of any external stimulation and are based on self-regulation of brain patterns through respective psychological or cognitive activities. The subject trains himself to generate specific brain rhythms through neurofeedback (Krusienski et al., 2007).

The evoked potentials are termed as SSEPs if these are elicited using a stimulus modulated at specific fixed frequencies. These steady-state responses may be the result of rapid auditory stimuli as in SSAEPs, visual stimuli as in SSVEPs, and sensory as in SSSEPs. For example, the onset of visual stimulations generates brain activity in the visual cortex and is captured as visual evoked potentials (VEPs) by placing scalp electrodes over visual cortex (Yijun et al., 2006). The high-amplitude VEPs are attained if the stimulus is placed nearby the visual field. Different stimulations can be used to obtain VEPs including flash stimulations (digits/flashing on any screen to generate SSVEPs); graphic patterns (lattice structure, dot map); light emitting diode (LED)/liquid crystal display (LCD)-based flashing lights; pattern reversals, etc. (Odom et al., 2004). While subject follows the above stimulations by moving their eye gaze, visual potentials are induced in visual cortex. These kinds of BCIs require minimal training and falls under the category of exogenous BCIs.

The endogenic P300 evoked potentials are one of the positive ERP components that are elicited about 250 ms after the onset of meaningful and less frequent auditory, visual, or somatosensory stimuli among many stimulus (Iversen et al., 2008). These can be usually observed over the central and parietal cortex as late positive ERP components that are known to occur due to subject's reaction to some selected stimuli rather than due to the stimuli itself. The higher amplitude of P300 potentials is usually obtained for less frequent stimulus. The occurrence, amplitude, and duration of P300 can be utilized as temporal features in the measurement of cognitive, auditory, visual, and somatosensory neural activities in BCI development. However, the subject's adaptability to these less probable stimuli may reduce the P300 amplitude and consequently it may deteriorate the designed BCI performance. A variety of BCI applications including control of wheelchair (Tanaka et al., 2005); controlling an internet browser (Mugler et al., 2010); and P300 speller (Brunner et al., 2010) have been successfully developed using P300 evoked potentials. The major advantage of P300 evoked potentials is that it requires minimal subject training and therefore, can be easily parameterized with respect to new user.

2.5.1.3 Slow Cortical Potentials

The other type of ERPs is the slow event-related variations in the cortical electrical activity and is known as SCPs. The source of SCPs is the variations in synchronization levels among certain group of dendrites of nerve cells. These are categorized as negative and positive SCPs. The more synchronized potentials and increased resultant cortical activity indicates negative SCPs whereas the more desynchronized potentials (decreased cortical activity) represent positive SCPs (Hinterberger et al., 2004). The user can learn to generate deliberate SCPs through neurofeedback and thus can be efficiently captured to control external devices such as cursor movement on a screen (Hinterberger et al., 2004). The vertical motion of cursor represents the amplitude of SCP variations and horizontal movements represents time period-related information.

The time domain features of EEG are frequently used for BCI development. However, due to their low amplitude (microvolts) and dominant background activity, it is difficult to detect the ERPs from correlated neural activity responses. Further, these set of features provide only temporal information and are unable to characterize the morphology of the acquired EEG waveform. This limitation can be overcome by implementing power spectral density (PSD) frequency domain techniques.

2.5.2 EEG Signal Representation in Frequency Domain

The acquired EEG signals are represented in frequency domain by applying the Fourier transform on these neural responses. The features used to characterize the neural signals in frequency domain are EEG subband power calculations and PSD features to capture power variations in specific EEG frequency bands. The FFT method is usually implemented to track amplitude modulations at a specific frequency by plotting the frequency spectrum of acquired EEG responses.

2.5.2.1 Band Power Features

Electroencephalogram signals carry subband power in delta, theta, alpha, beta, and gamma subbands, respectively. The computation of band power features involves the implementation of band-pass filter in a required frequency subband. The resultant output of filter is squared followed by averaging the sample values over a specific band of frequencies. For example, the two bands which are extensively used to extract band power features during motor imagery tasks are the *mu* band (8–12 Hz) and *beta* band (13–30 Hz). The success of BCIs utilizing band power features relies on the extent of accuracy with which dominant frequency bands are tuned. Pfurtscheller and Neuper (2001) utilized band power in *mu* and *beta* frequency bands successfully in motor imagery classification. Palaniappan (2005) and Yamanaka and Yamamoto (2010) utilized band power features while cognitive task classification. The band power features capture power information in only particular selected frequency band. However, another frequency domain technique PSD is calculated by dividing whole EEG signal into smaller segments and

calculating the power information in each subsegment. Therefore, is capable of extracting the overall frequency content of an EEG signal.

2.5.2.2 PSD Features

The PSD also known as power spectrum is the most widely used feature to identify the correlated neural activity in BCI development (Unde and Shriram, 2014). It estimates the power distribution of input EEG signal over a specific frequency range. This frequency domain feature captures the overall frequency content of specific neural activity and is expressed as Fourier transform of the autocorrelation of attained EEG signal. The extracted frequency information has the potential to consistently discriminate between distinct neural activities even using different type of classifiers (Hu et al., 2006). The PSD of input EEG signal can be computed by applying the periodogram approach as depicted in Fig. 2.8.

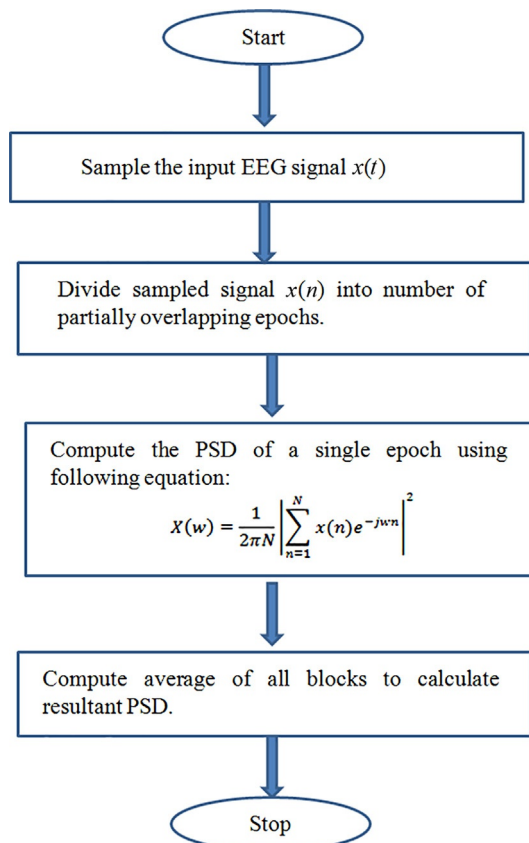


Fig. 2.8 Determination of power spectral density using periodogram approach.

In the periodogram approach of power spectrum estimation, the input EEG signal is divided into smaller data segments known as windows. The next step is to compute the DFT of each EEG subsegment followed by the squared magnitude of resultant DFT. The PSD is estimated by averaging these individual DFTs of overlapping segments. A wider EEG window may lead toward better frequency resolution. Another technique utilizing auto regressive (AR) modeling may also be implemented to estimate the PSD. This involves the calculation of AR parameters for each EEG window to correlate the original neural activity.

2.5.3 EEG Signal Representation in Time-Frequency Domain

The hybrid feature extraction techniques in both time and frequency domain can also be implemented to characterize the neurophysiological signals in BCI development. The neural signals possess properties in both the time and frequency domain. The advantage of representing EEG signals in time-frequency domain is that it is capable to capture both the random temporal and spectral variations. However, conventional frequency domain techniques characterize the signal variations by assuming the input EEG signal in a quasistationary state. The temporal and frequential EEG signal details can be extracted using short-time Fourier transform (STFT) or wavelet functions.

2.5.3.1 Short-Time Fourier Transform

The frequency and phase content-related information of overlapping segmented EEG signal can be determined using STFT. The STFT of input EEG signal $s(n)$ can be expressed as

$$\hat{S}(n, w) = \sum_{n=-\infty}^{\infty} s(n)w(n)e^{-jwn} \quad (2.9)$$

It is computed by first selecting a nonzero window function $w(n)$ over a short period of time. The selected window function is multiplied with input EEG signal and a Fourier transform of the resultant windowed EEG signal is computed (Zabidi et al., 2012). The fixed sized windowing provides similar temporal and spectral resolution in all EEG subbands. However, at higher frequencies, a higher temporal resolution is appreciated to analyze low amplitudes at higher frequencies more efficiently. A more robust wavelet-based analysis could be performed to overcome these limitations.

2.5.3.2 Wavelet Transform

The wavelet transform may also be implemented to estimate the power spectrum of input EEG signals, however, the resulting estimates possess temporal and frequential resolution on the basis of selected EEG subsegments. This method utilizes a set of wavelets to analyze the brain signals at different temporal and spectral resolution simultaneously. It makes

possible to analyze low-amplitude high-frequency segments with a high temporal resolution and high-amplitude low-frequency segments with a high spectral resolution. These properties of wavelets project them as an efficient tool to analyze EEG responses. The distinct set of wavelets has been applied efficiently for implementation of BCI systems, for example, Morlet wavelets ([Wang et al., 2010](#)), Daubechies wavelets, Mexican hat wavelets, etc.

2.5.4 EEG Signal Representation in Spatial Domain

Feature extraction in spatial domain aims toward the identification of specific brain regions where the neural activity is produced by plotting topographic patterns (scalp maps). This aids in selecting and focusing more on specific scalp electrodes/channels which are identified as major contributors/originators of specific neural activity. For example, the two-dimensional (2D)/three-dimensional (3D) topographic scalp maps of human brain show the potential distribution over scalp. This may subsequently aid in identifying the activated scalp regions (frontal, temporal, parietal, and occipital) in response to any specific brain activity.

The features capturing spatial and spectral information are mostly extracted in BCIs based on oscillatory activity such as SSVEP or ERD/ERS. However, the temporal and spatial information-related features are extracted in case of BCIs based on ERP. The spatial topographic maps reveal the information related to the activated regions of scalp during any brain activity. We know that the EEG signals are nonstationary, nonlinear, and non-Gaussian. Conventional linear power spectrum-based techniques suppress Fourier phase-related information while analysis of input EEG signals. The Fourier phase-related features contribute maximum toward morphology of the signal. Therefore, nonlinear signal analysis techniques such as higher-order spectra (bispectrum and trispectrum), Poincare plots, entropy analysis could be implemented to extract morphological features from input EEG signals ([Chua et al., 2010](#); [Pradhan et al., 2012](#)). Once the whole set of features is extracted, the feature selection algorithms based on PCA and ICA are implemented to select a more relevant and compact set of features.

2.6 CLASSIFICATION

In BCI systems, the feature extraction stage is followed by the classification/pattern recognition stage to translate the extracted feature set into operative commands and assign an appropriate class label to the set of features. The classification learning algorithms can be categorized as supervised (classifier is trained using a labeled EEG dataset), semisupervised (classifier is trained initially using a small labeled EEG dataset followed by online training with respect to input EEG data), and unsupervised learning (utilized with unlabeled dataset). The major concern related to implementation of efficient and robust classifiers is to deal with the size of the extracted feature vector. Larger is the size of feature vector, more

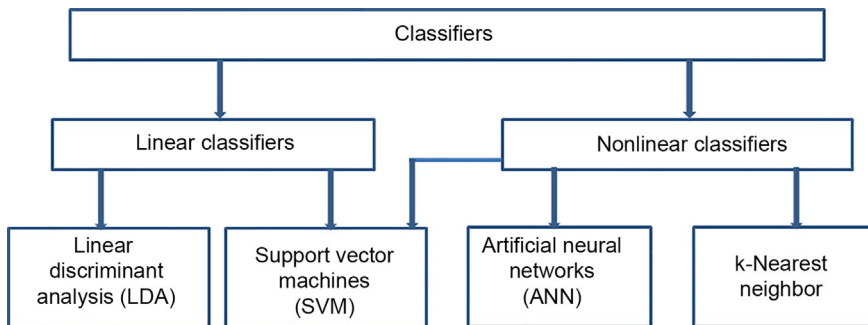


Fig. 2.9 Categorization of classifiers used in BCI systems.

will be the processing time of the classification system. The classification algorithms can be broadly categorized into linear and nonlinear classifiers as depicted in Fig. 2.9.

2.6.1 Linear Classifiers

Linear classifiers follow the principle of establishing a linear relationship/function between input and output variables of a classification system to categorize distinct classes of neural activity. These set of classifiers include linear discriminant analysis (LDA) and support vector machines (SVMs). LDA technique was developed by Fisher in 1936 and is based on the principle of linear separability of two class problems. It establishes a linear mathematical function known as hyperplane to separate the distinct neural activities from extracted feature set. For multiclass problems, a number of hyperplanes are established. The decision boundary is mathematically estimated as per Eq. (2.10):

$$f(x) = w^T x + w_o \quad (2.10)$$

where x represents input EEG feature vector, w is the weight vector, and w_o is the threshold to define decision boundaries. The input EEG is classified into the distinct classes depending on the sign of function $f(x)$. The LDA has been implemented in many BCI systems due to its simple, robust, and nonoverfit operation and computational requirements (Lotte et al., 2007; Muller et al., 2003).

The other type of linear classifiers SVMs works on the principle of estimating a decision boundary or a set of decision boundaries in order to maximize the margin between nearest training support vectors and the decision boundaries (Xiang et al., 2007). A SVM can also be implemented using a nonlinear and more flexible hyperplane to increase classification accuracy in multiclass nonlinear applications. The SVM-based classifiers work efficiently even with high-dimensionality feature set.

2.6.2 Nonlinear Classifiers

Nonlinear classifiers are implemented when it is impossible to construct any algorithmic solution among input and output variables of the classification system. These include artificial neural networks (ANNs), k-nearest neighbor classifier, and SVMs (can be implemented both ways: linear and nonlinear classifier). The ANNs are widely used in a variety of classification and pattern recognition tasks as they possess the capability to learn from training samples and thus classify the input samples accordingly. These work on the principle of developing a training algorithm to modify the weights assigned to individual input and hidden layer neurons in order to minimize the mean square error (difference between target and actual output). The multilayer perceptrons (MLPs) are the most widely used ANNs to classify multiclass neural activities efficiently ([Nakayama and Inagaki, 2006](#)).

The other category of nonlinear classifiers known as k-nearest neighbor utilize the concept that different class EEG features normally constitute separate clusters during feature mapping in feature space. On the other hand, very close neighbors are supposed to belong to the same class. The distance between test feature set and the neighbor is computed to classify the input feature vector efficiently in a multiclass environment ([Kayikcioglu and Aydemir, 2010](#)).

2.6.3 BCI Performance

Numerous parameters have been proposed to evaluate the performance of designed BCI. Few majorly used are enlisted as classification accuracy, sensitivity, specificity, and ITR. These statistical measures can be defined as:

- Classification rate/classification accuracy is defined as the number of correctly classified patterns to the total number of patterns. It can also be defined as the ratio of sum of true positives (*TP*) and true negatives (*TN*) to the total number of trials [sum of *TP*, false positives (*FP*), false negatives (*FN*), and *TN*].

$$\text{Classification Rate} = \frac{\text{True Positives} + \text{True Negatives}}{\text{True Positives} + \text{False Positives} + \text{False Negatives} + \text{True Negatives}} \quad (2.11)$$

The correctly classified patterns of particular class *A* are termed as *TP* whereas the patterns incorrectly assigned to class *A* are termed as *FP*. Similarly, the trials of class *A* that are assigned to another class are called *FN* and class patterns other than class *A* not assigned to class *A* are called *TN*.

Similarly, error rate can be computed as.

$$\text{Error Rate} = 1 - \text{Classification Rate} \quad (2.12)$$

$$\text{Error Rate} = \frac{\text{Number of incorrectly classified trials}}{\text{Total number of trials}} \quad (2.13)$$

- Sensitivity is defined as the ratio of TP to the sum of TP and FN (total number of trials of class A).

$$\text{Sensitivity} = \frac{\text{True Positives}}{\text{True Positives} + \text{False Negatives}} \quad (2.14)$$

This measure indicates the capability of an extracted feature set to identify the patterns of class A .

- Specificity is defined as the ratio of TN to the sum of FP and TN . It indicates the true negative rate.

$$\text{Specificity} = \frac{\text{True Negatives}}{\text{False Positives} + \text{True Negatives}} \quad (2.15)$$

- ITR is defined as the number of brain patterns (classes) that can be detected and classified quickly and reliably with high classification accuracy rates by a designed BCI. It constitutes of number of classified brain patterns, classification accuracy of BCI, and the time required by designed BCI to detect and classify these patterns of brain. It is measured in bits per minute. Higher the classification accuracy, higher would be the ITR as well. The BCIs with ITRs ranging from 30 bits per minute to 60 and 90 bits per minute have been designed successfully. However, these figures have been obtained in the excellent laboratory settings rather than real-world settings.

2.7 BCI APPLICATIONS

Brain power is being harnessed in amazingly surprising ways and with the advent of promising trends in computing technologies, brain-computer interface systems thus developed enable real-time solutions to complex needs. Brain-computer interfaces have conceivably, varied clinical and nonclinical applications as is briefed in Fig. 2.10. Major contributions in medical fields range from preventive to diagnostic to rehabilitative for patients suffering from locked-in syndrome (LIS), completely locked-in syndrome (CLIS) or even in healthy individuals (Berger et al., 2008; Neuper et al., 2003). Other major real-world applications that assist mutual understanding between human brain and the neighboring systems include neuroergonomics, smart home and environment, neuro-marketing, advertisement, education, games, entertainment, security, authentication, defence, and aerospace (Abdulkader et al., 2015; Mak and Wolpaw, 2009). Thus, as is obvious, the BCI technology is swiftly shifting from laboratory environments to everyday life useful products. Each application is reviewed in the subsequent subsections.

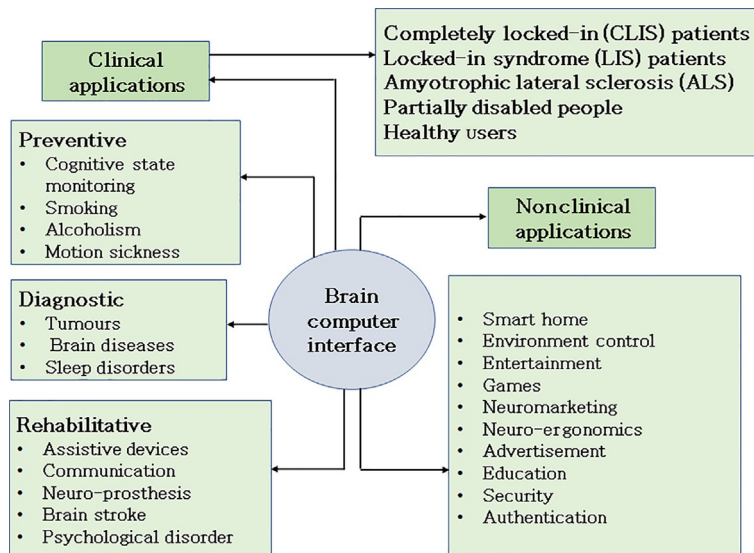


Fig. 2.10 Brain-computer interface applications.

2.7.1 BCI: Clinical Applications

Brain diseases that can affect an individual's ability to communicate could be a result of infections, tumours, or brain injuries viz. hematomas, blood clot, cerebral edema, or strokes. The neurodegenerative diseases like Huntington's, Parkinson's disease, Alzheimer's disease, dementia, amyotrophic lateral sclerosis (ALS), or Lou Gehrig's disease may develop as one grows old. There are certain genetic brain disorders like Tay-Sachs disease, and behavioral disorders, viz., depression, anxiety, bipolar disorder, or schizophrenia that hampers one's ability to connect to the external world. All such brain-related disorders can be taken care of using different BCI technologies which primarily depend on the degree of disability and not on the aetiology explains [Wolpaw et al. \(2006\)](#). Based on this theory, potential BCI applications can be categorized into following patient groups:

- Patients left with no visible neuromuscular control (CLIS).
- Patients with partial ability to control eye movements or a minor muscle twitch (LIS).
- Patients able to use conventional muscle-based assistive devices.

Different brain conditions damage CNS to different levels and so patients require diverse BCI technologies as assistive tools to communicate with the external world and go from one place to another and control movements.

2.7.1.1 BCI-Based Assistive Devices for Communication

Reinstating communication for brain-damaged patients has been the prime concern and a lot is being done in this field to prove the concept. EEG-based BCI for communication

purposes needs to be essentially a closed-loop real-time system and primarily depends on the following brain patterns:

- SCPs
- P300 ERPs
- SMRs

User can control positive and negative shifts in SCPs through extensive training and associated BCI interprets these changes to move and control objects on a computer monitor interface. Thus, disabled people are facilitated in sharing their ideas and views by the use of spelling devices (Birbaumer et al., 1999), thought translation devices (Birbaumer et al., 2000), and for basic and verbal communication as well (Kubler et al., 2001; Kubler and Birbaumer, 2008; Kaiser et al., 2002; Birbaumer, 2006; Birbaumer and Cohen, 2007). However, SCP-based systems are very sluggish and better solutions based on P300 and SMRs are considered and opted.

The μ (8–12 Hz) and β rhythms (18–26 Hz) of SMR which are traced from sensorimotor cortex site of the brain show variations due to movement, sensation, or motor imagery. Trained user is able to control SMR levels for communication purpose using motor imagery. Sufficient number of proofs of concept has been demonstrated to show word processing, spelling devices, cursor and mouse control, and icon identification applications of SMR-controlled BCI (Wolpaw et al., 1991; Wolpaw and McFarland, 2004; McFarland et al., 2008; Pfurtscheller et al., 2006a,b; Neuper et al., 2006; Kostov and Polak, 2000).

P300 is an event-related brain wave pattern obtained from the central and parietal regions in response to visual or auditory stimulus and BCIs based on P300 require minimal training. Inspired by initial development of visual input-based P300 speller by Donchin and Smith (1970), researchers have been assisting people with modified versions that make use of text-to-speech synthesizer or even a word-prediction algorithm (Sellers and Donchin, 2006; Nijboer et al., 2008; Piccione et al., 2006; Hoffmann et al., 2008; McCane et al., 2015). Patients with limited eye movement are also being supported by developing auditory stimulus-based P300 BCI (Kübler et al., 2009; Sellers et al., 2006; Furdea et al., 2009).

2.7.1.2 BCI-Based Assistive Devices for Locomotion and Movement

Independent mobility is most important for routine activities in case of differently abled and impaired individuals and BCI offers a ray of hope to this requirement. Reinstatement of motor control and wheelchair control powered by mind is being widely explored and applications built to address this need. McFarland and Wolpaw (2008) demonstrated that SMR-based BCI support control of prosthetic devices in multidimension. Researchers have been able to train tetraplegic patients to manage hand movements using electric orthosis through EEG inputs (Pfurtscheller et al., 2000). Tanaka et al. built an electric wheelchair in 2005 that could be commanded by EEG wave patterns. Wheelchair

navigation using tactile ERP-based BCI in virtual environment (Herweg et al., 2016) and in real-time (Kaufmann et al., 2014; Cao et al., 2014; Tonet et al., 2008), destination specific P300-based BCI (Rebsamen et al., 2007), and hybrid BCI based on P300 and μ rhythms to control simulated wheelchair (Long et al., 2012) have been successfully experimented. Galan et al. proved in 2008 and Kim et al. further reviewed in 2009 that mind controlled robotics can hugely impact and improve restoration of motor movements and thus quality of life.

2.7.1.3 BCI for Neurorehabilitation

Neurorehabilitation, a relatively novel field, offers multitude of healing solutions varying from psychological and creative to professional training to better understanding of the environment and ensures quality of life and independent living for an individual (Kitago and Krakauer, 2013; Dobkin, 2007). Neurorehabilitation is the culmination of varied technologies that offer the finest care for patients with nervous disorders or injuries. Enhancement in neuroimaging methods and robotics has made this realizable and assists in reducing recovery period as well.

Concept of using BCI for neurorehabilitation (Daly and Wolpaw, 2008; Buch et al., 2008; Sreedharan et al., 2013) is an emerging area and involves acquiring and understanding brain wave patterns when a task is being executed and using it as a feedback for improvement (van Dokkum et al., 2015). Applications include strengthening training session for illusioned motor tasks, achieve desired response in prosthetic limbs through sensory feedback and for better understanding of brain disorders and injuries. EEG-based BCI used for neurorehabilitation includes detection and classification of EEG features to be translated into feedback signal and better motor function control (Leamy et al., 2014). EEG wave patterns show signs of improvement after relearning sessions (Daly et al., 2006; Enzinger et al., 2008). Neurorehabilitation training assisted with robotics in the form of prosthetic limbs is an added advantage to the users and has proven out to be very successful in case of stroke (Daly et al., 2005). Huster et al. (2014) emphasized on the importance of EEG neurofeedback-based BCI for clinical trials and implementations of readymade solutions for neurorehabilitation. Use of smart phones with inbuilt cost-effective wireless EEG sensors has been demonstrated by Stopczynski et al. (2014) for real-time brain scanning in all kinds of set ups and is opening a new paradigm for neuroscience.

2.7.1.4 BCI for Cognitive State Analysis

BCI devices have the potential to portray an individual's cognitive and affective states that can be of great use in assisting disabled persons and prevent adversity in healthy users as well. Cognitive and volitional prostheses (Bai et al., 2015) facilitate improved feedback inputs to fine-tune BCI by analyzing conscious and unconscious states like alertness, attentiveness, drowsiness, frustrations, mood swings, intentions, confusions, etc.

Cognitive state monitoring may help in preventing disasters due to reduced attention level caused by smoking, alcohol consumption, motion sickness, etc.

Literature reports that prolonged cigarette smoking has adverse effects on the brain and cognitive abilities of humans which can lead to a risk of dementia or Alzheimer's disease (Centers for Disease Control and Prevention (CDC), 2008; Barnes and Yaffe, 2011; Corley et al., 2012; Karama et al., 2015). Erdozain et al. (2014) revealed that alcoholics tend to have protein variations in their brain which leads to certain neuronal and behavioral irregularity in them. They get prone to cognitive insufficiency in terms of learning and problem solving abilities, behavioral limitations like apprehension and hopelessness, and may get aggravated to Wernicke-Korsakoff disorder due to nutrition deficiency (Harper, 2007, 2009; Brust, 2010; Zahr et al., 2011; Thomson et al., 2012).

Noninvasive BCI is being vastly explored for early findings of motion sickness-based discomforts in drivers and commuters as a real-time application with an intention to reduce mishaps on roads due to reduced concentration and self-control in such a case. Efforts are in progress to develop an EEG-based cognitive monitoring system which can raise an alert on detecting motion sickness at an early stage and prevent accidents (Ko et al., 2011, 2013; Wei et al., 2011; Lin et al., 2013). Cognitive analysis using BCI may also give an indication/alarm when the driver is distracted or is exhausted and helps in devising an intelligent system to reduce disasters (Lin et al., 2010).

2.7.1.5 BCI for Medical Diagnostics

EEG-based BCI systems have the potential to predict the health of brain and assist in preventive care to curb brain issues like epileptic seizure, dyslexia, brain tumours, sleep disorder like rapid eye movement (REM), encephalopathy, Parkinson's disease, cerebro-vascular disorders, disorders of consciousness, and other health problems like cancer, etc. Sharanreddy and Kulkarni identified in 2013 (Sharanreddy and Kulkarni, 2013a,b) that EEG signal analysis can envisage disturbances in the brain signal and indicate epileptic seizure or brain tumor. Chen et al. (2014) worked on developing system-on-chip (SoC) prosthetic tool to acquire and analyze EEG signals in real time with an objective to reduce epileptic attack. Maksimenko et al. (2017) claim to have developed a predictive algorithm-based real-time system to control absence epilepsy in rat models. Sleep disorders like REM if analyzed through EEG signals can give an early indication of neurodegenerative diseases like Parkinson (Hansen et al., 2013; Christensen et al., 2014). Dyslexia, another brain disorder if diagnosed at an early stage using BCI can save a lot of embarrassment and help in confidence building (Al-Barhamtoshy and Motaweh, 2017). EEG-based noninvasive BCI provides diagnostic solution to certain chronic neurological problems like disorder of consciousness (Mikołajewska and Mikolajewski, 2014). EEG-based analysis has also opened a new paradigm of diagnostic and predictive approach to identify cancer (Poulos et al., 2012).

2.7.2 BCI: Nonclinical Applications

Brain-computer interfaces have advanced to such an extent that it is being offered to enrich normal life experiences. Several nonclinical applications based on intuitive human machine interactions in the field of neuroergonomics, smart home, internet of things (IOT), relaxation, music, entertainment, education, security, authentication, etc. are being explored.

2.7.2.1 BCI in Neuroergonomics

Neuroergonomics, an emerging research area initiated by Raja Parasuraman, deals with the study and analysis of brain using BCI to support enhancement of workplace by understanding worker's needs and wishes and understand the impact of fatigue on them and evolve a smart work place ([Mehta and Parasuraman, 2013](#); [Parasuraman and Wilson, 2008](#)). Funke et al. used Neuroergonomics in [2017](#) to show that people who are into vigilant duties feel oculomotor fatigue and tend to lose concentration. Researchers are also working on improving brain imaging techniques to noninvasively acquire and analyze brain data in dynamic conditions and automatically adapt to tasks at shop floors in manufacturing industries, team sports, health care units, etc. ([Jungnickel and Gramann, 2016](#)).

2.7.2.2 BCI for Smart Home

Integration of BCI to provide smart home environment is an exciting research field that has the potential to assist users control lightings and electronic equipments, security, etc. and offer feasible home automation ([Kosmyna et al., 2016](#)). Brennan et al. developed in [2015](#) autonomous systems using hybrid BCI with an objective to make older generation self-dependent. [Miralles et al. in 2015](#) developed "BackHome," a user-friendly BCI-based software application for smart home support and control, telemonitoring and provide cognitive inputs to reinstate liberty and freedom and ultimately improve standard of living.

2.7.2.3 BCI in Neuromarketing and Advertising

Use of BCI to assess cognitive brain functions for industrial product design is paving way for neuromarketing explorations ([Wriessnegger et al., 2015](#)). People are inclined toward products that are aesthetically appealing and make buying decisions purely based on visual impact. Neuromarketing attempts to comprehend user's response to marketing strategies and establishing a relation between human physiological parameters like EEG and art ([Chew et al., 2016](#)). [Vecchiato et al. \(2009\)](#) did a survey on the impact of political motivational speeches on general mass through TV messages and came to the conclusion that EEG data provide meaningful insights into the listener's brain activity. Researchers also have investigated effect of TV commercials and advertisements on human neural response and feel that certain words and pictures have a long-lasting effect on buyers,

thereby significantly effecting sales and marketing (Astolfi et al., 2008; Nomura and Mitsukura, 2015).

2.7.2.4 BCI for Games and Entertainment

Developers face continuing challenge in entertaining gamers with new technology and excitement. Concept of mind controlled gaming is a revolution and many companies are developing EEG-based entertainment apps as it has a huge market potential. BCI-based games recognize which event the gamer is interested in, whether he is getting stressed up or bored, his engagement level and can control commands merely by his mind. Video games are developed, flying objects can be controlled in 2D/3D virtual environment and even two players can play football using two sets of BCIs.

2.7.2.5 BCI for Security and Validation

Traditional security and validation systems available are vulnerable to certain shortcomings which are being addressed by BCI researchers. Security systems based on brain data claim to provide a reliable and robust solution to safety and authentication. Brain controlled commands for validation are perceived to be very secure as it is almost impossible to detect and imitate subtle changes in brain activity of an individual and breach the security.

2.8 CONCLUSION

Currently, development of EEG-based noninvasive, portable, and user-friendly brain-computer interfaces is a very dynamic and curious neuroscience research field. These BCIs possess the capability to be used in real-time applications outside the laboratory environment too. However, their reliability and calibration improvement could be done by developing and applying efficient machine learning-based classification algorithms on very large sample size of input EEG-based datasets. The potential robustness and efficiency of BCIs can be greatly improved by developing the efficient signal processing algorithms. This shall provide the most discriminative, invariant, and compact feature sets from acquired EEG signals. This could potentially lead toward decrease in processing time and increase in resultant efficiency of the developed BCI system. The enhancement in neuroscientific skills could also lead to development of the new brain pattern analysis techniques that may efficiently interpret the user's neural commands for control applications. BCI research must however address the following concerns:

- Poor reliability of brain-computer interfaces may lead to the misinterpretation of neural commands.
- Need of more comfortable, fully portable, and user-friendly EEG headsets with electrodes having less wear and tear which can perform well in all environments.

- Longer calibration times of mounted sensor electrodes and instrumentation. Improvements in electrode designing such as dry electrodes that do not require conductive gel and associated instrumentation are critical for the future of brain-operated computer interfaces.
- Correct capture, preprocessing, and analysis of brain patterns to translate these patterns into external device commands. Incorrect analysis may provide misleading results and conclusions.
- Limited reach to substantial users for rehabilitation.
- Low ITRs available with current BCIs which may hinder the development of BCI applications with minimal processing time.

With tremendous excitement in the emerging field of BCI research among neuroscientists, clinicians, and users; the future of developing wide range of EEG-based BCI applications seems to be very promising. Despite the present innovations in BCI research, further enhancements in brain signal acquisition and analysis techniques would eventually aid toward the improvement in BCI performance. Further, a need is there to transform BCI application prototypes from laboratory environment to actual use in practice by the external world. This could provide an efficient neural-based communication and control interface to restore useful life among people with severe neuromuscular/motor disabilities. Current BCI user population is limited; however, the evidence of its use in rehabilitation could contribute toward promoting the potential widespread BCI user population. Technological advancements in EEG-based BCIs reveal that EEG-BCIs possess the potential to be established as a neuroscientific tool for developing real time, portable, and fast brain-computer interfaces for neurorehabilitation.

REFERENCES

- Abdulkader, S.N., Mostafa-Sami, A.A., Mostafa, M., 2015. Brain computer interfacing: applications and challenges. *Egypt. Informat. J.* 16 (2), 213–230.
- Al-Barhamtoshy, H.M., Motaweh, D.M., 2017. Diagnosis of dyslexia using computing analysis. *J. Eng. Technol.* 0747-9964. 6 (2), 563–583.
- Astolfi, L., De Vico Fallani, F., Cincotti, F., Mattia, D., Bianchi, L., Marciani, M.G., Salinari, S., Colosimo, A., Tocci, A., Soranzo, R., Babiloni, F., 2008. Neural basis for brain responses to TV commercials: a high-resolution EEG study. *IEEE Trans. Neural Syst. Rehabil. Eng.* 16 (6), 522–531. <https://doi.org/10.1109/TNSRE.2008.2009784>.
- Babiloni, C., Pizzella, V., Gratta, C.D., Ferretti, A., Romani, G.L., 2009. Fundamentals of electroencephalography, magnetoencephalography, and functional magnetic resonance imaging. In: *Brain Machine Interfaces for Space Applications*. vol. 86. Academic Press, New York, NY, pp. 67–80.
- Bai, O., Kelly, G., Fei, D.-Y., Murphy, D., Fox, J., Burkhardt, B., Lovegreen, W., Soars, J., 2015. A Wireless, Smart EEG System for Volitional Control of Lower-Limb Prosthesis. In: *TENCON 2015 - 2015 IEEE Region 10 Conference*, 1-4 Nov, 2015, IEEE, Macao, China.
- Barnes, D.E., Yaffe, K., 2011. The projected effect of risk factor reduction on Alzheimer's disease prevalence. *Lancet Neurol.* 10 (9), 819–828.
- Berger, T.W., Chapin, J.K., Gerhardt, G.A., McFarland, D.J., Principe, J.C., Soussou, W.V., Taylor, D.M., Tresco, P.A., 2008. *Brain-Computer Interfaces: An International Assessment of Research and*

- Development Trends. Springer, Dordrecht. eBook. ISBN 978-1-4020-8705-9, Hardcover ISBN 978-1-4020-8704-2, p. 281.
- Bi, L., Fan, A.X., Liu, Y., 2013. EEG based brain controlled mobile robots: a survey. *IEEE Trans. Human-Machine Syst.* 43 (2), 161–176.
- Birbaumer, N., 2006. Breaking the silence: brain-computer interfaces (BCI) for communication and motor control. *Psychophysiology* 43 (6), 517–532.
- Birbaumer, N., Cohen, L.G., 2007. Brain-computer interfaces: communication and restoration of movement in paralysis. *J. Physiol.* 579 (Pt 3), 621–636.
- Birbaumer, N., Ghanayim, N., Hinterberger, T., Iversen, I., Kotchoubey, B., Kubler, A., Perelmouter, J., Taub, E., Flor, H., 1999. A spelling device for the paralysed. *Nature* 398 (6725), 297–298.
- Birbaumer, N., Kubler, A., Ghanayim, N., Hinterberger, T., Perelmouter, J., Kaiser, J., Iversen, I., Kotchoubey, B., Neumann, N., Flor, H., 2000. The thought translation device (TTD) for completely paralyzed patients. *IEEE Trans. Rehabil. Eng.* 8 (2), 190–193.
- Birvinskas, D., Jusas, V., Martišius, I., Damaševicius, R., 2013. Data compression of EEG signals for artificial neural network classification. *Inf. Technol. Control* 42 (3), 238–241.
- Blankertz, B., Tomioka, R., Lemm, S., Kawabata, M., Müller, K.R., 2008. Optimizing spatial filters for robust EEG single-trial analysis. *IEEE Signal Process. Mag.* 25 (1), 41–56.
- Boye, A.T., Kristiansen, U.Q., Billinger, M., do Nascimento, O.F., Farina, D., 2008. Identification of movement-related cortical potentials with optimized spatial filtering and principal component analysis. *Biomed Signal Process. Control*, 3, 300–304.
- Brennan, C.P., McCullagh, P.J., Galway, L., Lightbody, G., 2015. Promoting autonomy in a smart home environment with a smarter interface. *Conf. Proc. IEEE Eng. Med. Biol. Soc.* 2015, 5032–5035. <https://doi.org/10.1109/EMBC.2015.7319522>.
- Brunner, P., Joshi, S., Briskin, S., Wolpaw, J.R., Bischof, H., Schalk, G., 2010. Does the ‘P300’ speller depend on eye gaze? *J. Neural Eng.* 7, 056013.
- Brust, J.C., 2010. Ethanol and cognition: indirect effects, neurotoxicity and neuroprotection: a review. *Int. J. Environ. Res. Public Health* 7, 1540–1557.
- Buch, E., Weber, C., Cohen, L.G., Braun, C., Dimyan, M.A., Ard, T., Mellinger, J., Caria, A., Soekadar, S., Fourkas, A., Birbaumer, N., 2008. Think to move: a neuromagnetic brain-computer interface (BCI) system for chronic stroke. *Stroke* 39 (3), 910–917.
- Cao, L., Li, J., Ji, H., Jiang, C., 2014. A hybrid brain computer interface system based on the neurophysiological protocol and brain-actuated switch for wheelchair control. *J. Neurosci. Methods* 229, 33–43.
- Centers for Disease Control and Prevention (CDC), 2008. Smoking-attributable mortality, years of potential life lost, and productivity losses—United States, 2000–2004. *Morb. Mortal. Wkly Rep.* 57 (45), 1226–1228.
- Chao, Z.C., Nagasaka, Y., Fujii, N., 2010. Long-term asynchronous decoding of arm motion using electrocorticographic signals in monkeys. *Front. Neuroeng.* 3 (3), 1–10. <https://doi.org/10.3389/fneng.2010.00003>.
- Chen, W.-M., Chiueh, H., Chen, T.-J., Ho, C.-L., Jeng, C., Ker, M.-D., Lin, C.-Y., Huang, Y.-C., Chou, C.-W., Fan, T.-Y., Cheng, M.-S., Hsin, Y.-L., Liang, S.-F., Wang, Y.-L., Shaw, F.-Z., Huang, Y.-H., Yang, C.-H., Wu, C.-Y., 2014. A fully integrated 8-channel closed-loop neural-prosthetic CMOS SOC for real-time epileptic seizure control. *IEEE J. Solid State Circuits* 49 (1), 232–247 (6637111). <https://doi.org/10.1109/JSSC.2013.2284346>.
- Chew, L.H., Teo, J., Mountstephens, J., 2016. Aesthetic preference recognition of 3D shapes using EEG. *Cogn. Neurodyn.* 10 (2), 165–173. <https://doi.org/10.1007/s11571-015-9363-z>.
- Chi, Y.M., Jung, T.P., Cauwenberghs, G., 2010. Dry-contact and noncontact biopotential electrodes: methodological review. *IEEE Rev. Biomed. Eng.* 3, 106–119.
- Christensen, J.A., Zoetmulder, M., Koch, H., Frandsen, R., Arvastson, L., Christensen, S.R., Jennum, P., Sorensen, H.B., 2014. Data-driven modeling of sleep EEG and EOG reveals characteristics indicative of pre-Parkinson’s and Parkinson’s disease. *J. Neurosci. Methods* 235, 262–276. <https://doi.org/10.1016/j.jneumeth.2014.07.014>.
- Chua, K.C., Chandran, V., Acharya, U.R., Lim, C.M., 2010. Application of higher order statistics/spectra in biomedical signals—a review. *Med. Eng. Phys.* 32 (7), 679–689. <https://doi.org/10.1016/j.medengphy.2010.04.009>.

- Corley, J., Gow, A.J., Starr, J.M., Deary, I.J., 2012. Smoking, childhood IQ, and cognitive function in old age. *J. Psychosom. Res.* 73 (2), 132–138.
- Coyle, S.M., Ward, T.E., Markham, C.M., 2007. Brain-computer interface using a simplified functional near-infrared spectroscopy system. *J. Neural Eng.* 4 (3), 219–226. <https://doi.org/10.1088/1741-2560/4/3/007>.
- Crone, N.E., Miglioretti, D.L., Gordon, B., Sieracki, J.M., Wilson, M.T., Uematsu, S., Lesser, R.P., 1998. Functional mapping of human sensorimotor cortex with electrocorticographic spectral analysis. Alpha and beta event-related desynchronization. *Brain* 121, 2271–2299.
- Daly, J.J., Wolpaw, J.R., 2008. Brain-computer interfaces in neurological rehabilitation. *Lancet Neurol.* 7 (11), 1032–1043.
- Daly, J.J., Hogan, N., Perepezko, E.M., Krebs, H.I., Rogers, J.M., Goyal, K.S., Dohring, M.E., Fredrickson, E., Nethery, J., Ruff, R.L., 2005. Response to upper-limb robotics and functional neuromuscular stimulation following stroke. *J. Rehabil. Res. Dev.* 42 (6), 723–736.
- Daly, J.J., Fang, Y., Perepezko, E.M., Siemionow, V., Yue, G.H., 2006. Prolonged cognitive planning time, elevated cognitive effort, and relationship to coordination and motor control following stroke. *IEEE Trans. Neural Syst. Rehabil. Eng.* 14 (2), 168–171.
- Darvas, F., Scherer, R., Ojemann, J.G., Rao, R.P., Miller, K.J., Sorensen, L.B., 2010. High gamma mapping using EEG. *NeuroImage* 49, 930–938.
- Dobkin, B.H., 2007. Brain-computer interface technology as a tool to augment plasticity and outcomes for neurological rehabilitation. *J. Physiol.* 579 (Pt 3), 637–642.
- Donchin, E., Smith, D.B., 1970. The contingent negative variation and the late positive wave of the average evoked potential. *Electroencephalogr. Clin. Neurophysiol.* 29 (2), 201–203.
- Enzinger, C., Ropele, S., Fazekas, F., Loitfelder, M., Gorani, F., Seifert, T., Reiter, G., Neuper, C., Pfurtscheller, G., Muller-Putz, G., 2008. Brain motor system function in a patient with complete spinal cord injury following extensive brain-computer interface training. *Exp. Brain Res.* 190 (2), 215–223.
- Erdozain, A.M., Morentin, B., Bedford, L., King, E., Tooth, D., Brewer, C., Wayne, D., Johnson, L., Gerdes, H.K., Wigmore, P., Callado, L.F., Carter, W.G., 2014. Alcohol-related brain damage in humans. *PLoS One*. <https://doi.org/10.1371/journal.pone.0093586>.
- Fatourechi, M., Bashashati, A., Ward, R.K., Birch, G.E., 2007. EMG and EOG artifacts in brain computer interface systems: a survey. *Clin. Neurophysiol.* 118 (3), 480–494.
- Flexer, A., Bauer, H., Pripfl, J., Dorffner, G., 2005. Using ICA for removal of ocular artifacts in EEG recorded from blind subjects. *Neural Netw.* 18, 998–1005.
- Funke, M.E., Warm, J.S., Matthews, G., Funke, G.J., Chiu, P.Y., Shaw, T.H., Greenlee, E.T., 2017. The neuroergonomics of vigilance. *Hum. Factors* 59 (1), 62–75. <https://doi.org/10.1177/0018720816683121>.
- Furdea, A., Halder, S., Krusienski, D.J., Bross, D., Nijboer, F., Birbaumer, N., Kübler, A., 2009. An auditory oddball (P300) spelling system for brain-computer interfaces. *Psychophysiology* 46 (3), 617–625.
- Galan, F., Nuttin, M., Lew, E., Ferrez, P.W., Vanacker, G., Philips, J., Millan Jdel, R., 2008. A brain-actuated wheelchair: asynchronous and non-invasive brain-computer interfaces for continuous control of robots. *Clin. Neurophysiol.* 119 (9), 2159–2169.
- Gao, J., Yang, Y., Lin, P., Wang, P., Zheng, C., 2010. Automatic removal of eye-movement and blink artifacts from EEG signals. *Brain Topogr.* 23, 105–114.
- Grosse-Wentrup, M., Buss, M., 2008. Multi-class common spatial pattern and information theoretic feature extraction. *IEEE Trans. Biomed. Eng.* 55 (8), 1991–2000.
- Hansen, I.H., Marcussen, M., Christensen, J.A., Jennum, P., Sorensen, H.B., 2013. Detection of a sleep disorder predicting Parkinson's disease. *Conf. Proc. IEEE Eng. Med. Biol. Soc.* 2013, 5793–5796. <https://doi.org/10.1109/EMBC.2013.6610868>.
- Harper, C., 2007. The neurotoxicity of alcohol. *Hum. Exp. Toxicol.* 26, 251–257.
- Harper, C., 2009. The neuropathology of alcohol-related brain damage. *Alcohol* 44, 136–140.
- Herweg, A., Gutzeit, J., Kleih, S., Kübler, A., 2016. Wheelchair control by elderly participants in a virtual environment with a brain-computer interface (BCI) and tactile stimulation. *Biol. Psychol.* 121 (Pt A), 117–124.
- Hinterberger, T., Schmidt, S., Neumann, N., Mellinger, J., Blankertz, B., Curio, G., Birbaumer, N., 2004. Brain-computer communication and slow cortical potentials. *IEEE Trans. Biomed. Eng.* 51, 1011–1018.

- Hoffmann, U., Vesin, J.M., Ebrahimi, T., Diserens, K., 2008. An efficient P300-based brain-computer interface for disabled subjects. *J. Neurosci. Methods* 167 (1), 115–125.
- Hu, M., Li, J., Li, G., Tang, X., Ding, Q., 2006. In: Classification of normal and hypoxia EEG based on approximate entropy and welch power-spectral-density. The 2006 International Joint Conference on Neural Networks, IJCNN 06, pp. 3218–3222.
- Huster, R.J., Mokom, Z.N., Enriquez-Geppert, S., Herrmann, C.S., 2014. Brain-computer interfaces for EEG neurofeedback: peculiarities and solutions. *Int. J. Psychophysiol.* 91 (1), 36–45.
- Iwasaki, M., Kellinghaus, C., Alexopoulos, A.V., Burgess, R.C., Kumar, A.N., Han, Y.H., et al., 2005. Effects of eyelid closure, blinks, and eye movements on the electroencephalogram. *Clin. Neurophysiol.* 116, 878–885.
- Iversen, I.H., Ghanayim, N., Kübler, A., Neumann, N., Birbaumer, N., Kaiser, J.A., 2008. Brain-computer interface tool to assess cognitive functions in completely paralyzed patients with amyotrophic lateral sclerosis. *Clin. Neurophysiol.* 119, 2214–2223.
- Jasper, H.H., 1958. The ten-twenty electrode system of the International Federation. *Electroencephalogr. Clin. Neurophysiol.* 10, 371–375.
- Jinyin, Z., Sudre, G., Xin, L., Wei, W., Weber, D.J., Bagic, A., 2011. Clustering linear discriminant analysis for MEG-based brain computer interfaces. *IEEE Trans. Neural Syst. Rehabil. Eng.* 19, 221–231.
- Jungnickel, E., Gramann, K., 2016. Mobile brain/body imaging (MoBI) of physical interaction with dynamically moving objects. *Front. Hum. Neurosci.* 10, 306. <https://doi.org/10.3389/fnhum.2016.00306>.
- Kachenoura, A., Albera, L., Senhadji, L., Comon, P., 2008. ICA: a potential tool for BCI systems. *IEEE Signal Process. Mag* 25 (1), 57–68.
- Kaiser, J., Kubler, A., Hinterberger, T., Neumann, N., Birbaumer, N., 2002. A non-invasive communication device for the paralyzed. *Minim. Invasive Neurosurg.* 45 (1), 19–23.
- Karama, S., Ducharme, S., Corley, J., Chouinard-Decorte, F., Starr, J.M., Wardlaw, J.M., Bastin, M.E., Deary, I.J., 2015. Cigarette smoking and thinning of the brain's cortex. *Mol. Psychiatry* 20 (6), 778–785.
- Kaufmann, T., Herweg, A., Kübler, A., 2014. Toward brain-computer interface based wheelchair control utilizing tactually-evoked event-related potentials. *J. Neuroeng. Rehabil.* 11, 7. <https://doi.org/10.1186/1743-0003-11-7>.
- Kayikcioglu, T., Aydemir, O., 2010. A polynomial fitting and k-NN based approach for improving classification of motor imagery BCI data. *Pattern Recognit. Lett.* 31, 1207–1215.
- Keren, A.S., Yuval-Greenberg, S., Deouell, L.Y., 2010. Saccadic spike potentials in gamma-band EEG: characterization, detection and suppression. *NeuroImage* 49 (3), 2248–2263. <https://doi.org/10.1016/j.neuroimage.2009.10.057>.
- Kim, H.K., Park, S., Srinivasan, M.A., 2009. Developments in brain-machine interfaces from the perspective of robotics. *Hum. Mov. Sci.* 28 (2), 191–203.
- Kitago, T., Krakauer, J.W., 2013. Motor learning principles for neurorehabilitation. *Handb. Clin. Neurol.* 110, 93–103. <https://doi.org/10.1016/B978-0-444-52901-5.00008-3>.
- Kleber, B., Birbaumer, N., 2005. Direct brain communication: neuroelectric and metabolic approaches at Tübingen. *Cogn. Process.* 6, 65–74.
- Ko, L.-W., Wei, C.-S., Jung, T.-P., Lin, C.-T., 2011. In: Estimating the level of motion sickness based on EEG spectra. FAC'11 Proceedings of the 6th International Conference on Foundations of Augmented Cognition: Directing the Future of Adaptive Systems. Springer-Verlag, Berlin, Heidelberg, pp. 169–176.
- Ko, L.-W., Lee, H.-C., Tsai, S.-F., Shih, T.-C., Chuang, Y.-T., Huang, H.-L., Ho, S.-Y., Lin, C.-T., 2013. In: EEG-based motion sickness classification system with genetic feature selection. IEEE Symposium on Computational Intelligence, Cognitive Algorithms, Mind, and Brain (CCMB), pp. 158–164.
- Konrad, P., Shanks, T., 2010. Implantable brain computer interface: challenges to neurotechnology translation. *Neurobiol. Dis.* 38, 369–375.
- Kosmyna, N., Tarpin-Bernard, F., Bonnefond, N., Rivet, B., 2016. Feasibility of BCI control in a realistic smart home environment. *Front. Hum. Neurosci.* 10, 416. <https://doi.org/10.3389/fnhum.2016.00416>.
- Kostov, A., Polak, M., 2000. Parallel man-machine training in development of EEG-based cursor control. *IEEE Trans. Rehabil. Eng.* 8 (2), 203–205.
- Krusienski, D.J., Schalk, G., McFarland, D.J., Wolpaw, J.R., 2007. A mu-rhythm matched filter for continuous control of a brain-computer interface. *IEEE Trans. Biomed. Eng.* 54, 273–280.

- Kubler, A., Birbaumer, N., 2008. Brain-computer interfaces and communication in paralysis: extinction of goal directed thinking in completely paralysed patients? *Clin. Neurophysiol.* 119 (11), 2658–2666.
- Kubler, A., Neumann, N., Kaiser, J., Kotchoubey, B., Hinterberger, T., Birbaumer, N.P., 2001. Brain-computer communication: self-regulation of slow cortical potentials for verbal communication. *Arch. Phys. Med. Rehabil.* 82 (11), 1533–1539.
- Kübler, A., Furdea, A., Halder, S., Hammer, E.M., Nijboer, F., Kotchoubey, B., 2009. A brain-computer interface controlled auditory event-related potential (p300) spelling system for locked-in patients. *Ann. N. Y. Acad. Sci.* 1157, 90–100.
- Laureys, S., Boly, M., Tononi, G., 2009. Functional neuroimaging. In: Steven, L., Giulio, T. (Eds.), *The Neurology of Consciousness*. Academic Press, New York, NY, pp. 31–42.
- Leamy, D.J., Kocjan, J., Domijan, K., Duffin, J., Roche, R.A., Commins, S., Collins, R., Ward, T.E., 2014. An exploration of EEG features during recovery following stroke – implications for BCI-mediated neurorehabilitation therapy. *J. Neuroeng. Rehabil.* 11, 9. <https://doi.org/10.1186/1743-0003-11-9>.
- Lebedev, M., Nicolelis, M., 2006. Brain-machine interfaces: past, present and future. *Trends Neurosci.* 29 (9), 536–546.
- Lee, J., Ryu, J., Jolesz, F.A., Cho, Z.H., Yoo, S.S., 2009. Brain-machine interface via real-time fMRI: preliminary study on thought-controlled robotic arm. *Neurosci. Lett.* 450, 1–6.
- Levine, S.P., Huggins, J.E., BeMent, S.L., Kushwaha, R.K., Schuh, L.A., Passaro, E.A., Rohde, M.M., Ross, D.A., 1999. Identification of electrocorticogram patterns as the basis for a direct brain interface. *J. Clin. Neurophysiol.* 16, 439–447.
- Lin, C.-T., Chang, C.-J., Lin, B.-S., Hung, S.-H., Chao, C.-F., Wang, I.-J., 2010. A real-time wireless brain-computer interface system for drowsiness detection. *IEEE Trans. Biomed. Circ. Syst.* 4 (4), 214–222. <https://doi.org/10.1109/TBCAS.2010.2046415>.
- Lin, C.-T., Tsai, S.-F., Ko, L.-W., 2013. EEG-based learning system for online motion sickness level estimation in a dynamic vehicle environment. *IEEE Trans. Neural Netw. Learning Syst.* 24 (10), 1689–1700.
- Long, J., Li, Y., Wang, H., Yu, T., Pan, J., 2012. Control of a simulated wheelchair based on a hybrid brain computer interface. *Conf. Proc. IEEE Eng. Med. Biol. Soc.* 2012, 6727–6730.
- Lotte, F., Congedo, M., Lécuyer, A., Lamarche, F., Arnaldi, B., 2007. A review of classification algorithms for EEG-based brain computer interfaces. *J. Neural Eng.* 4 (1), 1–13.
- Mak, J.N., Wolpaw, J.R., 2009. Clinical applications of brain-computer interfaces: current state and future prospects. *IEEE Rev. Biomed. Eng.* 2, 187–199.
- Maksimenko, V.A., Heukelum, S.-V., Makarov, V.V., Kelderhuis, J., Lütjohann, A., Koronovskii, A.A., Hramov, A.E., Luijtelaar, G.-V., 2017. Absence seizure control by a brain computer interface. *Sci. Rep.* 7, 2487, <https://doi.org/10.1038/s41598-017-02626-y>.
- Margalit, E., Weiland, J.D., Clatterbuck, R.E., Fujii, G.Y., Maia, M., Tameesh, M., Torres, G., D'Anna, S.A., Desai, S., Piyathaisere, D.V., 2003. Visual and electrical evoked response recorded from subdural electrodes implanted above the visual cortex in normal dogs under two methods of anesthesia. *J. Neurosci. Methods* 123, 129–137.
- McCane, L.M., Heckman, S.M., McFarland, D.J., Townsend, G., Mak, J.N., Sellers, E.W., Zeitlin, D., Tenteromano, L.M., Wolpaw, J.R., Vaughan, T.M., 2015. P300-based brain-computer interface (BCI) event-related potentials (ERPs): people with amyotrophic lateral sclerosis (ALS) vs. age-matched controls. *Clin. Neurophysiol.* 126 (11), 2124–2131.
- McFarland, D.J., Wolpaw, J.R., 2008. Brain-computer interface operation of robotic and prosthetic devices. *Computer* 41 (10), 52–56.
- McFarland, D.J., McCane, L.M., David, S.V., Wolpaw, J.R., 1997. Spatial filter selection for EEG-based communication. *Electroencephalogr. Clin. Neurophysiol.* 103 (3), 386–394.
- McFarland, D.J., Krusienski, D.J., Sarnacki, W.A., Wolpaw, J.R., 2008. Emulation of computer mouse control with a noninvasive brain-computer interface. *J. Neural Eng.* 5 (2), 101–110.
- Mehta, R.K., Parasuraman, R., 2013. Neuroergonomics: a review of applications to physical and cognitive work. *Front. Hum. Neurosci.* 7, 889. <https://doi.org/10.3389/fnhum.2013.00889>.
- Mellinger, J., Schalk, G., Braun, C., Preissl, H., Rosenstiel, W., Birbaumer, N., Kübler, A., 2007. An MEG-based brain-computer interface (BCI). *NeuroImage* 36 (3), 581–593.

- Mikolajewska, E., Mikolajewski, D., 2014. Non-invasive EEG-based brain-computer interfaces in patients with disorders of consciousness. *Mil. Med. Res.* 2014 (1), 14. <https://doi.org/10.1186/2054-9369-1-14>.
- Miller, K.J., Den Nijs, M., Shenoy, P., Miller, J.W., Rao, R.P.N., Ojemann, J.G., 2007. Real-time functional brain mapping using electrocorticography. *NeuroImage* 37, 504–507.
- Miralles, F., Vargiu, E., Dauwalder, S., Solà, M., Müller-Putz, G., Wriessnegger, S.C., Pinegger, A., Kübler, A., Halder, S., Käthner, I., Martin, S., Daly, J., Armstrong, E., Guger, C., Hintermüller, C., Lowish, H., 2015. Brain computer interface on track to home. *Sci. World J.* 623896. <https://doi.org/10.1155/2015/623896> Epub 2015.
- Mousavi, E.A., Maller, J.J., Fitzgerald, P.B., Lithgow, B.J., 2011. Wavelet common spatial pattern in asynchronous offline brain computer interfaces. *Biomed. Signal Process. Control* 6, 121–128.
- Mugler, E.M., Ruf, C.A., Halder, S., Bensch, M., Kubler, A., 2010. Design and implementation of a P300-based brain-computer interface for controlling an internet browser. *IEEE Trans. Neural Syst. Rehabil. Eng.* 18, 599–609.
- Muller, K.-R., Kubler, A., 2007. Toward Brain Computer Interfacing. Massachusetts Institute of Technology, pp. 1–25.
- Müller, M.M., Bosch, J., Elbert, T., Kreiter, A., Sosa, M.V., Sosa, P.V., Rockstroh, B., 1996. Visually induced gamma-band responses in human electroencephalographic activity—a link to animal studies. *Exp. Brain Res.* 112, 96–102.
- Muller, K.R., Anderson, C.W., Birch, G.E., 2003. Linear and nonlinear methods for brain-computer interfaces. *IEEE Trans. Neural Syst. Rehabil. Eng.* 11, 165–169.
- Naeem, M., Brunner, C., Leeb, R., Graimann, B., Pfurtscheller, G., 2006. Separability of four-class motor imagery data using independent components analysis. *J. Neural Eng.* 3, 208–216. <https://doi.org/10.1088/1741-2560/3/3/003>.
- Nakayaman, K., Inagaki, K., 2006. In: A brain computer interface based on neural network with efficient pre-processing. Proceedings of the International Symposium on Intelligent Signal Processing and Communications (ISPACS'06), Yonago, Japan, December 2006, pp. 673–676.
- Navarro, A.A., Ceccaroni, L., Velickovski, F., Torrellas, S., Miralles, F., Allison, B.Z., Scherer, R.R., Faller, J., 2011. In: Context-awareness as an enhancement of brain-computer interfaces. International Workshop on Ambient Assisted Living (IWAAL 2011), pp. 216–223.
- Neuper, C., Muller, G.R., Kubler, A., Birbaumer, N., Pfurtscheller, G., 2003. Clinical application of an EEG-based brain-computer interface: a case study in a patient with severe motor impairment. *Clin. Neurophysiol.* 114 (3), 399–409.
- Neuper, C., Muller-Putz, G.R., Scherer, R., Pfurtscheller, G., 2006. Motor imagery and EEG-based control of spelling devices and neuroprostheses. *Prog. Brain Res.* 159, 393–409.
- Nijboer, F., Sellers, E.W., Mellinger, J., Jordan, M.A., Matuz, T., Furdea, A., Halder, S., Mochty, U., Krusienski, D.J., Vaughan, T.M., Wolpaw, J.R., Birbaumer, N., Kübler, A., 2008. A P300-based brain-computer interface for people with amyotrophic lateral sclerosis. *Clin. Neurophysiol.* 119 (8), 1909–1916.
- Nomura, T., Mitsukura, Y., 2015. EEG-based detection of TV commercials effects. *Procedia Comput. Sci.* 60, 131–140.
- Odom, J.V., Bach, M., Barber, C., Brigell, M., Marmor, M.F., Tormene, A.P., Holder, G.E., 2004. Visual evoked potentials standard. *Doc. Ophthalmol.* 108, 115–123.
- Palaniappan, R., 2005. In: Brain computer interface design using band powers extracted during mental tasks. 2nd International IEEE EMBS Conference on Neural Engineering, 2005 Conference Proceedings, pp. 321–324.
- Parasuraman, R., Wilson, G.F., 2008. Putting the brain to work: neuroergonomics past, present, and future. *Hum. Factors* 50 (3), 468–474.
- Pfurtscheller, G., Neuper, C., 2001. Motor imagery and direct brain-computer communication. *Proc. IEEE* 89 (7), 1123–1134.
- Pfurtscheller, G., Guger, C., Müller, G., Krausz, G., Neuper, C., 2000. Brain oscillations control hand orthosis in a tetraplegic. *Neurosci. Lett.* 292 (3), 211–214.
- Pfurtscheller, G., Müller-Putz, G.R., Schlögl, A., Graimann, B., Scherer, R., Leeb, R., Brunner, C., Keinrath, C., Lee, F., Townsend, G., Vidaurre, C., Neuper, C., 2006a. 15 years of BCI research at Graz University of Technology: current projects. *IEEE Trans. Neural Syst. Rehabil. Eng.* 14 (2), 205–210.

- Pfurtscheller, G., Brunner, C., Schlögl, A., Lopes da Silva, F.H., 2006b. Mu rhythm (de)synchronization and EEG single-trial classification of different motor imagery tasks. *NeuroImage* 31, 153–159.
- Piccione, F., Giorgi, F., Tonin, P., Prifitis, K., Giove, S., Silvoni, S., Palmas, G., Beverina, F., 2006. P300-based brain computer interface: reliability and performance in healthy and paralysed participants. *Clin. Neurophysiol.* 117 (3), 531–537.
- Polikov, V.S., Tresco, P.A., Reichert, W.M., 2005. Response of brain tissue to chronically implanted neural electrodes. *J. Neurosci. Methods* 148, 1–18.
- Poulos, M., Felekitis, T., Evangelou, A., 2012. Is it possible to extract a fingerprint for early breast cancer via EEG analysis? *Med. Hypotheses* 78 (6), 711–716. <https://doi.org/10.1016/j.mehy.2012.02.016>.
- Pradhan, C., Jena, S.K., Nadar, S.R., Pradhan, N., 2012. Higher-order spectrum in understanding nonlinearity in EEG rhythms. *Comput. Math. Methods Med.* 2012,206857, 8 p<https://doi.org/10.1155/2012/206857>.
- Ramoser, H., Muller-Gerking, J., Pfurtscheller, G., 2000. Optimal spatial filtering of single trial EEG during imagined hand movement. *IEEE Trans. Rehabil. Eng.* 8, 441–446.
- Rebsamen, B., Burdet, E., Guan, C., Zhang, H., Teo, C.L., Zeng, Q., Laugier, C., Ang, M.H., 2007. Controlling a wheelchair indoors using thought. *IEEE Intel. Syst.* 22 (2), 18–24.
- Sakkalis, V., 2011. Review of advanced techniques for the estimation of brain connectivity measured with EEG/MEG. *Comput. Biol. Med.* 41 (12), 1110–1117.
- Schalk, G., Schalk, G., Kubánek, J., Miller, K.J., Anderson, N.R., Leuthardt, E.C., Ojemann, J.G., Limbrick, D., Moran, D., Gerhardt, L.A., et al., 2007. Decoding two-dimensional movement trajectories using electrocorticographic signals in humans. *J. Neural Eng.* <https://doi.org/10.1088/1741-2560/4/3/012>.
- Schlögl, A., Lee, F., Bischof, H., Pfurtscheller, G., 2005. Characterization of four-class motor imagery EEG data for the BCI-competition. *J. Neural Eng.* 2, L14–L22.
- Sellers, E.W., Donchin, E., 2006. A P300-based brain-computer interface: initial tests by ALS patients. *Clin. Neurophysiol.* 117 (3), 538–548.
- Sellers, E.W., Kübler, A., Donchin, E., 2006. Brain-computer interface research at the University of South Florida Cognitive Psychophysiology Laboratory: the P300 speller. *IEEE Trans. Neural Syst. Rehabil. Eng.* 14 (2), 221–224.
- Sharanreddy, M., Kulkarni, P.K., 2013a. Automated EEG signal analysis for identification of epilepsy seizures and brain tumour. *J. Med. Eng. Technol.* 37 (8), 511–519.
- Sharanreddy, M., Kulkarni, P.K., 2013b. Brain tumor epilepsy seizure identification using multi-wavelet transform, neural network and clinical diagnosis data. *Int. J. Comput. Appl.* 67 (2), 10–17.
- Shibasaki, H., 2008. Human brain mapping: hemodynamic response and electrophysiology. *Clin. Neurophysiol.* 119, 731–743.
- Smith, S.W., 1999. *The Scientist & Engineer's Guide to Digital Signal Processing*. California Technical Publishing.
- Spüler, M., 2017. A high-speed brain-computer interface (BCI) using dry EEG electrodes. *PLoS One* 12 (2), e0172400. <https://doi.org/10.1371/journal.pone.0172400>.
- Sreedharan, S., Sitaram, R., Paul, J.S., Kesavadas, C., 2013. Brain-computer interfaces for neurorehabilitation. *Crit. Rev. Biomed. Eng.* 41 (3), 269–279.
- Stopczynski, A., Stahlhut, C., Petersen, M.K., Larsen, J.E., Jensen, C.F., Ivanova, M.G., Andersen, T.S., Hansen, L.K., 2014. Smartphones as pocketable labs: visions for mobile brain imaging and neurofeedback. *Int. J. Psychophysiol.* 91 (1), 54–66.
- Taga, G., Homae, F., Watanabe, H., 2007. Effects of source-detector distance of near infrared spectroscopy on the measurement of the cortical hemodynamic response in infants. *NeuroImage* 38, 452–460.
- Tanaka, K., Matsunaga, K., Wang, H.O., 2005. Electroencephalogram-based control of an electric wheelchair. *IEEE Trans. Robot.* 21 (4), 762–766.
- Tangermann, M., Winkler, I., Haufe, S., Blankertz, B., 2009. Classification of artifactual ICA components. *Int. J. Bioelectromagnetism* 11 (2), 110–114.
- Teplan, M., 2002. Fundamentals of EEG measurement. *Sci. Rev.* 2, 1–11.
- Thomson, A.D., Guerrini, I., Bell, D., Drummond, C., Duka, T., Field, M., Kopelman, M., Lingford-Hughes, A., Smith, I., Wilson, K., Marshall, E.J., 2012. Alcohol-related brain damage: report from a Medical Council on Alcohol Symposium. *Alcohol Alcohol.* 47 (2), 84–91.
- Tonet, O., Marinelli, M., Citi, L., Rossini, P.M., Rossini, L., Megali, G., Dario, P., 2008. Defining brain-machine interface applications by matching interface performance with device requirements. *J. Neurosci. Methods* 167 (1), 91–104.

- Unde, S., Shriram, R., 2014. In: Coherence analysis of EEG signal using power spectral density.2014 Fourth International Conference on Communication Systems and Network Technologies (CSNT), pp. 871–874.
- van Dokkum, L.E.H., Ward, T., Laffont, I., 2015. Brain computer interfaces for neurorehabilitation – its current status as a rehabilitation strategy post-stroke. *Ann. Phys. Rehabil. Med.* 58 (1), 3–8.
- Vecchiato, G., Astolfi, L., De Vico Fallani, F., Salinari, S., Cincotti, F., Aloise, F., Mattia, D., Marciani, M.G., Bianchi, L., Soranzo, R., Babiloni, F., 2009. The study of brain activity during the observation of commercial advertising by using high resolution EEG techniques. *Conf. Proc. IEEE Eng. Med. Biol. Soc.* 2009, 57–60. <https://doi.org/10.1109/IEMBS.2009.5335045>.
- Wadeson, A., Nijholt, C.S.N., 2015. Artistic brain-computer interfaces: current state-of-art of control mechanisms. *Brain Comput. Interfaces* 2 (2), 70–75.
- Waldert, S., Pistohl, T., Braun, C., Ball, T., Aertsen, A., Mehring, C., 2009. A review on directional information in neural signals for brain-machine interfaces. *J. Physiol. Paris* 103, 244–254.
- Wang, W., Sudre, G.P., Xu, Y., Kass, R.E., Collinger, J.L., Degenhart, A.D., Bagic, A.I., Weber, D.J., 2010. Decoding and cortical source localization for intended movement direction with MEG. *J. Neurophysiol.* 104, 2451–2461.
- Wei, C.-S., Chuang, S.-W., Wang, W.-R., Ko, L.-W., Jung, T.-P., Lin, C.-T., 2011. In: Implementation of a motion sickness evaluation system based on EEG spectrum analysis.2011 IEEE International Symposium on Circuits and Systems (ISCAS), pp. 1081–1084.
- Weiskopf, N., Mathiak, K., Bock, S.W., Scharnowski, F., Veit, R., Grodd, W., Goebel, R., Birbaumer, N., 2004. Principles of a brain-computer interface (BCI) based on real-time functional magnetic resonance imaging (fMRI). *IEEE Trans. Biomed. Eng.* 51, 966–970.
- Wolpaw, J., 2003. In: Brain-Computer interfaces: signals, methods, and goals. Proceeding of 1st International IEEE EMBS Conference on Neural Engineering. vol. 1, pp. 584–585.
- Wolpaw, J.R., McFarland, D.J., 2004. Control of a two-dimensional movement signal by a noninvasive brain-computer interface in humans. *Proc. Natl. Acad. Sci. USA* 101 (51), 17849–17854.
- Wolpaw, J.R., McFarland, D.J., Neat, G.W., Forneris, C.A., 1991. An EEG-based brain-computer interface for cursor control. *Electroencephalogr. Clin. Neurophysiol.* 78 (3), 252–259.
- Wolpaw, J.R., Loeb, G.E., Allison, B.Z., Donchin, E., do Nascimento, O.F., Heetderks, W.J., Nijboer, F., Shain, W.G., Turner, J.N., 2006. BCI meeting 2005—workshop on signals and recording methods. *IEEE Trans. Neural Syst. Rehabil. Eng.* 14 (2), 138–141.
- Wriessnegger, S.C., Hackhofer, D., Muller-Putz, G.R., 2015. Classification of unconscious like/dislike decisions: first results towards a novel application for BCI technology. *Conf. Proc. IEEE Eng. Med. Biol. Soc.* 2331–2334. <https://doi.org/10.1109/EMBC.2015.7318860>.
- Xiang, L., Dezhong, Y., Wu, D., Chaoyi, L., 2007. Combining spatial filters for the classification of single-trial EEG in a finger movement task. *IEEE Trans. Biomed. Eng.* 54, 821–831.
- Yamanaka, K., Yamamoto, Y., 2010. Single-trial EEG power and phase dynamics associated with voluntary response inhibition. *J. Cogn. Neurosci.* 22 (4), 714–727.
- Yijun, W., Ruiping, W., Xiaorong, G., Bo, H., Shangkai, G., 2006. A practical VEP-based brain-computer interface. *IEEE Trans. Neural Syst. Rehabil. Eng.* 14, 234–240.
- Yuen, T.G.H., Agnew, W.F., Bullara, L.A., 1987. Tissue response to potential neuroprosthetic materials implanted subdurally. *Biomaterials* 8, 138–141.
- Zabidi, A., Mansor, W., Lee, Y.K., Fadzal, C., 2012. In: Short-time fourier transform analysis of EEG signal generated during imagined writing.2012 International Conference on System Engineering and Technology (ICSET), pp. 1–4.
- Zahr, N.M., Kaufman, K.L., Harper, C.G., 2011. Clinical and pathological features of alcohol-related brain damage. *Nat. Rev. Neurol.* 7, 284–294.

FURTHER READING

- Lowish, H., 2015. Brain computer interface on track to home. *Sci. World J.* 2015, 623896. <https://doi.org/10.1155/2015/623896>.

CHAPTER 3

Real-Time EEG Acquisition

Dipali Bansal, Rashima Mahajan

Faculty of Engineering and Technology, Manav Rachna International Institute of Research and Studies, Faridabad, India

Contents

3.1	Introduction	73
3.2	Overview of Acquisition Units	76
3.2.1	Selection Criteria in Terms of Specifications	76
3.2.2	EEG Devices	77
3.3	Development of EEG-Based BCI for Eyeblink Acquisition	87
3.3.1	Selection of EEG Acquisition Unit	88
3.3.2	EMOTIV Test Bench	89
3.3.3	Understanding European Data Format (.edf)	91
3.3.4	Experiment Design for Eyeblink Acquisition	91
3.4	Import of EEG Data Into MATLAB	95
3.4.1	Selection of EEG Signal Analysis Toolbox	95
3.4.2	Import of EEG Data Into EEGLAB Toolbox	95
3.4.3	Import of EEG Data Into MATLAB Workspace	98
3.5	Import of EEG Data Into Simulink	102
3.6	Conclusion	103
	References	103
	Further Reading	105

3.1 INTRODUCTION

Progressive research in the field of brain-computer assistive technologies provides a platform to develop high performance and robust systems to control external devices/prosthetics via neural noninvasive methods. Traditionally, electroencephalography (EEG)-based brain-computer interfaces (BCIs) were aimed towards medical application domain only. The present emerging BCI research which includes user friendly and easily wearable EEG headsets and EEG signal analysis techniques have made possible to expand the BCI application areas toward gaming, entertainment, emotion recognition, e-learning, cyber world, automation, etc. This chapter highlights a step-by-step development of EEG-based BCI for control application using eyeblink-specific neural signal acquisition. This may help to improve/restore useful life among medically challenged subjects with motor disabilities.

A variety of techniques have been proposed in the literature to develop BCIs which are based on the generation of control signals via motor imagery, voluntary movements,

visual/audio stimulation, etc. These kind of human-machine interactions possess the potential of revolutionizing areas of medical prosthetics particularly neural controlled prosthetics. Since automatic control of external devices plays a significant role in the rehabilitation process of physically weak and handicapped subjects, the necessity and significance of automatic motor task identification has grown with the rising number of human-computer interface-based applications. Researchers are successfully utilizing noninvasive real-time EEGs to develop real-world control application-based interactive BCIs.

An early research work in 1988 utilized the P300 component of brain neuro-potentials to develop a communication system to assist subjects with speech-motor disabilities. The subjects were made to concentrate on letters displayed on the flashing screen and the subsequent P300 signals were analyzed to detect the selected letter on the screen ([Farwell and Donchin, 1988](#)). A noninvasive neural interface control system to assist paralyzed patients was developed by Birbaurmer et al. in early 1990 to control the cursor on a screen of a computer. The pioneering research in 1991 produced an EEG-based system to control screen cursor with just a thought of user ([Wolpaw et al., 1991](#)). Studies were also conducted to acquire EEG signals for left and right index finger movement control followed by the movement of right foot. The associated neural responses via EEG were recorded as three bipolar EEG channel data and 56 EEG channel data ([Kalcher et al., 1996; Peters et al., 1998](#)).

The grasping action using of prosthetic hand was controlled with the single trial neural responses acquired through single EEG electrode placed over the primary motor cortex region of human scalp ([Mahmoudi and Erfanian, 2002](#)). The EEG signals were recorded from subjects with physical disabilities (subjects amputated below elbow) instead of healthy normal subjects. The major concern of this research was to discriminate the grasping and opening of designed prosthetic hand by analyzing respective EEG signals corresponding to subject's imagination. Another communication interface developed between computer and human brain translated EEG-based human neural responses successfully into control signals for the movement of subject's left and right hand ([Jia et al., 2004](#)). The signals were specifically picked up from the sensory motor area of human brain during the left- and right-hand movement imagination. These types of control interfaces provide a platform to record the brain activity of user's imagination/intent to control external devices that may include wheel chair, prosthetic hand, cursor on a screen, robotic limb, etc. The EEG-based hybrid BCIs were also developed to extract multiple control signals from acquired brain EEGs to simultaneously control the movement of cursor on screen and wheelchair ([Li and Tianyou, 2015](#)). A prosthetic hand was successfully controlled by analyzing neural motor imagery signals acquired via EEG. The electroencephalogram signals were recorded using EMOTIV neuroheadset and processed using OpenVibe software platform to identify and classify the subject's intentions. The classified neural responses were translated into operative commands to control the

prosthetic hand movement ([Elstob and Secco, 2016](#)). These developments in neuro-based rehabilitation provide the awareness that such noninvasive EEG-based BCIs for control applications can improve the lives of severely handicapped patients remarkably ([Höhne et al., 2014](#)).

The motor prosthetic control applications primarily utilize the neural activity recorded from motor cortex region of cerebrum and are found to be more intuitive ([Hatsopoulos and Donoghue, 2009](#); [Schwartz, 2004](#)). However, the identification of cortical areas other than motor cortex for development of motor prosthetics is also gaining attention these days. This may lead to development of more versatile brain-computer interfaces for control applications. The recorded neural signals contain various artifacts including eyeblink artifacts. The researchers have innovatively started utilizing these eyeblinks particularly voluntary eyeblinks to generate control signals for designing control application specific BCIs.

A virtual keyboard has been demonstrated by analyzing eyeblink-specific neural EEG signals. The control signals were generated through deliberate eyeblinks to select characters/keys of the designed virtual keyboard ([Chambayil et al., 2010](#)). Another research picked up and analyzed eyeblink-specific EEG signals to control the electric wheelchair through a wireless interface established via Bluetooth. This was designed to assist paralyzed patients by capturing the voluntary eyeblink instances from recorded brain signals via EEG ([Lin et al., 2010](#)). The developed system was interfaced with brain-assisted devices like wheel chairs having DC motors controlled by the output of designed eyeblink algorithm ([Lin et al., 2010](#)).

Numerous control applications can be designed using eyeblink-specific neural responses. The development and utilization of such BCIs can contribute significantly to improve the quality of life for paralytic patients suffering from severe motor disabilities. For example, ALS (amyotrophic lateral sclerosis) patients with dead muscle controlling neurons may successfully utilize eyeblink, eye movement, thought related neural responses to develop brain assistive devices platform to bypass their motor disabilities. Several successful EEG-based BCI systems have been developed to assist such patients who may not be able to use conventional assistive platforms to control external devices and communicate with external world.

Number of robust and cost-effective neuroheadset units has been introduced in the market to acquire EEG-specific neural responses with high resolution at desired sampling rates. To develop mobile brain-computer interfaces, size and weight of the acquisition unit is a major concern. [Section 3.2](#) provides a comparative overview of available EEG acquisition units. A high resolution but bulky and large-sized EEG acquisition system was utilized by [Íñez et al. \(2009\)](#) to develop a BCI for controlling a robotic arm successfully. The large size limits the mobility feature of BCI. A compact and user-friendly EMOTIV neuroheadset was introduced in the market to provide more flexible option for BCI development with 14-electrode assembly and a nominal data resolution.

This unit has been utilized successfully by a number of researchers to develop brain assistive technologies for control applications by merely translating the thought patterns, voluntary eyeblinks, eye movements, etc. to respective control commands. This chapter details about the various EEG acquisition units followed by development of eyeblink-specific brain-computer interface for subsequent control applications.

3.2 OVERVIEW OF ACQUISITION UNITS

Owing to enormous applications of EEG technique in areas like medicine, brain-computer interfacing, prosthetic tools, psychological analysis, neuroscience, neuro-marketing, Internet of things (IOTs), gaming, and beyond; it has become imperative to design high end, economic, reliable, and robust EEG acquisition devices. Due to escalated market demand for quality EEG units, a large number of leading manufacturers are researching and investing to cater to specific requirements of users. Companies have unique features to offer to consumers in terms of advanced sensitivity, number of channels, sampling rate, ADC bits (resolution), electrode placement, acknowledged EEG paradigms, portability, compatible analytic software and tools, and other metrics' at competitive price. Explicit application decides which EEG headset to use and therefore a comparative analysis of consumer EEG units in terms of technical specifications and price is presented in subsequent subsections by taking reference from *IMOTIONS EEG 101 Guide* (imotions.com/blog/eeg/).

3.2.1 Selection Criteria in Terms of Specifications

Selection of EEG headset depends on the number and placement of electrodes, sampling frequency required, montage, and ADC bits, that is, resolution of the signal.

Number and Placement of Electrodes: Depending on the EEG paradigms to be recorded in a particular application, a certain number of electrodes are required. Strong response comes from certain sites only; accordingly a particular product needs to be selected. As an example, Muse EEG unit does not help in acquiring Motor Imagery data as it has fixed electrodes. Instead Open BCI comes out useful as sensors can be placed as wished.

Sampling rate: Depending on the frequency of the acquired EEG data, sampling rate is generally set 2.5 times higher than base frequency of interest. The minimum conventional rate in most of the devices is 256 samples per second, but in some applications a higher sampling rate is required. For example, there are applications which need to record brain activity directly from the surface which are of the tune of 200 Hz, so in such cases EEG systems are set to a sampling rate of 480 Hz. If these sampling rates are not maintained then recovery of analog signal from digitized version may get distorted. Sampling skew is also to be looked into in EEG acquisition units to maintain accuracy. Sampling skew is a phenomenon that happens when all acquisition channels are not sampled simultaneously which leads to time lag between sampling of each channel.

To overcome this issue, burst mode sampling is used in acquisition units which raises the speed of consecutive channel's sampling and reduces the extent of sampling skew.

Montage: Montage refers to the way of connecting channel electrodes pairs to each amplifier in the brain response (EEG) acquisition unit. The standard montages are common-reference, average-reference, or bipolar derivation. In common-reference arrangement, every amplifier section captures the difference value between a scalp electrode of interest and a mentioned reference electrode. The electrode designated as reference is same for all the channel electrodes. Recordings from each and every channel electrodes are noted, summed up together and averaged in average referencing mode. The averaged value is then applied and made to pass through a connected high value resistance. The resultant acts as a reference value and is applied as a second input value to each amplifier stage in acquisition unit. In *bipolar derivation mode* electrodes are sequentially linked together generally in straight line arrangement from scalp front to the back of the scalp or the arrangement of electrodes can be in transverse mode across the scalp. EEG units can change the montage online or offline. This re-montaging is possible only if recordings are done with a common reference electrode. This makes possible displaying of data using different montages at a later instant.

ADC Bits: Analog-to-digital converter (ADC) bits helps in estimating the acquisition voltage range and is the resolution of the signal which refers to the conversion of analog voltage into digital values. For example, a 2-bit digital system having “0” and “1” as symbols can represent four different numbers (00, 01, 10, and 11). Now if a voltage input range of 0–10 V is required to be measured using 2-bit system, it has to be divided into four portions (0–2.5, 2.5–5.0, 5.0–7.5, and 7.5–10.0 V) providing a 2.5 V per bit of voltage resolution. Similarly, a digital system based on 3-bits represents 2^3 distinct voltage levels, 12-bit gives 4096 (2^{12}) levels, and a 16-bit system can represent 65,536 (2^{16}) voltage levels. More number of ADC bits, however, does not necessarily mean better acquisition quality.

3.2.2 EEG Devices

Commercially available EEG units have been categorized price range wise as follows:

Low-end units (99–1000 USD) shown in Fig. 3.1.

- Emotiv Epoc/E poc +(14 channels).
- Emotiv Insight (5 channels).
- Muse (4 channels).
- NeuroSky (1 channel).
- OpenBCI (8–16 channels).

Low cost of EEG headset is primarily due to lesser number of electrodes provided for acquiring brain signal. NeuroSky EEG headset is single channel and Muse unit is with four channels, but they still offer neurofeedback to assist meditation and sleep.

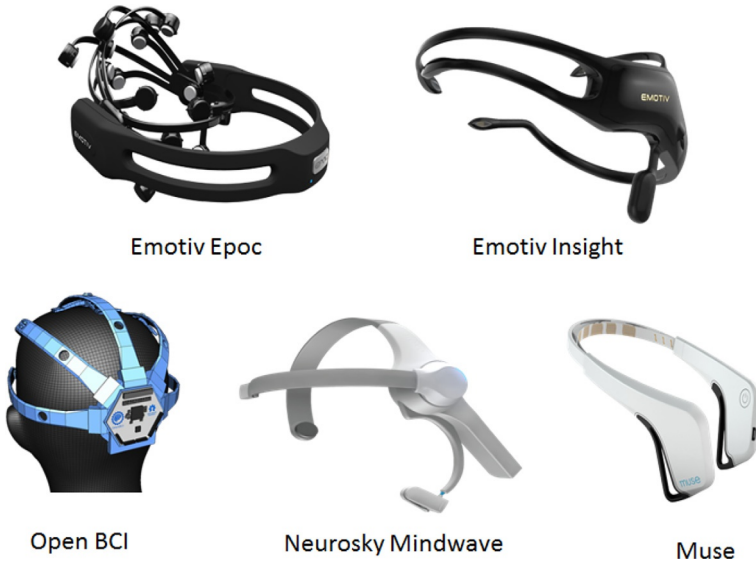


Fig. 3.1 Lower price range EEG units.

Emotiv deals in two types of electrode assemblies (5 and 14 channel), with distinct built-in hardware (including amplifiers, ADC) to improve the acquisition of brain signals and transmit wirelessly. The OpenBCI platforms being an open source present a cost-effective solution for EEG signal analysis.

Mid-end units (1000–25,000 USD) shown in Fig. 3.2 are listed as follows:

- Wearable sensing headset supports (7–24 channels).
- ANT Neuro—eegort/eego sports cap supports (8–32 channels).
- Neuro-electrics cap supports (8–32 channels).
- G.tec-Nautilus wireless acquisition unit/Nautilus PRO wireless acquisition unit supports (8–64 channels).
- BioSemi recording unit supports (16–64 channels).
- Cognionics headset supports (20–30 channels).
- mBrain Train EEG cap supports (24 channels).
- Brain products Live-Amp headset supports (32 channels).

As the number of electrodes increases, so does the price. Most of the manufacturers (Wearable Sensing, ANT Neuro, Cognionics, G.tec, mBrainTrain, Neuroelectrics, Brain Products LiveAmp, and BioSemi) offer wireless solutions in mid-price range, enabling increased mobility and comfort. In most cases, EEG data can be collected without the use of conductive gel thus reducing acquisition time. The number of channels available has a wider range up to 64 electrodes and has a flexible system. These units are supported by well-articulated and validated metrics that offer rapid and valuable insight into the cognitive state of brain.

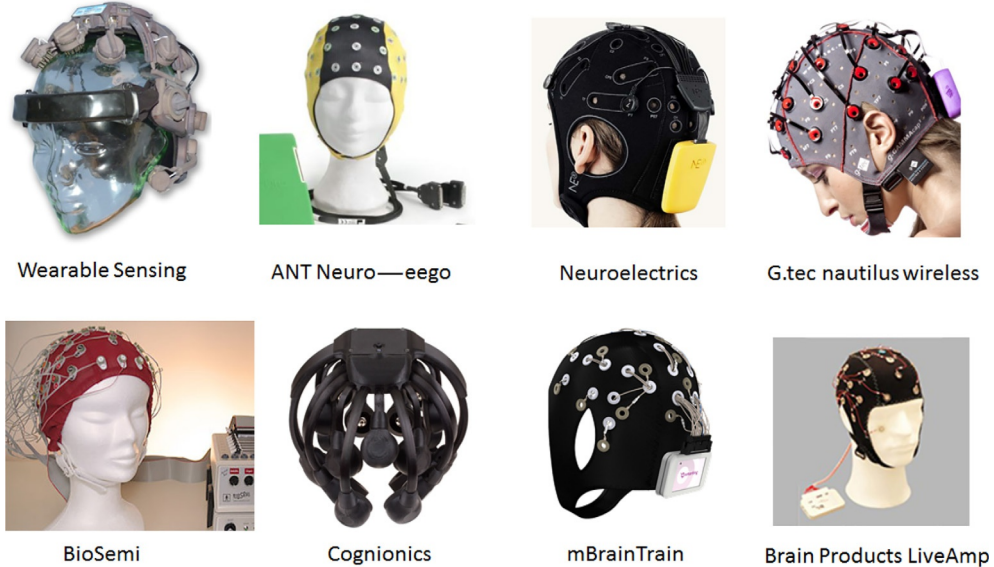


Fig. 3.2 Middle price range EEG units.

High-end units (25,000+ USD)

- ANT Neuro—eego/eego sports unit (64 channels).
- ANT Neuro—eegomylab unit (32–256 channels).
- Brain Products actiCHamp unit (32–160 channels).
- BioSemi unit (32–256 channels).

Large number of electrode channels is offered in this range thus enabling high-resolution EEG signal acquisition. The range starts at 32 and goes up to 160 in actiCHamp (Brain Product), 256 channels in BioSemi, 64 channels in ANT Neuro going up to 256 electrodes.

3.2.2.1 Emotive EPOC/EPOC + Headset

One of the most user friendly, popular, and initially available commercial Neuroheadset is Emotiv EPOC (www.emotiv.com/epoch/). It is a high resolution, 14 channel portable unit, cost effective, and has an easy development platform that comes with proprietary software and so is the most widely used EEG unit for DIY projects. It allows real-time analysis of brain data. Features and technical specifications are listed in the following and in [Table 3.1](#).

Features

- possess stylish and user friendly easy-to-set flexible design
- supports wireless transmission

Table 3.1 Technical specifications of EEG Emotiv EPOC headset (www.emotiv.com/epoc/)

Technical specifications	EEG Emotiv EPOC headset
Number of channels	14
Reference electrodes	CMS/DRL at P3/P4 sites
Electrode placement	AF3, F7, F3, FC5, T7, P7, O1, O2, P8, T8, FC6, F4, F8, AF4
Sampling technique	Sequential; single ADC 14/16 bits
Sampling rate	128 or 256 samples per second (2048 Hz internal)
Bandwidth allowed	0.2–45 Hz
Power-line removal	Digital-notch filters: 50 Hz, 60 Hz
Filters	Digital sinc filter; fifth order
Coupling mode	AC coupled
Battery	Lithium polymer, 680 mAh, life: 12 h typical
Frequency response	0.16–43 Hz
Least significant bit resolution	0.51 μV at 14 bit/0.13 μV at 16 bit
Dynamic amplitude range	± 4.17 mV
Connectivity	Wireless 2.4 GHz (USB reception dongle)
Recordable EEG paradigms	Variety of Facial expression/activities
Compatibility	Windows, OSX, Linux, Android, and iOS

- high spatial resolution to ensure complete neuro analysis
- wet electrodes using saline solution
- able to capture and provide raw EEG dataset
- allows real-time analytics
- access performance metrics, able to capture human emotion states, thought-based commands and facial activity
- possess ability to provide feedback in real-time mode and can be used for neuro-marketing applications
- allows adaptive interfaces in real time
- better interpretation due to artificial intelligence

Emotiv EPOC+

Emotiv EPOC+ is the most credible award winning and cost-effective EEG headset available in the market offering high resolution and full spatial resolution for contextual research and progressive innovations in BCI applications. Its features are all similar to Emotiv EPOC. This headset can connect wirelessly to computers, tablets, and smart phones. The system requirements for various platforms are

- Windows: Intel Pentium G (or equivalent); MS windows 7, 8, or 10; 2 GB RAM; 200 MB disk space; 2.0 USB ports.
- MAC: OS (10.11.x, 10.12.x); 2 GB RAM; 500 MB Hard-disk; 2.0 USB ports.
- Linux: Intel Pentium G; Ubuntu version 16.04 or recent upgraded versions, Fedora v 20; with 2GB RAM; hard-disk 200 MB; 2.0 USB ports.

- Android: OS: Android 4.3.4+; Bluetooth SMART functionality; USB-OTG functions implementing HID host Mode.
 - iOS 9.0 and higher, iPhone 5 and above, iPod Touch 6, iPad 3 or later, iPad mini.

3.2.2.2 Emotiv Insight

Emotiv Insight was the second invention launched into the market by Emotiv to cater to everyday need of monitoring cognitive health at an affordable price. Supported by intensive research and experience, Emotiv Insight has come out as the next-gen EEG headset. It is 5 sensors +2 reference sensors wireless EEG Unit equipped with advanced technology that gives optimized, robust, and noise-free meaningful signal. The features of EEG Emotiv Insight are highlighted in the following and [Table 3.2](#) enlists the respective technical specifications (www.emotiv.com/epoc/):

Features

- sophisticated, light in weight, instinctive, and has ergonomic design
 - delivers high spatial resolution ensuring deeper insight into brain signal
 - permits real-time simulations of brain patterns
 - hydrophilic polymer bioSensor—wireless connectivity to phone, tablet, and PC
 - comes with motion sensors for recording of head location and movements precisely
 - capable to provide raw EEG stream of data and comes with proprietary software
 - permits multiple degrees of freedom for control applications

Table 3.2 Technical specifications of EEG Emotiv Insight

Technical specifications	EEG Emotiv Insight
Number of channels	Five
Reference channels	CMS/DRL in noise cancellation configuration
Electrode placement	AF3, AF4, T7, T8, Pz
Sampling technique	15 bits
Sampling rate	128 samples per second per channel
Bandwidth	0.2–45 Hz
Power-line removal	Digital notch filters: 50 Hz and 60 Hz
Filters	Digital sinc filter; fifth order
Coupling mode	AC coupled
Battery	Lithium polymer, 480 mAh, life: 08 h typical
Frequency response	0.5–43 Hz
Least significant bit resolution	0.51 µV at 14 bit
Dynamic range	±4.17 mV
Connectivity	2.4 GHz wireless USB dongle
Recordable EEG paradigms	Facial expression
Compatibility	Windows, OSX, Linux, Android, and iOS

- allows performance metrics, capturing emotion states, mental states, and facial expressions
- covers all prime areas of the scalp. It captures activity in frontal region (decision-making functions), the parietal-temporal cortex (auditory, spatial/coordination), and the parietal-occipital cortex (visual). This enables insight into emotional states, mental activity, and memory processing
- advanced algorithm enables modeling of brain regions

MyEmotiv is a latest and advanced version of Emotiv Insight App and is a companion to Emotiv Insight and EPOC + EEG acquisition Neuroheadsets.

Features

- acquire, record, save, and playback recordings of neural activities
- Quantifies 6 prime cognitive and emotional metrics: focus, stress, excitement, relaxation, interest, and engagement
- helps exploration in real time with three-dimensional (3D) BrainViz viewer
- allows comparison with previous sessions and the Emotiv community
- monitors routine life to improve focus and manage stress
- compatibility with operating system iOS 9.0 and higher. Recommended devices: iPhone 5 and above, iPod Touch 6

3.2.2.3 Muse

Muse is an EEG device which makes meditation easy and elevates the experience. It gradually escorts meditation through changing soundscapes based on user's real-time state of mind. This results in deeper sense of focus, motivates, and helps in reducing symptoms associated with stress, depression, and anxiety and enhances quality of life. It has exercises recommended by meditation experts to benefit one's learning.

Features

- number of channels are four with one reference and two ground electrodes
- static electrode placement is at AF7 and AF8 sites
- sampling rate set is 256 Hz
- assists in focused meditation
- primary soundscapes available are Beach, Rainforest, Desert
- sets milestones and gives reward points for self-motivation
- creates multiple accounts and allows sharing with family and friends
- provides analytics and measures progress
- dry electrodes
- compatible with Windows, Mac, Linux, Android, IOS
- recordable EEG paradigms are relaxation and concentration levels, frontal asymmetry, P300

3.2.2.4 OpenBCI

The Open BCI is an open-source EEG headset unit that has a maximum of 16 channels and 4 channel system also which is available at a cheaper rate. It was designed as a 2013 Kick starter project, but has stretched to include an open-source 3D printed cap.

Features

- allows flexible electrode placement
- comes with both dry and wet electrodes
- sampling rate is set to 256Hz
- channel resolution is 24 bits
- high gain low noise ADC
- has eight biopotential input channels: EEG, EMG, and ECG (inverted common mode noise)
- Arduino compatible (5 GPIO pins)
- wireless communication: RF Digital RFD 22301, bluetooth low energy (BLE), high data rate radio via USB
- high-powered analog front end
- three-axes accelerometer (16 bit data output)
- Open-source software and hardware
- can record any EEG paradigm which needs only 16 channels or less

3.2.2.5 Neurosky Mindwave

Neurosky Mindwave is a single channel simple and affordable EEG acquisition unit that permits easy-to-perceive brain signals. The EEG biosensor technology used provides crisp inputs for distinct applications that give health and wellness, educational, and research inputs for varied control applications. It can be categorized as a high-performance physiological signal acquisition and analysis solution via single chip for precise brain signal acquisition and subsequent processing. Products for EEG acquisition made available by Neurosky are TGAT1/TGAM1 and TGAT2 (<http://neurosky.com/biosensors/eeg-sensor/>).

Features of TGAT1/TGAM1

- direct connect: dry electrode
- rigid electrode placement at AFz
- advanced filter with high noise immunity
- sampling rate 512Hz
- resolution: 12 bits
- bandwidth: 3–100Hz
- recordable EEG paradigms: raw EEG dataset while performing distinct activities

Features of TGAT2

- wider bandwidth: 0.5–100 Hz
- better common mode rejection ratio for noise reduction compact size
- very high ADC resolution of 16 bits

3.2.2.6 Wearable Sensing

Wearable sensing's product DSI-24 is a wireless and portable research-grade headset unit that allows high-quality brain data acquisition via EEG and has made various applications possible in real-time settings. It can be worn comfortably for almost 8 h and starts recording EEG signal in <5 min. The salient features of wearable sensing EEG Headset are listed in the following and technical specifications are tabulated in **Table 3.3** (<http://www.wearablesensing.com/DSI24.php>).

Features

- 21 electrode positioning as per the standard 10–20 International System
- battery: lithium ion
- dry electrode sensors capable to capture continuous EEG/EMG/ECG data, enables long-term recording and monitoring
- no requirement of applying gel to electrodes

Table 3.3 Technical specifications of wearable sensing EEG headset

Technical specifications Wearable sensing EEG headset (DSI-24)

Number of channels	Twenty electrodes positioned as per International 10/20 System
Electrode placement	Fp1, Fp2, Fz, F3, F4, F7, F8, Cz, C3, C4, T3, T4, T5, T6, P3, P4, O1, O2, A1, and A2
Common mode voltage follower	Pz sensor as voltage follower
Ground electrode	One ground electrode is provided at Fpz
Amplifier/digitizer	A 24 channel amplifier/digitizer
Sampling frequency	300 Hz
Run-time	>Continuous (hot-swappable batteries)
Bandwidth	0.003–150 Hz
Digital input	Eight bit digital input
Analog-to-digital converter	ADC with 16-bit resolution
Analog/Digital resolution:	0.317 μ V with respect to input
Gain	60
Common mode rejection ratio	>120 dB
Maximum input range	10 mV peak to peak
Noise (1–50 Hz)	<3 μ V peak to peak

- possess both online and offline signal analysis
- enables cognitive state analysis and identification in quantitative mode
- wireless transmission mode (range 10m) to transmit acquired signal data to interfaced machine
- proprietary software provides efficient learning algorithms capable enough to interpret acquired data

3.2.2.7 Ant Neuro (*eegomylab*)

Eegomylab is a product sensibly planned by Ant Neuro to attend to the needs of present researchers. It allows recordings from 32 to 256 EEG channels and offers flexibility of splitting into different 64 channel mobile units for individual applications. *It provides high-speed data at a sampling rate of up to 16kHz so that no information is lost.* The amplifier system has ultrahigh input impedance of $1\text{ G}\Omega$, preparation time is less for acquisition so the quality of recordings is optimized. It is ideal for recording EEG paradigms, such as (SS) VEP, AEP, MMN, P300. Third-party devices can be synced through the 8-bit TTL trigger input port.

Eego mylab comes with loads of software options designed for spontaneous performance. It can be used in combination with a shielded waveguard cap thus allowing recording of high-quality EEG even in adverse conditions when access to shielded rooms is not available. Shielded wave guard protects brain signal from getting corrupted by 50/60Hz noise interference and reduces the need of additional preamplifiers at the cap.

3.2.2.8 Neuroelectrics (*Enobio 32*)

Neuroelectrics is a *brain health corporation* that assists in researching, diagnosing, and treating brain disorders. Enobio 32 is a Neuroelectric's product which captures high-density EEG signal. It has an integrated user interface, spectrogram and allows 3D visualization of spectral data in real time. The important features of Enobio 32 acquisition unit (www.neuroelectrics.com/products/enobio/enobio-32/) are listed in the following and Table 3.4 highlights the respective technical specifications.

Features

- excellent S/N ratio, wide dynamic range available
- records EEG in frequency subbands (delta; theta; alpha; beta; gamma)
- collects 100S/s triaxial accelerometer recording simultaneously with brain EEG
- begins recording in <5 min
- wireless, lightweight, comfortable, and rechargeable system
- able to record EEG data in "Holter" mode
- headset cap available for both kids and adults
- compatible with real-time data in Matlab using MatNIC toolkit

Table 3.4 Technical specifications of neuroelectrics (Enobio 32) EEG headset

Technical specifications	Neuroelectrics (Enobio 32) EEG headset
Number of channels	32
Sampling technique	24 bits
Sampling rate	500 SPS
Bandwidth	0 (DC) to 125 Hz
Output	European data format, raw EEG data, ASCII
Battery	Lithium Ion, 14 h typical
Input impedance	1 GΩ
LSB resolution	0.05 μV at 24 bit
Measurement noise	<1 μV RMS
Connectivity	Bluetooth 2.1
Recordable EEG paradigms	Motor imagery ERD, SSVEP and P300, neuromodulation, user affective state, biometry
Compatibility	Windows seven, eight, and Mac-OS-X, Mat-NIC toolbox available for networked device control, neuroelectrics NUBE cloud

3.2.2.9 Brain Products': LiveAmp (32 channels)

LiveAmp is Brain Products' innovative compact wearable solution for superior quality mobile wireless EEG acquisition. It is widely used for *sports research*, *sleep research*, *cognitive states research* or for analysis of workload under realistic circumstances, or while performing complicated tasks (e.g., piloting a jet fighter). The various technical specifications of LiveAmp (32 channels) headset (<http://www.brainproducts.com/productdetails.php?id=63>) are provided in Table 3.5.

3.2.2.10 Brain Products: ActiChamp

Brain products actiChamp is an innovative change that allows measurement of human electrophysiological parameters in a user friendly and affordable manner. It is a 24-bit unit with up to 160 channels for EEG measurement. The features of this unit are listed in the following and Table 3.6 highlights the major technical specifications (www.brainvision.com/actichamp.html).

Features

- 24-bit, active channel unit with actiCAP electrodes
- availability in 32, 64, 96, 128, and 168 EEG channel assembly
- complete range of bio-signal sensors for distinct measurements
- possess high sampling frequency (range up to 100 kHz) and provides a wide bandwidth range
- provision for increasing number of channels
- compatible with certain open-source recorders to acquire brain signals

Table 3.5 Technical specifications of LiveAmp (32 channels)

Technical specifications	Brain Products': LiveAmp (32 channels)
Number of channels	32 unipolar channels or 24 unipolar and 8 bipolar channels
Resolution	24 bits
Sampling rate	1000 Hz
Low pass filters	Third-order sinc filter with –3 dB frequency depending on the sample rate: 1000 Hz: 262 Hz; 500Hz: 131 Hz; 250 Hz: 65 Hz
Gain factor	12
Battery	Built-in rechargeable battery, capacity: 1000 mAh
Resolution	40.7 nV/bit
Dynamic range	±341.6 mV
Input noise	<2 µVpp (0.01 Hz to 65 Hz at 250 Hz sample rate)
Connectivity	In 2.402–2.480 GHz ISM band
Compatibility	Windows 7, 32- and 64-bit, Windows 8.1, 64-bit, Windows 10, Software: BrainVision Recorder as of version 1.21.0001.NET 4

Table 3.6 Technical specifications of Brain Products: ActiChamp

Technical specifications	Brain Products: ActiChamp
Number of electrodes per unit	32
Maximum number of electrodes	160
Bandwidth	DC–20 kHz
ADC bits	24 bits
Input noise	2 µVpp (0.1–30 Hz)
Dynamic range	0–100 kΩ
Input voltage range	±409 mV
Resolution	0.0487 µV per bit
Common-mode rejection (CMR)	>100 dB
Power supply	External battery (actiPOWER)
Maximum sampling rate	100 kHz
Battery	Lead accumulator

3.3 DEVELOPMENT OF EEG-BASED BCI FOR EYEBLINK ACQUISITION

The primary procedure to develop an efficient BCI for control applications includes the selection of efficient and reliable evoking techniques for the generation of neural-specific control signals. As stated in the literature, evoking procedure may include motor imagery, eye movement, voluntary eyeblink, etc. The aim of study included in this chapter is to develop an EEG-based BCI system for eyeblink acquisition and subsequent control application that could facilitate rehabilitation of physical disabled/paralytic patients. Therefore, the motor task to be performed for the above-stated study is deliberate

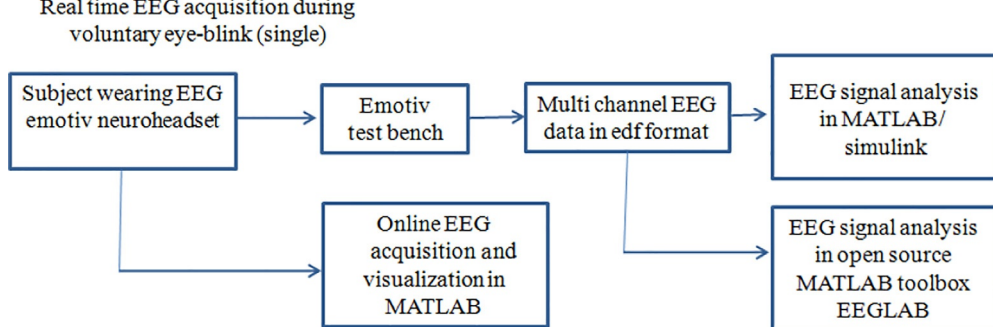


Fig. 3.3 Framework to develop EEG-based BCI to acquire real-time EEG during voluntary eyeblink.

eyeblink. This system shall include a stage for EEG signal acquisition in real time, EEG signal preprocessing and analysis in real-time online and off-line mode followed by translation of extracted feature set from signal analysis into device control commands for designed application as depicted in Fig. 3.3. This whole framework is designed to discriminate the deliberate single eyeblink instant from normal relaxed state.

3.3.1 Selection of EEG Acquisition Unit

Based on the analysis of neuroheadsets for EEG signal acquisition as detailed in Section 3.2, the unit selected to acquire real-time raw EEG recordings is EMOTIV neuroheadset (<https://www.emotiv.com>). This cost-effective commercial unit is available with 14-electrodes to capture the real-time EEG signals over the scalp. It provides an acceptable compromise between cost and overall efficiency including 16-bit resolution, sequential sampling and 0.2–45 Hz of selective bandwidth. The set of 14-electrodes include frontal electrodes (AF3, AF4, F7, F8, F3, F4, FC5, FC6); temporal electrodes (T7, T8); parietal electrodes (P7, P8); and occipital electrodes (O1, O2) as shown in Fig. 3.4. The two reference electrodes (CMS and DRL) are also provided to adjust and position the headset electrodes appropriately for correct operation of headset. These reference electrodes are placed on the scalp bone at neck interface just behind the left and right ear lobe. The two front electrodes AF3 and AF4 are placed around the height of three fingers above the eyebrows to ensure the proper positioning of neuroheadset. Each of the EEG channel location is set according to the international 10–20 electrode system to cover all scalp regions evenly as explained in Fig. 2.2.

The EMOTIV neuroheadset acquires EEG data by sampling it at 128 Hz. This unit captures subject's brain responses, converts to digital format, processes for necessary amplification and filtering, and transmits wirelessly to interfaced computer through USB receiver. A software development kit (SDK) is provided with EMOTIV headset unit

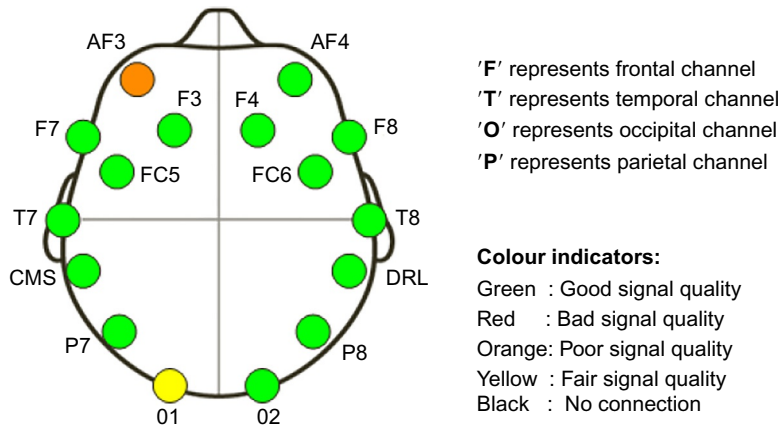


Fig. 3.4 Channels of EMOTIV neuro-headset unit.

to acquire raw EEG data from this neuroheadset device. This raw EEG data are transmitted by the unit in the form of encrypted data packets. These data packets are picked up by EMOTIV test bench software installed at interfaced computer. On reception, these packets are decrypted to automatically display each sampled data point over 14-EEG locations on the graphical user interface (GUI).

3.3.2 EMOTIV Test Bench

The test bench application provided with EMOTIV headset collects and displays the real-time multichannel EEG data packets through USB receiver as shown in Fig. 3.5. Along with real-time visualization of 14-channel EEG data, this proprietary test bench software also provides the provision to record these time-specific EEG signals for further offline analysis and playback in .edf (European data format). An .edf to .csv (comma separated values) format converter is also included to provide and store EEG data in .csv format. The important features of EMOTIV test bench are listed as follows:

- Test bench provides a real-time EEG signal display window with a rolling time of 5 s.
- The status pane at the left panel of test bench setup screen (Fig. 3.5) indicates the quality of electrode-scalp contact status. Saline is applied on the electrodes before using to ensure proper contact for the best quality signal acquisition. The change of sensor's color from red to green indicates the good quality contact as depicted in Fig. 3.4. Thus, provides an efficient calibration system using an interactive GUI.
- It also facilitates the inclusion of real time and playback mode timed markers into the incoming acquired real-time EEG data stream. The setting of markers ensures the synchronized neural activity with specific performed task.

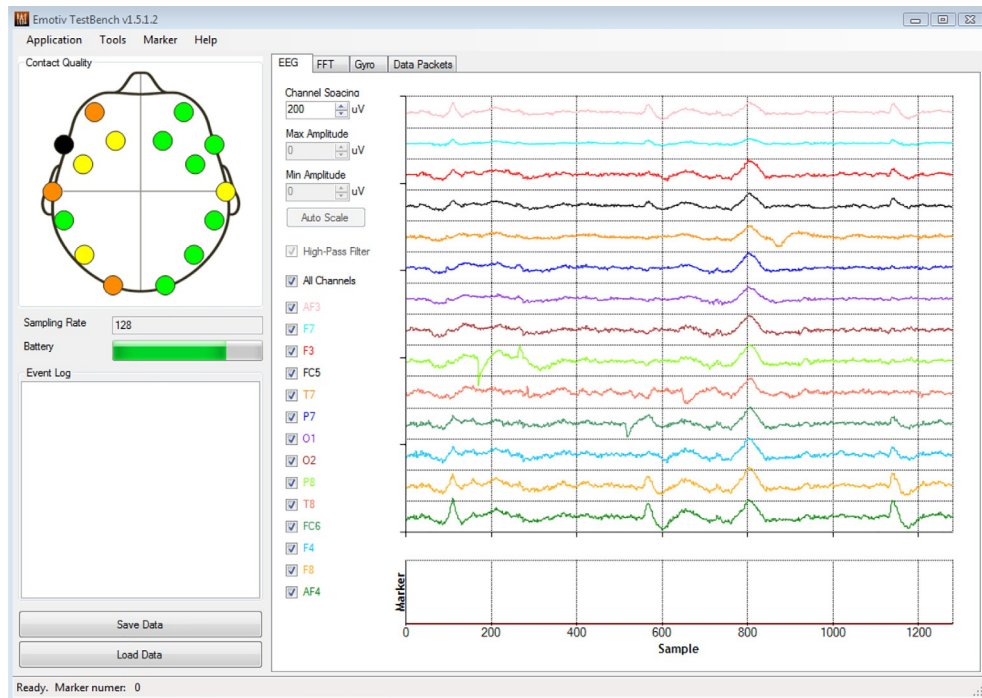


Fig. 3.5 EMOTIV test bench.

- The number of channels on the right panel of EMOTIV test bench can be selected for single/multichannel real-time EEG signal acquisition as per the selected application.
- An inbuilt high-pass filter with cut-off frequency 0.16 Hz is provided to adjust DC offset values and correct baseline by rejecting the background spurious signals.
- Able to display power and amplitude calculation in both volts and decibel mode.
- It also incorporates the FFT (fast Fourier transform) suite to display power spectrum (graph between powers in decibel versus frequency in Hertz) of the selected channel in real time.
- Power level of incoming EEG signal in the specific EEG frequency subbands (delta, theta, alpha, and beta) is displayed using customized EEG subband histogram display.
- A facility to select the type of FFT filter window (Hamming, Hanning, Blackman, rectangle, etc.) and length of samples required to obtain FFT is also included. The tapered window functions are usually selected to remove the warping artifacts which may otherwise induce noise in the resulting power spectrum.
- Data packet display with a rolling time of 5 s is provided to indicate the count of lost data packets while wireless EEG signal transmission via Bluetooth USB dongle.

3.3.3 Understanding European Data Format (.edf)

The EMOTIV unit acquires EEG signals in standard binary format known as European data format (.edf) which came into existence in 1992. It is used extensively for efficient exchange of multichannel electrophysiological data. A single data file in .edf includes one uninterrupted/continuous digitized EEG recording. Each data file contains header information followed by a single or multiple EEG data records. Each header includes general subject details (subject identification, start date and time, number of records, duration of records, etc.) and technical details of each recorded EEG signals (sampling rate, calibration, filter specifications, channel names, electrode types, etc.). The data file includes successive fixed duration samples (epochs) of EEG recording acquired at each scalp channel.

The sampling rate of EMOTIV neuroheadset with 14-channel assembly is 128 kHz. This indicates that for 1-s time slice of data there will be 128 samples. Therefore, each data file will incorporate 128 rows for 128 data samples and each row will show data slice corresponding to 1/128 s time. Each column of the acquired data file corresponds to the signal values of an individual channel location. All the 14-channel information is incorporated by 14 columns of each data file.

3.3.4 Experiment Design for Eyeblink Acquisition

This section details the experiment protocol followed and technical details to implement a noninvasive BCI via EEG signal acquisition for developing neuro assistive control applications. The experiments to capture cerebral activities of a subject related to deliberate eyeblink have been designed and presented. Two frameworks have been discussed to acquire the required neural signals:

- First framework discusses the acquisition of real-time EEG signals using EMOTIV test bench. The acquired brain patterns in .edf format are ready to be analyzed in off-line mode. This is done by importing neural signals into MATLAB workspace by developing required algorithmic solutions as well as by utilizing any available open-source brain mapping toolbox of MATLAB.
- The second cognitive framework is based on the online analysis and processing of real-time EEG feed acquired directly in MATLAB using Bluetooth-enabled USB receiver supporting transmission/reception at 2.4 GHz wireless band of IEEE802.11b/g standards.

As per the previous studies in brain-computer interfacing, the motor cortex region is responsible for generating the neural signals corresponding to any voluntary motor movement/task ([Hatsopoulos and Donoghue, 2009](#); [Schwartz, 2004](#)). The motor cortex region is located in the frontal lobe of cerebral cortex as depicted in Fig. 1.3. To develop control application, the motor task to be performed in this study is deliberate single eyeblink. Based on the above discussion, the hypothesis of this study is that the frontal channels shall contribute more toward the acquisition of neural responses responding to

deliberate eyeblink. The proposed frameworks shall be implemented to verify the stated hypothesis for eyeblink-related study presented here.

3.3.4.1 Acquisition of EEG Signals Using EMOTIV Test Bench

Real-time EEG recordings have been obtained from subjects (mean age 30 ± 8 years) who volunteered for this study. All the participants were healthy and reported to be under no effect of any neurological illness or medicine prior to the test to design a baseline BCI system. Extra care was taken to ensure that no source of electromagnetic interference was present in the environment. The participants were briefed about the experiment and the type of neural responses to be recorded. It has been explained that single eyeblink-based BCI system is to be designed and whole framework has been discussed. The voluntary eyeblink-related EEG database was constructed according to the experiment protocol explained in Fig. 3.6.

Each trial started and terminated with the subject in relaxed state for 5 s. All the subjects were instructed to perform no eyeblink during this instant. This relaxed state phase is recorded to have a baseline EEG to identify the instant of eyeblink during analysis. The following steps were followed during conduct of the experiment:

- Initially, a subject was directed to sit in a relaxed state of mind to record a baseline EEG signal for first 5 s.
- At $t = 5$ s, a “start” marker was sent manually and a subject was instructed to perform a voluntary single eyeblink.

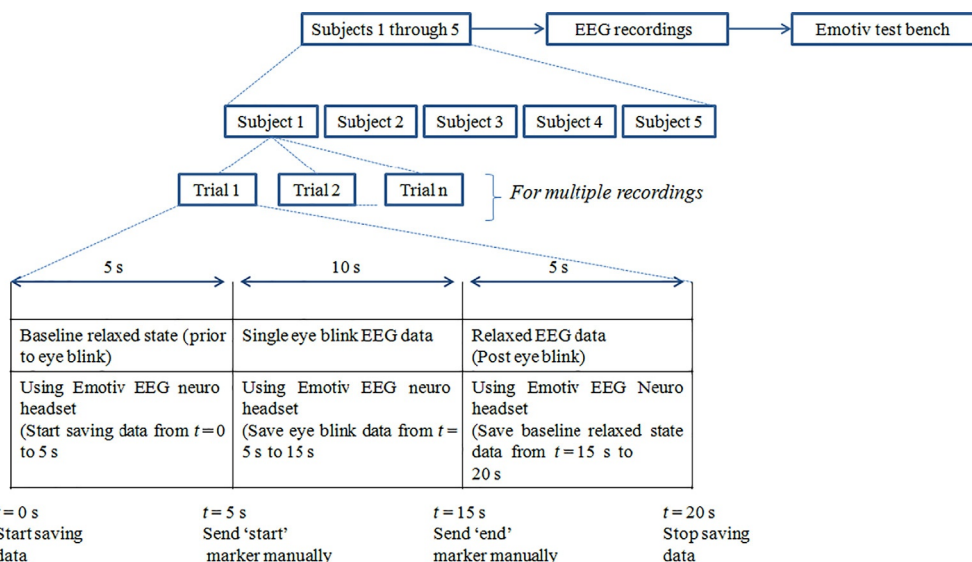


Fig. 3.6 Experiment protocol for Eyeblink acquisition (single).

- Another marker “stop” was sent at $t=15\text{ s}$ indicating an eyeblink activity was performed during this duration of $t=5$ to $t=15\text{ s}$.
- This was followed by capturing EEG signal recording for next 5 s during normal relaxed baseline state.

Multiple recordings were attained to prepare a robust database of single eyeblink-specific EEG responses with each record of 20 s duration. Each 20-s multichannel EEG records acquired by 14-scalp electrodes of EMOTIV neuroheadset were transmitted to receiver laptop through a Bluetooth USB and were displayed on test bench software. These records were saved in .edf file for further analysis in time and frequency domain to identify the performed eyeblink activity. The whole step-by-step procedure has been depicted in Fig. 3.7.

3.3.4.2 Acquisition of Online EEG Signals Directly in MATLAB

The real-time multichannel online EEG data feed can be directly received in MATLAB instead of acquiring EEG responses using EMOTIV test bench and then importing it for off-line analysis. The live EEG signal acquisition may limit the possibility of information loss which otherwise may occur while storing neural responses in database through test bench. It also facilitates live EEG signal visualization and analysis without any delay. Such online BCI systems could assist paralyzed patients efficiently and can be developed as a promising tool to

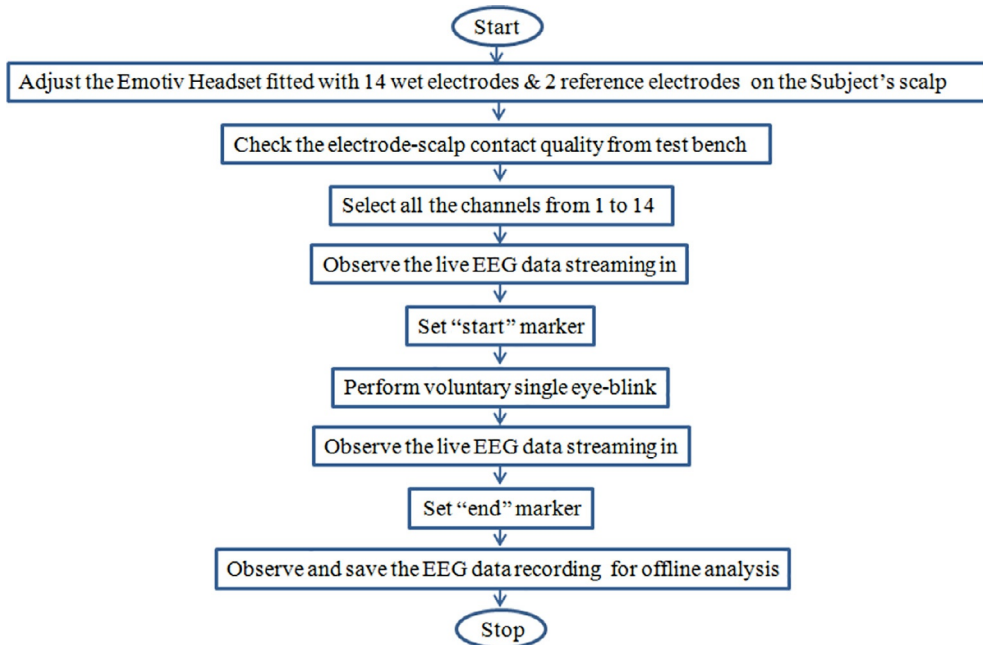


Fig. 3.7 Procedure to acquire EEG signals using EMOTIV test bench.

aid medical prosthetics. It can be implemented using customized application program interface along with an EEG acquisition device EMOTIV EEG unit. The acquired data can be analyzed by developing efficient physiological signal processing algorithms to understand the related neural pattern dynamics. The online EEG acquisition and display system is capable to overcome the limitations of proprietary test bench-based application interface software provided with EMOTIV unit. It utilizes the EDK library of EmotivEEG headset toolbox to display the acquired EEG responses in real time and for subsequent storage. To design any real-time application utilizing live EEG feed from acquisition unit, certain Emotiv dynamic linked library files (edk.dll, edk_utils.dll) are required along with header files EmoStateDLL.h, edk.h, edkErrorCode.h, and mat file EmotivEEG.m. The steps to acquire online brain responses directly in MATLAB environment are listed as follows (<https://in.mathworks.com/matlabcentral/fileexchange/36111-emotiveeg-headset-toolbox>):

- Download open-source MATLAB-based neuroheadset toolbox in directory1: EmotivEEG.
- Add the following Emotiv research edition files in directory1:
 - i. edk.dll
 - ii. edk_utils.dll
 - iii. EmoStateDLL.h
 - iv. edk.h
 - v. edkErrorCode.h
- Add this directory1 to the MATLAB toolbox directory.
- Switch on the headset unit with 14-electrode assembly and position it well over subject's scalp as discussed in [Section 3.3.1](#).
- Connect the Bluetooth-enabled USB dongle to wirelessly transmit acquired EEG signals to interfaced computer.
- Open MATLAB software.
- Write the following command into command line window of MATLAB to initiate the application programming interface "EmotivEEG":
`>>help EmotivEEG`
- Create the object to acquire online EEG data as following:
`>>x=EmotivEEG`
- Set sampling frequency, acquisition time, time period and plot time period.
- Acquire latest EEG data continuously in real-time mode using following command:
`>>x.Run`
- The online acquired EEG data values can be plotted using a command:
`>>x.Plot`
- The online feed can also be recorded and saved in a .mat file for future offline analysis using a command:
`>>x.Record(50)`. It will record 50s of EEG data
- The created library can be disconnected and unloaded as follows:
`>>delete (x)`

The continuous EEG data feed can be obtained in MATLAB environment by creating an input object to first set up a connection between Emotiv acquisition unit and MATLAB. The established connection will start to acquire single eyeblink-specific neural data. This online data feed can be analyzed in time/frequency domain to understand the associated EEG dynamics and extract the discriminative feature set. The related feature set can be translated into command signals to develop a relevant brain-assisted control application. Once the required task-specific brain data are attained and analyzed, the signal acquisition is terminated and associated memory space in MATLAB is cleared.

3.4 IMPORT OF EEG DATA INTO MATLAB

The acquired multichannel single eyeblink-specific EEG data using EMOTIV test bench has been imported to MATLAB for further analysis. The scripts can be written in MATLAB workspace to load and analyze EEG data or available brain mapping toolboxes could be used as well for subsequent signal analysis.

3.4.1 Selection of EEG Signal Analysis Toolbox

To start the whole development step by step, the first task is to enlist and review the available open-source toolboxes for brain pattern analysis via EEG. A variety of EEG-based brain mapping toolboxes is available, viz., OpenVibe ([Renard et al., 2010](#)), BioSig ([Vidaurre et al., 2011](#)), FieldTrip ([Oostenveld et al., 2011](#)), LIMOESEG ([Pernet et al., 2011](#)), PyEEG ([Bao et al., 2011](#)), BCILAB ([Schalk et al., 2004](#)), EEGLAB ([Delorme and Makeig, 2004](#)), eConnectome ([He et al., 2011](#)), and EEGNET ([Hassan et al., 2015](#)). [Table 3.7](#) provides a comprehensive comparative summary of all the above available EEG signal processing toolboxes.

As clear from the detailed analysis, the EEGLAB: open-source software provides an interactive platform with a rich set of functions to import, preprocess, and analyze acquired EEG responses. Therefore, EEGLAB toolbox has been selected to analyze and map single eyeblink-related brain signals.

3.4.2 Import of EEG Data Into EEGLAB Toolbox

The recorded single eyeblink-specific EEG data is imported to EEGLAB toolbox for subsequent analysis and development of designed control application. The following steps are followed to load acquired brain responses into EEGLAB toolbox using Windows platform ([Delorme and Makeig, 2004](#)):

- Download and install latest version of open-source MATLAB-based toolbox eeglab.
- Start MATLAB and write “`>>eeglab`” in the command line window: A eeglab main window will appear as shown in [Fig. 3.8A](#).

Table 3.7 EEG signal processing toolboxes

EEG signal processing toolbox	Implementation software	Features
OpenVIBE	C++	<ul style="list-style-type: none"> Provides an online signal processing platform to load, preprocess, analyze and classify EEG signals Also supports signal classification after extracting suitable set of features
BioSig	C/C++, MATLAB/ Octave	<ul style="list-style-type: none"> Possess the capability to accept EEG signals in distinct data formats for subsequent signal visualization and analysis in time domain, frequency domain and hybrid time-frequency domain Supports efficient EEG signal classification using extracted feature set in both (time and frequency transformations) including common spatial pattern and blind source-based separation
FieldTrip	MATLAB	<ul style="list-style-type: none"> Does not provide any interactive GUI rather available with an interactive environment to work directly with MATLAB scripts and functions Rich platform of high- and low-level MATLAB functions required to analyze averaged potential distribution across entire scalp regions followed by EEG spectral analysis in online and offline mode as per the requirement
LIMO EEG	MATLAB	<ul style="list-style-type: none"> Provision for robust statistical signal analysis till second level with maximum statistics and parametric tests is available for one and two-dimensional temporal clustering analysis Evoked event-related potentials over all scalp regions can be analyzed in all time and space dimensions
PyEEG	Python	<ul style="list-style-type: none"> Wide feature space is available including a set of nonlinear features along for EEG signal analysis and feature vector mapping in both real and complex domain Being an open-source platform, suffers with bugs in some programming domains
BCILAB	MATLAB	<ul style="list-style-type: none"> BCILAB is a plugin of another EEG signal processing toolbox EEGLAB; supports feature extraction using both linear and nonlinear set of features including slow cortical potentials, power spectrum analysis, and common spatial patterns Ability of nonlinear EEG signal classification based on statistical learning including Bayesian classification, linear discriminant analysis-based classification

Table 3.7 EEG signal processing toolboxes—cont'd

EEG signal processing toolbox	Implementation software	Features
EEGLAB	MATLAB	<ul style="list-style-type: none"> The most user-friendly EEG signal analysis open-source MATLAB-based toolbox able to investigate variability in evoked brain responses trial wise Provision for efficient independent component analysis using higher-order (third-order and fourth-order) spectral functions to reject artifacts Rich set of functions to analyze event-related potentials, channel spectral analysis, cross-coherence analysis of imported EEG responses Open source and freely available interactive GUI to facilitate structural and functional neural connectivity of recorded EEG as well as electrocorticogram (ECoG) at both the scalp regions and cerebral cortical levels Developed for both single and multiple trial events-related EEG datasets to preprocess and map electrophysiological signals in time, frequency, and spatial domain Supports event-related cortical source imaging/identification, brain connectivity pattern analysis of selected region of interest (ROI), imaging and visualization to understand the time-varying localized neural functions from multivariate time-series EEG and ECoG data
eConnectome	MATLAB	
EEGNET	MATLAB	<ul style="list-style-type: none"> Unique EEG signal processing and neural network visualization tool that provides a provision for both EEG functional connectivity analysis along with network characterization Offers functional brain network analysis based on graph theory to compute network measures such as modularity, neural density, node strength, neighborhood edge analysis, shortest path edge length, clustering coefficient etc. Supports functional neural connectivity analysis and color-based visualization using cross-coherence/correlation, mutual information and mean phase coherence

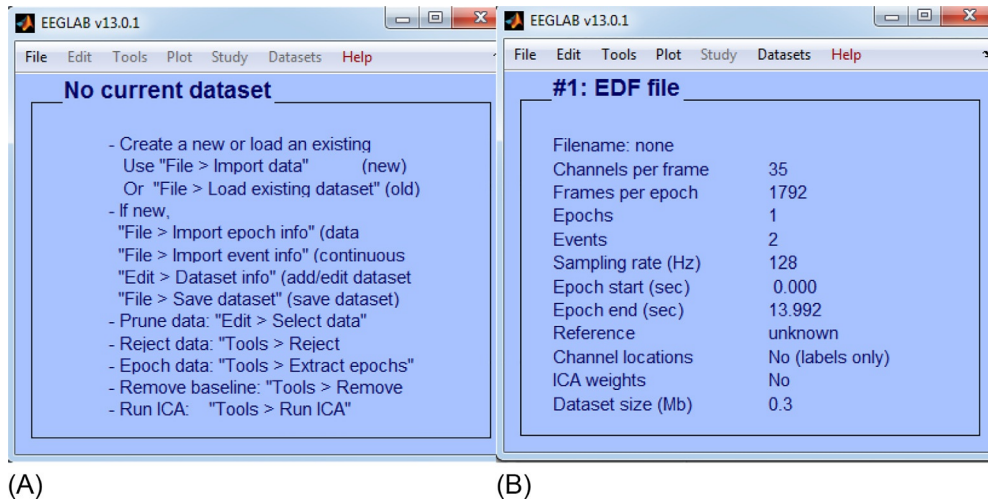


Fig. 3.8 Loading of EEG dataset into EEGLAB toolbox. (A) EEG lab main window. (B) Loaded EEG dataset information.

- Click on “File” menu in EEGLAB main window, select “Import data” from sub menu, click on “using EEGLAB functions and plugins” followed by selecting “from EDF files” to load selected multichannel EEG data into EEGLAB.

The loading of dataset in eeglab is done and the following window (Fig. 3.8B) appears with the relevant data information. This includes number of EEG channels, frames per epoch, number of epochs, sampling rate, epoch start and end time, data set size, etc. of loaded EEG dataset.

The voluntary eyeblink-specific EEG dataset loaded into EEGLAB toolbox is plotted using command “eegplot” to visualize the correlated EEG dynamics. Fig. 3.9 shows multichannel EEG responses acquired using Emotiv neuroheadset unit while performing a single eyeblink. It is clear that eyeblink-related neural activity is maximally captured by frontal channels as highlighted by green outlines in Fig. 3.9. This primary observation shall be verified while performing time, frequency, and spatial domain analysis of acquired responses in subsequent chapters.

3.4.3 Import of EEG Data Into MATLAB Workspace

The acquired deliberate single eyeblink-specific EEG responses are imported to MATLAB workspace to analyze the related variations in neural patterns. A function “edfread” is called to load EEG records in MATLAB. The epochs in the recorded EEG dataset corresponding to performed voluntary action of interest are identified to analyze the associated electrical activity of neurons. The step-by-step procedure to load EEG data into MATLAB is depicted in Fig. 3.10. The multichannel EEG signals attained using Emotiv neuroheadset are baseline corrected after importing to MATLAB workspace and are plotted in Fig. 3.11 for one subject.

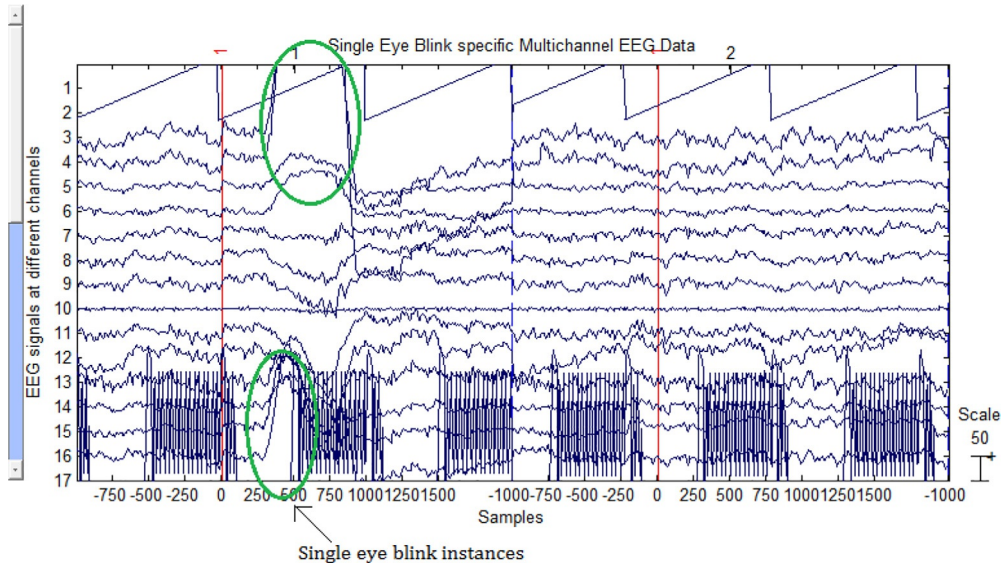


Fig. 3.9 Single eyeblink-specific multichannel EEG data loaded in EEGLAB toolbox.

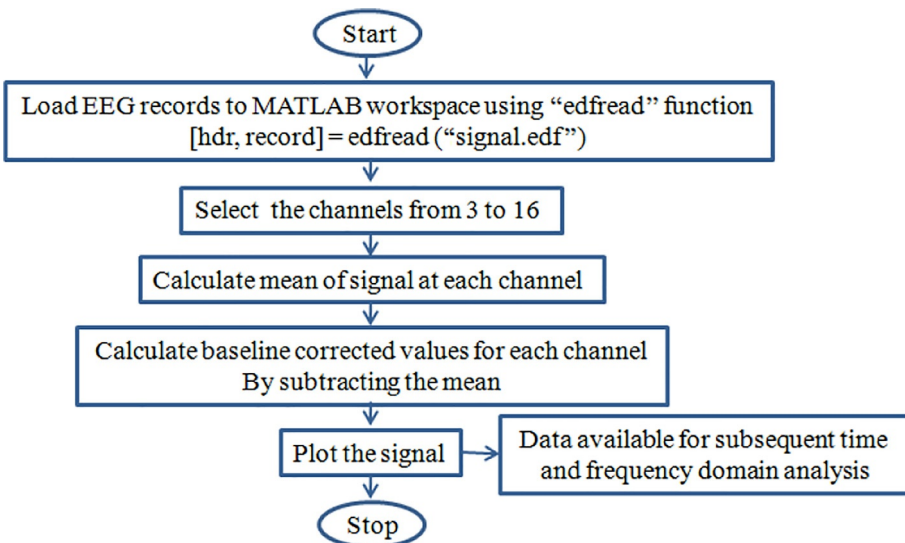


Fig. 3.10 Procedure to load EEG data into MATLAB.

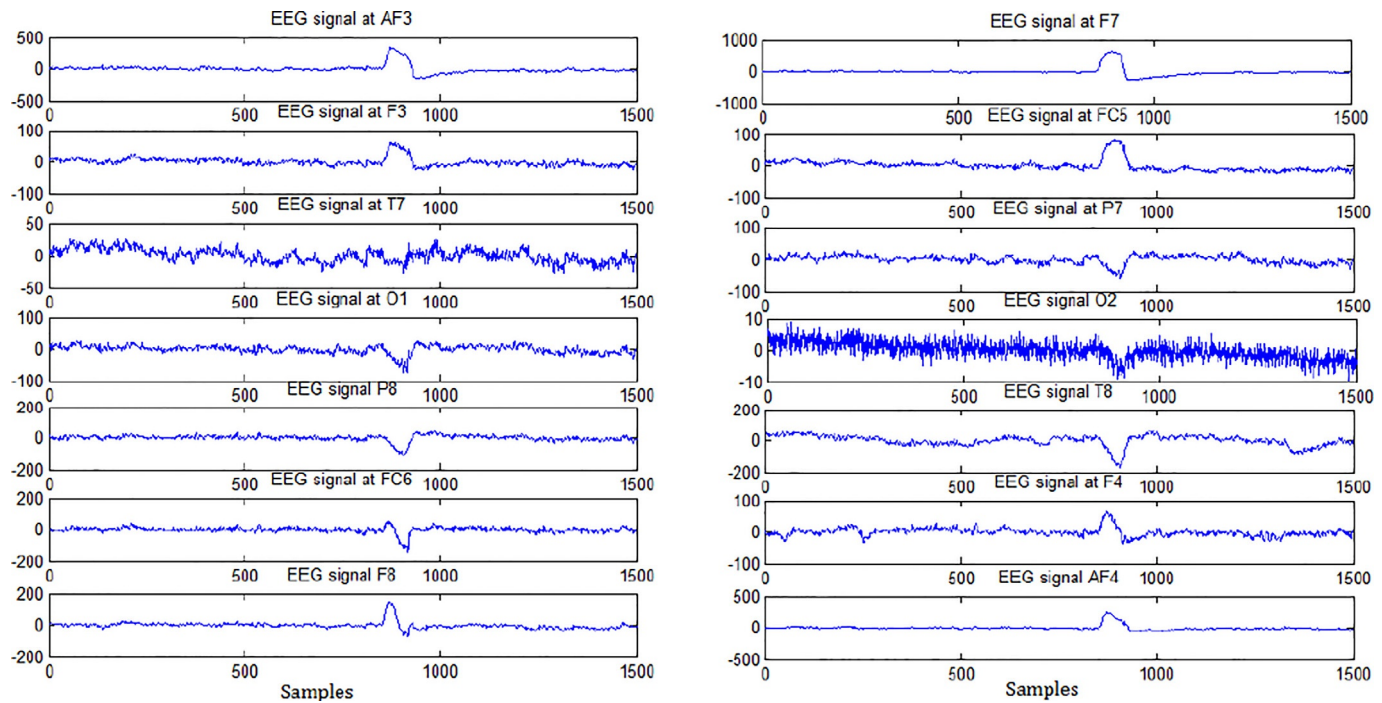


Fig. 3.11 Single eyeblink-specific multichannel EEG data.

The MATLAB function “`edfread`” reads the signal values from selected record (x.edf) of interest passed as a function argument. The syntax of called function is:

```
[hdr, record] = edfread('x.edf');
```

It returns two structures (header and record) with the entire general and technical specifications in “header” and all the signal information in other structure “record.” The following screenshots in Fig. 3.12A and B shows the header and record information, respectively of a multichannel EEG data “x” acquired during voluntary eyeblink.

The frame format of header is depicted in Table 3.8. The first 256 bytes of header indicates the version of data format, subject and record information, time information of the imported EEG record, number of data records, and finally followed by the number of signal channels (n) in each data record. The next 256 bytes specify the channel labels of device used for EEG signal acquisition, calibrated amplitude values followed by sampling rate of each data record.

Therefore, total header bytes are $256 + n \times 256$, “n” being number of channels in each record. Each header is followed by associated signal record containing data values at each sample for all the scalp channel locations from 1 to 36. The EEG Emotiv headset unit utilizes only 14 scalp channels with two reference electrodes as depicted in Fig. 3.11B. Thus, 14-channel EEG data acquired while performing voluntary eyeblink (single) is loaded and used for subsequent analysis to develop control applications.

The image shows two MATLAB variable browser windows side-by-side. The left window, titled 'Variables - hdr', displays the structure of the header (hdr). It contains fields such as 'ver' (0), 'patientID' ('6'), 'recordID' ('6'), 'startdate' ('16.02.14'), 'starttime' ('18.29.55'), 'bytes' (9472), 'records' (14), 'duration' (1), 'ns' (36), and various cell arrays for 'label', 'transducer', 'units', and ranges ('physicalMin', 'physicalMax', 'digitalMin', 'digitalMax'). The right window, titled 'Variables - record', displays the structure of the record (record). It shows a 1792x6 matrix of double precision values, representing 1792 samples across 6 channels. The first few rows of the matrix are: Row 1: 94, 95, 96, 97, 98, 0; Row 2: 0, 0, 0, 0, 0, 0; Row 3: 4.3856e+03, 4.3810e+03, 4.3846e+03, 4.3985e+03, 4.4010e+03, 4.4010e+03; Row 4: 4.5497e+03, 4.5508e+03, 4.5482e+03, 4.5554e+03, 4.5559e+03, 4.5559e+03; Row 5: 4.2482e+03, 4.2436e+03, 4.2456e+03, 4.2472e+03, 4.2467e+03, 4.2467e+03; Row 6: 4.0154e+03, 4.0097e+03, 4.0154e+03, 4.0221e+03, 4.0205e+03, 4.0154e+03; Row 7: 4.7195e+03, 4.7144e+03, 4.7123e+03, 4.7190e+03, 4.7174e+03, 4.7195e+03; Row 8: 4.6682e+03, 4.6677e+03, 4.6682e+03, 4.6677e+03, 4.6600e+03, 4.6682e+03; Row 9: 4.4979e+03, 4.5010e+03, 4.5036e+03, 4.5056e+03, 4.4959e+03, 4.4979e+03; Row 10: 4.2969e+03, 4.2959e+03, 4.2959e+03, 4.2923e+03, 4.2954e+03, 4.2969e+03; Row 11: 4.1790e+03, 4.1826e+03, 4.1754e+03, 4.1759e+03, 4.1744e+03, 4.1790e+03; Row 12: 4.6046e+03, 4.6005e+03, 4.5918e+03, 4.5923e+03, 4.5892e+03, 4.5604e+03; Row 13: 4.4995e+03, 4.4944e+03, 4.5000e+03, 4.5097e+03, 4.4995e+03, 4.4995e+03; Row 14: 4.3467e+03, 4.3431e+03, 4.3390e+03, 4.3364e+03, 4.3333e+03, 4.3467e+03; Row 15: 4.0328e+03, 4.0318e+03, 4.0328e+03, 4.0349e+03, 4.0338e+03, 4.0328e+03; Row 16: 4.2518e+03, 4.2492e+03, 4.2467e+03, 4.2503e+03, 4.2482e+03, 4.2518e+03.

Field	Value	Min	Max
ver	0	0	0
patientID	'6'	...	
recordID	'6'	...	
startdate	'16.02.14'		
starttime	'18.29.55'		
bytes	9472	9472	9472
records	14	14	14
duration	1	1	1
ns	36	36	36
(1) label	<1x36 cell>		
(1) transducer	<1x36 cell>		
(1) units	<1x36 cell>		
physicalMin	<1x36 double>	0	0
physicalMax	<1x36 double>	16000	16000
digitalMin	<1x36 double>	0	0
digitalMax	<1x36 double>	16000	31200
(1) prefilter	<1x36 cell>		
samples	<1x36 double>	128	128

1	2	3	4	5	
1	94	95	96	97	98
2	0	0	0	0	0
3	4.3856e+03	4.3810e+03	4.3846e+03	4.3985e+03	4.4010e+03
4	4.5497e+03	4.5508e+03	4.5482e+03	4.5554e+03	4.5559e+03
5	4.2482e+03	4.2436e+03	4.2456e+03	4.2472e+03	4.2467e+03
6	4.0154e+03	4.0097e+03	4.0154e+03	4.0221e+03	4.0205e+03
7	4.7195e+03	4.7144e+03	4.7123e+03	4.7190e+03	4.7174e+03
8	4.6682e+03	4.6677e+03	4.6682e+03	4.6677e+03	4.6600e+03
9	4.4979e+03	4.5010e+03	4.5036e+03	4.5056e+03	4.4959e+03
10	4.2969e+03	4.2959e+03	4.2959e+03	4.2923e+03	4.2954e+03
11	4.1790e+03	4.1826e+03	4.1754e+03	4.1759e+03	4.1744e+03
12	4.6046e+03	4.6005e+03	4.5918e+03	4.5923e+03	4.5892e+03
13	4.4995e+03	4.4944e+03	4.5000e+03	4.5097e+03	4.4995e+03
14	4.3467e+03	4.3431e+03	4.3390e+03	4.3364e+03	4.3333e+03
15	4.0328e+03	4.0318e+03	4.0328e+03	4.0349e+03	4.0338e+03
16	4.2518e+03	4.2492e+03	4.2467e+03	4.2503e+03	4.2482e+03

Fig. 3.12 (A) Header and (B) record information of acquired multichannel EEG data.

Table 3.8 Frame format of header in .edf record

Specification	Bytes
Version of European data format	8
Subject information	80
Subject recording	80
Date of data recording/acquisition (dd-mm-yyyy format)	8
Time of data recording/acquisition	8
Total number of bytes used for header information	8
Reserved bytes	44
Total number of acquired data recordings	8
Duration of each data recording (seconds)	8
Total number of acquired signals in particular data record (n):	4
Number of activated channels	
Label (channel names)	$n * 16$
Transducer type (Emotiv electrodes)	$n * 80$
Physical dimension (μ V)	$n * 8$
Physical minimum values allowed	$n * 8$
Physical maximum values allowed	$n * 8$
Digital minimum values allowed	$n * 8$
Digital maximum values allowed	$n * 8$
Prefiltering (notch/low-pass/high-pass filter specifications)	$n * 80$
Sampling rate specifications of each data record	$n * 8$
Reserved bytes	$n * 32$

3.5 IMPORT OF EEG DATA INTO SIMULINK

The multichannel EEG data can also be loaded into Simulink as it offers a rich library to design and simulate the models to interface external devices. The single eyeblink-specific brain responses analyzed in MATLAB are imported to Simulink using “simin” source library to develop various control applications of interest. A vast set of packages are available to interface certain controller boards such as Arduino, Raspberry-Pi, etc. to control interfaced external devices via input trigger signals received through designed Simulink model. The EEG responses recorded while performing voluntary eyeblink (single) are analyzed in MATLAB to identify the instant of eyeblink. The resultant workspace variable is exported to Simulink and acts as a trigger to control external brain assisted devices interfaced to Simulink through required controllers.

The EEG signal data from MATLAB workspace can be loaded into Simulink by selecting a block “simin” from “source” library. It reads brain signal data from MATLAB workspace and gives output as a signal. The following steps are followed to import data in Simulink:

- Import multichannel EEG data in MATLAB workspace and create a variable in workspace to represent the EEG data to be loaded.

- Select “simin” block from source library of Simulink and add to a new model.
- Add a block “from workspace” to a selected Simulink model.
- Select the output block and connect the output of “simin” block to it.
- Click on the block “from workspace” and configure the:
 - i. data from workspace to be loaded
 - ii. indicate data format
 - iii. process of data to be loaded with information about sample time, missing data points and zero crossing points

3.6 CONCLUSION

A detailed framework to design and understand the real-time acquisition of voluntary single eyeblink-specific brain patterns using EEG has been discussed. It has been highlighted that rather than considering eyeblink as an artifact, customization of the system could be possible to utilize eyeblink as a trigger to develop interactive brain-computer interfaces for control applications. This could facilitate the automation of external devices by merely using the neural responses of the subject. The resultant system of brain assistive devices would definitely possess the potential to assist physically challenged subjects having severe motor disabilities. The feature-specific analysis of available EEG acquisition units has been detailed. The candidature of Emotiv EEG neuroheadset to select it as a neural pattern acquisition device has been discussed. The detailed experiment protocol designed to acquire real-time synchronized single eyeblink-related neural activity using Emotiv EEG test bench has been presented. The recorded patterns can be used for offline analysis to study the task-specific EEG dynamics. It is followed by the procedure for online neural activity acquisition using MATLAB-based Emotiv EEG toolbox. The roadmap to analyze acquired brain responses in time, frequency, and spatial domain has been discussed in subsequent chapters. Overall, the related research and development opens up the perspectives to offer an alternative means of interaction with external environment for subjects with serious motor disabilities.

REFERENCES

- Bao, F.S., Liu, X., Zhang, C., 2011. PyEEG: an open source Python module for EEG/MEG feature extraction. *Comput. Intell.Neurosci.* 406391, 7 p.<https://doi.org/10.1155/2011/406391>
- Chambayil, B., Singla, R., Jha, R., 2010. In: Virtual keyboard BCI using eye blinks in EEG. 2010 IEEE 6th International Conference on Wireless and Mobile Computing, Networking and Communications (WiMob). 2010. <https://doi.org/10.1109/WIMOB.2010.5645025>.
- Delorme, A., Makeig, S., 2004. EEGLAB: an open source toolbox for analysis of single-trial EEG dynamics. *J. Neurosci. Methods* 134, 9–21.
- Elstob, D., Secco, E.L., 2016. A low cost EEG based BCI prosthetic using motor imagery. *Int. J. Inf. Technol. Converg. Serv.* 6 (1), 23–36.

- Farwell, L.A., Donchin, E., 1988. Taking off the top of your head: toward a mental prostheses utilizing event-related brain potentials. *Electroencephalogr. Clin. Neurophysiol.* 70 (6), 510–523. [https://doi.org/10.1016/0013-4694\(88\)90149-6](https://doi.org/10.1016/0013-4694(88)90149-6).
- Hassan, M., Shamas, M., Khalil, M., El Falou, W., Wendling, F., 2015. EEGNET: an open source tool for analyzing and visualizing M/EEG connectome. *PLoS One* 10 (9), e0138297. <https://doi.org/10.1371/journal.pone.0138297>.
- Hatsopoulos, N.G., Donoghue, J.P., 2009. The science of neural interface systems. *Annu. Rev. Neurosci.* 32, 249–266.
- He, B., Dai, Y., Astolfi, L., Babiloni, F., Yuan, H., Yang, L., 2011. eConnectome: a MATLAB toolbox for mapping and imaging of brain functional connectivity. *J. Neurosci. Methods* 195 (2), 261–269. <https://doi.org/10.1016/j.jneumeth.2010.11.015>.
- Höhne, J., Holz, E., Staiger-Sälzer, P., Müller, K.R., Kübler, A., Tangermann, M., 2014. Motor imagery for severely motor-impaired patients: evidence for brain-computer interfacing as superior control solution. *PLoS One* 9(8) e104854, <https://doi.org/10.1371/journal.pone.0104854>.
- Iáñez, E., Furió, M.C., Azorín, J.M., Huizzi, J.A., Fernández, E., 2009. Brain robot interface for controlling a remote robot arm. *Bioinsp. Appl. Artif. Nat. Comput.* 353–361.
- Jia, W., Zhao, X., Liu, H., Gao, X., Gao, S., Yang, F., 2004. Classification of single trial EEG during motor imagery based on ERD. *Conf. Proc. IEEE Eng. Med. Biol. Soc.* 1, 5–8.
- Kalcher, J., Flotzinger, D., Neuper, C., Golly, S., Pfurtscheller, G., 1996. Graz brain-computer interface II—towards communication between humans and computers based on online classification of three different EEG patterns. *Med. Biol. Eng. Comput.* 34, 382–388.
- Li, Y., Tianyou, Y., 2015. In: EEG based hybrid BCIs and their applications. 2015 3rd International Winter Conference on Brain Computer Interface (BCI), IEEE Xplore, South Korea. <https://doi.org/10.1109/IWFW-BCI.2015.7073035>.
- Lin, J.S., Chen, K.C., Yang, W.C., 2010. In: EEG and eye-blinking signals through a brain-computer interface based control for electric wheelchairs with wireless scheme. IEEE New Trends in Information Science and Service Science (NISS), 2010 4th International Conference on, Gyeongju, South Korea, 11–13 May 2010.
- Mahmoudi, B., Erfanian, A., 2002. In: Single-channel EEG-based prosthetic hand grasp control for amputee subjects, engineering in medicine and biology. Proceedings of the Second Joint 24th IEEE Annual Conference and the Annual Fall Meeting of the Biomedical Engineering Society EMBS/BMES Conference. <https://doi.org/10.1109/IEMBS.2002.1053347>.
- Oostenveld, R., Fries, P., Maris, E., Schoffelen, J.M., 2011. FieldTrip: open source software for advanced analysis of MEG, EEG, and invasive electrophysiological data. *Comput. Intell. Neurosci.* 2011. 9 p.
- Pernet, C.R., Chauveau, N., Gaspar, C., Rousselet, G.A., 2011. LIMO EEG: a toolbox for hierarchical linear modeling of electro encephalo graphic data. *Comput. Intell. Neurosci.* 2011, 831409, 11 p.
- Peters, B.O., Pfurtscheller, G., Flyvbjerg, H., 1998. Mining multichannel EEG for its information content: an ANN-based method for a brain-computer interface. *Neural Netw.* 11, 1429–1433.
- Renard, Y., Lotte, F., Gibert, G., Congedo, M., Maby, E., 2010. OpenViBE: An Open-Source Software Platform to Design, Test and Use Brain-Computer Interfaces in Real and Virtual Environments, Presence: Teleoperators and Virtual Environments. vol. 19(1) Massachusetts Institute of Technology Press, pp. 35–53.
- Schalk, G., McFarland, D.J., Hinterberger, T., Birbaumer, N., Wolpaw, J.R., 2004. BCI2000: a general-purpose brain-computer interface (BCI) system. *IEEE Trans. Biomed. Eng.* 51 (6), 1034–1043.
- Schwartz, A.B., 2004. Cortical neural prosthetics. *Annu. Rev. Neurosci.* 27, 487–507.
- Vidaurre, C., Sander, T.H., Schlögl, A., 2011. BioSig: the free and open source software library for biomedical signal processing. *Comput. Intell. Neurosci.* 935364, 12 p. <https://doi.org/10.1155/2011/935364>
- Wolpaw, J., McFarland, D., Neat, G., Forneris, C., 1991. An EEG-based brain-computer interface for cursor control. *Electroencephalogr. Clin. Neurophysiol.* 78 (3), 252–259. [https://doi.org/10.1016/0013-4694\(91\)90040-B](https://doi.org/10.1016/0013-4694(91)90040-B).

FURTHER READING

- Bio-medical, <https://bio-medical.com/>. [(Accessed 12 January 2018)].
- Brainproducts, <http://www.brainproducts.com/productdetails.php?id=63>. [(Accessed 12 January 2018)].
- Brainvision, www.brainvision.com/actichamp.html. [(Accessed 12 January 2018)].
- Emotiv, <https://www.emotiv.com/epoch/>. [(Accessed 12 January 2018)].
- Imotions, <https://imotions.com/blog/eeg/>. [(Accessed 12 January 2018)].
- Lievesley, R., Wozencroft, M., Ewins, D., 2011. The Emotiv EPOC neuroheadset: an inexpensive method of controlling assistive technologies using facial expressions and thoughts? *J. Assist. Technol.* 5 (2), 67–82.
- Mathworks, <https://in.mathworks.com/matlabcentral/fileexchange/36111-emotiveeg-headset-toolbox>. [(Accessed 6 January 2018)].
- Neuroelectrics, www.neuroelectrics.com/products/enobio/enobio-32/. [(Accessed 12 January 2018)].
- Neurosky, <http://neurosky.com/biosensors/eeg-sensor/>. [(Accessed 14 January 2018)].
- Poor, G.M., Leventhal, L.M., Kelley, S., Ringenbergs, J., Jaffee, S.D., 2011. Thought cubes: exploring the use of an inexpensive brain-computer interface on a mental rotation task. *The Proceedings of the 13th International ACM O'Connor 30 SIGACCESS Conference on Computers and Accessibility (ASSETS '11)*, pp. 291–292.
- Wearablesensing, <http://www.wearablesensing.com/DSI24.php>. [(Accessed 14 January 2018)].

CHAPTER 4

Cognitive Analysis: Time Domain

Dipali Bansal, Rashima Mahajan

Faculty of Engineering and Technology, Manav Rachna International Institute of Research and Studies, Faridabad, India

Contents

4.1 Introduction	107
4.2 Preprocessing	110
4.2.1 Prefiltering	111
4.2.2 ICA of Filtered EEG Data	113
4.3 Channel ERP Analysis	116
4.4 ERP Scalp Map Analysis at Different Latencies	117
4.5 Result and Analysis	118
4.6 Conclusion	118
References	136
	137

4.1 INTRODUCTION

The acquisition procedure of voluntary eyeblink-based neural responses via EEG has been detailed in the previous chapter. This chapter highlights the processes and algorithms involved in cognitive analysis of acquired single eyeblink-related brain activity in time domain. Neural activity controlled robotics are providing new horizons of mobility and medical diagnostics for differently abled subjects and thus ensuring improved independent life (Bi et al., 2013). This opens up the possibilities to control external devices and design rehabilitative systems by characterizing and correlating merely single voluntary eyeblink-related neural responses using signal processing tools. Therefore, the selection and utilization of eyeblink as a useful control signal rather than considering it as an artifact in brain signals has seen a phenomenal growth in this decade. The designing and implementation of such neural-based rehabilitation equipments including medical robotics via interactive brain-computer interfaces (BCIs) is gaining attention progressively. Assistive external devices and robotics designed using interactive man-machine interfaces (MMIs) for medically challenged subjects are the major application outcomes in the field of rehabilitation. The utilization of neural controlled automation is not only intended for physically handicapped subjects, but it can certainly contribute toward improving the living standards of healthy users also. The primary requirement to design efficient brain activity controlled systems is the development of an efficient and accurate BCI. This shall include an accurate acquisition of specific neural patterns, analysis of

recorded patterns to identify the instant of interest followed by utilization of identified signal instances as commands to develop neural controlled applications.

The neural responses acquired through scalp electrodes are produced as electrical impulses of neurons in time domain. The analysis of captured brain patterns in time domain includes the characterization of neural variations to extract temporal correlates of associated neuronal activity (motor, cognitive, stimulated, etc.). The epochs related to the performed cognitive/motor/stimulus-based neuronal activity are extracted for subsequent analysis in time domain. The nonsignificant epochs with inconsistent phase relationships are responsible for background artifacts/oscillations only and thus rejected during preprocessing phase. The related activity of interest is extracted through the most relevant epochs of specific brain activity. The subsequent neuronal activity variations are characterized in terms of amplitude variations with respect to time followed by variations in time segments between selected data points and duration of distinct events.

The most appropriate parameter as stated in the literature to capture the specific activity in time domain is brain potential and is expressed as event-related potential (ERP). As stated in Section 2.5.1, the ERPs can be categorized as event-related synchronization (ERS)/desynchronization (ERD), evoked potentials (steady-state-evoked potential, steady-state-visually evoked potential (SSVEP), steady-state-auditory-evoked potential, steady-state-somatosensory-evoked potential, P300 evoked potential), and slow cortical potentials. A fair amount of work has been published to control external devices by extracting above potentials from the acquired EEGs. The single-trial induced potentials in the sensorimotor area of cerebral cortex have been recorded in terms of ERS and ERD potentials to successfully identify the left-hand or right-hand movement (Jia et al., 2004). The captured ERS/ERD potentials are quantized as per the intensity of imagination of movement task to obtain high classification and information transfer rate of designed BCI. There is no mandatory requirement of external stimuli to characterize brain activity using ERS/ERD. However, a long training period is required.

The eyeblink-specific EEG signals have also been utilized to design and implement a BCI system for selecting characters/keys on the virtual keyboard. The platform used to implement the BCI was LabVIEW. The peakedness in terms of kurtosis coefficient of acquired EEG responses in fusion with the associated amplitude variations have been used primarily to characterize the eyeblink-related neural instances (Chambayil et al., 2010). A group of researchers have utilized P300 evoked potentials to characterize neural variations in acquired EEGs even with high efficiency of 85%–90% even using a short training period of signals (Shi et al., 2010; Cecotti and Graser, 2011; Escolano et al., 2012; Pathirage et al., 2013). A fusion of ERPs such as P300 with SSVEP has also been utilized to successfully control the position of cursor on the screen (Li and Yu, 2015). The combination of P300 with motor imagery signals has been successfully implemented to control the horizontal and vertical position of cursor on computer screen with short training period and even high efficiency of 85%–90%.

It has also been reported in late sixties (1969) itself that the neural correlates of any planned or performed voluntary motor task/movement are well captured by the brain cortical potentials (Deecke, 1969). This reflects the potential of brain cortical potentials to be used as control signals for specific applications including cursor movement, home automation, development of prosthetics, wheelchair movement, etc. (Kalcher et al., 1996). The characterization of 56-channel recorded EEG was done successfully using brain cortical potentials to identify and discriminate motor movements, viz., right-foot movement from the both hand index finger movement (Peters et al., 1998). These types of slow cortical potentials are also known as movement-related cortical potentials (MRCP) and are extensively used for detection of motor movements/intentions for subsequent triggering of external devices. The MRCPs captured from scalp EEG electrodes can be used to develop closed loop-brain control interfaces capable of generating commands to control devices efficiently in real time (Xu et al., 2014). However, a high training period is required to attain high classification accuracy and possess a comparatively low-information transfer rate.

The control potentials used in BCIs can also be evoked by external stimulations (auditory or visual). The frequency of generated potentials in response to external stimulations is made to map with an input of interfaced computer. The received EEG responses with evoked potentials are analyzed on computer to identify the neural correlates of interest (Smith et al., 2014). The potentials evoked through visual stimulations possess a high immunity toward noise artifacts arising due to eye movements and other body movements. Therefore, visual stimulation-based BCIs possess high signal-to-noise ratio, high accuracy, high information transfer rate, short training periods and are thus, preferred to assist differently abled subjects (Ahmad et al., 2016). The fact behind the reception of high-noise immune EEG responses is the low-frequency noise generated by these body and eye movements than the visual stimulation frequency. This leads to the requirement of minimal filter stages during preprocessing of acquired EEG signals.

This work implements a simple and robust BCI based on exploring ERPs as a discriminative feature to be used as a trigger to develop control applications driven by deliberate eyeblink-specific neural responses. The cognitive BCIs based on ERP possess the capability to exploit the spatial domain information of acquired EEG responses. This aids the selection of specific-activated scalp channels for subsequent analysis. The brain activity related to voluntary single eyeblink captured using 14-channel EMOTIV EEG neuro-headset has been analyzed in time and spatial domain to design a control application. The framework designed for cognitive analysis of real-time EEGs acquired during voluntary eyeblink is as shown in Fig. 4.1.

Each of the 20-s duration brain patterns has been recorded via EEG and is analyzed in time domain to identify deliberate eyeblink activity. The statistically independent components are identified using fourth-order moment-based independent component analysis (ICA) to locate the most relevant epochs of the imported EEG dataset. The channel

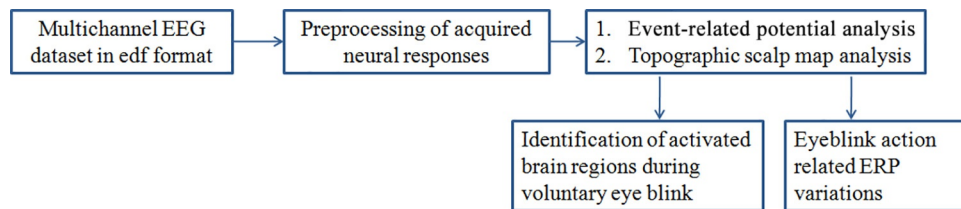


Fig. 4.1 Cognitive analyses of acquired real-time EEG during voluntary eyeblink: time domain.

ERP distributions along with topographic scalp maps have been analyzed to identify the activated scalp channels and correlated neural activity during voluntary eyeblink. The detailed time domain (by extracting ERPs) and spatial domain [by plotting two-dimensional (2D) and three-dimensional (3D) scalp maps] analysis of recorded brain activity is included in the subsequent sections.

4.2 PREPROCESSING

The time-domain analysis of recorded EEG activity has been performed using MATLAB-based standalone application software toolbox EEGLAB v 13.2.2.b and in MATLAB workspace of release 2015a. The primary aim is to extract a multi domain feature set to identify the instance of a thoughtful single eyeblink successfully. The eyeblink-specific acquired EEG dataset through EMOTIV test bench was imported to EEGLAB and in MATLAB workspace directly as detailed in [Chapter 3](#). The 14-channels placed over scalp to capture EEG data were located across the brain regions as depicted in [Fig. 4.2](#). The EEG data components have been acquired through EEG electrodes from the source locations as visualized in 2D ([Fig. 4.2A](#)) and 3D ([Fig. 4.2B](#)) scalp maps. The channels AF3, F3, F7, and FC5 are the left frontal channels and AF4, F4, F8, and FC6 are the right frontal channels.

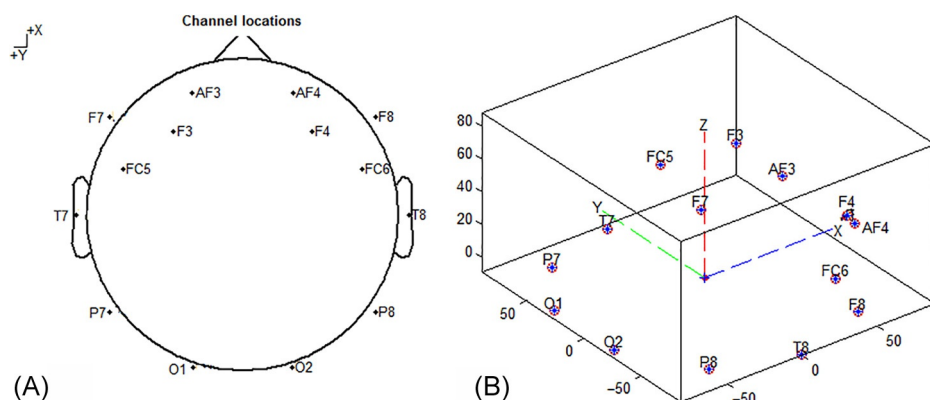


Fig. 4.2 (A) Channel locations across 2D scalp maps and (B) channel locations across 3D maps.

constitute the right frontal channel group. The pair of temporal channels has been located as T7 (left temporal) and T8 (right temporal) locations. The left- and right-parietal channels consist of P7 and P8, respectively. The occipital region is covered by two occipital electrodes O1 (left) and O2 (right), respectively, to capture brain waves from specified locations. The channel locations in 3D map are shown at specific azimuth and elevation angle to locate the electrodes across subject's scalp periphery.

The deliberate eyeblinks are required to be identified significantly by rejecting various artifacts including involuntary eyeblinks also. Number of techniques has been documented in the literature to detect the desired instances from acquired EEG responses. This first includes the preprocessing of EEG-related neural activity recorded by scalp electrodes. The preprocessing primarily aims toward the rejection of spurious artifacts including both physiological (ECG, EMG, eye movements, involuntary eyeblinks) and nonphysiological artifacts (power line interference, dry scalp electrode contact, electrode impedance fluctuations). The preprocessing step includes pre-filtering and ICA of filtered EEG data.

4.2.1 Prefiltering

To locate the maximally activated channels during single eyeblink activity, the acquired EEG dataset is first filtered to reject the spurious data epochs. It is recommended to filter the acquired continuous EEG dataset rather than applying separate filtering operation to each epoch. This leads to minimization of filtering artifacts which otherwise gets introduced at EEG data epoch boundaries. A 2536-point zero-phase finite impulse response (FIR) band-pass filter has been implemented with lower cut-off frequency of 0.25 Hz and higher cut-off frequency of 50 Hz. The filter characteristics of the designed FIR filter are as plotted in [Fig. 4.3](#). The designed filter provides output with a transition bandwidth of 0.25 Hz. The selected bandwidth of 0.25–50 Hz allows capturing all the variations in ERPs of recorded EEGs in the designated bandwidth. This automatically rejects the high line-noise artifacts at 50–60 Hz followed by rejection of movement-related artifacts, low-frequency skin, and sweat artifacts.

However, implementation of FIR band-pass filter may introduce phase delays sometimes which need to be nullified to accurately identify the intended instances. This is followed by reverse filtering to remove the introduced phase delays. A MATLAB function *filtfilt()* is used to perform reverse filtering. The following steps are followed to perform digital filtering with zero phase:

- filter the input data coefficients in the forward direction;
- reverse the resultant filtered output coefficients; and
- perform the filtering operation again and repeat the whole process.

The above sequential operations ensure the nullification of the phase lags introduced during filtering, thus minimizing starting and ending transients. This in turn ensures the

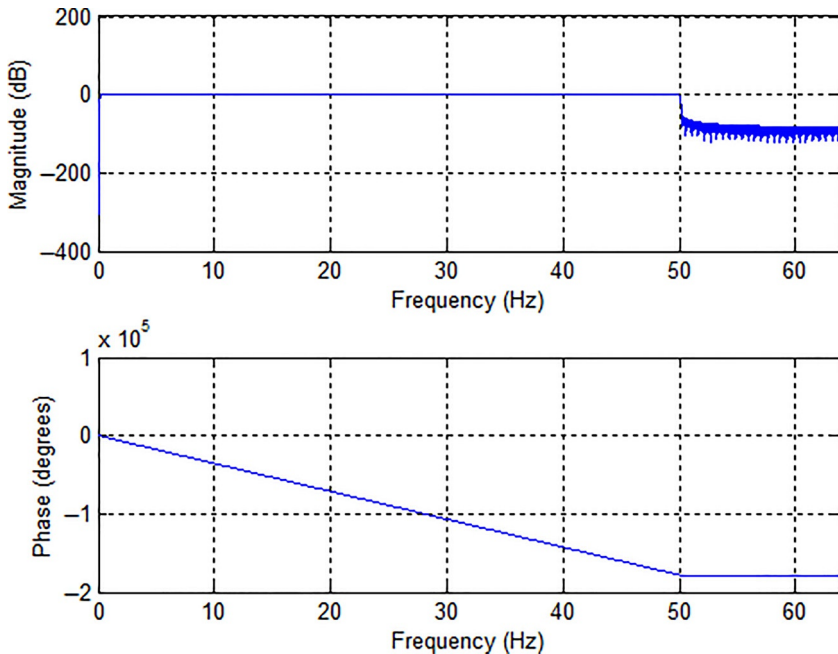


Fig. 4.3 Filter characteristics of a 2536-point zero-phase FIR band-pass filter with passband range (0.25–50 Hz).

smooth transition between passband and stop band. The above operation utilizes the time-reversal property of the discrete-time Fourier transform (DTFT) as follows:

If

$$x(n) \xleftrightarrow{DTFT} X(e^{j\omega}) \quad (4.1)$$

then

$$x(-n) \leftrightarrow X(e^{-j\omega}) \text{ or } X^*(e^{j\omega}) \quad (4.2)$$

Here, $x(n)$ represents the input sequence and $X(e^{j\omega})$ represents the Fourier transform of $x(n)$. The time reversal of $x(n)$ corresponds to replacement of ω by $-\omega$ in frequency domain. It indicates data filtering in forward direction followed by filtering in backward direction. The block diagram of this forward-backward filtering operation is explained as in [Fig. 4.4](#).

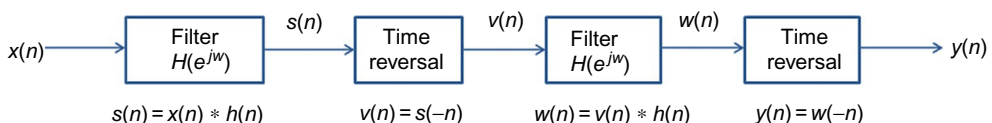


Fig. 4.4 Implementation of forward and reverse digital filtering operation.

The input signal $x(n)$ is applied to filter having transfer function $H(e^{j\omega})$. The result of first forward filter is:

$$S(e^{j\omega}) = H(e^{j\omega}) X(e^{j\omega}) \quad (4.3)$$

Here, $H(e^{j\omega})$ is the Fourier transform of impulse response of filter $h(n)$. The time reversal of resultant $S(e^{j\omega})$ gives output as per the following equation:

$$V(e^{j\omega}) = S^*(e^{j\omega}) = H^*(e^{j\omega}) X^*(e^{j\omega}) \quad (4.4)$$

The result of second filter is given as

$$\begin{aligned} W(e^{j\omega}) &= H(e^{j\omega}) V(e^{j\omega}) \\ &= H(e^{j\omega}) H^*(e^{j\omega}) X^*(e^{j\omega}) \\ &= |H(e^{j\omega})|^2 X^*(e^{j\omega}) \end{aligned} \quad (4.5)$$

The spectrum of output signal $Y(e^{j\omega})$ is obtained as time reversal of $W(e^{j\omega})$ as follows:

$$\begin{aligned} Y(e^{j\omega}) &= W^*(e^{j\omega}) \\ &= |H(e^{j\omega})|^2 X(e^{j\omega}) \end{aligned} \quad (4.6)$$

Therefore,

$$H_{overall} = |H(e^{j\omega})|^2 \quad (4.7)$$

It shows that the overall frequency response (transfer function) of the forward-backward filtering is equal to the squared magnitude of the transfer function of the filter in forward direction. It is clear from Eq. (4.6) that the output spectrum is obtained by using a filter with frequency response $|H(e^{j\omega})|^2$. This resultant transfer function is purely a real value with zero phases and subsequently free from phase distortions.

A fusion of filters can also be used to reject artifacts in the acquired EEG responses. The median filter to preprocess the eyeblink-related EEG signals along with a mode filter to select the most significant samples of the selected instances from EEG signals can also be implemented (Varela, 2015). The selected samples are analyzed to extract the most relevant and informative feature set to identify the corresponding brain patterns related to deliberate eyeblinks with high classification accuracy.

4.2.2 ICA of Filtered EEG Data

The reverse filtered EEG data is further decomposed into maximally independent components by applying ICA algorithm in EEGLAB toolbox. It blindly separates the statistically and temporally independent neural signals corresponding to specific (cognitive, motor, stimulated) neural activity present in the acquired multichannel EEG data

(Delorme and Makeig, 2004; Bugli and Lambert, 2007). The remarkable potential of ICA algorithm to identify and separate out distinct component activities contained in recorded dataset has been well explained by Onton and Makeig (2006). It is based on computation of higher-order spectral components of input signals specifically third-order (bispectrum) and fourth-order spectral (trispectrum) components to identify voluntary single eyeblink-related instances in the recorded neural patterns through EEG scalp electrodes. The third-order statistics is a measure of symmetry (skewness) of sample variations in the acquired neural activity (Pradhan et al., 2012). It is capable of extracting and identifying the non-Gaussian patterns from recorded EEG-based brain patterns. The fourth-order statistics is a measure of peakedness (kurtosis) of amplitude variations in the acquired neural activity (Collis et al., 1998). It is capable of extracting and identifying unusual peak amplitude variations and distributions among recorded EEG signal samples. Therefore, it also provides a basis to automatically identify and reject temporal as well as spatial artifacts along with bad epochs from acquired and imported EEG signals.

A fourth-order moment-based ICA algorithm has been implemented on acquired EEG signals of 20-s duration each to detect the brain patterns related to performed voluntary single eyeblink activity. The principle behind the decomposition of recorded EEG signals into independent components is based on maximizing the non-Gaussian distribution and measuring the Fourier-phase relationships among individual input signal samples. This provides direct access to individual sample components which otherwise are difficult to be observed and analyzed for subsequent feature extraction. The morphology-related exact information gets suppressed in principal component analysis (PCA)-based decomposition algorithm (Subasi and Gursoy, 2010). Since it utilizes the second-order spectra to analyze the recorded input EEG signals which suppress the Fourier-phase relation among sample values (Joyce et al., 2004). The kurtosis of input EEG signal is computed as (Delorme et al., 2007)

$$K = M_4 - 3M_2^2 \text{ and } M_n = E\{(x - M_1)^n\} \quad (4.8)$$

where M_n indicates the n th-order moment around the sample mean and E represents an overall sample average envelope function. The high positive and negative values of kurtosis for imported EEG sample values as per Eq. (4.8) represents high-peak artifacts whereas values lying near to zero represents highly Gaussian behavior of samples (Delorme et al., 2007). The EEG signal components with high positive or negative kurtosis values are rejected to obtain clean and artifact-free single eyeblink-specific neural dataset.

An EEG signal at single scalp channel is basically the sum of potential differences between distinct voltage source projections to the selected scalp data channel and one or more than one reference data channels. It is represented by a single row of EEG data recording matrix as each row data corresponds to distinct channel data, respectively. The decomposition of recorded EEG data using ICA algorithm provides a linear

transformation of EEG data attained across single scalp electrodes into spatially distinct components. Thus, it implements a linear spatial filtering operation. Once the ICA-based decomposition is performed, individual row of resultant EEG data matrix now indicates the activity of single component of selected channel across the whole course of time. It is labeled as a single component activity operation which is temporally and spatially filtered from a selected channel EEG signals. These component activities are basically extracted from the volumetric conduction mixtures of recorded neuronal variations through EEG scalp electrodes. The volumetric conduction mixing phenomenon utilized to record distinct source contributions is purely passive (no additional information is added to dataset) and linear. Each independent component is computed as a set of contributions of relative synchronous/partially synchronous cortical activity strengths of specific component projections to the recording scalp channels and is termed as scalp map.

Though the volumetric mixtures of neuronal and peripheral activity recorded by adjacent scalp channels are highly similar, however, the individual ICA component variations are found to be maximally distinct over the course of time. This is also the case even with overlapped scalp maps. Therefore, the complex macroscopic dynamics related to un-averaged cortical activity through ICA components represent more informative response in time domain as compared to the averaged or clustered cortical response at specific EEG scalp channel. From the above discussion, it can be concluded that ICA algorithm is very well capable to separate averaged EEG signals coming from linearly mixed source data points over scalp. It determines individual components by maximizing the non-Gaussianity of sources and thus, indicates that ICA is not applicable to signal sources with perfect Gaussianity.

Following are the algorithmic steps to perform ICA of EEG sources:

- i.** Compute the matrix M in such a way that for any $i \neq j$, the components of EEG signal x_i and x_j are highly uncorrelated and the resultant transformed components $g(x_i)$ and $g(x_j)$ are also uncorrelated. Here, g and h represents nonlinear transformations applied to components x_i and x_j , respectively. This is known as the principle of nonlinear decorrelation.
- ii.** Compute a linear combination using matrix M , i.e., $x = Ms$ such that, s is possessing constant variance. Now, locate the local maxima of existing non-Gaussianity of above linear relation $x = Ms$. This is known as principle of maximum non-Gaussianity.

Each of the computed local maxima indicates individual independent component of the input EEG signal. If the various sample values of input EEG signal at different instances are $s_1(t), s_2(t), \dots, s_n(t)$; where t is the time duration of acquired signal trial, the computation of independent components include the estimation of matrix M and various $x_i(t)$ values from recorded $s_i(t)$ sample values. The artifact-free EEG signals are obtained by identifying and rejecting the individual noisy EEG components which possess very high positive or negative kurtosis values as depicted in Fig. 4.5.

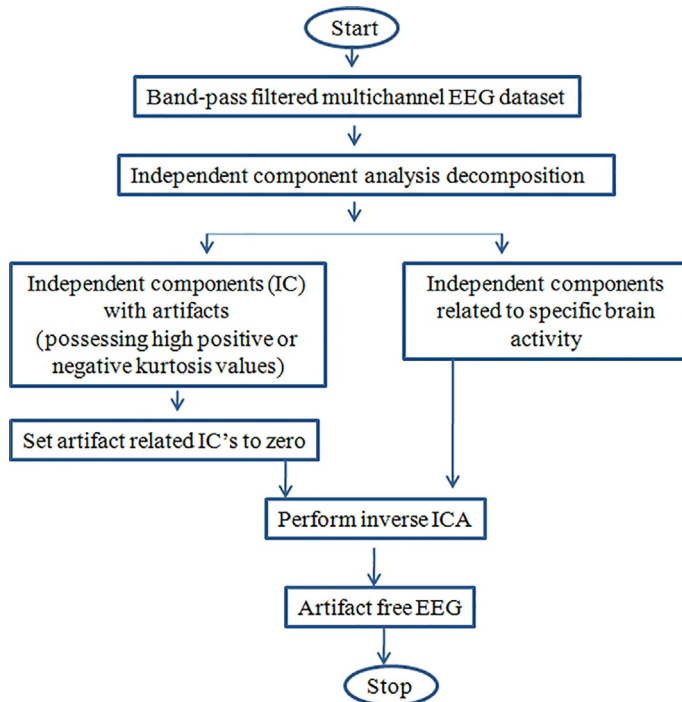


Fig. 4.5 Independent component analysis (ICA) to obtain artifact-free EEG.

4.3 CHANNEL ERP ANALYSIS

ERPs are averaged EEG signals captured by scalp electrodes. These signals are acquired in response to specific neural task. The averaged EEG neural waveforms are consisted of positive and negative ERP components. It is represented by the sum average of all neural activities related to distinct processes involved in specific task (Luck, 2005). The ERP analysis involves the determination of minute voltage variations in the neural activity acquired by scalp electrodes. The recorded neural activity is time locked to specific events. The artifact-free EEG records are analyzed to extract the specific event-related data epochs from continuously acquired EEG data records. The detailed analysis related to EEG-signal dynamics at specific instant provide the information of EEG-signal epochs which are time locked to distinct voluntary events/actions of subject's/application developer's interest. For example, EEG-signal epochs that are time locked precisely to some stimulated experimental task such as cognitive task (critical thinking, problem solving), onset of voluntary actions, motor tasks, affective tasks (related to positive or negative emotions), memory-related tasks (recalling or remembering an incidence), sensory-related tasks (determination of shape, color, audio stimulus, video stimulus), etc. are extracted.

The preprocessed voluntary eyeblink action-specific EEG neural response has been selected and analyzed to characterize the associated variations in time domain. The ERP-related features generally extract the temporal information of the input EEG signals. It includes the record of variation of amplitude of neural responses via EEG with respect to time. The extraction of ERP-related features includes the following steps:

- Acquired single eyeblink-specific EEG signals are band-pass filtered in the frequency range 0.25–50 Hz as explained in [Section 4.2](#).
- The filtered signals are down sampled to reduce the dimensionality of the acquired signals by limiting the number of EEG data time points.
- The amplitude variations are recorded at distinct data points to obtain the resultant ERP values.

The neural variations in time domain are mostly related to the amplitude variations of brain signals in response to voluntary motor event/action. These fluctuations in amplitude of acquired brain EEG responses are termed as ERPs. It is to be noted that the performed event must be recorded for an accurate and sufficient measurable duration of time. The instant of the start of the task or presentation of the stimulus to the subject is termed as trigger instant of the event. This event is captured in terms of related brain activity using EEG. The variations in brain potentials are expected in response to any performed voluntary event and are represented as waveforms. The corresponding neural variations are measured as ERP amplitudes. However, the nature of ERPs is extremely varied according to the context of their occurrence as follows:

- It can be visualized as an indicator of application of abrupt stimulation to observe specific response.
- On the other hand, the polarity of recorded ERPs may also be observed in response of any neural activity. A decrease or increase in amplitude of acquired ERP indicates the correlation of respective ERPs with specific activity of neurons.

Voluntary single eyeblink-based ERP result and analysis performed in this work is detailed in [Section 4.5](#).

4.4 ERP SCALP MAP ANALYSIS AT DIFFERENT LATENCIES

The ERP scalp map analysis is performed in EEGLAB at selected latencies to determine the activated regions of brain in response to the specific stimulation or cognitive/motor action. The spatial information of recorded eyeblink-specific EEG response is extracted. These topographic scalp maps indicate the potential distribution across distinct cerebrum regions using different color scheme. The red color shows the highest potential values and hence indicates the maximum activation across specific region of brain. However, the lowest activation is indicated by blue color as per the color-coding scheme utilized in EEGLAB toolbox of MATLAB. The 2D and 3D scalp maps have been plotted for thoughtful single eyeblink-specific EEG responses. The whole spatial domain analysis

is typically performed to identify and focus exclusively on specific-activated channel neural data instead of extracting the relevant feature set from highly data intensive entire multichannel EEG dataset.

The timing of occurrence of event via ERPs also indicates the level of neural cognition and processing involved in specific task. Early signal components occurring after 20 ms of onset of the specific event trigger are mostly related to the automatic natural actions. These may extend from 20 to 100 ms. These types of early negative components of ERPs are designated as N100 wave (for auditory stimulation) and N1 wave (for visual stimulation). Their amplitude lies between low and average values; however, it can be modulated if the action is performed with high attention. A set of late ERP signal components occurring approximately after 200–300 ms of the onset of neural event trigger are considered to be related to the high level of neural cognition and processing. These types of positive late ERP components are designated as P300 waves. These components occur approximately after 300 ms of the application of stimulus to the subject involved in specific neural task. Voluntary single eyeblink-based 2D and 3D scalp map analysis done in our work at different latencies is presented in [Section 4.5](#).

4.5 RESULT AND ANALYSIS

This section presents the detailed results and subsequent analysis of performed experimentation. The presented approach for thoughtful single eyeblink identification has been developed using MATLAB tool. In this experiment, the neural activity of five human subjects while performing a deliberate single eyeblink action is recorded via EEG. The acquired multichannel EEG-specific neural dataset has been analyzed by extracting specific feature set in time domain. The ERP and scalp map analysis results of five subjects are presented and discussed in detail to identify an instant of a thoughtful eyeblink. In this experimentation, the human subjects were made to relax first and then perform a deliberate single eyeblink activity. Each of the corresponding brain patterns via EEG are recorded for 20-s duration via scalp electrodes of EMOTIV Neuroheadset unit. The acquired dataset is imported to EEGLAB toolbox of MATLAB for the subsequent analysis in time domain. The first step is to obtain the signal at band of frequencies lying between 0.25 and 50 Hz. A zero-phase FIR band-pass filter has been implemented in MATLAB to obtain a desired set of EEG signals. The fourth-order spectral-based ICA of signals has been performed to separate action specific components from the acquired EEG response mixtures. The maximum temporally and spatially distinct components related to voluntary single eyeblink action are identified as per the process depicted in [Section 4.2.2](#). The high peak artifacts are removed by incorporating fourth-order statistics-based ICA decomposition to extract the clean EEG-signal epochs related to thoughtful single eyeblink action.

The primary aim is to determine the regions of brain (frontal, temporal, parietal, and occipital) activated during performed voluntary eyeblink. The understanding obtained shall be used to select the corresponding scalp channels of EMOTIV EEG neuroheadset unit (frontal: AF3, AF4, F7, F8, F3, F4, FC5, FC6; temporal: T7, T8; parietal: P7, P8, and occipital: O1, O2) for subsequent analysis. The frontal channels are further subdivided as left frontal (AF3, F7), centrally frontal (F3, FC5, F4, FC6), and right frontal (AF4, F8). The single eyeblink-specific filtered artifact-free multichannel EEG dataset is invoked for ERP and subsequent topographic scalp map analysis at distinct set of latencies. It is aimed to identify the deliberate single eyeblink action using detailed time-domain analysis. The ERP analysis primarily determines averaged ERPs of all EEG epochs acquired across 14 scalp electrodes of EMOTIV EEG neuroheadset. It is plotted across all latency points (millisecond scale) of input EEG signals acquired from subject one as shown in [Fig. 4.6](#).

Each single trace in the generated plot determines the ERP variations in microvolts recorded across respective scalp channel during a selected course of time. A 2D scalp map is plotted above ERP traces to indicate the average potential distribution across distinct regions of cerebral cortex during the performed eyeblink action. The plotted topographic scalp map at latency of 619 ms indicates the maximum potential distribution across frontal regions of brain (bright red color) during voluntary eyeblink. The corresponding event-related data variance across the selected latency point is also found to be maximum. The topographic analysis can be performed at different latencies. The corresponding scalp

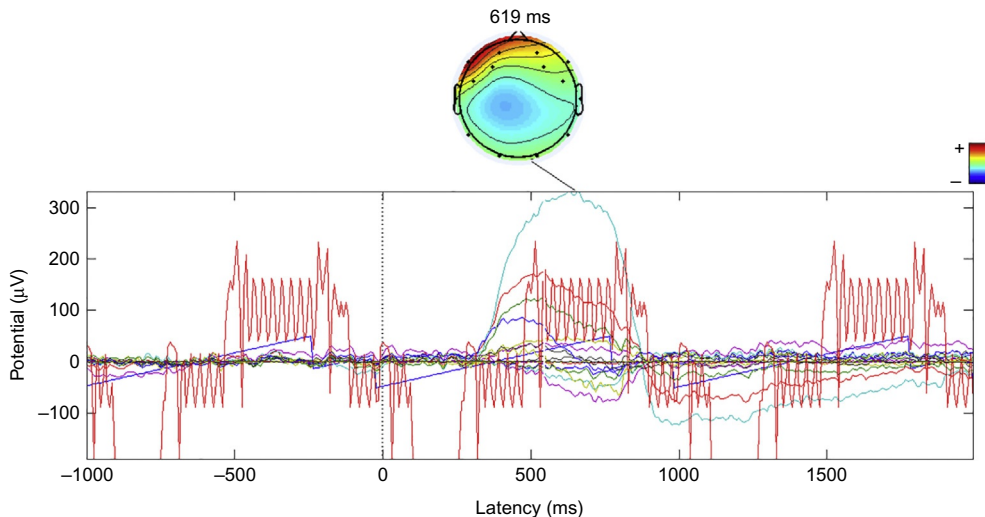


Fig. 4.6 Forced single eyeblink-specific average event-related potential waveform plot of subject one. A 2D scalp map plotted at latency 619 ms indicates maximum potential concentration (*bright red color*) across left frontal regions.

maps can be plotted at specific latencies of interest by clicking on the acquired ERP waveform in MATLAB workspace of EEGLAB toolbox. Here, the latency point is selected to show the average potential concentration across the instant of peak ERP amplitude (619 ms). The single eyeblink-specific ERP components are found approximately after 300 ms of onset of the performed action. It is also observed that being a voluntary action, it involves a high level of neural cognition. The onset of action is indicated by a “start” marker (vertical blue line) introduced at 0 ms.

The topographic analysis has been elaborated by plotting single eyeblink-specific scalp map series at distinct set of latencies. A set of 2D and 3D scalp maps have been plotted at latencies 400, 500, 600, 700, 800, and 900 ms in Figs. 4.7 and 4.8, respectively. These scalp maps indicate an average distribution of forced eyeblink-specific ERPs across the distinct regions of cerebral cortex. The bright red color indicates the maximum potential concentration followed by green and blue. Therefore, the maximum neural component activity is found at red-colored scalp regions and minimum neural component activity is found around blue-colored scalp regions. It can be observed from Figs. 4.7 and 4.8 that the left frontal regions of cerebral cortex are found to possess maximum potential distribution during the performed action. The scalp maps are plotted around the latency points

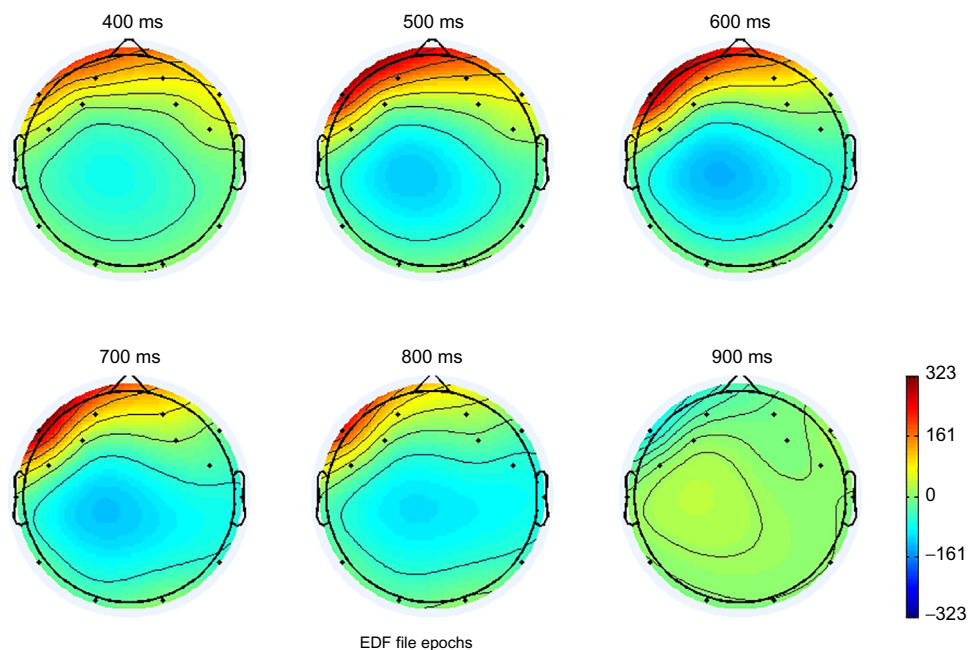


Fig. 4.7 Forced single eyeblink-specific 2D scalp map series plotted at distinct latency points for subject one. Left frontal regions of cerebral cortex plotted around the latency points (600 ms) of maximum ERP amplitude are found to possess maximum potential concentration (*bright red color*) during the performed action. The potential concentration decreases at the latency points farther than the voluntary action onset points as shown by the scalp map plotted at latency point of 900 ms.

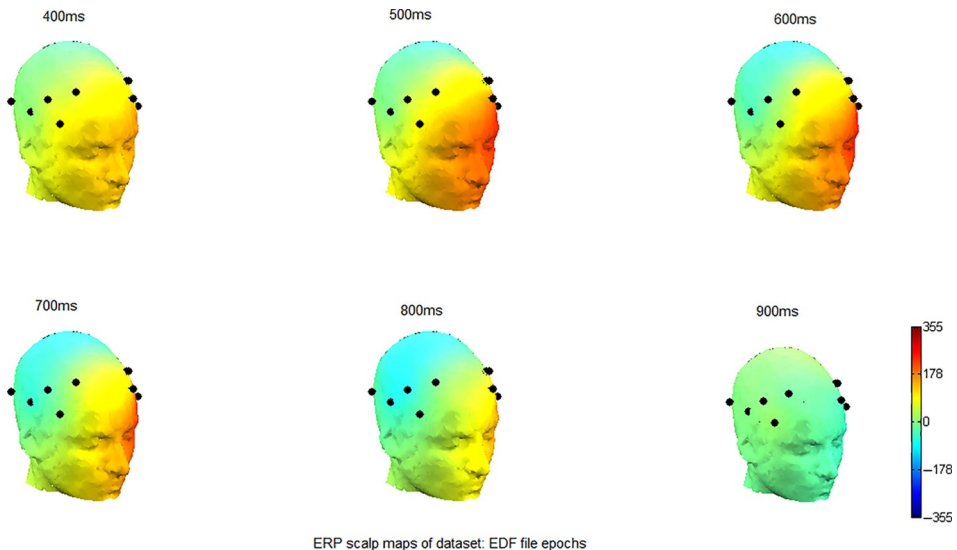


Fig. 4.8 Forced single eyeblink-specific 3D scalp map series plotted at distinct latency points for subject one. Left frontal regions of cerebral cortex plotted around the latency points of maximum ERP amplitude are found to possess maximum potential concentration (*bright red color*) during the performed action. The potential concentration decreases at the latency points farther than the voluntary action onset points as shown by the scalp map plotted at latency point of 900ms.

of maximum ERP amplitude to observe the activated brain regions. The left frontal regions include AF3 and F7 scalp channels of EMOTIV headset unit. It reflects that the neural activity correlated to deliberate single eyeblink action can be captured prominently at the left frontal channels of EMOTIV neural head set unit and hence, is selected for further analysis.

The single eyeblink-specific individual EEG-signal epochs captured at distinct frontal, temporal, parietal, and occipital scalp channels have also been plotted as shown in [Fig. 4.9](#). The acquired multichannel EEG dataset has been imported to EEGLAB and individual channel epochs for single eyeblink action have been extracted. A high variation in ERP is reflected at frontal channels AF3, F7, AF4, and F8. If we observe more precisely, the left frontal channels AF3 and F7 are found to show even higher potential activation as compared to right frontal channels AF4 and F8. Keeping these primary observations as reference, the EEG signals captured at channel AF3 and F7 are selected for further analysis and algorithm development. The topographic map analysis and extracted EEG-signal epochs at each scalp channel represents the index of neuronal activity during the selected cognitive, motor, affective, and any stimulated task. The individual EEG-signal epoch traces of subject one captured at left frontal scalp channels AF3 and F7 corresponding to the performed voluntary eyeblink action are plotted in [Figs. 4.10](#) and [4.11](#), respectively.

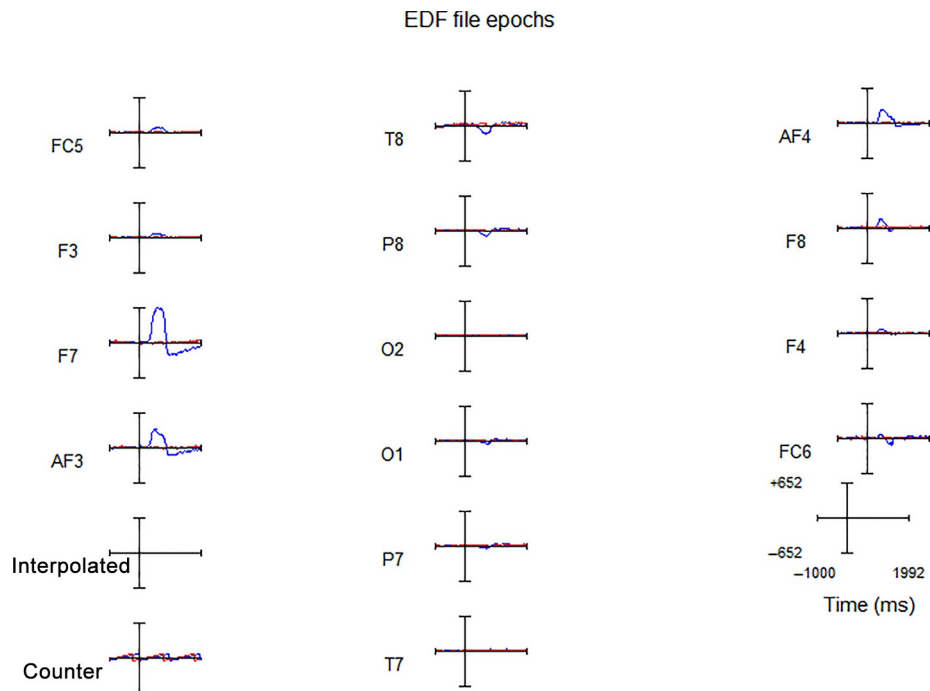


Fig. 4.9 Single eyeblink-specific EEG-signal epochs of subject one captured at distinct scalp channels of EMOTIV EEG neuroheadset unit.

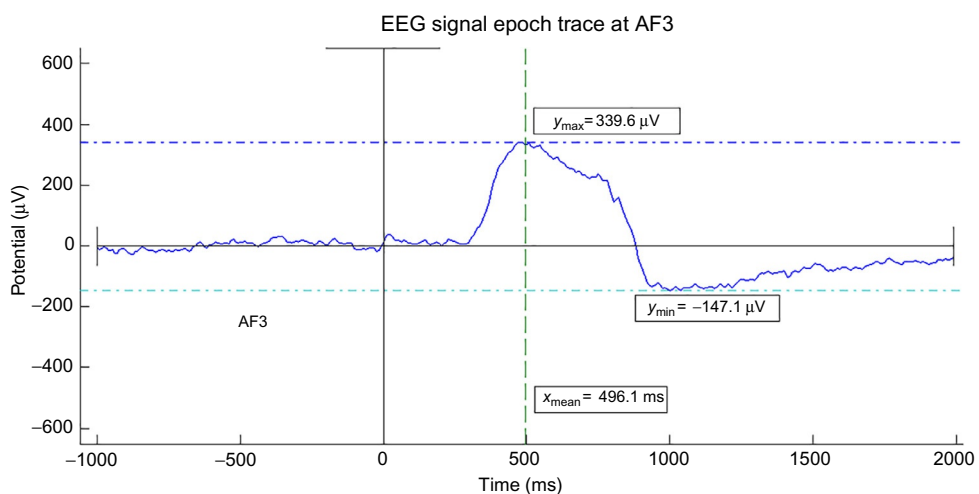


Fig. 4.10 Forced single eyeblink-specific EEG-signal epoch trace at left frontal channel AF3.

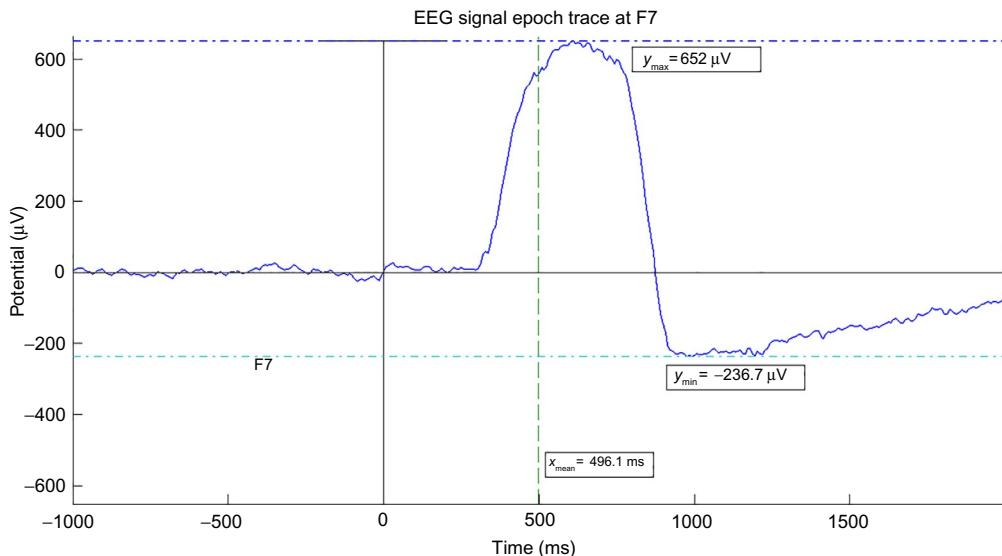


Fig. 4.11 Forced single eyeblink-specific EEG-signal epoch trace at left frontal channel F7.

The performed thoughtful action can be perfectly identified by a substantial increase in the corresponding ERP from 0 to $339.6 \mu\text{V}$ at channel AF3 and from 0 to $652 \mu\text{V}$ at channel F7, respectively. The ERP amplitudes specific to forced single eyeblink are observed at late latencies after around 300 ms of onset of the performed action. More precisely, the ERPs are found to be maximum around 500 ms at both left frontal channels AF3 and F7 as depicted in Figs. 4.10 and 4.11, respectively. This indicates the high level of cognition and neural processing involved in a thoughtful eyeblink action. The detailed ERP analysis including minimum/maximum values, mean, median, mode, standard deviation, and range are calculated for both the channels (AF3 and F7) and are tabulated in Tables 4.1 and 4.2, respectively.

Table 4.1 Forced eyeblink-specific event-related potential (ERP) analysis at channel AF3

ERP specifications	Latency values (ms)	Potential amplitude (μV)
--------------------	---------------------	---------------------------------------

Minimum ERP	-1000	-147.1
Maximum ERP	1992	339.6
Mean ERP	496.1	11.47
Median	496.1	-7.332
Mode	-1000	8.309
Standard deviation	867.2	121.4
Range	2992	486.7

Table 4.2 Forced eyeblink-specific event-related potential (ERP) analysis at channel F7

ERP specifications	Latency values (ms)	Potential amplitude (μ V)
Minimum ERP	-1000	-236.7
Maximum ERP	1992	652
Mean ERP	496.1	26.95
Median	496.1	-3.101
Mode	-1000	-3.87
Standard deviation	867.2	241.5
Range	2992	888.7

This section also includes channel statistics analysis performed for the activated channel during forced single eyeblink action. It has been observed that left frontal lobe channels AF3 and F7 show maximum ERP activation. The correlated channel statistics are obtained by calculating deviation from Gaussian channel activity distribution and are depicted in Fig. 4.12. The plot shows the component activation across the scalp channel—3 (AF3) of EMOTIV EEG neuroheadset unit. A voluntary single eyeblink action-specific acquired EEG dataset at channel AF3 has been plotted with respect to normal distribution trace. A deviation in distribution trace of acquired EEG dataset from normal distribution is clearly visible in the data versus standard normal plot. Therefore, the performed eyeblink action is identified as the resultant deviation in the traces. Instead of normal distribution plot for relaxed neural state, a right skewed (with skewness value 1.97) and highly peaked (with kurtosis value 5.22) non-Gaussian distributed plot is attained for a thoughtful eyeblink action.

The set of results obtained by analyzing EEG-signal dataset of rest of four subjects is also presented and discussed in detail. The averaged ERPs of multichannel EEG epochs acquired from subject two, three, four, and five are plotted in Fig. 4.13A–D, respectively.

The averaged ERPs are found to be maximum at the selected latency points, viz., 1039 ms (Fig. 4.13A: subject two), 875 ms (Fig. 4.13B: subject three), 813 ms (Fig. 4.13C: subject four), and 1188 ms (Fig. 4.13D: subject five), respectively. The scalp maps plotted above ERP traces at the selected latencies indicate the maximum potential distribution across frontal regions of cerebral cortex during voluntary single eyeblink action. The detailed 2D and 3D scalp map topographic analysis has been presented at different set of latencies for all the subjects. The activated scalp regions have been identified by plotting scalp maps around the latency points of maximum ERP amplitudes. For subject two, the peak ERP values are obtained at latency point 1039 ms (Fig. 4.13A). As a result, the corresponding 2D and 3D scalp maps have been plotted at latencies 700, 800, 900, 1000, 1100, and 1200 ms as depicted in Fig. 4.14A and B, respectively. Similarly,

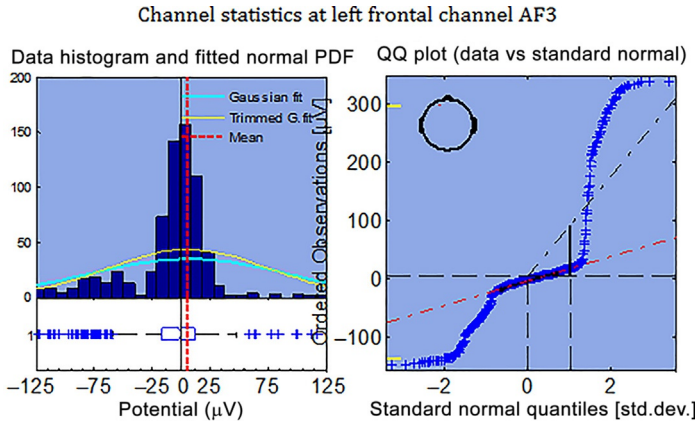


Fig. 4.12 Forced eyeblink-specific channel statistics captured at channel AF3.

the peak ERP values for third subject are obtained at latency point 875 ms ([Fig. 4.13B](#)). The corresponding 2D and 3D scalp maps have been plotted at latencies 600, 700, 800, 900, 1000, and 1100 ms as depicted in [Fig. 4.15A](#) and B, respectively. For fourth subject, the peak ERP values are obtained at latency point 813 ms ([Fig. 4.13C](#)). The corresponding 2D and 3D scalp maps have been plotted at latencies 600, 700, 800, 900, 1000, and 1100 ms as depicted in [Fig. 4.16A](#) and B, respectively. For fifth subject, the peak ERP values are obtained at latency point 1188 ms ([Fig. 4.13D](#)). The corresponding 2D and 3D scalp maps have been plotted at latencies 900, 1000, 1100, 1200, 1300, and 1400 ms as depicted in [Fig. 4.17A](#) and B, respectively. It is clearly observed from scalp maps plotted for all the subjects that maximum potential distribution is found across left frontal regions of cerebral cortex during voluntary eyeblink action.

The ERPs across activated regions of brain have been quantified by extracting the single eyeblink-specific multichannel EEG-signal epochs. The EEG epochs captured at individual scalp regions for each subject have been plotted in [Fig. 4.18A](#) (subject two), [4.18B](#) (subject three), [4.18C](#) (subject four), and [4.18D](#) (subject five), respectively.

It can be clearly observed from the above multichannel EEG traces that left frontal channels AF3 and F7 possess high event-related potentials in all plotted set of waveforms. The similar set of observations have been recorded during the EEG-signal analysis of subject one. The single eyeblink-specific ERP variations have been further quantified by plotting EEG-signal traces of each subject across left frontal channels AF3 and F7. The resultant EEG-signal epochs are plotted in [Fig. 4.19A](#) (AF3 channel, subject two), [4.19B](#) (F7 channel, subject two); [Fig. 4.20A](#) (AF3 channel, subject three), [4.20B](#) (F7 channel, subject three); [Fig. 4.21A](#) (AF3 channel, subject four), [4.21B](#) (F7 channel, subject four); and [Fig. 4.22A](#) (AF3 channel, subject five), [4.22B](#) (F7 channel, subject five), respectively.

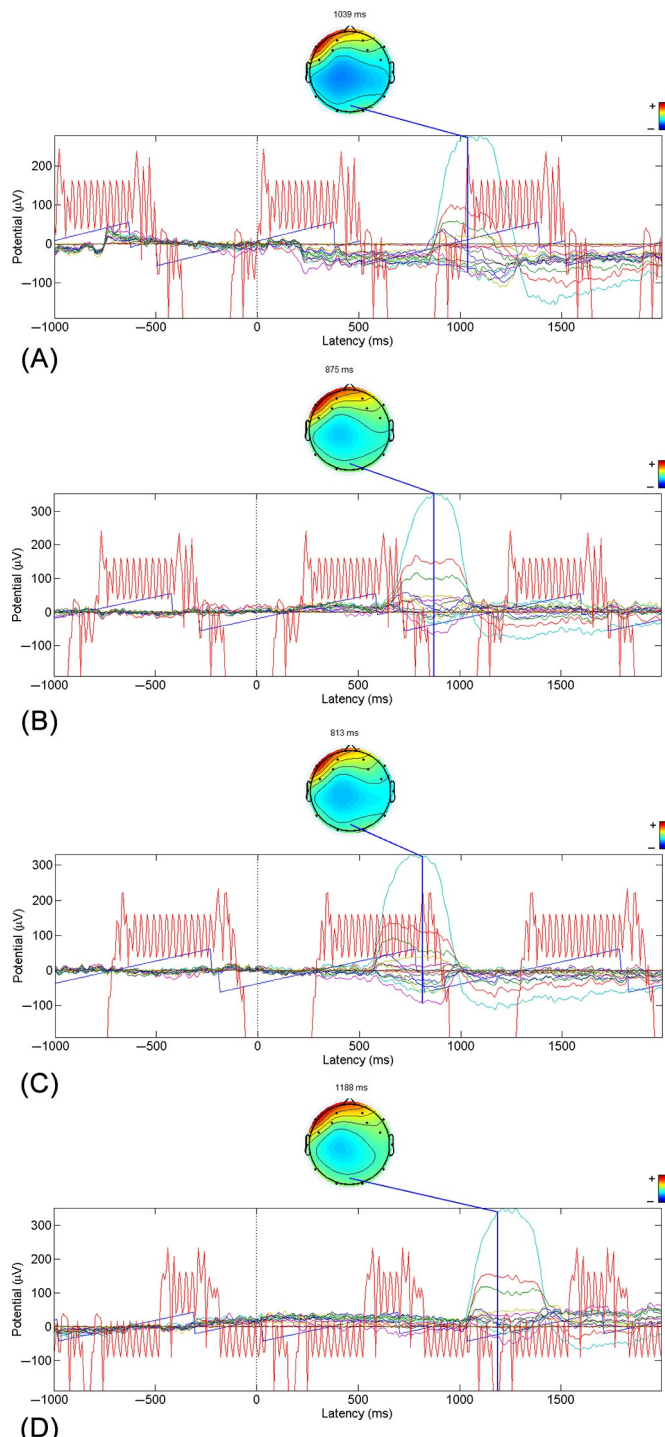


Fig. 4.13 Forced single eyeblink-specific average event-related potential waveform (A) plot of subject two. A 2D scalp map plotted at latency 1039 ms indicates maximum potential concentration (bright red color) across left frontal regions. (B) Plot of third subject. A 2D scalp map plotted at latency 875 ms indicates maximum potential concentration across left frontal regions. (C) Plot of fourth subject. A 2D scalp map plotted at latency 813 ms indicates maximum potential concentration across left frontal regions. (D) Plot of fifth subject. A 2D scalp map plotted at latency 1188 ms indicates maximum potential concentration across left frontal regions.

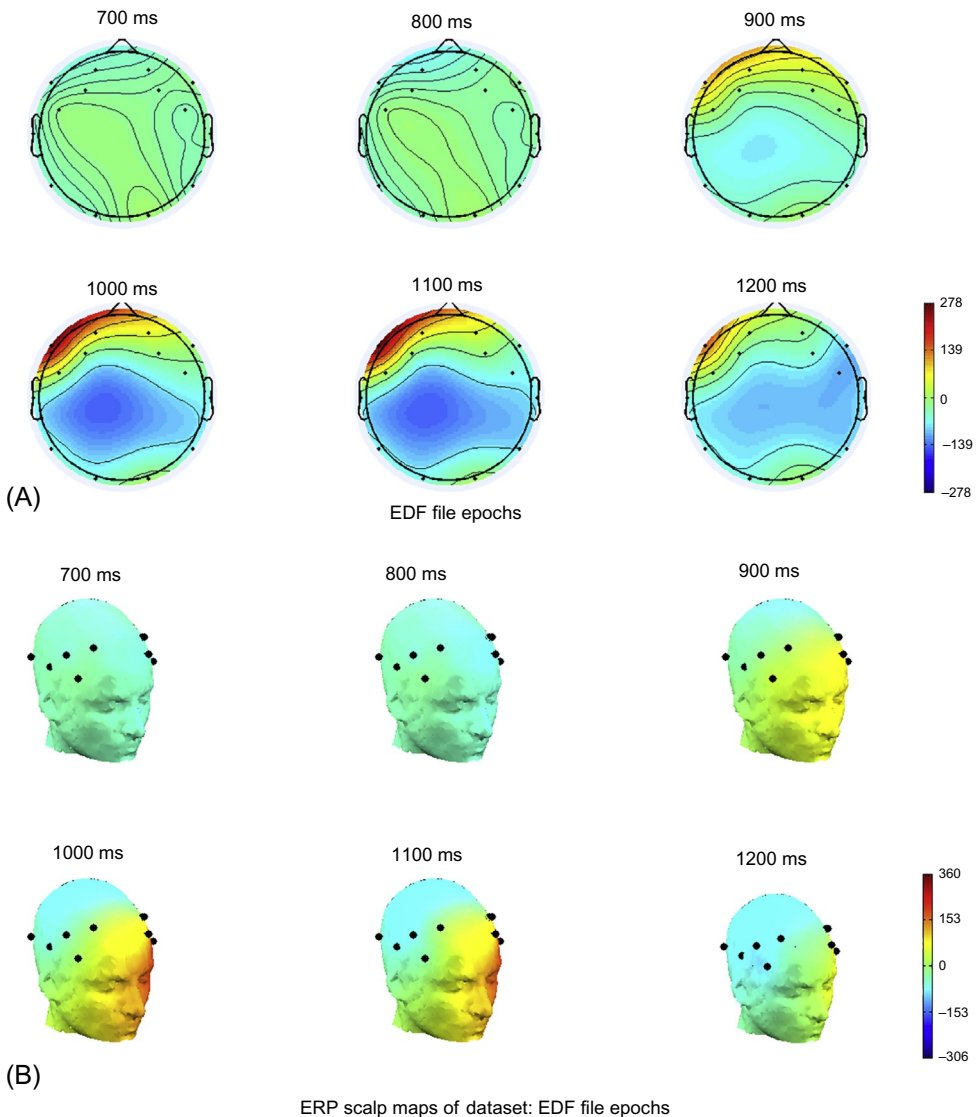


Fig. 4.14 Forced single eyeblink-specific (A) 2D and (B) 3D scalp map series plotted at distinct latency points for second subject. Left frontal regions of cerebral cortex plotted around the latency points (1000 ms) of maximum ERP amplitude are found to possess maximum potential concentration during the performed action. The potential concentration decreases at the latency points farther than the voluntary action onset points as shown by the scalp maps plotted at latency points of 700, 800, and 1200 ms.

The thoughtful action performed by subject two can be perfectly identified by a substantial increase in the corresponding ERP from 0 to $99.67\mu\text{V}$ at channel AF3 and from 0 to $278.4\mu\text{V}$ at channel F7, as shown in Fig. 4.19A and B, respectively. A similar incidence of results has been observed for rest of the EEG dataset acquired from subject number three, four, and five, respectively. Fig. 4.20A and B show rise in ERPs from

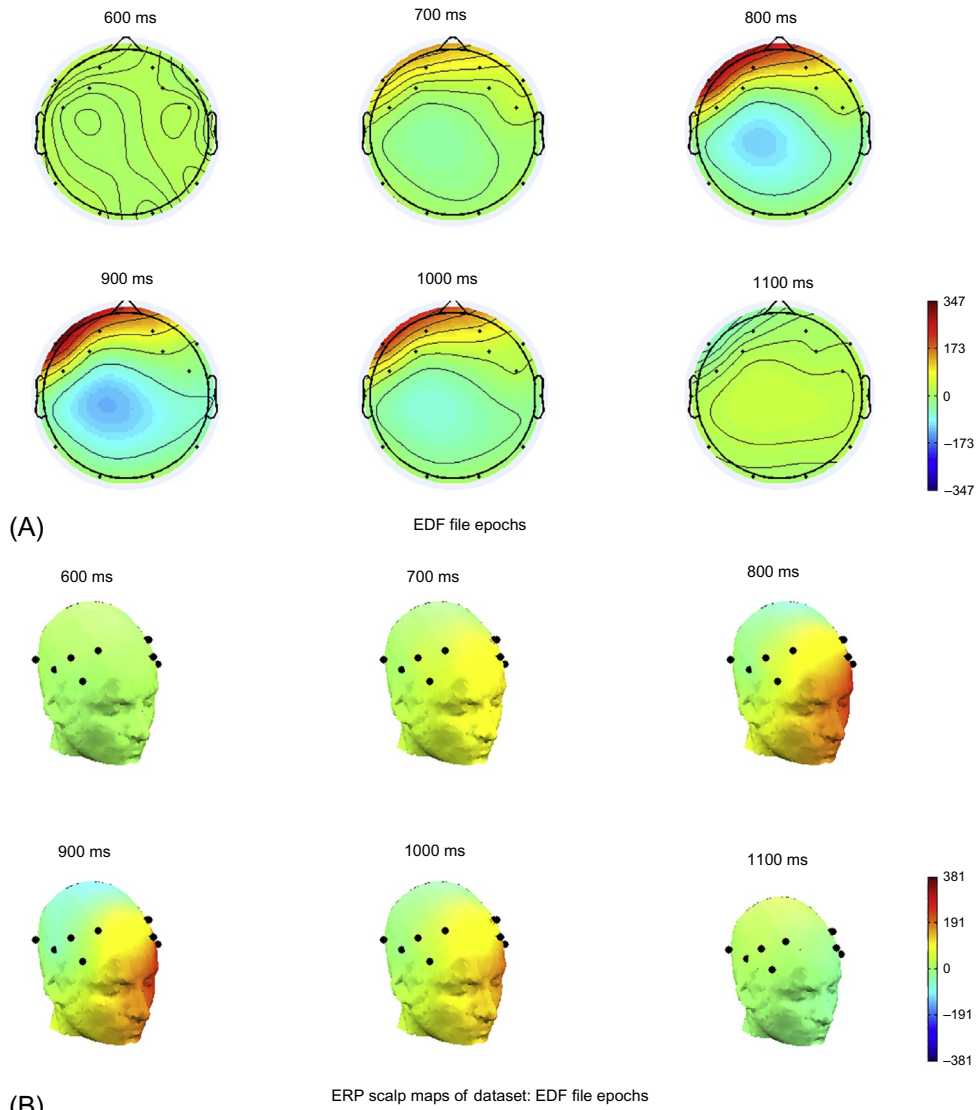


Fig. 4.15 Forced single eyeblink-specific (A) 2D and (B) 3D scalp map series plotted at distinct latency points for third subject. Left frontal regions of cerebral cortex plotted around the latency points (875 ms) of maximum ERP amplitude are found to possess maximum potential concentration during the performed action. The potential concentration decreases at the latency points farther than the voluntary action onset points as shown by the scalp maps plotted at latency points of 600 and 1100 ms.

0 to 168.5 μ V at AF3 and 0 to 352.9 μ V at F7 electrode for third subject. The EEG epoch traces of subject number four also show a similar increasing trend in respective ERP amplitudes at AF3 channel (from 0 to 136.2 μ V) and F7 channel (from 0 to 331.1 μ V) as plotted in Fig. 4.21A and B, respectively. The rise in deliberate single eyeblink-specific

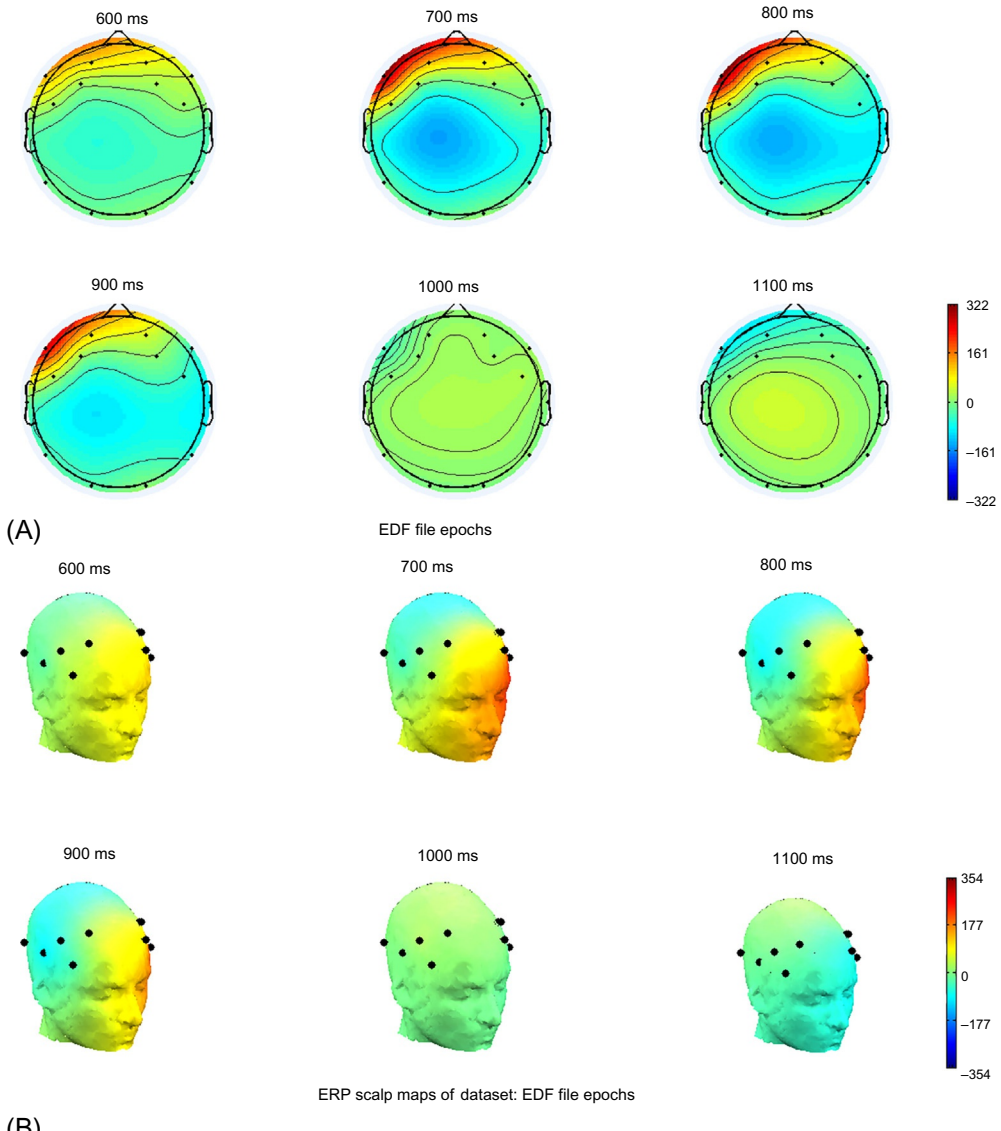


Fig. 4.16 Forced single eyeblink-specific (A) 2D and (B) 3D scalp map series plotted at distinct latency points for fourth subject. Left frontal regions of cerebral cortex plotted around the latency points (813 ms) of maximum ERP amplitude are found to possess maximum potential concentration during the performed action. The potential concentration decreases at the latency points farther than the voluntary action onset points as shown by the scalp maps plotted at latency points of 1000 and 1100 ms.

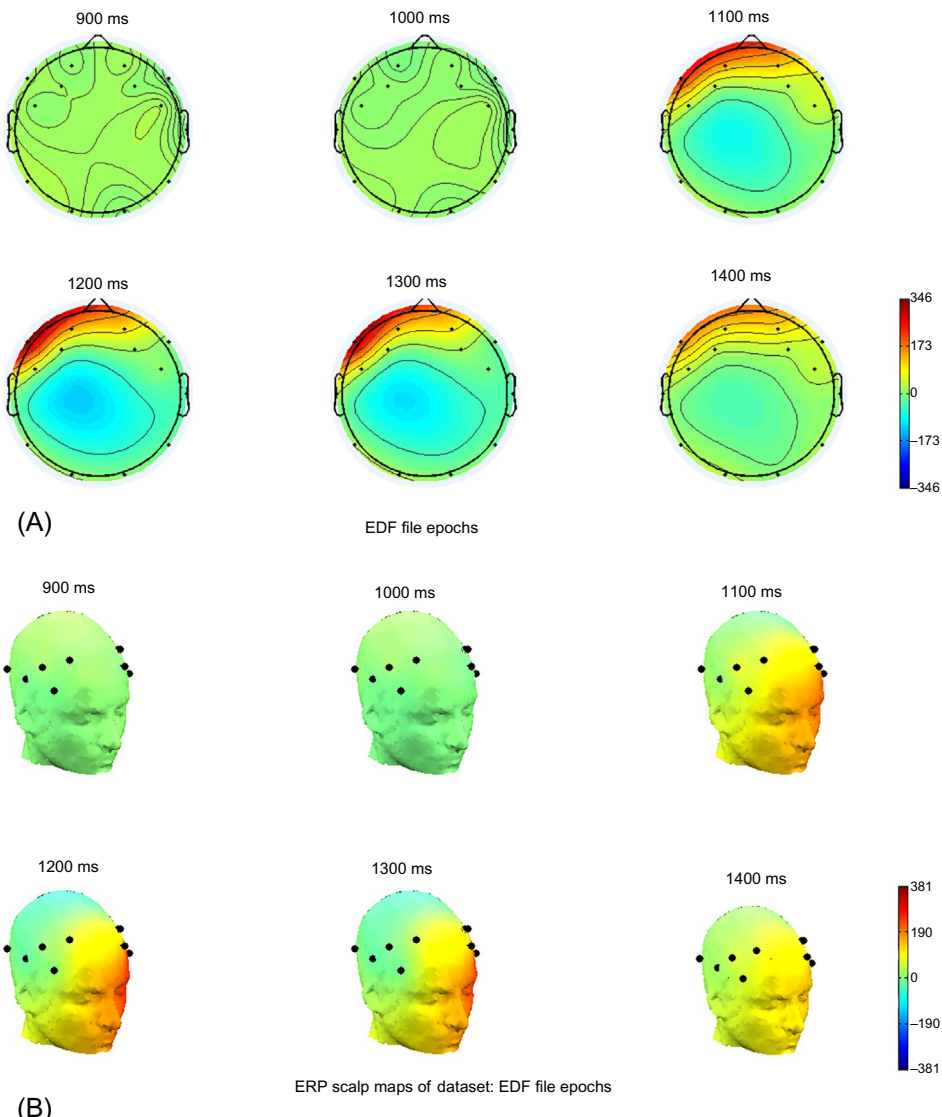


Fig. 4.17 Forced single eyeblink-specific (A) 2D and (B) 3D scalp map series plotted at distinct latency points for fifth subject. Left frontal regions of cerebral cortex plotted around the latency points (1188 ms) of maximum ERP amplitude are found to possess maximum potential concentration during the performed action. The potential concentration decreases at the latency points farther than the voluntary action onset points as shown by the scalp maps plotted at latency points of 900 and 1000 ms.

ERPs at channel AF3 (from 0 to 155.6 μ V) and channel F7 (from 0 to 351.9 μ V) for subject number five has been recorded as shown in Fig. 4.22A and B, respectively. It is clearly observed that a high incidence of similarity in time-domain analysis results has been found with EEG dataset of all the five subjects.

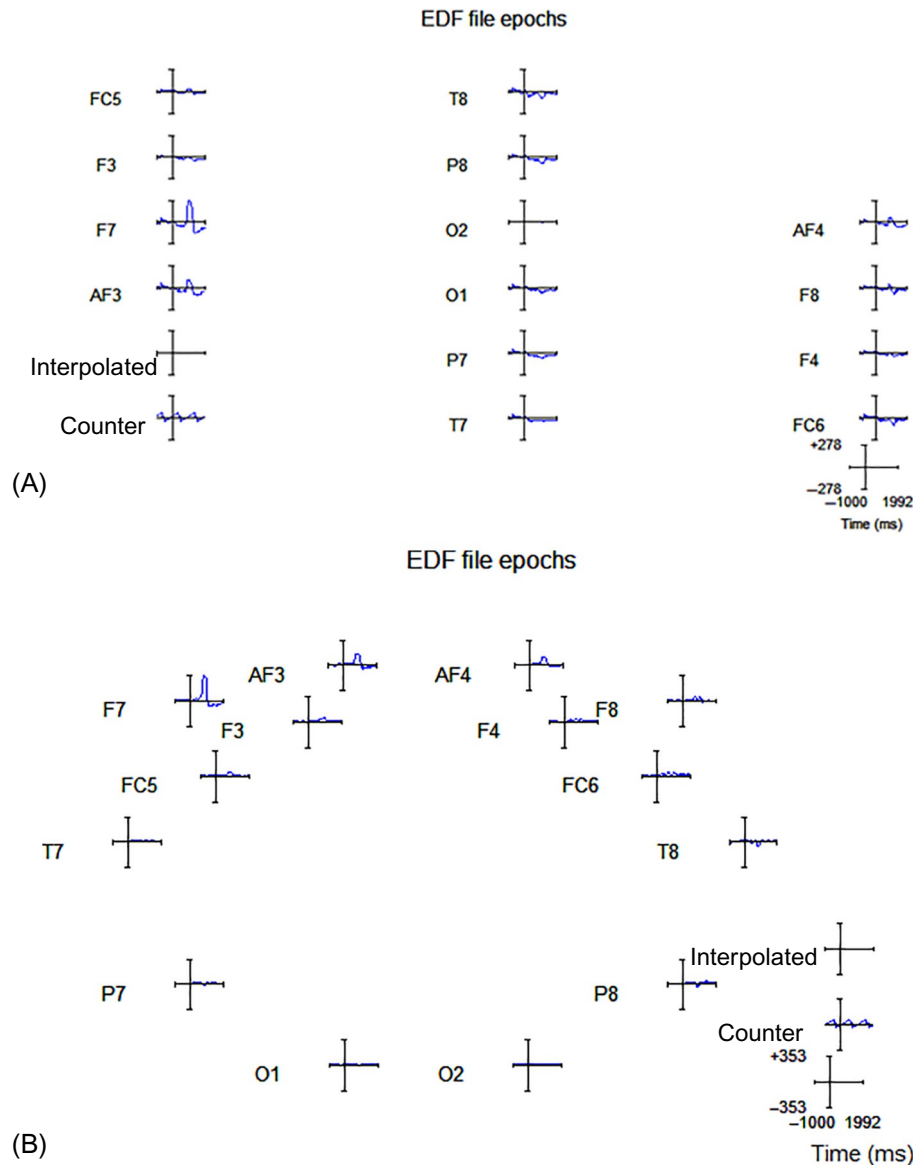


Fig. 4.18 Single eyeblink-specific EEG-signal epochs of (A) subject two, (B) third subject,
(Continued)

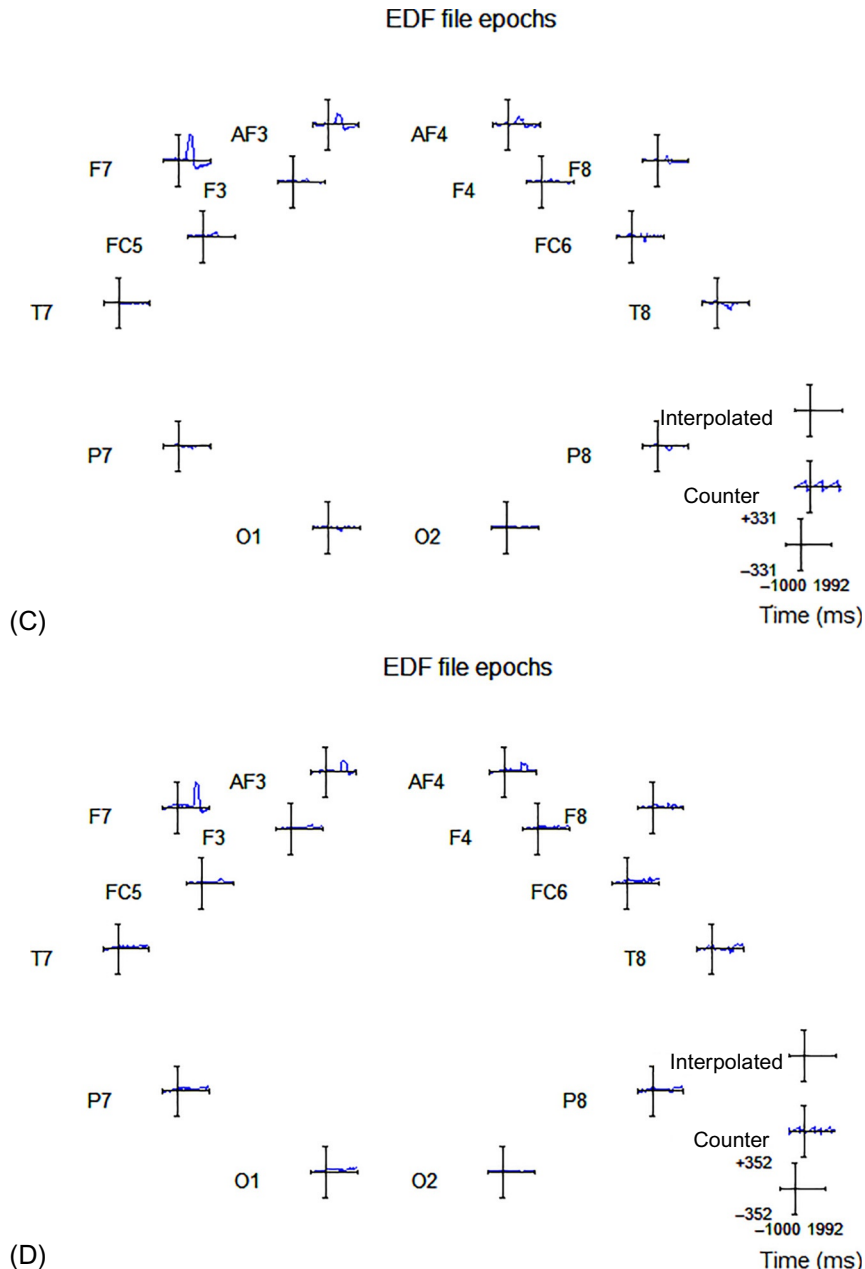


Fig. 4.18—cont'd (C) fourth subject, and (D) fifth subject, captured at distinct scalp channels of EMOTIV EEG neuroheadset unit.

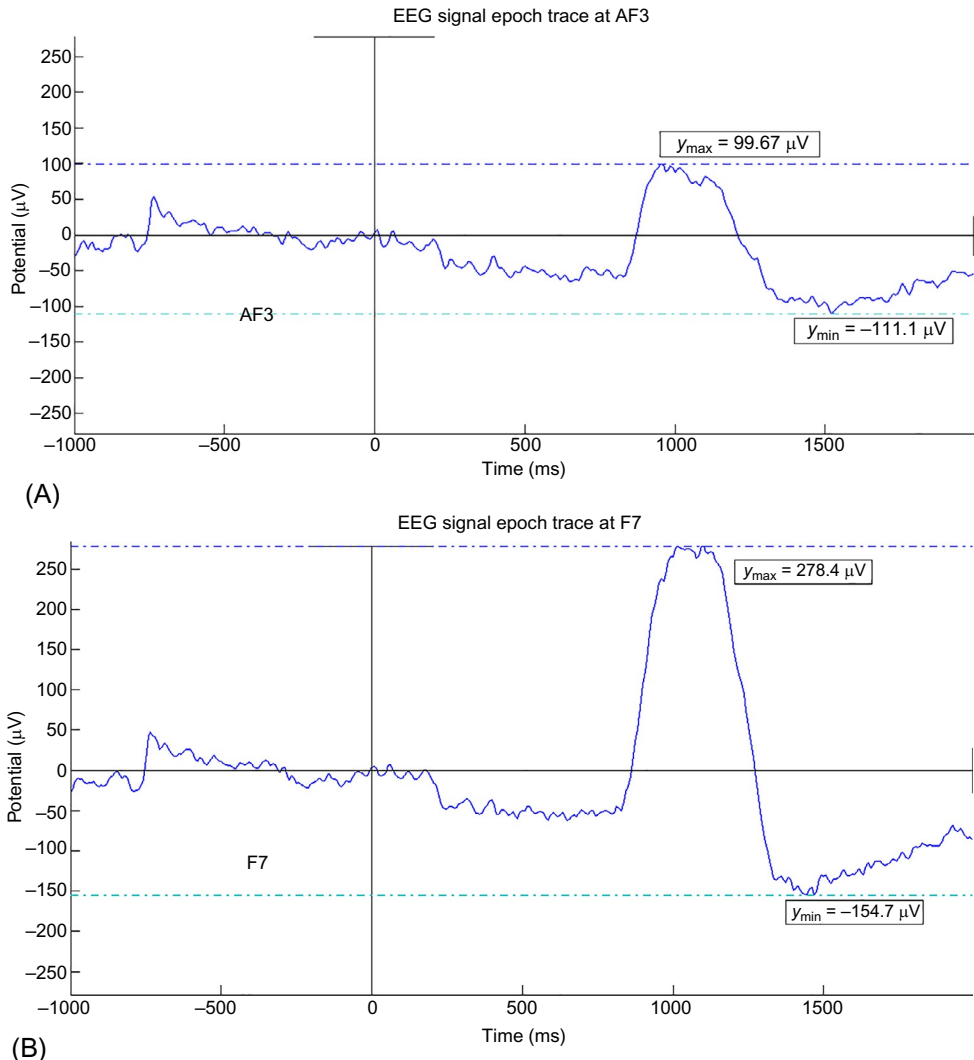


Fig. 4.19 Forced single eyeblink-specific EEG-signal epoch trace captured at left frontal channel (A) AF3 and (B) F7 of subject two.

The obtained values of ERPs at left frontal channels justify our initial hypothesis of neural component activation in response to a thoughtful eyeblink action. An identified high variation in ERPs on the onset of deliberate action shall be utilized as control signal to design an algorithm and framework to implement neural control applications of interest. A set of in house control applications has been developed to translate attained neural ERP component activation into action, viz., to automatically play a MATLAB audio file “*handel.mat*” (Bansal et al., 2015) and to control the glowing instances of a light-emitting

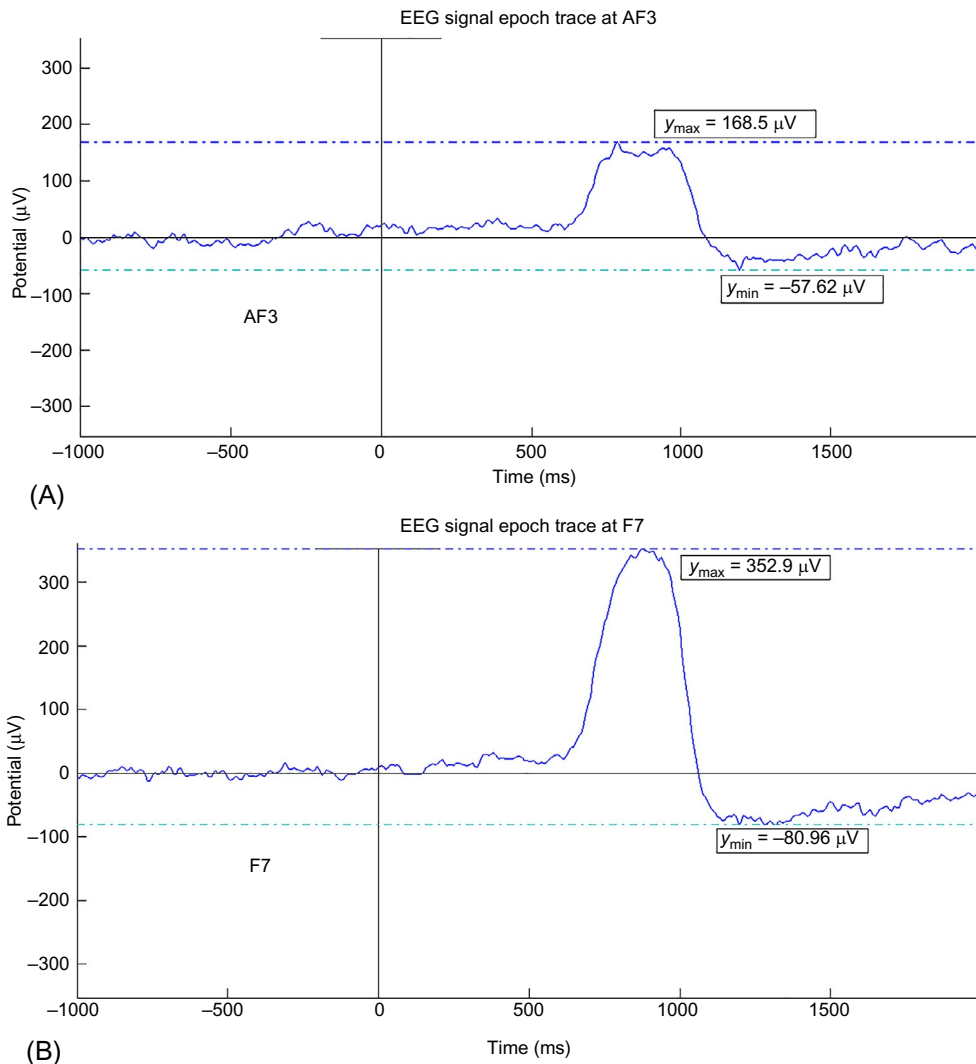


Fig. 4.20 Forced single eyeblink-specific EEG-signal epoch trace captured at left frontal channel (A) AF3 and (B) F7 of subject three.

diode (LED) (Mahajan and Bansal, 2017). It has been implemented by interfacing a LED with ARDUINO board. The identified high ERP component variations from MATLAB workspace have been translated into control commands to drive the interfaced device (LED here) via ARDUINO. The step-by-step detailed procedure is included in Chapter 6. This reflects that the intentional eyeblink-specific EEG-activated components have the potential to be used as a trigger to develop rehabilitative BCIs. Furthermore, the

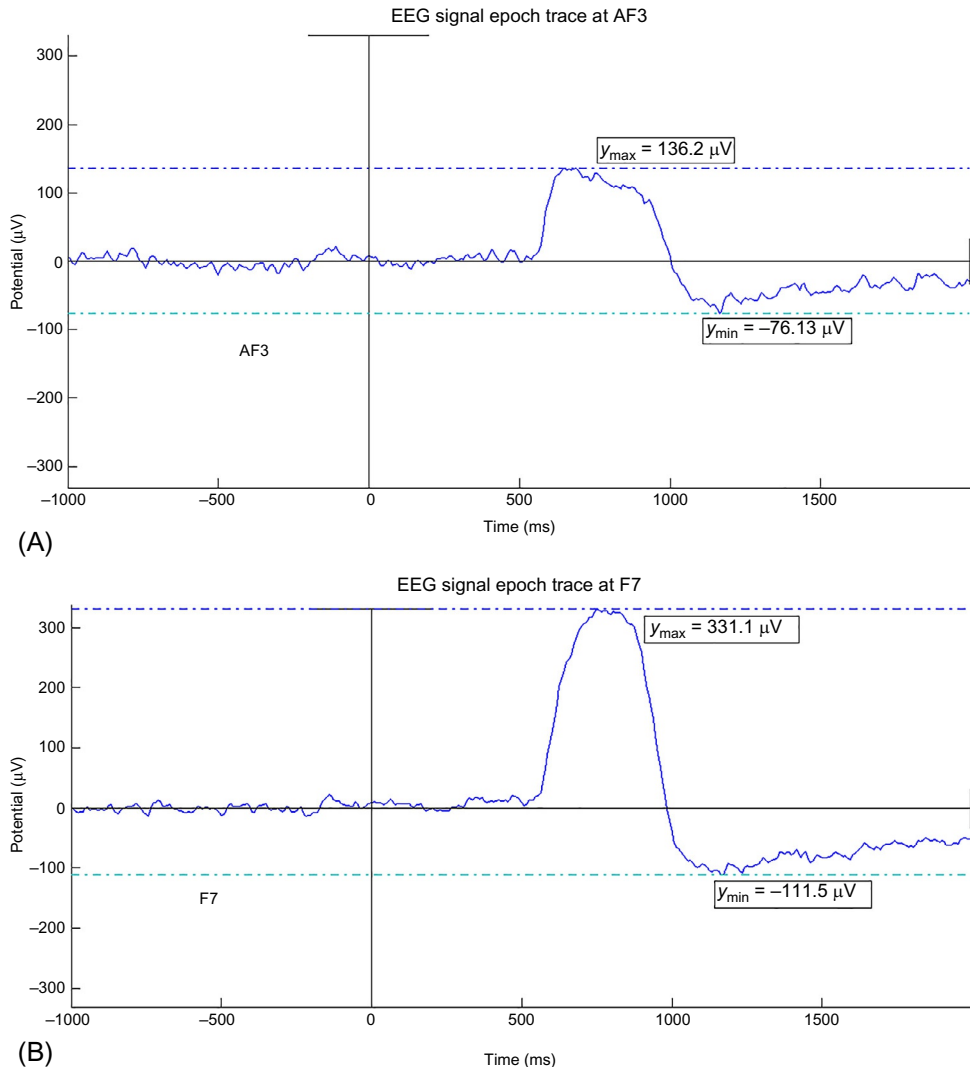


Fig. 4.21 Forced single eyeblink-specific EEG-signal epoch trace captured at left frontal channel (A) AF3 (B) F7 of subject four.

ERP-based BCIs possess high throughput due to their short latency period. However, ERP are low amplitude signals and are mostly suppressed by the background neural activity. Therefore, an attempt has been made in [Chapter 5](#) to use hybrid features of EEG (combination of both time domain: ERP related and frequency domain: power spectrum-related features) instead of individual domain features to detect the correlated neural state.

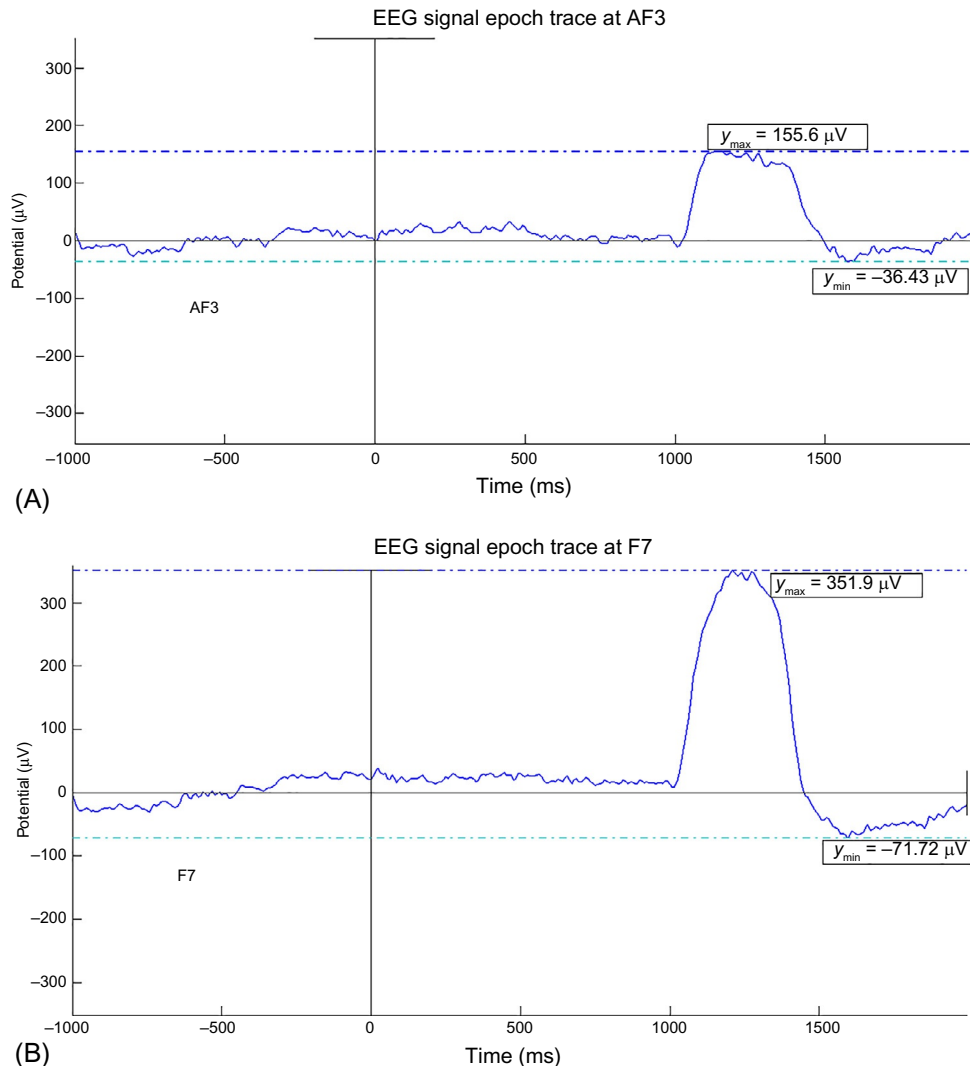


Fig. 4.22 Forced single eyeblink-specific EEG-signal epoch trace captured at left frontal channel (A) AF3 and (B) F7 of subject five.

4.6 CONCLUSION

An exponential growth has been observed in the development of BCIs. However, Cognitive neuroscience particularly for the development of efficient BCIs for device control applications is gaining importance in the current scenario. The remarkable innovations toward implementation of more interactive and control application specific BCIs has been proved to provide enhanced assistance to paralytic subjects to restore a normal life.

This chapter presents a framework to implement a real-time BCI for control applications using forced eyeblink action-specific EEG responses. A detailed methodology to preprocess and analyze the acquired multichannel brain patterns has been discussed. The eyeblink activity-related maximum temporally and spatially independent distinct neural components have been identified by exploring a fourth-order spectra-based ICA. The artifact-free clean EEG patterns have been analyzed in time and spatial domain to identify the action correlated neural state and activated lobes of cerebral cortex. The topographic analysis of 2D and 3D scalp maps has been performed. A high potential concentration is found across left frontal scalp channels (AF3 and F7) of EMOTIV EEG neuroheadset unit. Distinct EEG-signal epochs at individual channels have been extracted from acquired multichannel EEG dataset. This aims toward understanding the underlying neural dynamics locked to cognitive/motor/affective/stimulated action of interest. A significant rise in ERPs has been observed at left frontal brain regions. The corresponding EEG component epochs have been extracted to visualize and record the ERP variations at the onset of forced eyeblink action. The recorded ERP variations in eyeblink specific EEGs have been utilized to develop a control algorithm in MATLAB. It uses captured EEG variations as a trigger to perform selected control actions/or control an output interfaced device. The details have been included in Chapter 6. The above findings reflect that the captured ERP variations from input EEG dataset possess the potential to be used as a trigger to implement device control applications. The cognitive analysis findings in time domain can further be utilized to develop intelligent interfaces for neural output driven assistive devices. It is implemented by translating thoughtful intentions into device control signals which could drive external assistive devices for rehabilitation of physically locked-in patients.

REFERENCES

- Ahmad, N., Ariffin, R., Ghazilla, R., Hakim, M.Z., Azizi, M.D., 2016. Steady state visual evoked potential based Bci as control method for exoskeleton: a review. *Malaysian J. Public Health Med.* 1, 86–94.
- Bansal, D., Mahajan, R., Roy, S., Rathee, D., Singh, S., 2015. Real time man machine interface and control using deliberate eye blink. *Int. J. Biomed. Eng. Technol.* 18 (4), 370–384.
- Bi, L., Fan, X.A., Liu, Y., 2013. EEG-based brain-controlled mobile robots: a survey. *IEEE Transact. Human-Mach. Syst.* 43 (2), 161–176.
- Bugli, C., Lambert, P., 2007. Comparison between principal component analysis and independent component analysis in electroencephalograms modeling. *Biom. J.* 49 (2), 312–327.
- Cecotti, H., Graser, A., 2011. Convolutional neural networks for P300 detection with application to brain-computer interfaces. *IEEE Trans. Pattern Anal. Mach. Intell.* 33 (3), 433–445.
- Chambayil, B., Singla, R., Jha, R., 2010. In: Virtual keyboard BCI using eye blinks in EEG. IEEE 6th International Conference on Wireless and Mobile Computing, Networking and Communications (WiMob). <https://doi.org/10.1109/WIMOB.2010.5645025>.
- Collis, W.B., White, P.R., Hammond, J.K., 1998. Higher-order spectra: the bispectrum and trispectrum. *Mech. Syst. Signal Process.* 12 (3), 375–394.
- Deecke, L., 1969. Distribution of readiness potential, pre-motion positivity, and motor potential of the human cerebral cortex preceding voluntary finger movement. *Exp. Brain Res.* 7, 158–168.

- Delorme, A., Makeig, S., 2004. EEGLAB: an open source toolbox for analysis of single-trial EEG dynamics. *J. Neurosci. Methods* 134, 9–21.
- Delorme, A., Sejnowski, T., Makeig, S., 2007. Enhanced detection of artifacts in EEG data using higher-order statistics and independent component analysis. *NeuroImage* 34, 1443–1449.
- Escolano, C., Antelis, J.M., Minguez, J., 2012. A telepresence mobile robot controlled with a noninvasive brain—computer interface. *IEEE Trans. Syst. Man Cybern. B* 42 (3), 793–804.
- Jia, W., Zhao, X., Liu, H., Gao, X., Gao, S., Yang, F., 2004. Classification of single trial EEG during motor imagery based on ERD. *Conf. Proc. IEEE Eng. Med. Biol. Soc.* 1, 5–8.
- Joyce, C.A., Gorodnitsky, I.F., Kutas, M., 2004. Automatic removal of eye movement and blink artifacts from EEG data using blind component separation. *Psychophysiology* 41 (2), 313–325.
- Kalcher, J., Flotzinger, D., Neuper, C., Golly, S., Pfurtscheller, G., 1996. Graz brain-computer interface II: towards communication between humans and computers based on online classification of three different EEG patterns. *Med. Biol. Eng. Comput.* 34 (5), 382–388.
- Li, Y., Yu, T., 2015. In: EEG-based hybrid BCIs and their applications.3rd International Winter Conference on Brain-Computer Interface (BCI), IEEE Xplore. <https://doi.org/10.1109/IWW-BCI.2015.7073035>.
- Luck, J.S., 2005. An Introduction to the Event-Related Potential Technique. MIT Press. pages 374, 0262122774, 9780262122771.
- Mahajan, R., Bansal, D., 2017. Real time EEG based cognitive brain computer interface for control applications via Arduino interfacing. *Procedia Comput. Sci.* 115, 812–820.
- Onton, J., Makeig, S., 2006. Information-based modeling of event-related brain dynamics. *Prog. Brain Res.* 159, 99–120. [https://doi.org/10.1016/S0079-6123\(06\)59007-7](https://doi.org/10.1016/S0079-6123(06)59007-7).
- Pathirage, I., Khokar, K., Klay, E., Alqasemi, R., Dubey, R., 2013. In: A vision based P300 brain computer interface for grasping using a wheelchair-mounted robotic arm.2013 IEEE/ASME International Conference on Advanced Intelligent Mechatronics (AIM), pp. 188–193.
- Peters, B.O., Pfurtscheller, G., Flyvbjerg, H., 1998. Mining multichannel EEG for its information content: an ANN-based method for a brain-computer interface. *Neural Netw.* 11, 1429–1433.
- Pradhan, C., Jena, S.K., Nadar, S.R., Pradhan, N., 2012. Higher-order spectrum in understanding nonlinearity in EEG rhythms. *Comput. Math. Methods Med.* 2012. 206857, 8 pages. <https://doi.org/10.1155/2012/206857>.
- Shi, B.G., Kim, T., Jo, S., 2010. Non-invasive Brain Signal Interface for a Wheelchair Navigation. In: Proceedings of International Conference on Control Automation and Systems, Gyeonggi-do, Korea, pp. 2257–2260.
- Smith, D.J., Varghese, L.A., Stepp, C.E., Guenther, F.H., 2014. Comparison of steady-state visual and somatosensory evoked potentials for brain-computer interface control. *Conf. Proc. IEEE Eng. Med. Biol. Soc.*, 1234–1237. <https://doi.org/10.1109/EMBC.2014.6943820>.
- Subasi, A., Gursoy, M.I., 2010. EEG signal classification using PCA, ICA, LDA and support vector machines. *Expert Syst. Appl.* 37 (12), 8659–8666.
- Varela, M., 2015. In: Raw EEG signal processing for BCI control based on voluntary eye blinks.Central American and Panama Convention (CONCAPAN XXXV), 2015 IEEE Thirty Fifth, pp. 1–5. <https://doi.org/10.1109/CONCAPAN.2015.7428477>.
- Xu, R., Jiang, N., Lin, C., Mrachacz-Kersting, N., Dremstrup, K., Farina, D., 2014. Enhanced low-latency detection of motor intention from EEG for closed-loop brain-computer interface applications. *IEEE Trans. Biomed. Eng.* 61 (2), 288–296.

CHAPTER 5

Cognitive Analysis: Frequency Domain

Dipali Bansal, Rashima Mahajan

Faculty of Engineering and Technology, Manav Rachna International Institute of Research and Studies, Faridabad, India

Contents

5.1 Introduction	139
5.2 Channel Spectral Analysis	142
5.3 Subband Power Analysis	143
5.4 EEG Coherence Analysis	144
5.5 Result and Analysis	147
5.6 Conclusion	162
References	165
Further Reading	166

5.1 INTRODUCTION

A lot of physically challenged population worldwide is compelled to live a dependent life as they are not able to perform muscular/motor actions. Along with regular treatment, a research to improve their day-to-day life by developing automated control systems is the need of the hour. An exponential growth has been witnessed in physiological signal-based external device control systems. The neural responses via EEG are the most widely used physiological responses for control applications (Wolpaw et al., 2002; Tanaka et al., 2005; Nielsen et al., 2006; Galán et al., 2008; Lecuyer et al., 2008; Cho et al., 2009). The mental task, eyeblink, imagery thought, eye movement, visual/auditory/affective stimulation, etc. of physically challenged subjects are the instances which are generally captured via neural patterns. The acquired responses are analyzed and translated into operative control signals to develop control application-based brain-computer interfaces (BCIs). The performance of developed system is solely dependent on decoding ability of the algorithm (Cabrera et al., 2008). Therefore, neural pattern translation algorithm is the core component of any BCI system.

Cognitive analysis of EEG-based neural responses in majority of the research work involves the extraction of event-related potential (ERP) distribution across distinct regions of cerebral cortex. The detailed analyses of single eyeblink specific brain activity via EEG in time domain are presented in Chapter 4. The time-domain analysis of recorded neural patterns through scalp electrodes is focused toward the characterization

of even minute neural signal variations. The aim is to extract amplitude variations with respect to time followed by variations in time segments between selected data points and duration of distinct events. However, time-domain analysis requires several number of EEG trials to be averaged to determine resultant ERP amplitudes (DeBoer et al., 2006). Furthermore, if the peak amplitude variations are not much prominent, it is difficult to classify the correlated neural states.

A channel spectral analysis in frequency domain has been proved to be an efficient technique to characterize neural variations during specific cognitive, affective, or motor action (Dressler et al., 2004; Jatupaiboon et al., 2013). This chapter highlights the processes and algorithms involved in cognitive analysis of acquired single eyeblink-related brain activity in frequency domain. The frequency-domain analysis of recorded EEG signals involves the application of Fourier transform to estimate the respective spectral details. The fast Fourier transform (FFT) is usually implemented to track amplitude modulations at a specific frequency by plotting the frequency spectrum of acquired EEG responses. The spectral analysis is aimed to determine the feature set consisting of EEG subband power specifications in response to the performed single eyeblink action. This indicates the respective power variations in specific EEG frequency bands. The prime EEG subbands of the brainwave signals are beta, alpha, theta, gamma, and delta. A delta band has the lowest frequency range (0–4 Hz) followed by theta (4–8 Hz), alpha (8–12 Hz), beta with a range between 12 and 31 Hz and gamma is in the range beyond 31 Hz (Teplan, 2002). The EEG subband power variations are associated with specific brain activity. Thus, by identifying these spectral variations and analyzing them, it is possible to characterize the correlated cognitive neural states as stated by Wolpaw et al. (2000), Iversen et al. (2008), and Sakkalis (2011). The motive is to analyze the brain activity of human subjects using EEG signals and develop a technique to implement BCIs for control applications.

The normalized delta, alpha, and beta waves have been successfully used to characterize meditation- and attention-related neural patterns acquired through EEG (Lin et al., 2010). The aim was to develop an interactive BCI to control the movement of electric wheelchair for physically locked-in patients. The neural activity was captured using a unipolar electrode placed over the frontal scalp region near forehead. The meditation- and attention-specific acquired EEG responses were analyzed in frequency domain to extract the relevant feature set. An efficient and convenient interface was developed by translating a feature vector into control signals for wheelchair movement.

With a vision to suggest a solution to improve the life of paralyzed patients, the power spectral density (PSD)-based features were extracted from recorded EEG signals to classify the left-hand and right-hand imaginary movement (Saa and Gutierrez, 2010). The results suggested that the PSD estimation via parametrical techniques (Castanié, 2013) can contribute efficiently toward the improvement of classification accuracy of designed BCI. The classified signal features can possibly be utilized further to control external devices including computer systems. An early research in 1990s has also

investigated the EEG responses acquired during the left and right motor imagery action by extracting the relevant features using parametrical spectral estimation (Pregenzer and Pfurtscheller, 1999). The EEG signals were specifically picked up from left and right areas of central cerebral cortex using two bipolar electrodes. An autoregressive modeling (AR) of the order of six was incorporated to develop a reduced dimensionality feature vector. The aim of the research was to introduce an efficient BCI to control hand grasping in subjects amputated below elbow. A more efficient autoregressive moving average (ARMA) model has been implemented by Sakkalis et al. (2008) to analyze the EEG-related brain activities of young children with mild epilepsy. The tests were conducted on EEG data segments each of 10.24-s duration to extract the associated biomarkers. A classification accuracy of perfect 100% has been obtained using parametric modeling approach across all channel dataset.

Another research highlights the use of closed eye-related EEG responses to control the movement of electric wheelchair (Ming et al., 2014). The EEG signals with subject's eyes closed for >1 s were analyzed in frequency domain. The forward, backward, left, and right direction movement of wheelchair was controlled by extracting the subband power spectral features of multichannel EEG dataset. The amplitude of alpha wave in EEG power spectrum has been monitored and the subsequent variations have been translated into control signals for wheelchair movement. An average successful control rate of 81.3% has been achieved using the developed BCI.

As per the above discussion, nonparametric and parametric spectral approaches can be applied to acquire EEG responses for spectral estimation and subsequent neural state classification as depicted in Fig. 5.1. The spectral analysis using nonparametric techniques is performed once the recorded dataset is preprocessed to filter out the various physiological and nonphysiological artifacts. This process in turn enhances the required

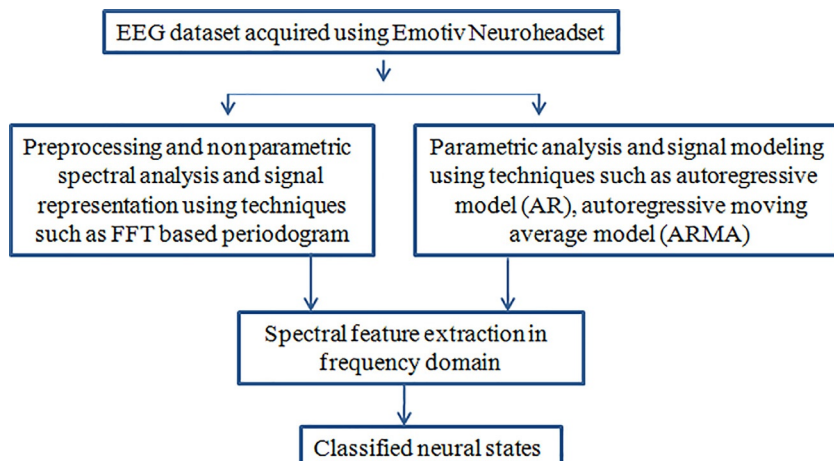


Fig. 5.1 Nonparametric and parametric techniques for spectral estimation and subsequent neural state classification.

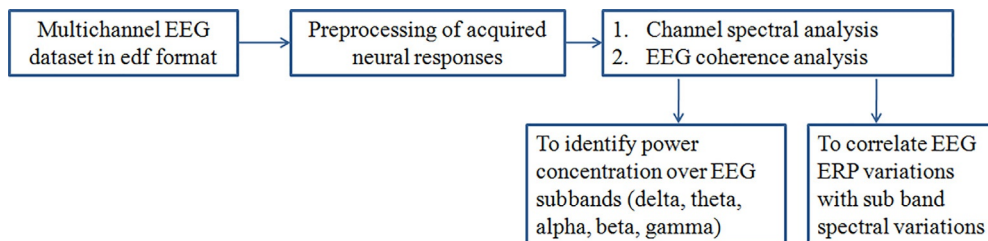


Fig. 5.2 Cognitive analyses of acquired real-time EEG during voluntary eyeblink: frequency domain.

information-specific brain activity patterns present in raw EEG records. It is followed by spectral analysis of preprocessed EEG signals to extract the most discriminative feature set to classify the correlated neural state. On the other hand, parametric spectral analysis can be performed directly on acquired EEG dataset (Sakkalis et al., 2008). The parametric spectral estimation techniques offer various advantages over nonparametric techniques. These minimize the spectral leakage across boundaries resulting due to the applied window function and provide high-frequency resolution (Gath et al., 1992) followed by minimum computational complexity (Tavainen et al., 2004).

This work implements a BCI based on subband power spectral and EEG coherence-related features to identify deliberate eyeblink-specific instants in acquired neural responses. The cognitive BCIs based on spectral parameters involve the exploration of frequency-domain information of EEG responses. The frequency response analysis involves the separation of entire range of EEG frequencies in subfrequency bands. It includes delta (0–4 Hz), theta (4–8 Hz), alpha (8–12 Hz), beta (12–30 Hz), and gamma (>30 Hz) rhythms. The brain activity related to voluntary single eyeblink captured using 14-channel EMOTIV EEG neuroheadset has been analyzed in frequency domain to extract the relevant feature set. The framework designed for cognitive spectral analysis of real-time EEGs acquired during voluntary eyeblink is as shown in Fig. 5.2.

The forced eyeblink-specific brain patterns have been acquired via EEG from five subjects and are analyzed in frequency domain to identify respective power concentration in distinct EEG subfrequency bands. The detailed frequency-domain analysis (by extracting channel spectral- and coherence-related features) of recorded brain activity is included in the subsequent sections.

5.2 CHANNEL SPECTRAL ANALYSIS

The frequency-domain analysis of recorded EEG activity has been performed using MATLAB-based standalone application software toolbox EEGLAB v 13.2.2.b (Delorme and Makeig, 2004) and in MATLAB workspace of release 2015a. The preprocessed multi-channel EEG dataset is used for channel spectral analysis to extract the all channel power spectrum (16-channel as acquired using Emotiv EEG neuroheadset). A finite impulse

response (FIR) band-pass filter has been implemented on input EEG signals to select a bandwidth of 0.25–50 Hz as discussed in [Chapter 3](#). The selected bandwidth allows capturing all the ERP and frequency variations in the single eyeblink-specific EEG signals. The subtle oscillatory variations in EEG are often visualized by recording the respective power variations. To capture the event-related power variations, the channel spectral analysis is performed. The power content at specific frequency points can be quantized by computing the PSD of input EEG signal. PSD is the most widely used feature to identify the correlated neural activity in BCI development ([Unde and Shriram, 2014](#)). It determines the squared amplitude at different frequency points (in $\mu\text{V}^2/\text{Hz}$) and is represented as energy per unit frequency ([Sanei and Chambers, 2007](#)).

The channel spectral analysis of 16-channel EEG data is performed across the selected frequency points in the given bandwidth range. An all channel spectrum has been plotted with different color traces representing the respective spectrum of an EEG activity across individual scalp channel. The resulting spectrum has been computed using FFT-based periodogram technique. A sliding latency Hanning windowing technique is applied to smooth the truncation of data to minimize the leakage effect and subsequent noise elimination across the spectrum. The PSD of input EEG signal is determined as Fourier transform of its autocorrelation. The steps to compute PSD using periodogram approach are listed as follows:

- i. sample the input EEG signal $x(t)$;
- ii. divide sampled signal $x(n)$ into smaller overlapped EEG data segments. A wider EEG segment may lead toward better frequency resolution;
- iii. compute the discrete Fourier transform (DFT) of each EEG subsegment followed by the squared magnitude of resultant DFT. The following equation is used to compute DFT:

$$X(w) = \frac{1}{2\pi N} \left| \sum_{n=1}^N x(n) e^{-jwn} \right|^2 \quad (5.1)$$

- iv. compute average of individual DFTs of respective overlapping segments to estimate resultant EEG power spectrum.

The topographic scalp maps have been plotted above EEG channel spectrum traces at selected frequencies lying within the selected bandwidth. Each scalp map shows the distribution of power across distinct scalp regions (frontal, temporal, parietal, and occipital) at individual frequency.

5.3 SUBBAND POWER ANALYSIS

The neural activity of neurons is often associated with variations in power of captured signal in response to any external stimuli, motor action or event. To capture the specific

event-related power variations, a standard frequency-domain technique based on Fourier transform of correlation of signals known as power spectral analysis is the most commonly used. It is also termed as power spectrum of EEG signal. The acquired EEG signals can be quantified by determining the power content in particular EEG frequency subband and is known as EEG subband power analysis. It shows the power distribution or squared amplitude distribution among distinct EEG frequency components, viz., delta, theta, alpha, beta, and gamma ([Stein et al., 1999](#); [Mahajan and Bansal, 2015](#)).

Electroencephalogram signals carry subband power in delta, theta, alpha, beta, and gamma subbands. The computation of band power features involves the implementation of band-pass filter in a required frequency subband. The resultant output of filter is squared followed by averaging the sample values over a specific band of frequencies. The input eyeblink specific EEG-based time-series neural responses are subjected to Fourier transform to obtain the resultant power spectrum. It decomposes the input EEG signal into real (cosine component of EEG response) and imaginary component (sine component of EEG response) for each and every frequency points. Therefore, a complex representation of input EEG signal is obtained at successive frequency points. The resulting spectrum is a set of complex values at specific frequency points selected in the range. The log power spectrum is obtained by converting the resulting spectra into a logarithmic scale.

The success of BCIs utilizing band power features relies on the extent of accuracy with which dominant frequency bands are tuned. The band power features have been extensively utilized to classify motor imagery ([Pfurtscheller and Neuper, 2001](#)) and cognitive tasks ([Palaniappan, 2005](#); [Yamanaka and Yamamoto, 2010](#)). The band power features capture power information in only particular selected frequency band. However, another frequency-domain technique PSD is calculated by dividing whole EEG signal into smaller segments and calculating the power information in each subsegment. Therefore, it is capable of extracting the overall frequency content of an EEG signal. The subband power analysis has been performed in EEGLAB. The channel properties are plotted for selected scalp channels to understand the single eyeblink-related neural variations in ERP image plot and activity spectrum.

5.4 EEG COHERENCE ANALYSIS

The similarity relationship between two input EEG signals at different electrodes can be observed by understanding the degree of their phase adjustment to each other. This can be determined by using a parameter known as coherence among input signals captured at different scalp electrode pairs. The computation of coherence at distinct selected electrode pairs provides a method to determine the respective stability of associated phase coupling. It represents the degree of relation in terms of frequency between two time signals or spectra determined at different time and frequency points.

The degree of similarity among neighboring brain signals through EEG coherence can be estimated by computing the respective Fourier transform-based spectrograms. The process to determine the spectrogram includes the analysis of EEG responses in time-frequency domain using short-time Fourier transforms (STFTs). An input EEG signal $x(t)$ is sampled at N instants to convert it into a discrete time signal $x(n)$ having total of N samples. The resultant signal can be analyzed using DFT/FFT and is defined using the following equation:

$$X(k) = \sum_{n=0}^{N-1} x(n) e^{-j2\pi kn/N}, \quad k = 0, 1, 2, \dots, N-1 \quad (5.2)$$

where $X(k)$ represents DFT of finite duration signal $x(n)$ at the different frequency points given as $f = k/N$.

The inverse DFT is used to obtain the signal $x(n)$ back from $X(k)$ as.

$$x(n) = \frac{1}{N} \sum_{k=0}^{N-1} X(k) e^{j2\pi kn/N}, \quad n = 0, 1, 2, \dots, N-1 \quad (5.3)$$

Here, an extra term $1/N$ is introduced and is known as a scaling factor.

In terms of matrix notation, Eqs. (5.1) and (5.2) can be represented as

$$x = \frac{1}{N} F X \quad (5.4)$$

$$X = \bar{F} x \quad (5.5)$$

where \bar{F} represents the complex conjugate of Fourier matrix F .

The output elements obtained in the DFT vector $X(k)$ are the Fourier coefficients calculated at the frequencies $f = 0, 1/N, 2/N, \dots, (N-1)/N$, respectively. The frequency content in the resultant DFT, $X(k)$, is depicted graphically using two plots, viz., magnitude plot, $|X(k)|$ and the phase angle plot, $\arg X(k)$.

Now, to calculate the spectrogram of the input EEG signal, following are the algorithmic steps:

- i. Record the input EEG signal $x(t)$.
- ii. Sample input signal at N sample points to obtain a digitized signal $x(n)$ with length N .
- iii. Divide the whole signal $x(n)$ into successive overlapping segments of length m .
- iv. Constitute a matrix Y with successive overlapping input segments placed as successive columns of matrix. It can be formed as

First column of Y : $[x(0), x(1), \dots, x(m-1)]^T$.

Second column of Y : $[x(1), x(2), \dots, x(m)]^T$ and so on. This will lead to a formation of highly redundant matrix Y from input signal segments.

- v. Compute individual DFT of the columns of matrix Y . This will constitute the spectrogram $Y(k)$ of input signal $x(n)$ with window length m . The output spectrogram

matrix $Y(k)$ is constituted of columns obtained from DFTs of the columns of matrix Y . The rows of $Y(k)$ are indexed in terms of frequency and the columns are indexed in terms of time. Each point in $Y(k)$ is represented in terms of frequency and time. This is known as time-frequency representation of input signal $x(n)$.

To summarize, the spectrogram is created by using DFT/FFT of input digitized signal. Initially, the acquired EEG signals are sampled in time domain. The sampled EEG data are divided into smaller and similar length overlapped consecutive data segments arranged as columns in a matrix. A DFT/FFT for each subdivided data segment is computed to determine the magnitude of resultant frequency spectrum. The obtained FFTs represent a column in the resultant spectrogram image (magnitude vs frequency representation for a specified time instant). These FFT spectrums are placed together side by side to form the resultant colored image plot. It indicates the variations in frequency components of input EEG signal with respect to time (Tuncel et al., 2010; Bajaj and Pachori, 2013). In spectrogram image plot, the differences in amplitude are coded with different colors. However, the similar color represents the uniform amplitudes of input signal. The resolution of spectrogram is dependent on the length of window (overlapped segment). A short length of segment leads toward improved time resolution but degraded frequency resolution, however, a long length of segment provides improved frequency resolution but degraded time resolution of image spectrogram. Therefore, an optimized segment length and subsequent overlapping can provide enhanced visualization of image-based time-frequency spectrograms (Ricardo Ramos-Aguilar et al., 2017).

The coherence between different scalp channel neural signals in terms of EEG has been obtained to understand the eyeblink-related variations. It has been observed between either pair of left frontal channels (frontal frontal): AF3 (channel number 3)-F7 (channel number 4) or frontal channels with respect to reference electrodes (frontal reference). The left frontal channels have been selected for coherence analysis as the neural activity correlated to deliberate single eyeblink action can be captured prominently at left frontal channels of EMOTIV neural head set unit (refer result and analysis Section 4.5).

EEG coherence analysis between neural activities of selected electrode pairs has been accomplished by computing their Fourier transform-based spectrograms. The coherence parameter is a ratio of squared magnitude of cross-spectral density between selected electrode pair (three pairs have been selected for present analysis: AF3-F7; AF3-reference electrode; F-reference electrode) and product of their individual power-spectral densities (Mathewson et al., 2012). The coherence function between EEG scalp electrodes AF3 (Channel-3) and F7 (Channel-4) is given as:

$$C_{3-4} = \frac{(|(P_{3-4}(f))|)^2}{(P_{3-3}(f)P_{4-4}(f))} \quad (5.6)$$

where $P_{3-3}(f)$ and $P_{4-4}(f)$ indicates the auto power-spectral density of channel number “3” (AF3) and channel number “4” (F7), respectively, at selected frequency f . The cross power-spectral density between left frontal channels AF3 and F7 is represented as $P_{3-4}(f)$. The coherence function C_{3-4} determines the degree to which signal at channel number “4” may be estimated/predicted from signal at channel number “3” by implementing an optimum least-square-linear function. It provides a measure of synchronization among signals captured at selected electrode pair. A value “one” reflects perfect association between the brain activity recorded at selected channel locations and a value “zero” represents completely uncorrelated brain activity at respective scalp channels (Mathewson et al., 2012). The enhanced stabilization of phase coupling leads to even coherence values greater than unity. EEG channel coherence results between three distinct electrode pairs for five subjects have been retrieved to understand the instants of maximum association during a thoughtful single eyeblink action.

5.5 RESULT AND ANALYSIS

This section presents the detailed results and subsequent frequency-domain analysis for single eyeblink identification through EEG-based neural responses. The channel spectral analysis has been performed to extract all-channel power spectrum of acquired multi-channel EEG dataset. The subband power analysis and EEG coherence analysis results of five subjects are presented and discussed in detail to identify an instant of a thoughtful eyeblink. The subjects were asked to perform a deliberate single eyeblink activity. Each of the corresponding brain patterns via EEG are recorded through scalp electrodes of EMO-TIV neuroheadset unit. The acquired dataset is imported to EEGLAB toolbox of MATLAB for the subsequent analysis in frequency domain.

The power spectral analysis has been performed to determine the power distribution across different EEG frequency points for all channel EEG data. The topographic distribution above the plots depicts the spatial power distribution across distinct scalp regions at different frequency values. It is important to understand that which particular scalp region contribute most strongly toward which band of frequencies (delta, theta, alpha, beta, gamma) in the acquired EEG data. The channel spectra and corresponding topographic maps at different frequencies are plotted to extract the related information.

The individual colored trace in the resulting spectra represents the mean log power spectrum of neural activity captured at one scalp electrode for successive frequency points. The topographic scalp maps show the power concentration over distinct scalp regions at selected frequencies in different EEG subbands (delta, theta, alpha, and beta). The leftmost topographic map indicates the distribution of spectral power at 2 Hz (present in delta frequency band). The other topographic maps indicate the respective power

distribution at 6 Hz (present in theta frequency band), 9 Hz (present in alpha frequency band), and 20 Hz (present in beta frequency band).

The detailed ERP analysis and topographic scalp map analysis has been discussed in [Chapter 4](#). The left frontal regions of cerebral cortex were found to possess maximum potential distribution during the performed action. As the left frontal regions include AF3 (channel number 3) and F7 (channel number 4) scalp channels of EMOTIV headset unit, hence are selected for further analysis. The power distribution across left frontal scalp regions is found to be high across delta (2 Hz) to alpha (9 Hz) frequency subband of EEG as visualized (red color across left frontal regions of scalp) in [Fig. 5.3](#).

The subband power analysis of multichannel EEG dataset has been performed across all left frontal (AF3 and F7), occipital (O1 and O2), parietal (P7 and P8), and temporal (T7 and T8) channel EEG data to identify the instant of a thoughtful single eyeblink action. The channel activity properties with ERP image plot captured at left frontal channels AF3 and F7 of EMOTIV EEG neuroheadset have been obtained. The results are plotted and discussed for five subjects in the subsequent sections. The channel activities extracted from EEG signals of subject 1 acquired at left frontal channel AF3 during single eyeblink action are plotted in [Fig. 5.4](#).

It shows a scalp map with selected channel location as red mark (here channel 3: AF3), ERP image plots indicating neural activity occurring across selected trials and EEG activity spectrum with a set of spectral peaks at distinct EEG frequencies, respectively. An ERP image plot is a color-coded plot in which the ERP amplitudes related to specific neural activity are represented by distinct color bars. A red bar in ERP image plot is indicative of maximum amplitude of ERP and hence enhanced neural activity followed by yellow, green, and blue colored bars, respectively. This ERP image plot at upper right

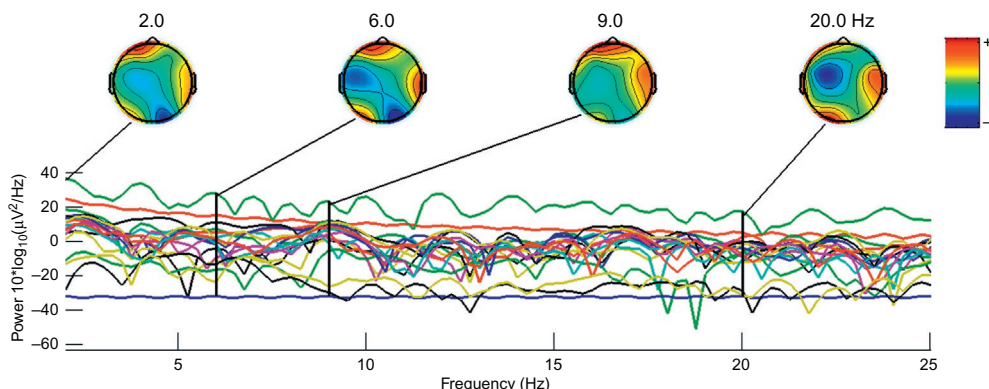


Fig. 5.3 Channel spectra plots of deliberate single eyeblink-specific multichannel EEG data. The left frontal scalp regions are found to possess high-power distribution across delta (2 Hz) to alpha (9 Hz) frequency subband of EEG. The *red color* shows maximum power distribution which is followed by *yellow, green, and blue color*.

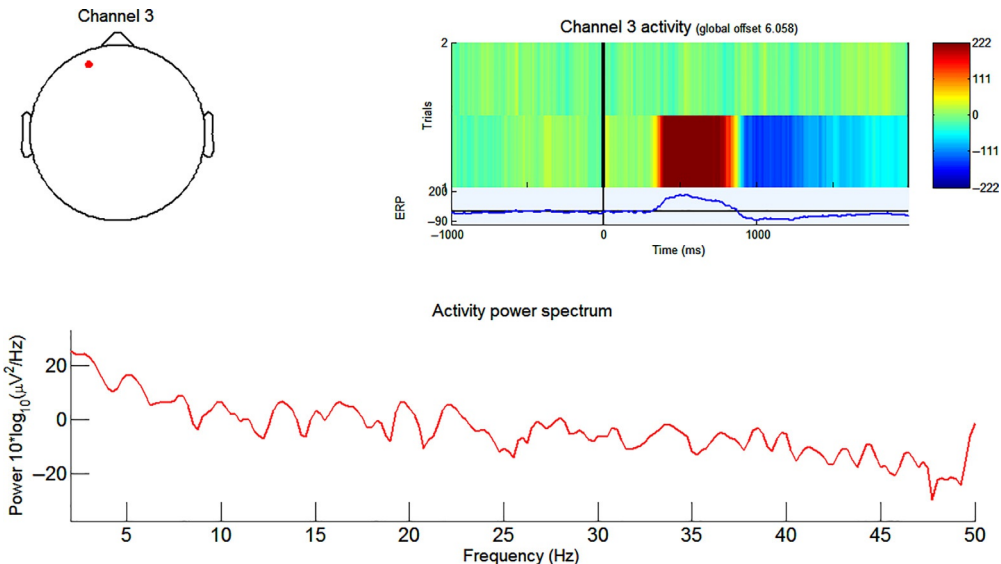


Fig. 5.4 Channel activity properties with event-related potential (ERP) image plot of subject 1 during single eyeblink action captured at channel AF3. The red dot in 2-D scalp map at the upper left position depicts the selected left frontal channel number 3 (AF3). The ERP image plot at upper right position shows the increased neural activity with high potential concentration (*red color bar*) and *blue color trace* shows the EEG signal epoch trace, respectively during single eyeblink action. The EEG power spectrum at the lower position indicates high delta (0–4 Hz) power till alpha subband power (8–12 Hz).

position depicts the increased potential concentration (*red color bar*) in captured neural activity during the performed single eyeblink action. The corresponding EEG signal variations are shown by *blue color trace* under ERP image plot. It shows the averaged ERP amplitude values of the recorded and epoched EEG signals with respect to selected latency points. The increased ERP amplitudes are obtained during the instant of a thoughtful single eyeblink action. The ERP amplitude varies from -40 to $200 \mu\text{V}$ during latency range 400 – 900 ms as shown in Fig. 5.4. This corresponds to a dark red colored vertical bar also and thus is indicative of increased neuronal activity captured in EEG signal. The EEG power spectrum at the bottom shows the corresponding spectral variations of recorded EEG signals in terms of power amplitude ($\mu\text{V}^2/\text{Hz}$) vs frequency (Hz) plot. The maximum spectral power amplitude is found to be $24 \mu\text{V}^2/\text{Hz}$. A high delta (0–4 Hz) power till alpha subband power (8–12 Hz) can be observed from Fig. 5.4. It depicts the activation of these low-frequency EEG subbands during deliberate single eyeblink actions.

Further evidence to above results came from the channel activity results extracted from EEG signals of subject 1 acquired at another left frontal channel F7 during a deliberate single eyeblink action are plotted in Fig. 5.5. A two-dimensional scalp map at the

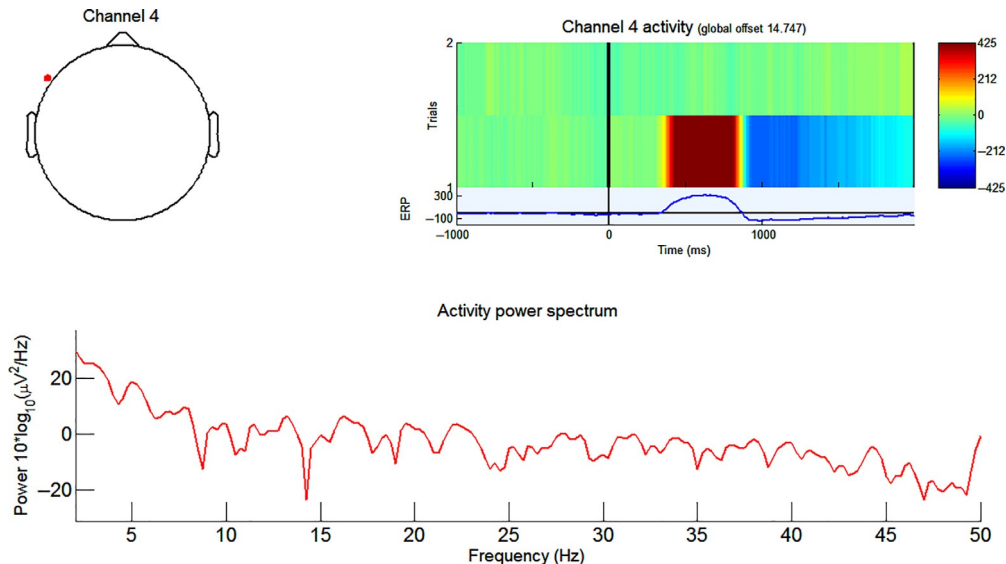


Fig. 5.5 Channel activity properties with event-related potential (ERP) image plot of subject 1 during single eyeblink action captured at channel F7. The red dot in 2-D scalp map at the upper left position depicts the selected left frontal channel number 4 (F7). The ERP image plot at upper right position shows the increased neural activity with high potential concentration (red color bar) and blue colored trace shows the EEG signal epoch trace, respectively during single eyeblink action. The EEG power spectrum at the lower position indicates high delta (0–4 Hz) power up to alpha subband power (8–12 Hz).

top left position shows selected channel location channel 4: F7 as red mark. An increase in neuronal activity across selected trials of a thoughtful single eyeblink action is noted through ERP image plot (red colored bar indicating maximum potential concentration and ERP amplitudes) and blue colored ERP trace showing increased averaged ERPs of acquired EEG signals during 400–900 ms. The ERP amplitude varies from -100 to $300 \mu\text{V}$ during latency range 400–900 ms as shown in Fig. 5.5. The spectral power amplitudes are also found to be dominated during low-EEG frequency subbands (delta, theta, and alpha). The maximum spectral power amplitude is found to be $24 \mu\text{V}^2/\text{Hz}$.

The set of results obtained by analyzing EEG signal dataset of rest of four subjects is also presented and discussed in detail. The channel activity results extracted from EEG signals captured at left frontal channel 3: AF3 from subject 2, 3, 4, and 5 during a deliberate single eyeblink action are plotted in Fig. 5.6A–D, respectively. These are comprised of respective ERP image plots, averaged ERP traces, and activity power spectra. Similarly, the channel activity results extracted from EEG signals captured at next left frontal channel 4: F7 from subject 2, 3, 4, and 5 during a deliberate single eyeblink action are plotted in Fig. 5.7A–D, respectively.

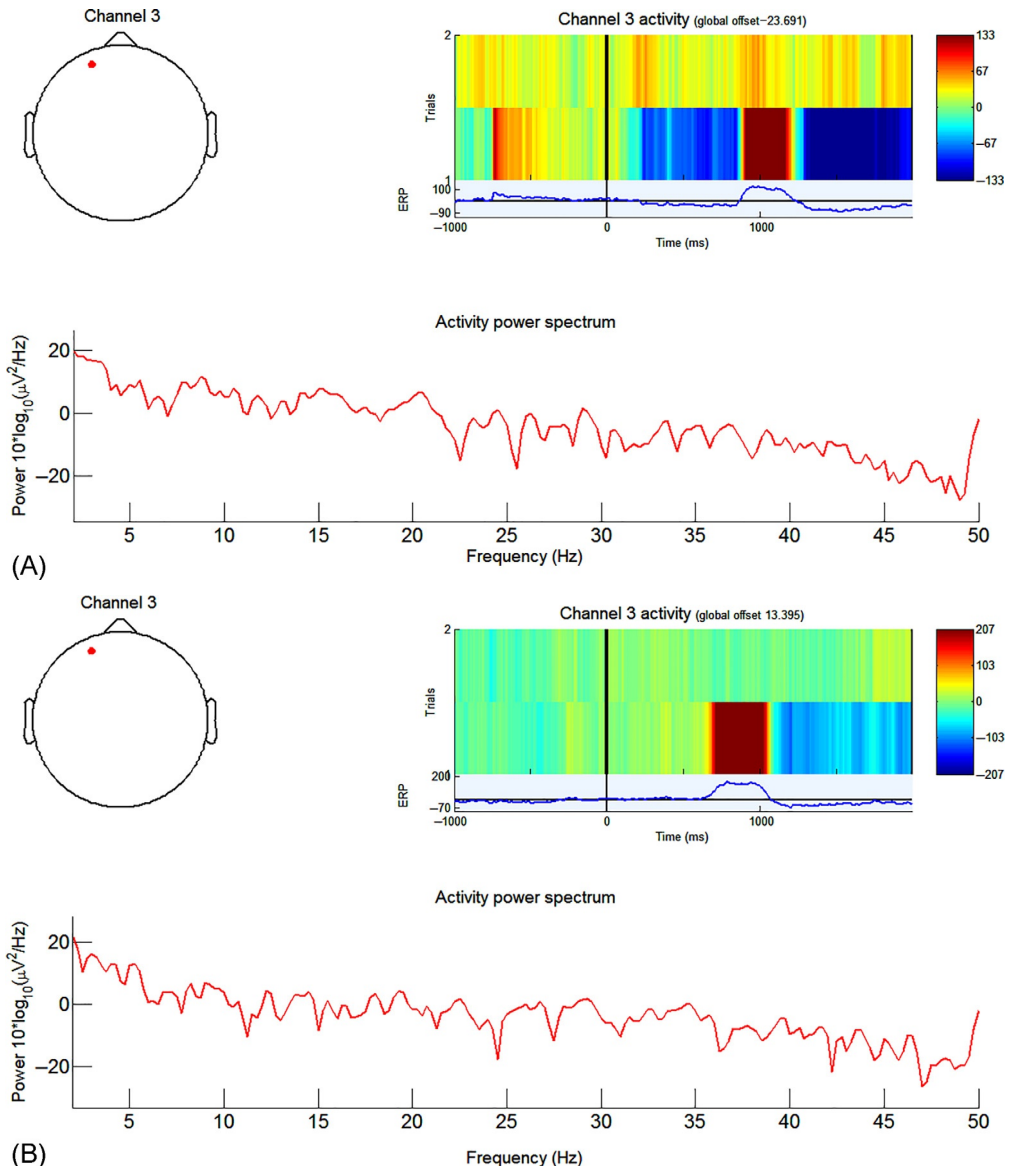
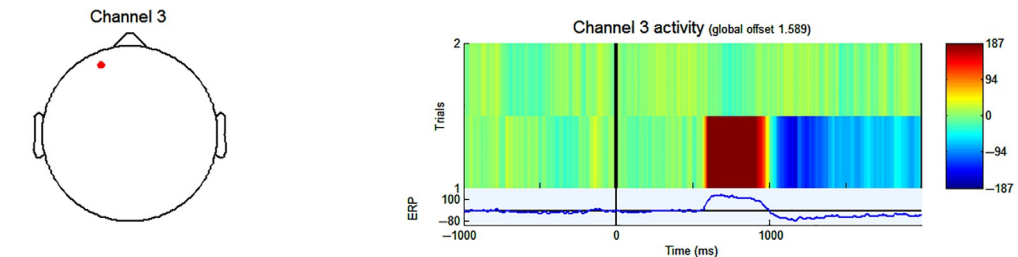
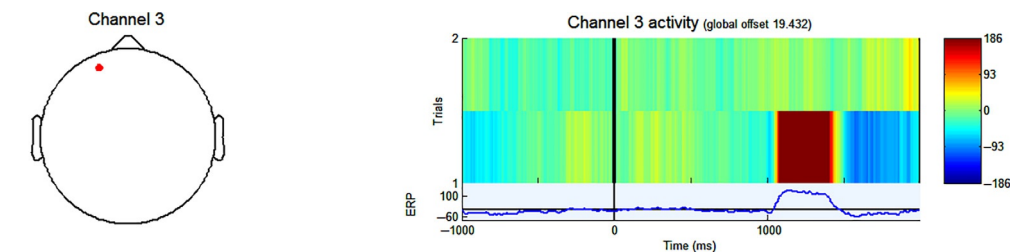


Fig. 5.6 Channel activity properties with event related-potential (ERP) image plot of (A) subject 2, (B) subject 3, (C) subject 4, and (D) subject 5 during single eyeblink action captured at channel AF3. The red dot in 2-D scalp map at the upper left position depicts the selected left frontal channel number 3 (AF3). The ERP image plot at upper right position shows the increased neural activity with high potential concentration (red color bar) and blue color trace shows the EEG signal epoch trace, respectively, during single eyeblink action. The EEG power spectrum at the lower position indicates high delta (0–4 Hz) power till alpha subband power (8–12 Hz).



(C)



(D)

Fig. 5.6, Cont'd

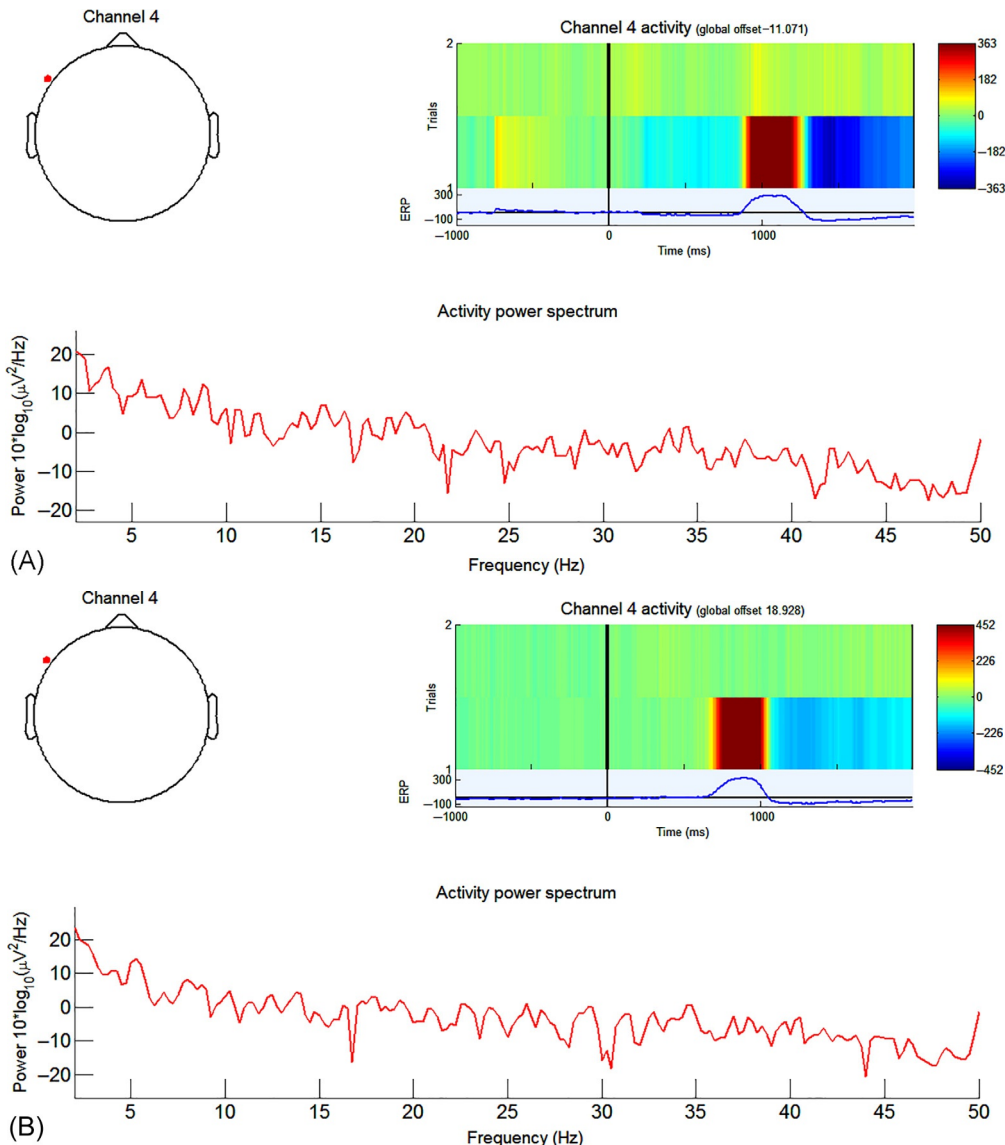


Fig. 5.7 Channel activity properties with event-related potential (ERP) image plot of (A) subject 2, (B) subject 3, (C) subject 4, and (D) subject 5 during single eyeblink action captured at channel F7. The red dot in 2-D scalp map at the upper left position depicts the selected left frontal channel number 4 (F7). The ERP image plot at upper right position shows the increased neural activity with high potential concentration (red color bar) and blue color trace shows the EEG signal epoch trace, respectively during single eyeblink action. The EEG power spectrum at the lower position indicates high delta (0–4 Hz) power till alpha subband power (8–12 Hz).

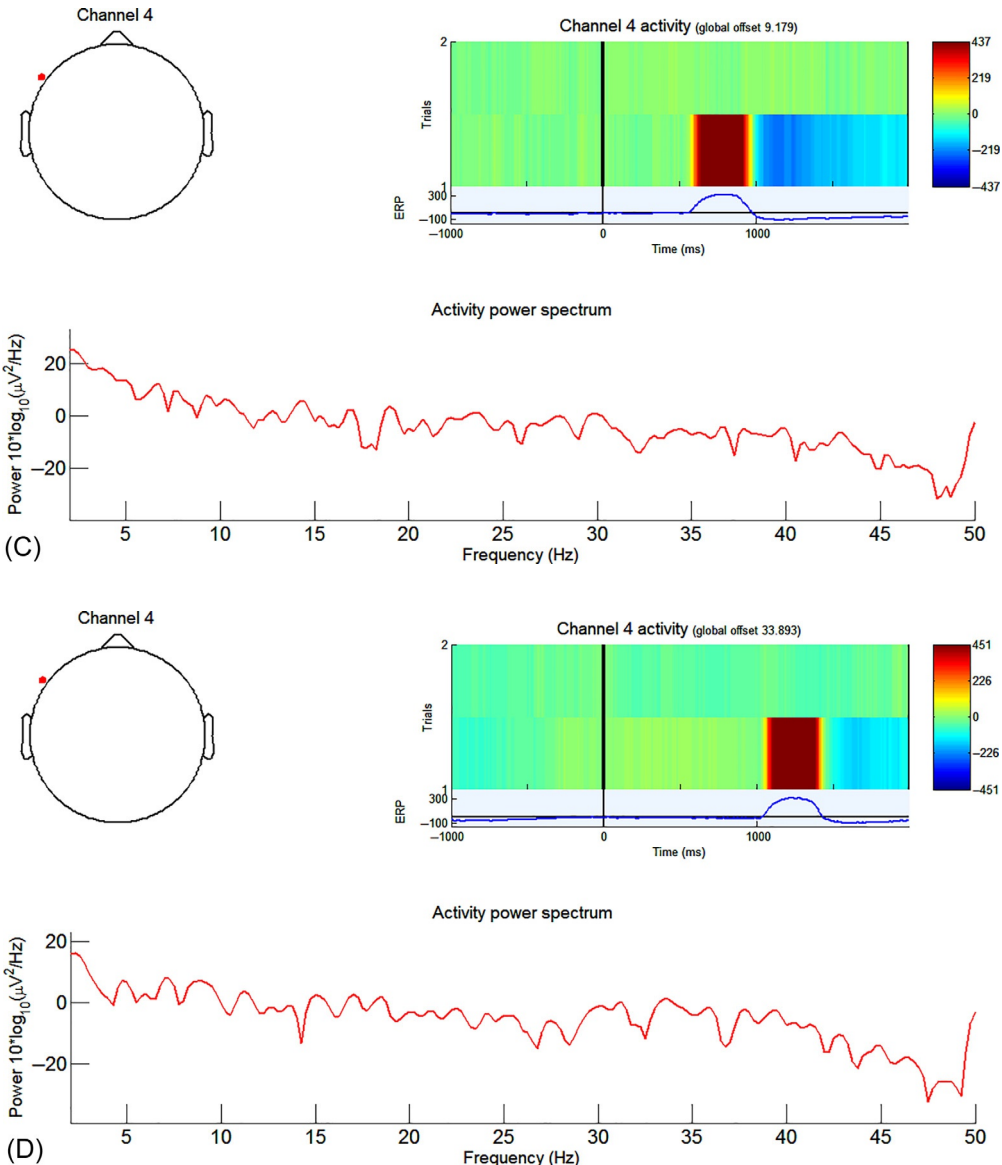


Fig. 5.7, Cont'd

The averaged ERPs at channel AF3 and F7 are found to be maximum at the selected latency range, viz., around 1000 ms (Figs. 5.6A and 5.7A: subject 2), 600–1050 ms (Figs. 5.6B and 5.7B: subject 3), 500–1000 ms (Figs. 5.6C and 5.7C: subject 4), and 1000–1500 ms (Figs. 5.6D and 5.7D: subject 5). These latency ranges indicate the duration

of performed single eyeblink action. For subject 2, the ERP amplitude at channel AF3 varies from -50 to $100\text{ }\mu\text{V}$ and at channel F7 varies from -100 to $300\text{ }\mu\text{V}$ around latency points 1000 ms . The maximum spectral power amplitude is found to be $20\text{ }\mu\text{V}^2/\text{Hz}$ during low-EEG frequency subbands. For subject 3, the ERP amplitude at channel AF3 varies from -70 to $200\text{ }\mu\text{V}$ and at channel F7 varies from -100 to $300\text{ }\mu\text{V}$ at 600 – 1050 ms . The maximum spectral power amplitude across both the channels (AF3 and F7) is found to be $20\text{ }\mu\text{V}^2/\text{Hz}$ during low-EEG frequency subbands. The subject 4 also shows the similar trends, the ERP amplitude at channel AF3 varies from -80 to $100\text{ }\mu\text{V}$ and at channel F7 varies from -100 to $300\text{ }\mu\text{V}$ at 500 – 1000 ms . The maximum spectral power amplitude across channels AF3 and F7 is found to be 20 and $24\text{ }\mu\text{V}^2/\text{Hz}$, respectively during low-EEG frequency subbands. For subject 5, the ERP amplitude at channel AF3 varies from -60 to $100\text{ }\mu\text{V}$ and at channel F7 varies from -100 to $300\text{ }\mu\text{V}$ at 600 – 1050 ms . The maximum spectral power amplitude across both the channels (AF3 and F7) is found to be $18\text{ }\mu\text{V}^2/\text{Hz}$ during low-EEG frequency subbands. The channel activity results extracted from EEG signals captured at left frontal channels AF3 and F7 from subject 1, 2, 3, 4, and 5 during a deliberate single eyeblink action are tabulated in [Table 5.1](#).

However, the channel activity results of subject 1 found at occipital, temporal, and parietal channels do not show such prominent increase in ERP amplitudes and spectral power amplitudes as they have been visualized across frontal channels AF3 and F7. The results have been analyzed at left occipital channel O1 ([Fig. 5.8A](#)) and right occipital channel O2 ([Fig. 5.8B](#)) to identify the instances of a thoughtful single eyeblink action. The very low ERP amplitudes are found across O1 (maximum $40\text{ }\mu\text{V}$) and O2 ($3\text{ }\mu\text{V}$).

Table 5.1 Channel activity parameters observed at left frontal channels AF3 and F7

Subjects	Channels			
	Channel number 3 (AF3)	Channel number 4 (F7)		
	ERP amplitude variations	Maximum spectral power amplitude	ERP amplitude variations	Maximum spectral power amplitude
Subject 1	-40 to $200\text{ }\mu\text{V}$ at 400 to 900 ms	$24\text{ }\mu\text{V}^2/\text{Hz}$	-100 to $300\text{ }\mu\text{V}$ at 400 to 900 ms	$24\text{ }\mu\text{V}^2/\text{Hz}$
Subject 2	-50 to $100\text{ }\mu\text{V}$ around latency points 1000 ms	$20\text{ }\mu\text{V}^2/\text{Hz}$	-100 to $300\text{ }\mu\text{V}$ around latency points 1000 ms	$20\text{ }\mu\text{V}^2/\text{Hz}$
Subject 3	-70 to $200\text{ }\mu\text{V}$ at 600 to 1050 ms	$20\text{ }\mu\text{V}^2/\text{Hz}$	-100 to $300\text{ }\mu\text{V}$ at 600 to 1050 ms	$20\text{ }\mu\text{V}^2/\text{Hz}$
Subject 4	-80 to $100\text{ }\mu\text{V}$ at 500 to 1000 ms	$20\text{ }\mu\text{V}^2/\text{Hz}$	-100 to $300\text{ }\mu\text{V}$ at 500 to 1000 ms	$24\text{ }\mu\text{V}^2/\text{Hz}$
Subject 5	-60 to $100\text{ }\mu\text{V}$ at 1000 to 1500 ms	$18\text{ }\mu\text{V}^2/\text{Hz}$	-100 to $300\text{ }\mu\text{V}$ at 1000 to 1500 ms	$18\text{ }\mu\text{V}^2/\text{Hz}$

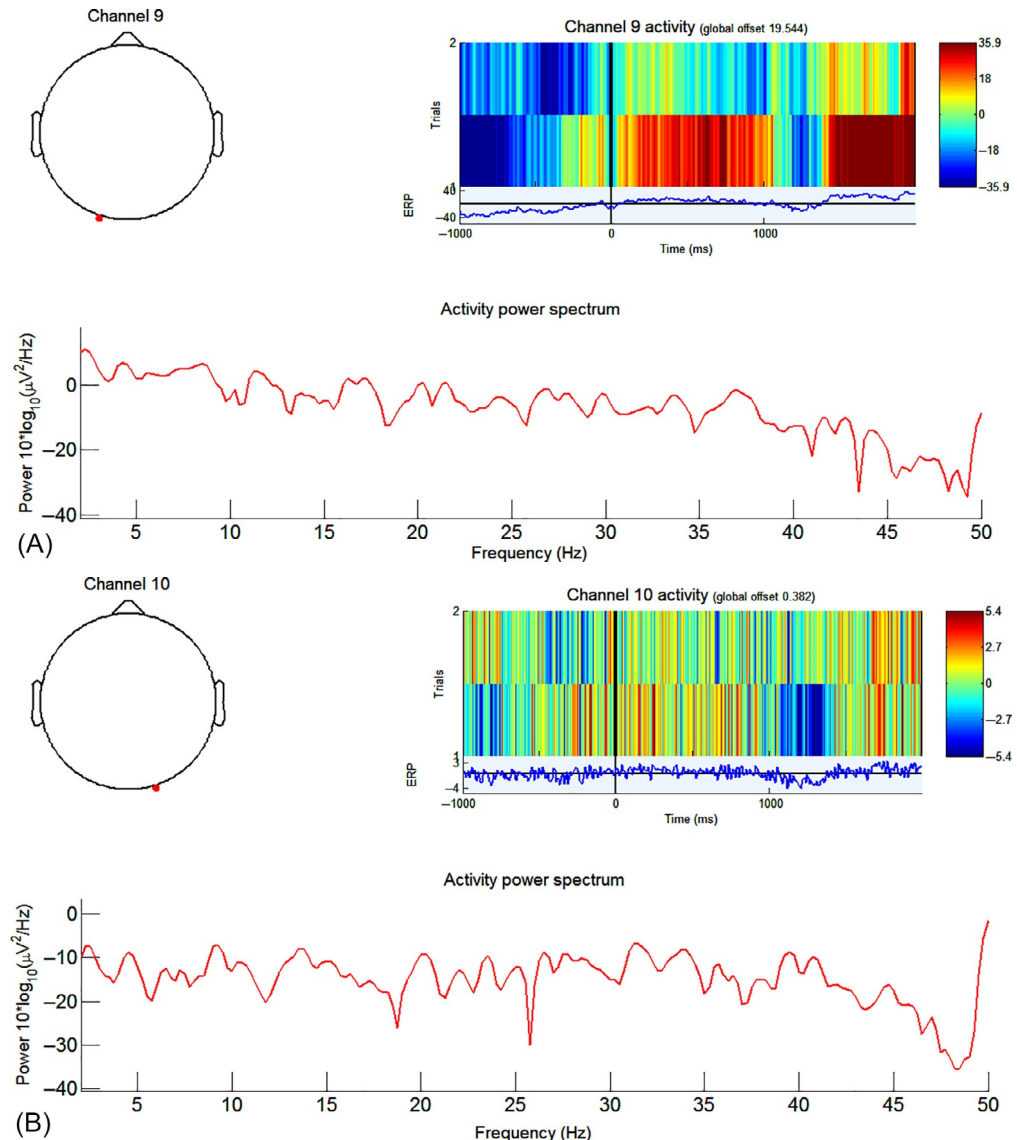


Fig. 5.8 Channel activity properties with event-related potential (ERP) image plot of subject 1 during single eyeblink action captured at (A) left occipital channel O1 and (B) right occipital channel O2. The red dot in 2D scalp map at the upper left position depicts the selected (A) left occipital channel number 9 (O1) and (B) right occipital channel number 10 (O2). The ERP image plot at upper right position and blue color EEG epoch trace shows that no increased neural activity is captured at occipital regions of brain during single eyeblink action. The EEG power spectrum is shown at the lower position with no dominant subpower bands.

[Fig. 5.9 A and B](#) shows channel activity results of subject 1 at temporal channels T7 and T8, respectively. The ERP amplitudes found across T7 (maximum 30 μ V) and T8 (maximum 60 μ V), are very low. The similar trends of low ERP amplitudes are observed at parietal channels P7 and P8 (maximum 40 μ V) as shown in [Fig. 5.10 A and B](#), respectively. There are no dominant subpower bands of EEG found across the EEG power spectrum at the bottom across occipital, temporal, and parietal channels.

The EEG coherence analysis has been performed between either pair of left frontal channels (frontal-frontal): AF3 (channel number 3)-F7 (channel number 4) or frontal channels with respect to reference electrodes (frontal-reference). The subsequent inspection of coherence results obtained at mentioned pair of electrodes (frontal-frontal and frontal-reference) reveals that eyeblink-specific neural activity varies tremendously with respect to time during onset of planned action. A high level of local synchronization of brain activity is evidenced in the results of all the subjects. It represents high coherence or synchronization between activated frontal regions of cerebral cortex. The EEG coherence results for single eyeblink activity have been computed using FFT-based spectrogram method. It represents power spectral variations as a function of time and frequency. In a spectrogram image plot, horizontal dimension shows time points, vertical dimension shows frequency points, and the leftover third dimension shows spectral amplitude intensity across time-frequency points. The spectral power intensity is color coded.

The set of EEG coherence results has been obtained by analyzing EEG signal dataset of five subjects and is presented in [Figs. 5.11–5.15](#), respectively. The coherence results for single eyeblink activity performed by subject 1 have been plotted between reference and left frontal channel AF3 ([Fig. 5.11A](#)), between reference and left frontal channel F7 ([Fig. 5.11B](#)), and between both the left frontal channels AF3 and F7 ([Fig. 5.11C](#)). The spectrogram image plot depicts the average event-related variations in EEG subband power at each time instant and frequency point of recorded EEG signal. It shows power variations (minor red colored variations) at about 7000 ms between 0 and 5 Hz indicating high delta band coherence. It is depicted from mean power spectrum (plotted in left panel) obtained during single eyeblink activity. The green color coherence plot below spectrogram image shows significantly increased EEG activity and high coherence during performed action.

The EEG coherence results of five subjects reveal that significantly high coherence strength have been observed around 6500 and 7000 ms for left frontal channel pairs (AF3-F7) and reference-left frontal channel pairs (Ref-AF3; Ref-F7) for a thoughtful single eyeblink action. The instants of high coherence are found to be related with high power values in particular frequency subbands. These are found dominant in lower frequency bands as depicted by the mean power spectrum plots shown in the left panel. Furthermore, the stated results have been found to be stable in all the five subjects showing similar coherence and spectral measures during performed activity. Therefore, the left frontal regions show a high interconnectivity across lower frequency bands.

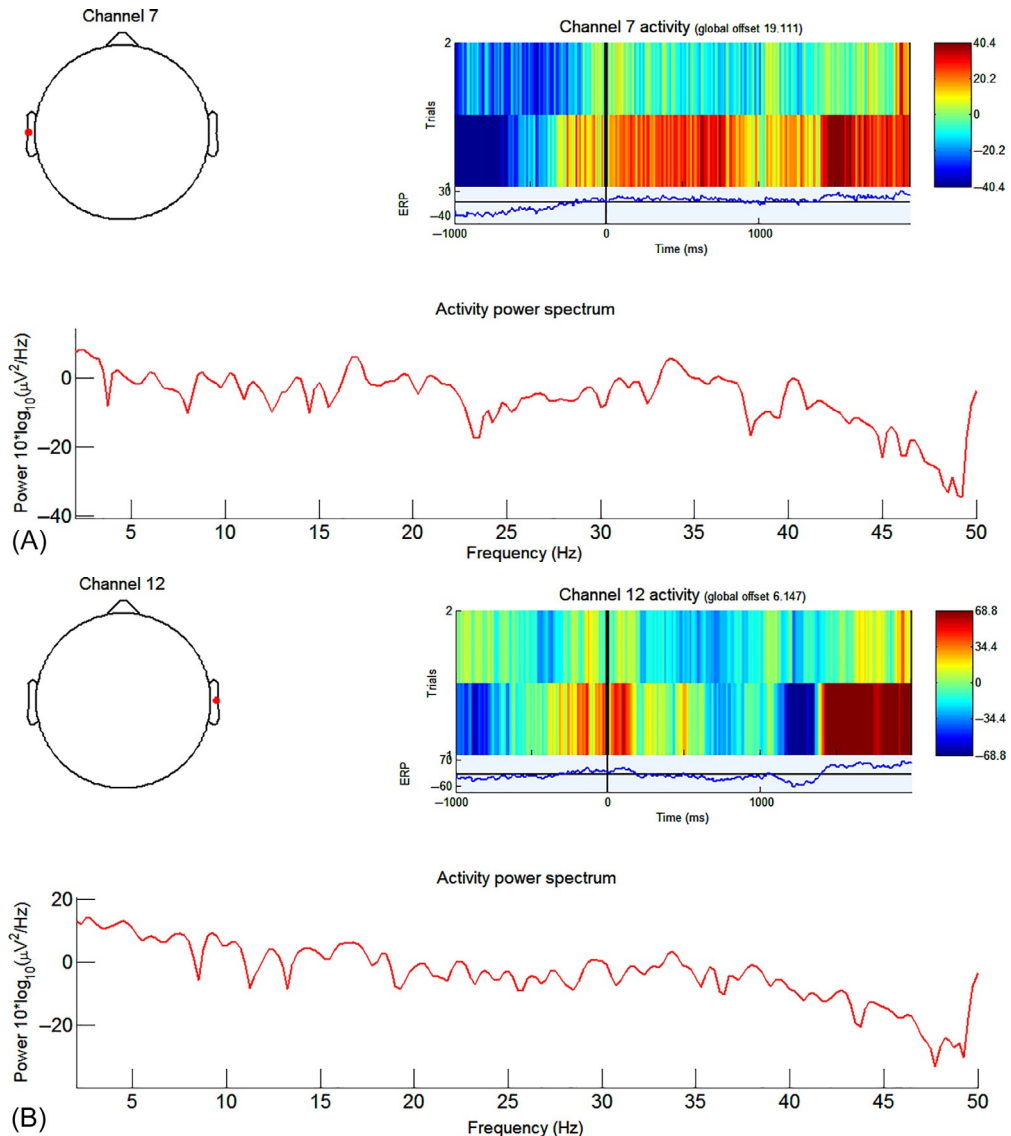


Fig. 5.9 Channel activity properties with event-related potential (ERP) image plot of subject 1 during single eyeblink action captured at (A) left temporal channel T7 and (B) right temporal channel T8. The red dot in 2D scalp map at the upper left position depicts the selected (A) left temporal channel number 7 (T7) and (B) right temporal channel number 12 (T8). The ERP image plot at upper right position and blue color EEG epoch trace shows that no increased neural activity is captured at temporal regions of brain during single eyeblink action. The EEG power spectrum is shown at the lower position.

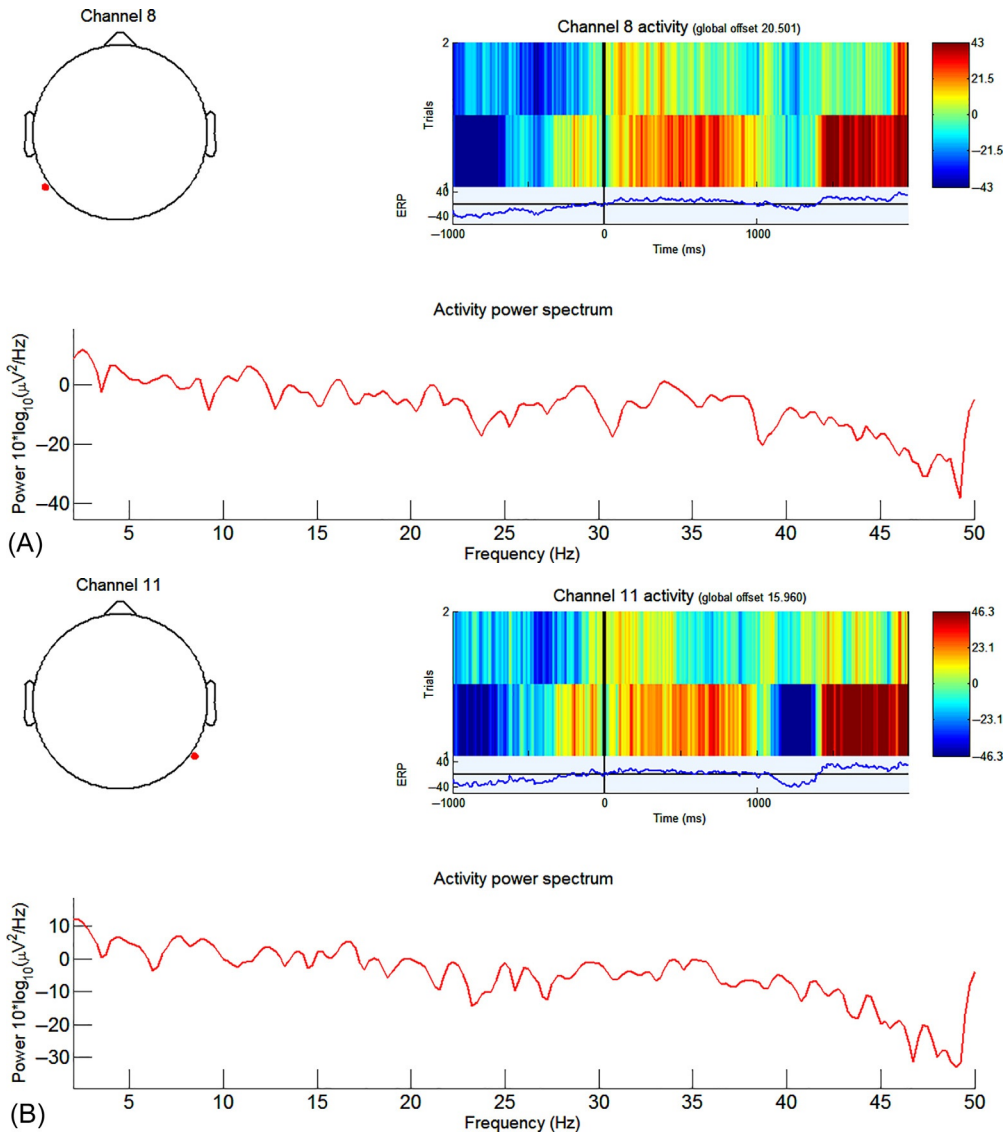


Fig. 5.10 Channel activity properties with event-related potential (ERP) image plot of subject 1 during single eyeblink action captured at (A) left parietal channel P7 and (B) right parietal channel P8. The red dot in 2D scalp map at the upper left position depicts the selected (A) left parietal channel number 8 (P7) and (B) right parietal channel number 11 (P8). The ERP image plot at upper right position and blue color EEG epoch trace shows that no increased neural activity is captured at temporal regions of brain during single eyeblink action. The EEG power spectrum is shown at the lower position.

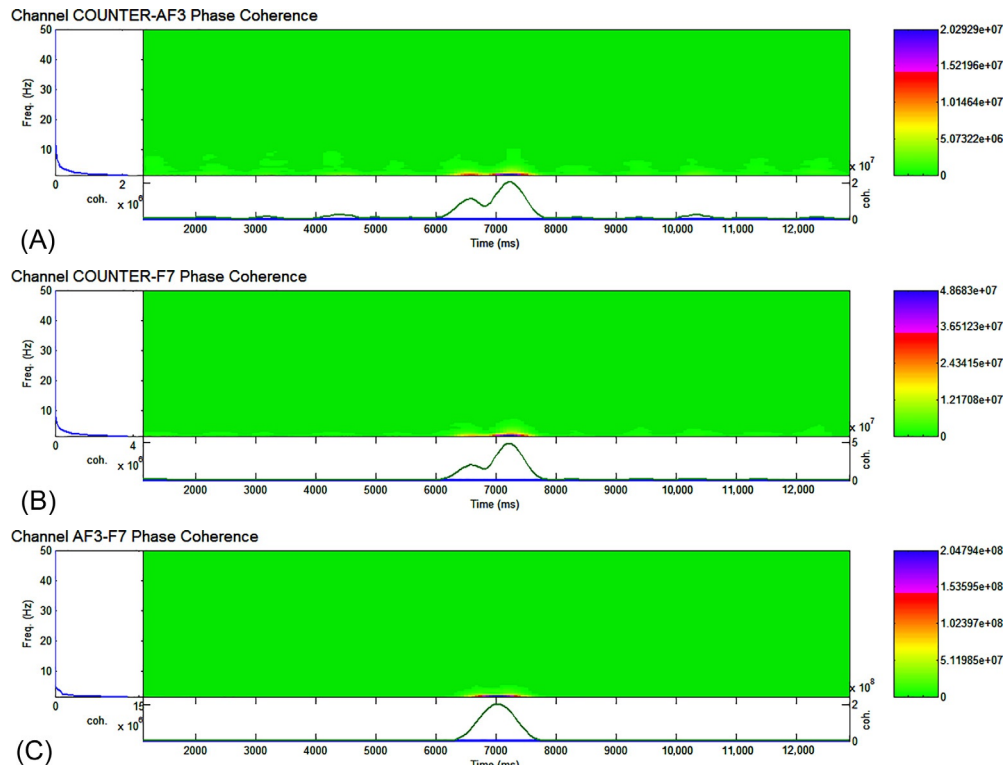


Fig. 5.11 EEG coherence plots between distinct pair of electrodes for single eyeblink activity performed by subject 1 (A) reference channel-AF3 channel, (B) reference channel-F7 channel, and (C) left frontal channels AF3-F7. The spectrogram image plot shows power variations at about 7000ms at 0–5Hz indicating high delta band coherence. The left panel indicates the mean power spectrum during single eyeblink activity. The green color coherence plot below spectrogram image shows significantly increased EEG activity and high coherence during performed action.

As stated earlier, the ERP-based brain-computer interfaces possess high throughput due to their short latency period. However, ERPs are low amplitude signals and are mostly suppressed by the background neural activity. It has also been stated in the literature that time-domain analysis of EEG signals require several number of individual trials to be averaged to determine resultant ERP amplitudes. Therefore, an attempt has been made in this chapter to explore the frequency (power spectrum features) and spatial domain (spectrogram-dependent features) feature set to detect and identify an instance of thoughtful single eyeblink action. Therefore, instead of utilizing the individual feature set (time domain: ERP analysis; frequency domain: power spectral amplitude analysis and spatial domain: EEG coherence analysis) in isolation, it would be more efficient to use a

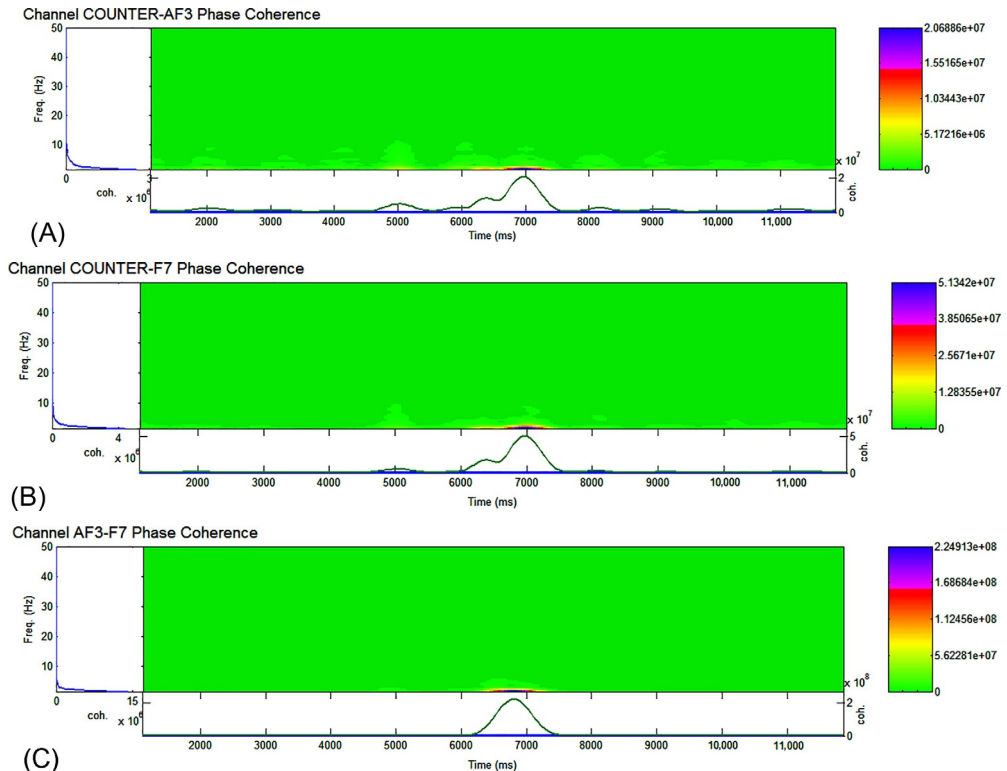


Fig. 5.12 EEG coherence plots between distinct pair of electrodes for single eyeblink activity performed by subject 2 (A) reference channel-AF3 channel, (B) reference channel-F7 channel, and (C) left frontal channels AF3-F7. The spectrogram image plot shows power variations at about 7000ms at 0–5Hz indicating high delta band coherence. The left panel indicates the mean power spectrum during single eyeblink activity. The green color coherence plot below spectrogram image shows significantly increased EEG activity and high coherence during performed action.

combined feature set to develop a more robust BCI. Such BCIs utilizing a multiple domain feature set are termed as hybrid BCIs. The combination of distinct feature set may lead to more translation of efficient control signals and thus enhance the overall efficiency of BCIs for control applications.

The single eyeblink action specific values of ERPs at left frontal channels along with spectral power amplitudes over specific EEG power subband and EEG coherence values can be utilized as a hybrid feature set to develop a more efficient BCI for control applications. An identified high variation in ERPs from ERP image plots and low-frequency EEG power subband (delta, theta, alpha) dominance on the onset of deliberate action can be utilized as control signal to develop a framework for implementation of neural control applications of interest.

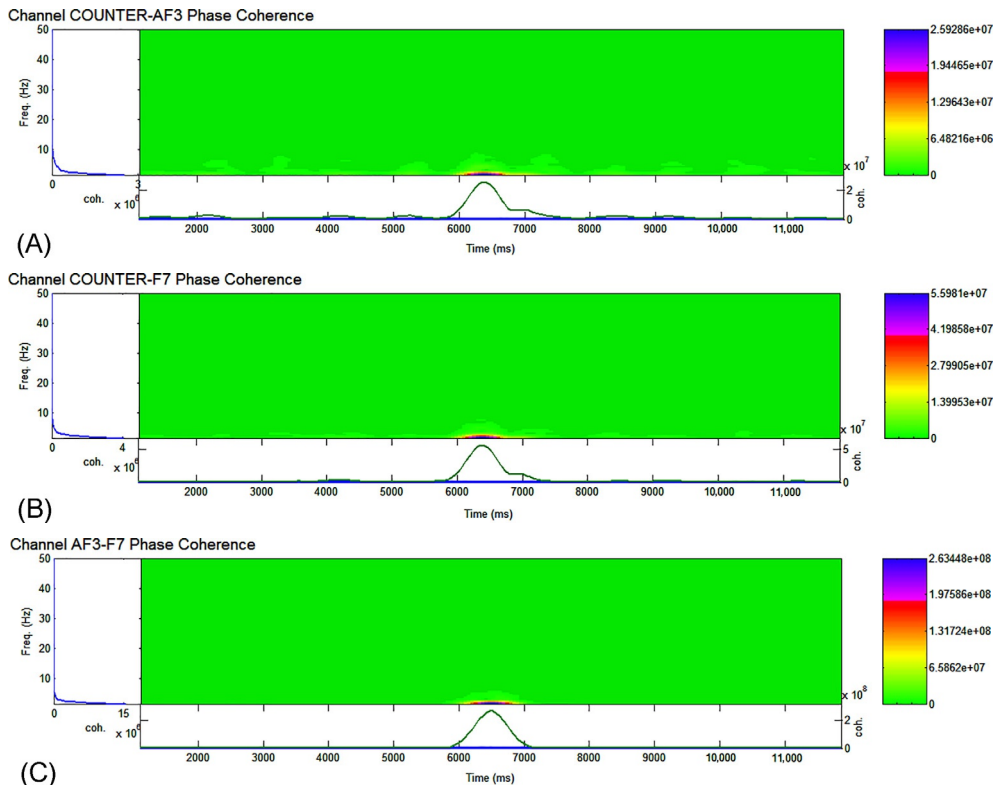


Fig. 5.13 EEG coherence plots between distinct pair of electrodes for single eyeblink activity performed by subject 3 (A) reference channel-AF3 channel, (B) reference channel-F7 channel, and (C) left frontal channels AF3-F7. The spectrogram image plot shows power variations at about 6500ms at 0–5Hz indicating high delta band coherence. The left panel indicates the mean power spectrum during single eyeblink activity. The green color coherence plot below spectrogram image shows significantly increased EEG activity and high coherence during performed action.

5.6 CONCLUSION

A substantial growth has been observed in the development of brain-computer interfaces utilizing spectral features of acquired EEG signals. Particularly, EEG signal processing in frequency domain is gaining importance for the development of efficient BCIs for device control applications in the current scenario. Brain-computer interfacing in this era is augmented toward implementation of more interactive and control applications to provide enhanced assistance to mankind to restore a normal life. This chapter presents a framework to implement a real-time BCI for control applications by analyzing forced eyeblink action-specific EEG responses in frequency domain. A detailed methodology to analyze the acquired multichannel brain patterns to identify the instant of a thoughtful single

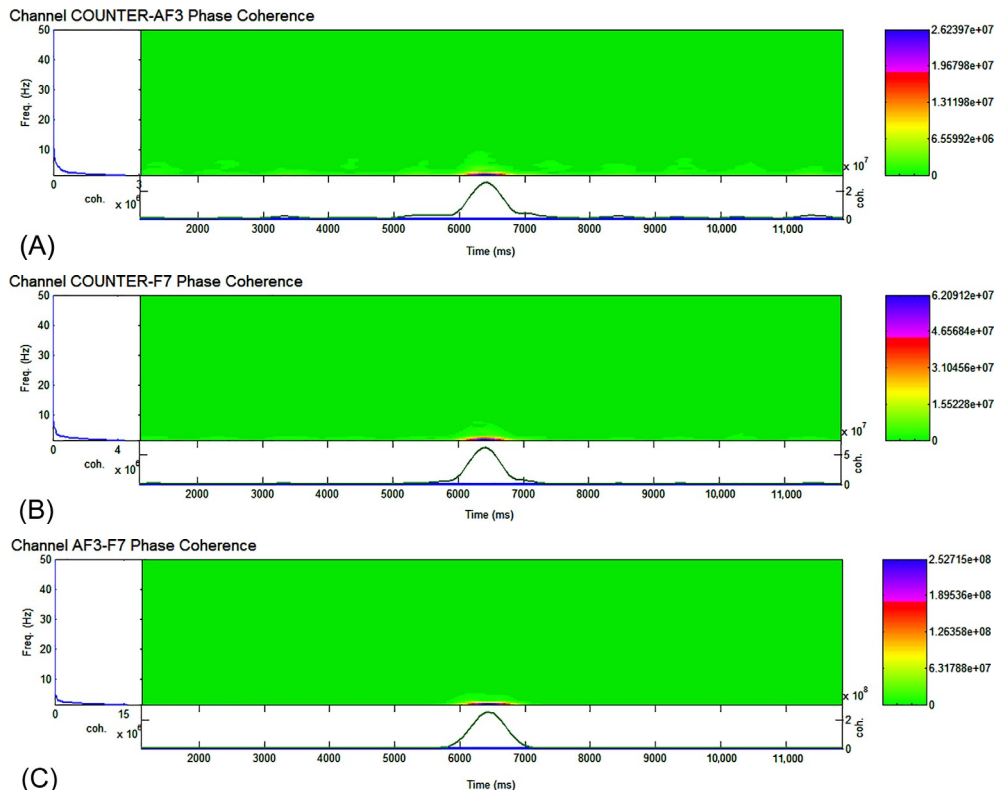


Fig. 5.14 EEG coherence plots between distinct pair of electrodes for single eyeblink activity performed by subject 4 (A) reference channel-AF3 channel, (B) reference channel-F7 channel, and (C) left frontal channels AF3-F7. The spectrogram image plot shows power variations at about 6500 ms at 0–5 Hz indicating high delta band coherence. The left panel indicates the mean power spectrum during single eyeblink activity. The green color coherence plot below spectrogram image shows significantly increased EEG activity and high coherence during performed action.

eyeblink action has been discussed. The artifact-free clean multichannel EEG dataset has been analyzed in frequency and spatial domain to identify the action correlated neural state and activated lobes of cerebral cortex. The channel spectral analysis of EEG signals has been performed to determine the power distribution across different EEG frequency points for all channel EEG data. The power distribution across left frontal scalp regions is found to be high across delta (2 Hz) to alpha (9 Hz) frequency subband of EEG. It depicts the activation of these low-frequency EEG subbands during deliberate single eyeblink actions. The channel activity analysis comprising of respective ERP image plots, averaged ERP traces, and activity power spectra has been performed across all left frontal (AF3 and F7), occipital (O1 and O2), parietal (P7 and P8), and temporal (T7 and T8) channel EEG data. The left frontal channels show increase in ERPs in response to a

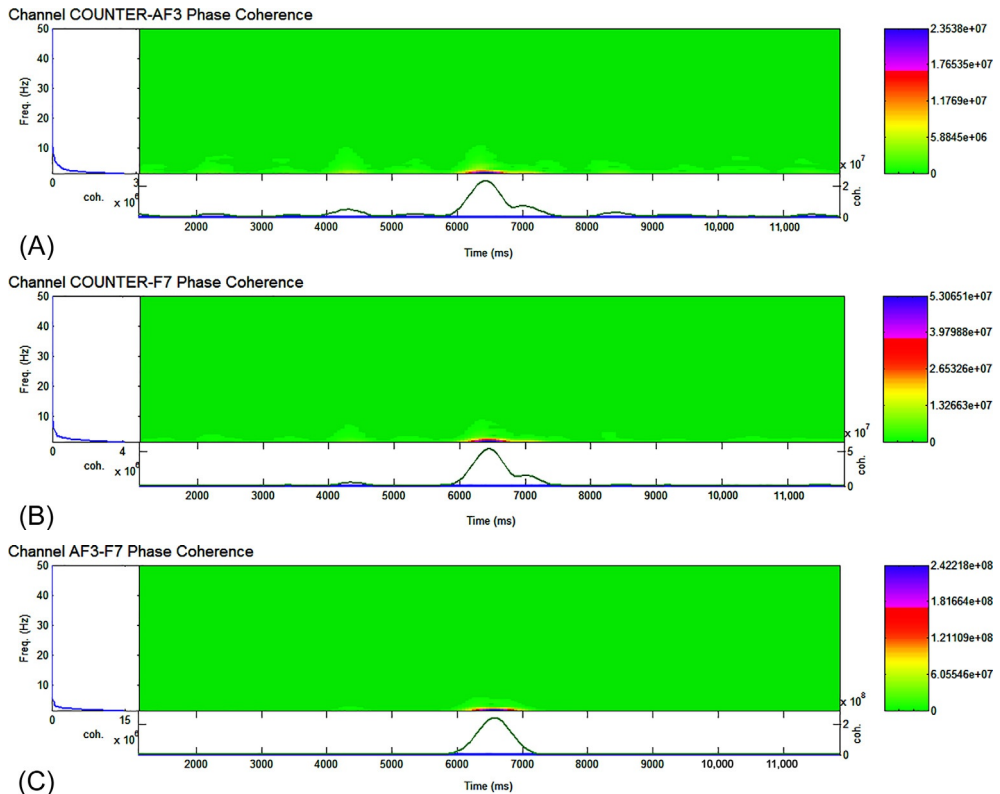


Fig. 5.15 EEG coherence plots between distinct pair of electrodes for single eyeblink activity performed by subject 5 (A) reference channel-AF3 channel, (B) reference channel-F7 channel, and (C) left frontal channels AF3-F7. The spectrogram image plot shows power variations at about 6500 ms at 0–5 Hz indicating high delta band coherence. The left panel indicates the mean power spectrum during single eyeblink activity. The green color coherence plot below spectrogram image shows significantly increased EEG activity and high coherence during performed action.

deliberate single eyeblink activity. The spectral power amplitudes are also found to be high across low-frequency bands (delta, theta, and alpha). However, the channel activity results of subject 1 found at occipital, temporal, and parietal channels do not show such prominent increase in ERP amplitudes and spectral power amplitudes as they have been visualized across frontal channels AF3 and F7. This is followed by spatial domain analysis to determine EEG coherence between either pair of left frontal channels (frontal-frontal): AF3 (channel number 3)-F7 (channel number 4) or frontal channels with respect to reference electrodes (frontal-reference). The EEG coherence results for single eyeblink activity have been computed using FFT-based spectrogram method. A high level of coherence or synchronization between activated frontal regions of cerebral cortex has

been witnessed. The instants of high coherence are found to be correlated with high EEG subband power amplitude values in particular frequency subband. The high-power amplitudes are found across lower frequency bands as depicted by the mean power spectrum plots. The above findings reflect that the captured ERP variations in time domain, spectral power amplitude variations in frequency domain, and coherence analysis in spatial domain of input EEG dataset possess the potential to be used as a trigger to implement device control applications. The cognitive analysis findings in time, frequency, and spatial domain can further be utilized to develop BCIs and have neural output driven assistive devices. The thoughtful actions/intentions can be translated into device control signals to drive external assistive devices for rehabilitation of medically/physically disabled subjects. Research in BCI has a focused approach toward improving quality of life for everyone. The potential clinical application of this work shall be to develop interactive platforms to control devices by merely using the eyeblink specific neural signals. Effective machine learning algorithms can be applied to develop a more efficient control application tool.

REFERENCES

- Bajaj, V., Pachori, R.B., 2013. Automatic classification of sleep stages based on the time-frequency image of EEG signals. *Comput. Methods Prog. Biomed.* 112 (3), 320–328. <https://doi.org/10.1016/j.cmpb.2013.07.006>.
- Cabrera, A.F., Nascimento, O.F., Farina, D., Dremstrup, K., 2008. Brain-computer interfacing: how to control computers with thoughts. *First International Symposium on Applied Sciences on Biomedical and Communication Technologies*, pp. 1–4.
- Castanié, F., 2013. Spectral analysis by parametric modeling. In: *Digital Spectral Analysis: Parametric, Non-parametric and Advanced Methods*. Wiley Online Library, pp. 143–168. <https://doi.org/10.1002/9781118601877>.
- Cho, S.-Y., Vinod, A.P., Cheng, K.W.E., 2009. Towards a brain-computer interface based control for next generation electric wheelchairs. *Int. Conf. Power Electron. Syst. Appl.*, 1–5.
- DeBoer, T., Scott, L.S., Nelson, C.A., 2006. *Methods of Acquiring and Analyzing Infant EEG and Event-Related Potentials*. Psychology Press, London, pp. 5–38.
- Delorme, A., Makeig, S., 2004. EEGLAB: an open source toolbox for analysis of single-trial EEG dynamics. *J. Neurosci. Methods* 134, 9–21.
- Dressler, O., Schneider, G., Stockmanns, G., Kochs, E.F., 2004. Awareness and the EEG power spectrum: analysis of frequencies. *Br. J. Anaesth.* 93 (6), 806–809.
- Galán, F., Nuttin, M., Lew, E., Ferrez, P.W., Vanacker, G., Philips, J., Mill'an, J.d.R., 2008. A brain-actuated wheelchair: asynchronous and noninvasive brain-computer interfaces for continuous control of robots. *Clin. Neurophysiol.* 119, 2159–2169.
- Gath, I., Feuerstein, C., Pham, D.T., Rondouin, G., 1992. On the tracking of rapid dynamic changes in seizure EEG. *IEEE Trans. Biomed. Eng.* 39 (9), 952–958.
- Iversen, I.H., Ghanayim, N., Kübler, A., Neumann, N., Birbaumer, N., Kaiser, J., 2008. A brain-computer interface tool to assess cognitive functions in completely paralyzed patients with amyotrophic lateral sclerosis. *Clin. Neurophysiol.* 119, 2214–2223.
- Jatupaiboon, N., Pannum, S., Israsena, P., 2013. Real-time EEG-based happiness detection system. *Sci. World J.* 2013, 618649. 12 pages.
- Lecuyer, A., Lotte, F., Reilly, R.B., Leeb, R., Hirose, M., Slater, M., 2008. Brain-computer interfaces virtual reality and videogames: current applications and future trends. *IEEE Comput.* 41 (10), 66–72.

- Lin, J.S., Chen, K.C., Yang, W.C., 2010. In: EEG and eye-blinking signals through a brain-computer interface based control for electric wheelchairs with wireless scheme. 2010 4th International Conference on New Trends in Information Science and Service Science (NISS), pp. 731–734.
- Mahajan, R., Bansal, D., 2015. Depression diagnosis and management using EEG based affective brain mapping in real time. *Int. J. Biomed. Eng. Technol.* 18 (2), 115–138.
- Mathewson, K.J., Jetha, M.K., Drmic, I.E., Bryson, S.E., Goldberg, J.O., Schmidt, L.A., 2012. Regional EEG alpha power, coherence, and behavioral symptomatology in autism spectrum disorder. *Clin. Neurophysiol.* 123, 1798–1809.
- Ming, D., Fu, L., Chen, L., et al., 2014. Electric wheelchair control system using brain-computer interface based on alpha-wave blocking. *Trans. Tianjin Univ.* 20 (5), 358–363. <https://doi.org/10.1007/s12209-014-2235-5>.
- Nielsen, K., Cabrera, A., Nascimento, O., 2006. EEG based BCI-towards a better control: brain-computer interface research at Aalborg University. *IEEE Trans. Neural Syst. Rehabil. Eng.* 14 (2), 202–204.
- Palaniappan, R., 2005. Brain computer interface design using band powers extracted during mental tasks. In: 2005 Conference Proceedings, 2nd International IEEE EMBS Conference on Neural Engineering, pp. 321–324.
- Pfurtscheller, G., Neuper, C., 2001. Motor imagery and direct brain-computer communication. *Proc. IEEE* 89 (7), 1123–1134.
- Pregenzer, M., Pfurtscheller, G., 1999. Frequency component selection for an EEG-based Brain Computer Interface (BCI). *IEEE Trans. Rehabil. Eng.* 7, 413–419.
- Ricardo Ramos-Aguilar, J., Olvera-López, A., Olmos-Pineda, I., 2017. Analysis of EEG signal processing techniques based on spectrograms. *Res. Comput. Sci.* 145, 151–162.
- Saa, J.F.D., Gutierrez, M.S., 2010. In: EEG signal classification using power spectral features and linear discriminant analysis: a brain computer interface application. Eighth LACCEI Latin American and Caribbean Conference for Engineering and Technology (LACCEI'2010) Innovation and Development for the Americas, June 1–4, Arequipa, Perú. WE1-1–WE1-7.
- Sakkalis, V., 2011. Review of advanced techniques for the estimation of brain connectivity measured with EEG/MEG. *Comput. Biol. Med.* 41 (12), 1110–1117.
- Sakkalis, V., Cassar, T., Zervakis, M., et al., 2008. Parametric and nonparametric EEG analysis for the evaluation of EEG activity in young children with controlled epilepsy. *Comput. Intell. Neurosci.* 2008, 462593 15 pages. <https://doi.org/10.1155/2008/462593>.
- Sanei, S., Chambers, J., 2007. EEG Signal Processing. John Wiley & Sons, p. 55.
- Stein, A., Rappelsberger, P., Sarnthein, J., Petsche, H., 1999. Synchronization between temporal and parietal cortex during multimodal object processing in man. *Cereb. Cortex* 9, 137–150.
- Tanaka, K., Matsunaga, K., Wang, H.O., 2005. Electroencephalogram-based control of an electric wheelchair. *IEEE Trans. Robotics* 21 (4), 762–766.
- Tarvainen, M.P., Hiltunen, J.K., Ranta-Aho, P.O., Karjalainen, P.A., 2004. Estimation of nonstationary EEG with Kalman smoother approach: an application to event-related synchronization (ERS). *IEEE Trans. Biomed. Eng.* 51 (3), 516–524.
- Teplan, M., 2002. Fundamentals of EEG measurement. *Meas. Sci. Rev.* 2, 1–11.
- Tuncel, D., Dizibuyuk, A., Kiymik, M.K., 2010. Time frequency based coherence analysis between EEG and EMG activities in fatigue duration. *J. Med. Syst.* 34 (2), 131–138.
- Unde, S., Shriram, R., 2014. Coherence analysis of EEG signal using power spectral density. In: 2014 Fourth International Conference on Communication Systems and Network Technologies (CSNT), pp. 871–874.
- Wolpaw, J.R., McFarland, D.J., Vaughan, T.M., 2000. Brain-computer interface research at the Wadsworth center. *IEEE Trans. Rehabil. Eng.* 8, 222–226.
- Wolpaw, J.R., Birbaumer, N., McFarland, D.J., Pfurtscheller, G., Vaughan, T.M., 2002. Brain-computer interfaces for communication and control. *Clin. Neurophysiol.* 113 (6), 767–791.
- Yamanaka, K., Yamamoto, Y., 2010. Single-trial EEG power and phase dynamics associated with voluntary response inhibition. *J. Cogn. Neurosci.* 22 (4), 714–727.

FURTHER READING

- Bansal, D., Mahajan, R., Singh, S., Rathee, D., Roy, S., 2014. Real time acquisition and analysis of neural response for rehabilitative control. *Int. J. Electr. Robot. Electron. Commun. Eng.* 8 (5), 697–701.

CHAPTER 6

EEG Based BCI—Control Applications

Dipali Bansal, Rashima Mahajan

Faculty of Engineering and Technology, Manav Rachna International Institute of Research and Studies, Faridabad, India

Contents

6.1	Introduction	167
6.2	In-House Development of Eyeblink-Based BCI for Control	171
6.2.1	Control Triggers Using MATLAB Software	173
6.2.2	Arduino Uno Hardware Interfacing for Control Applications	176
6.3	Possible Other Control Applications Using EEG-Based BCI	180
6.3.1	National Instruments' (NI) LabVIEW-Enabled Control Using BCI	180
6.3.2	Mathworks' MATLAB/Simulink-Enabled Control Using BCI	188
6.4	Conclusion	191
	References	191
	Further Reading	192

6.1 INTRODUCTION

Beethoven, the most recognized music composer and pianist started losing his hearing abilities when he was in his late 20s. Musicians of the century believe that his near deafness made him even more creative and an influential composer. However, due to the sensory loss, he stopped making public appearances and doing concerts. It makes one wonder that if brain-computer interfacing was possible in that era, then may be Beethoven would have been able to communicate his musical composition with the world in a better manner.

Research in brain-computer interface (BCI) has a focused approach toward improving quality of life for everyone. The disabled and even healthy users are deriving benefits from BCI research. Advancements in BCI technology assist in identifying efficient and low latency ways of getting voluntary changes in electroencephalography (EEG) signals for communication and control. That is, these BCI systems permit modulations in brain signals through external stimulation which can be further utilized as a control trigger for plethora of applications. BCIs are often used for cognitive monitoring of a user and thus improve their way of life through real-time neurofeedback.

“Hold that Thought” an article by Mike Richardson gives a cover story published in 2007 on how neurological signals tapped through BCI helps disable people control the external environment. The article reports that cofounder and CEO of “Ambient,” Michael Callahan was instrumental in prototyping an assistive device for patients with

symptoms of amyotrophic lateral sclerosis (ALS) and cerebral palsy or with injury in the spinal cord to overcome the challenges of social and environmental access. This device called “The Audeo” developed converts thoughts of a disabled person into speech which can further be used to control a motorized wheelchair and relied on LabVIEW application software developed by the National Instruments (NIs). Audeo was tested on an elderly gentleman who had never spoken in his life to communicate the word “Yes” to the world. The smile that appeared on his face is a motivation for BCI researchers. Mark Manasas representing “Cambridge Consultants,” a group which is into BCI research remarked that their team was successful in turning a complex, expensive, and limited to research BCI applications into affordable compact unit ready to be used in home environments for everyday use. They created a matrix of graphical user interface (GUI)-based icons for easy navigation of requirements. A BCI-based application that enables us to SEE what a locked-in patient is THINKING, can bring a change to the entire human race, as is the classic case of Prof. Stephen Hawking.

Robotics community has been exploring humanoid robots to assist mankind in performing real-time tasks that are required to be done in areas difficult to reach or are dangerous in nature. Humanoid robotics clubbed with neuroscience is gaining a lot of interest and proof of concept is being presented for controlling humanoid robots using BCI ([Bryan et al., 2011](#); [Bell et al., 2008](#); [Chae et al., 2011](#); [Millan et al., 2004](#)). Control of humanoid robots require appropriate management of high degrees of freedom inherent in them and so were handled using joysticks, speaker identification, visual response, etc. Using BCI as an alternate approach to achieve control of humanoid robots is cumbersome and yields low throughput. Noninvasive BCIs based on EEG signals further add to the problem as they offer low bandwidth for control due to low signal-to-noise ratio. A solution experimented by [Bryan et al. \(2011\)](#) to address this issue is adaptive hierarchical BCI (HBCI) design which was explored only for navigational assignments previously. HBCI works on the principle of training the BCI user initially to high skills using low-level commands which later gets translated to high-level commands. This way the humanoid robot is able to obey complex commands using BCI relating to various state spaces.

The hierarchical architecture of HBCI follows a modular concept and can be applied as explained below:

- The user is subjected to visual stimulus based on light-emitting diodes (LEDs) and the BCI depends on steady-state visually evoked potential (SSVEP). Use of LEDs offers broader range of frequencies thus allowing higher degrees of freedom.
- In the application developed by Bryan et al., EEG signals were captured using Gold electrodes positioned at FPZ on the forehead and OZ placed on the back of the skull in the center. The acquisition unit used is developed by *gUSBamp, Guger Technologies, Graz, Austria*.

- A Willow Garage PR2 humanoid robot is being trained in this application and the robot arm is simulated to pour milk into a bowl.
- Fast Fourier transform tool is used to estimate the power spectrum and for classifying the EEG signal frequency spread. Highest average frequency is selected for sending commands to the humanoid robot and the menu system.
- Menu system serves as the interface with the user to control the robot and also assists during the training session to acquire new high-end skills. Commands set on the menu initially are to train, navigate, and playback.
- HBCI architecture allows user to learn arm trajectories, rotation, and gripping as low-level primal commands to define skills of higher-level learning sequence.
- The subroutines available in an open-source software ROS (robot operating system) presented by [Quigley et al. \(2009\)](#) was made use to train on low-level commands.
- A camera is placed on the robot's head to continuously provide real-time visual stimulus.
- Cognitive exertion by the user is largely reduced in HBCI set up due to reduced number of command required to execute a task, thus improving the throughput of the system.

Another mentionable project was published in 2011 by the IEEE Computer Society in IEEE Intelligent Systems where a wheelchair was controlled safely and efficiently inside a building using thoughts acquired from P300 EEG signals. The authors Rebsamen et al. demonstrated a working prototype of a brain-actuated wheelchair navigation indoors. Control strategy adopted here depends on P300 EEG-based BCI where the user has the liberty to choose the final destination to reach available on the menu. Wheelchair user follows the destined defined path safely and with minimal effort. Paths defined for a particular environment are software controlled and so are dynamic in nature and can be modified. Context-dependent command menu is flashed randomly to the wheelchair user and the P300 BCI identifies the requirement. Options are to choose different floors or various locations on a particular floor to navigate. Critical parameters to be kept in mind to ensure error-free selection of target destination are error rate, response time, and false acceptance rate. A compromise has to be made based on these factors for setting optimum threshold for a particular application. Implementation of this project is done as per details below:

- A high-quality, cost-effective 40-channel EEG acquisition set “NuAmps” manufactured by Neuroscan is used.
- The prototype is developed on Yamaha's JW-1 power wheelchair.
- A bar code scanner “Symbol M2004 Cyclone” used by shopkeepers to read price code is installed for global positioning.
- Two optical rotary encoders are used for odometry which are attached to the glidewheels.

- The programming language used is “C” operating on Ubuntu Linux 6.06 platform. To enable real-time application, it is linked with RT (real time) application interface version 3.3.

The system developed is very user friendly and easy to set up in real time. Simple tools enable design of guiding maps and involve least user’s input and concentration. Since the path navigated becomes predictable, the user is relaxed during the movement.

Today, the world is witnessing “Information Tsunami” and a large amount of spatial/temporal data is being captured and stored and it is becoming increasingly difficult to extract relevant information and make quick decisions based on them. Futuristic developments are dependent on such information and decisions and so it is imperative to make technological advancements to handle this. Human capacity to perceive information and draw inferences is still unsurpassed and so EEG-based BCI systems that can combine human vision and computer vision to understand large database of images/videos is being researched. Such BCI is called “cortically coupled computer vision” (C3-Vision) that utilizes the capability of a human being and a computer, where neurological signals communicate with the user’s intent and cognitive condition (Pohlmeyer et al., 2011; Gerson et al., 2006).

A BCI unit must be executable in real time and should be flexible enough to adapt to specific user’s needs. Delorme et al. contributed a chapter titled “*MATLAB-Based Tools for BCI Research*” in 2010 which describes the requirements for BCI software development and the environment. Facilitation in flexibility of design and computational and performance efficiency are very critical elements of a BCI unit. As researchers of versatile domains viz. psychologists, doctors, mathematicians, scientists, engineers, signal processing experts, etc. take interest in BCI development, it becomes essential that the development environment should be user friendly. A BCI system involving EEG data acquisition in real time must critically look into data streaming, online data processing, and feedback mechanism for its use as a control application (Delorme et al., 2010). Mostly, EEG data streaming between the acquisition unit and the software is done by calling a dynamically linked library (.dll) file. For example, in MATLAB, a .dll subroutine is called to set up interface using “Realtime Workshop.” MATLAB also permits use of transmission control protocol/internet protocol (TCP/IP) protocol along with “Instrument Control Toolbox” for data streaming over a network. Data streaming is also performed for buffering so as to avoid delay in real-time data acquisition process when repeated computation takes place in the system. Online data processing in a BCI unit includes signal processing, feature extraction, and classification algorithms. Based on the classification, a neurofeedback is generated and applications are controlled.

Optimum usability of a BCI system is hugely impacted by specified input methods, display paradigms, and control interface used. Control interfaces provide cues for doing mental tasks, give updates on system feedback, and represent the subject’s neural response. Control interfaces also translate the coherent control outputs generated by the classifier algorithm into meaningful control outputs to manage the device

mechanism. To be able to control a device, a BCI user needs to perform “control tasks” which are mental endeavors made to bring voluntary changes in the neural responses. The control task includes visualized or physical movements, entity identification, focused mind, singing or counting, meditation, etc. and can be categorized into exogenous and endogenous paradigms. Exogenous or the evoked paradigm is where the user is made to focus on a set of stimuli which generates automatic predefined responses to be picked by a BCI. One such example is the activation of P300 signal in the parietal brain region after 300 ms, when the user is exposed to visual or auditory stimuli. In endogenous or self-generated model, the user voluntarily does the mental task of imagined movement, meditation or counting, etc. to produce subtle changes in the neural response. Examples are slow cortical potentials (SCPs) and mu rhythm responses which are used to select targets like positioning of a cursor by means of endogenous input similar to imagined hand movement. Biofeedbacks also have a vital role to play in guiding response of endogenous control interfaces ([Jackson and Mappus, 2010](#)).

Control outputs from a BCI unit enable replacement, restoration, and enhancement and they also supplement the natural brain signal output to bring changes in the manner in which one interacts with the internal and external environment. BCI output can replace impaired natural ability of an individual to speak by helping them to spell words or even speak using a speech synthesizer. BCI also assists in restoring natural limb movement which may be lost due to spinal cord injury by implanting electrodes that control stimulation of paralyzed limbs. Bladder control lost due to multiple sclerosis can also be restored using a BCI output that can trigger stimulation outputs to the nerves that control urination. Concentration spans and attention levels can be enhanced using BCI and mishaps can be avoided. Natural central nervous system (CNS) output can be further supplemented and improved by a BCI output control mechanism as in case of maneuvering a robotic arm designed to do a specific task ([He et al., n.d.](#); [Springer, 2013](#)). Certain interesting control applications designed using BCI are explained in the below sections. [Section 6.2](#) details in-house development of eyeblink-based BCI in MATLAB environment for control applications and [Section 6.3](#) explains possible other methods for control using BCI developed so far by various researchers.

6.2 IN-HOUSE DEVELOPMENT OF EYEBLINK-BASED BCI FOR CONTROL

Medical robotics has contributed phenomenally over the years toward clinical procedures, viz., surgery, prosthetics, orthotics, BCIs, etc. Research publications in the domain of brain-controlled applications have covered not only medical needs but also has catered to the requirements of healthy users in their day-to-day life. Most of the work is concentrated around acquisition of EEG signal for BCI however other modalities are also researched. In this section, attempt has been made to detect brain activity relating to a thoughtful single eyeblink which has been acquired through a 14-channel

EEG neuroheadset unit “Emotiv” and its subsequent use as trigger for control applications. The EEG-based neural patterns attained while performing a voluntary motor action (eyeblink) is imported and analyzed using EEGLAB version 13.0.1 toolbox in MATLAB. Left frontal scalp regions corresponding to channel AF3 of Emotiv unit are observed as the prominent points of eyeblink-related brain pattern acquisition. The acquired EEG patterns are preprocessed and ICA is applied to identify the maximum independent EEG components (in spatial and temporal domain) related to performed single eyeblink action. A prominent increase in the potential concentration has been recorded while being almost constantly varying when the subject is relaxed.

The single eyeblink-specific multichannel EEG dataset is used for event-related potential (ERP) and subsequent topographic scalp map analysis at distinct set of latencies. The highest potential distribution is found across frontal scalp regions during the performed action of eyeblink. The spectral map analysis indicates the dominance of particular EEG subbands during performed action (details are in [Chapters 4 and 5](#)). This high variation captured in ERPs on the onset of deliberate eyeblink action has been utilized as a control signal to design an algorithm and framework to implement neural control applications of interest, viz., to play a “*handel.mat*” audio file in MATLAB environment and to control the glowing instances of a LED. The identified high ERP component variations from MATLAB workspace have been translated into control commands. The control application-based BCIs possess the potential to be developed as a real-time assistive tool for rehabilitation of differently abled subjects suffering from certain motor disorders.

Functional block diagram (BD) of BCI system developed in-house to acquire and identify voluntary single eyeblink in real time using Emotiv EEG neuroheadset and its use to trigger a control application is sketched in [Fig. 6.1](#). The system enables capturing of EEG data from Emotiv unit in wireless mode through Bluetooth. Signal processing is done in MATLAB application software to identify deliberate eyeblink information from the EEG dataset. An algorithm is further developed to trigger a control command based on a subsequent rise in ERP related to forced eyeblink captured from the neural EEG patterns through scalp electrodes.

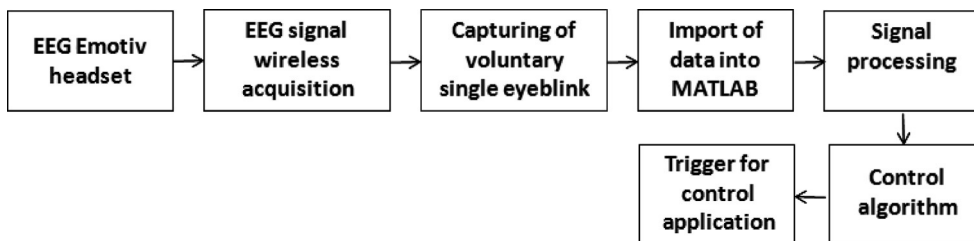


Fig. 6.1 Block diagram to capture neural activity via electroencephalography (EEG) for eyeblink-based control.

Ten healthy subjects (seven females and three males), aged 14–18 years, who had not consumed any medication before the experiment have been allowed to participate for EEG data acquisition and subsequent signal database formulation. The consent from all the participants has been documented before conducting the planned research work. The participants were briefed about the experiment and the type of neural responses to be recorded. Each participant wearing EEG Emotiv unit has been asked to be seated in a designated disturbance free room. Initially, a settlement time has been given to make them feel relaxed and was directed to perform a forced single eyeblink action. A set of almost 50 EEG signal trials were recorded by acquiring five signal sequences per subject. The Emotiv unit helped in acquiring EEG brain patterns while performing voluntary eyeblink action using scalp electrodes which include frontal electrodes (AF3, AF4, F7, F8, F3, F4, FC5, and FC6); temporal electrodes (T7 and T8); parietal electrodes (P7 and P8), and occipital electrodes (O1 and O2). The EMOTIV neuroheadset acquires EEG data by sampling it at 128 Hz and wirelessly transmits to the interfaced computer unit. The transmitted dataset in .edf format is first received and displayed in EMOTIV test bench software installed at interfaced computer. The real-time multichannel online EEG data feed can be directly received in MATLAB (.mat format) instead of acquiring EEG responses using EMOTIV test bench which may facilitate live EEG signal visualization and analysis without any introduced delay.

The preprocessing, time domain and frequency domain analysis of recorded EEG activity has been performed using MATLAB-based stand-alone application software toolbox EEGLAB v 13.2.2.b and in MATLAB workspace of release 2016b. Initially, the eyeblink specific acquired EEG dataset through EMOTIV test bench was imported to EEGLAB and in MATLAB workspace. The recorded neural activity is time locked to specific events. The EEG records are analyzed to extract the specific event-related data epochs from continuously acquired EEG data through scalp electrodes. It has been found that the brain response correlated to deliberate single eyeblink act can be observed majorly at left frontal scalp channels (AF3 and F7) and right frontal scalp channels (AF4 and F8) of EMOTIV headset unit as shown in Fig. 6.2.

The BCI developed in-house has been used to trigger a musical output using software control in MATLAB ([Bansal et al., 2014](#)) and also to control hardware using Arduino Uno interfacing based on eyeblink data. Detail of the applications developed is presented in sections further.

6.2.1 Control Triggers Using MATLAB Software

Fig. 6.3 presents the algorithm developed in MATLAB for triggering an external device control application through a thoughtful single eyeblink-based EEG data. EEG data acquired and stored for voluntary eyeblink is exported to MATLAB environment for the purposeful subsequent analysis. EEG signal information is loaded and stored in a

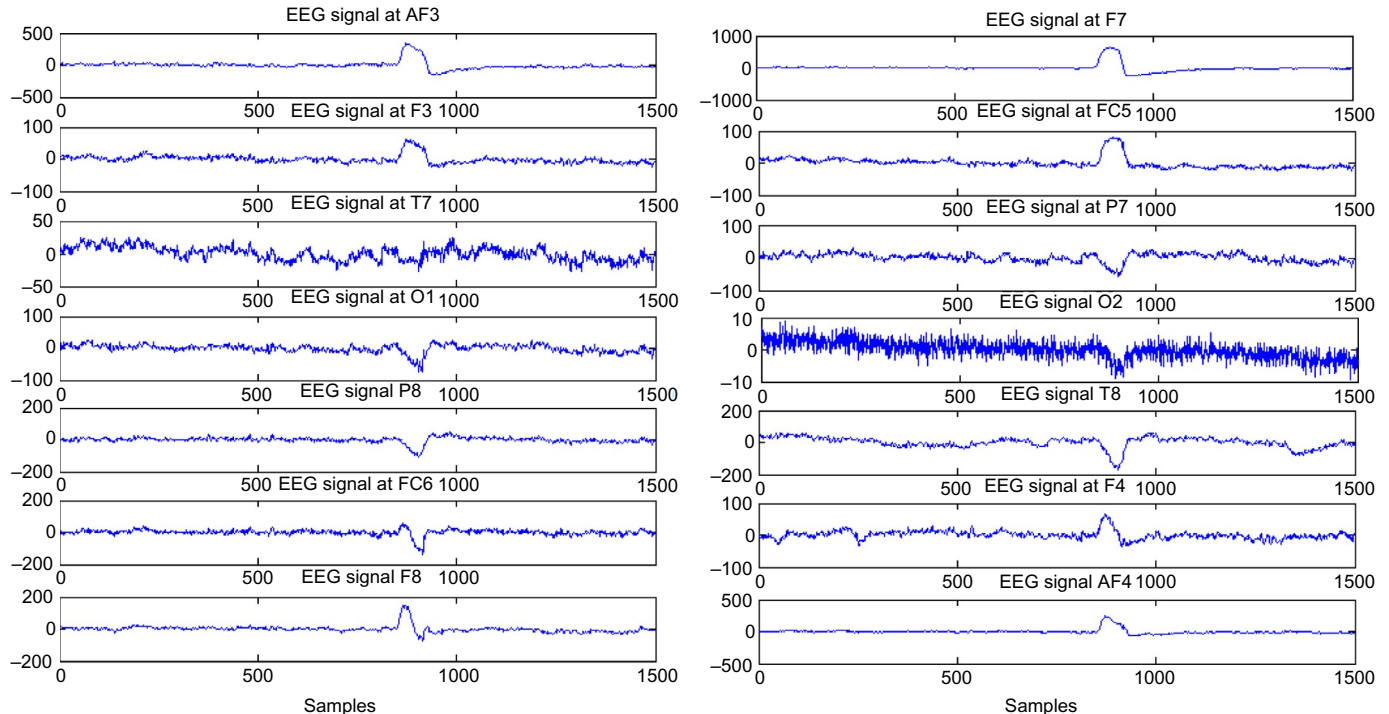


Fig. 6.2 Eyeblink-related EEG acquired using Emotiv EEG neuroheadset.

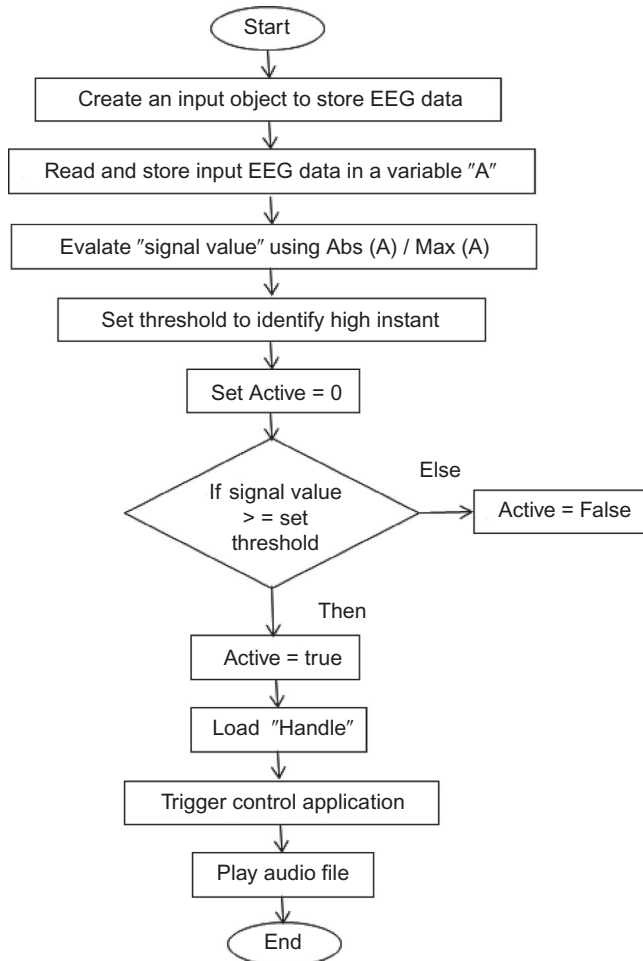


Fig. 6.3 Algorithm in MATLAB to use eyeblink-specific brain activity via EEG to develop device control application.

variable created in MATLAB. The absolute/maximum value is evaluated further for the variable created. The signal is passed through a band-pass filter and the corresponding mean is computed from the preprocessed EEG data to find the “threshold ERP” value to be set as reference. The input EEG signal samples at each and every time point are compared with the set threshold ERP value. If the signal amplitude at certain point is found more than the selected threshold ERP value, the performed single eyeblink action is used as software-based trigger for control applications. A “handle” is then loaded into MATLAB. In the present application, an audio file “handel.mat” is played when an “active high” output is generated. Thus, using single eyeblink information captured in human EEG data, the BCI developed is able to play music using software.

6.2.2 Arduino Uno Hardware Interfacing for Control Applications

A countable research has been documented to use eyeblink-based neural activity via EEG to trigger a device control application. Further, the use of Arduino board as an interfacing unit to control the specific application as per the acquired and translated neural activity needs to be explored. Having a vision to establish the proposed concept, the functional BD of the developed BCI with Arduino Uno hardware interfacing is given in Fig. 6.4. It includes Emotiv EEG acquisition device to record correlated brain patterns while performing a forced eyeblink action, EEG data import block to attain signals in MATLAB workspace, signal processing/analysis stage to capture subtle details in recorded EEG dataset. The extracted feature set is translated to operative control signals and is further applied to the interfaced microcontroller unit (Arduino Uno), the output instances of which are used for specific controlling action.

The neural activity recorded via electroencephalogram at left frontal scalp electrode AF3 as shown in Fig. 6.2 has been analyzed and encoded to further develop a LED control application. It has been implemented by interfacing a LED with Arduino board. The identified high ERP component variations from MATLAB workspace have been translated into control commands to drive the interfaced device (LED here) via Arduino. At first, the mean value of captured EEG signals from frontal electrode AF3 is calculated. This is followed by subtraction of mean from input signal to obtain a scaled EEG signal for subsequent analysis. Next step is to calculate the threshold (T) value of a scaled signal. It is compared with peak ERP amplitude (ERP_{peak}) at each instance. If $ERP_{peak} > T$, a D11 pin of interfaced Arduino Uno microcontroller board will receive ‘high’ input to be further used for glowing interfaced LED. The whole process is explained in Fig. 6.5.

Arduino Uno support packages were installed and the board was interfaced with both MATLAB and Simulink release 2016a. A “com port” is created using the device manager for setting up a “communication channel” between MATLAB and Arduino Uno microcontroller board. An object “a” is generated in MATLAB to configure Arduino via port “5.” Once the communication is launched, a “high” output is generated at pin “D11” of Arduino board, if output exceeds the threshold being set. This switches ON the LED whose anode is attached to pin D11 of microcontroller board and cathode is grounded. The MATLAB command used is as follows:

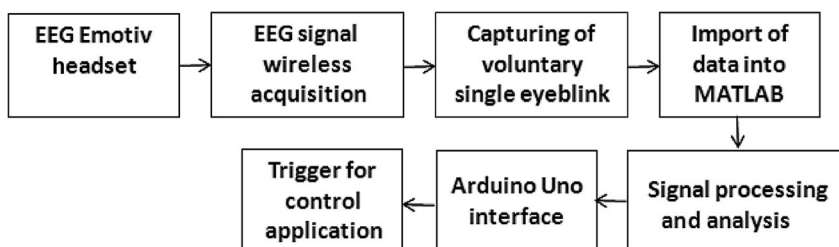


Fig. 6.4 Block diagram of in-house developed brain-computer interface (BCI) with Arduino Hardware interfacing for control.

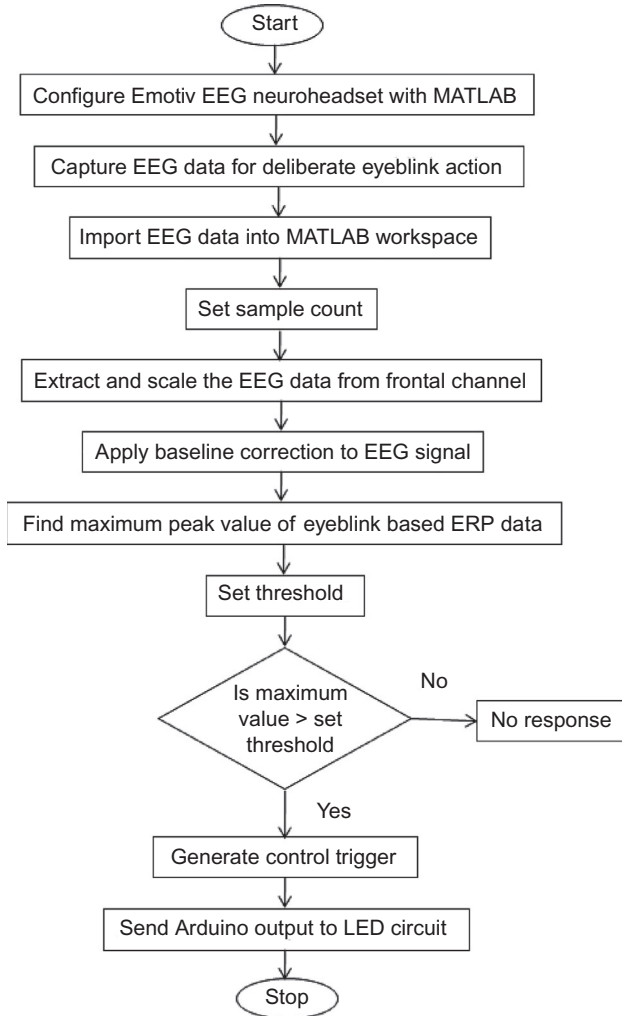


Fig. 6.5 Algorithm for EEG-based eyeblink controlled light-emitting diode (LED) through Arduino board.

```

a = arduino ('com5', 'uno');
writeDigitalPin (a, 'D11', 1);
  
```

An interfacing between Arduino Uno board and Simulink has also been established, so that the model could be used independently for other control applications. A “Simin-Block” was used from “Simulink Source Library” to bring in forced eyeblink-specific neural responses from MATLAB Workspace. Output obtained was then interfaced with Arduino Uno microcontroller hardware board using “Arduino Digital Block” and interconnections were done to create the complete model. Output from Simulink model was attained at “D11” pin of microcontroller board. Interfacing of Arduino board with MATLAB and Simulink environment is presented in Fig. 6.6.

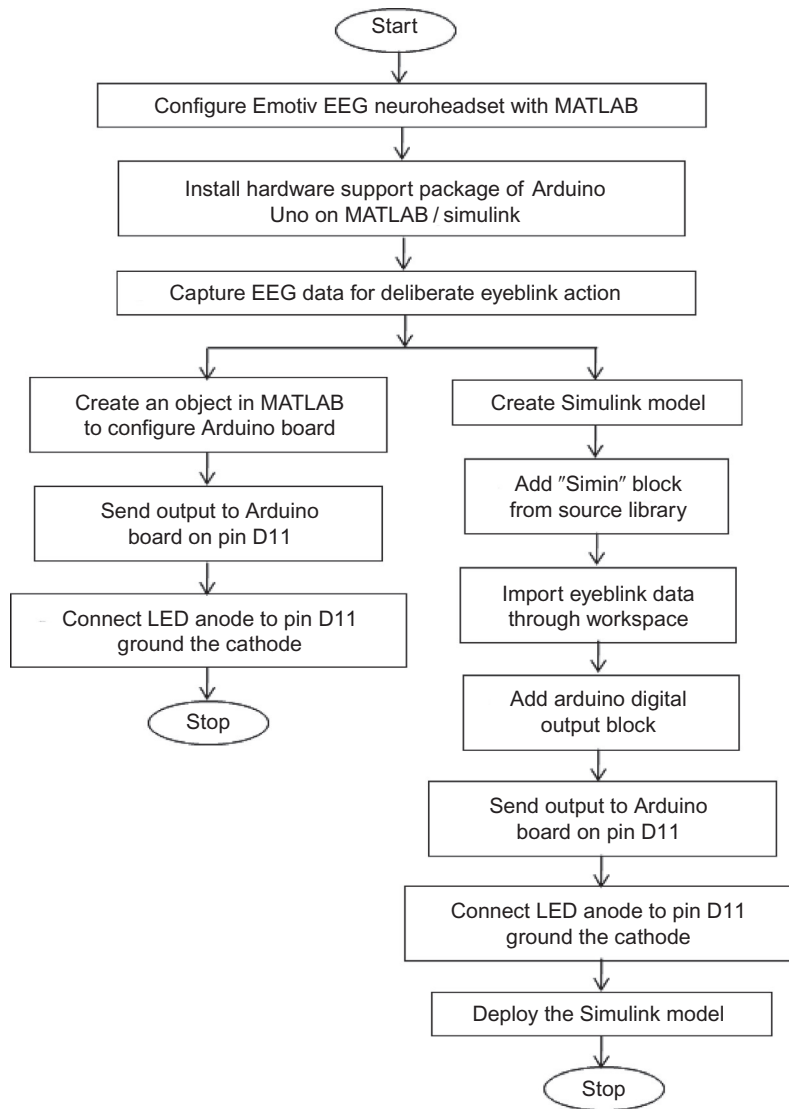


Fig. 6.6 Interfacing of Arduino board with MATLAB/Simulink environment.

At first, the neural responses via EEG are captured when subject is in relaxed state and is plotted in Fig. 6.7A. Further, the subjects were directed to perform single eyeblink action and corresponding signal is presented in Fig. 6.7B. The increased ERP amplitude is encircled red for better understanding. The recorded changes in peak potential amplitudes are compared with the calculated threshold. The moment the ERP amplitude becomes higher than calculated threshold particularly during samples values from 800 to 1000 (shown in Fig. 6.7B), a control output is triggered. This “high” output is interfaced to pin number 11 of microcontroller board through the “com 5” port. The

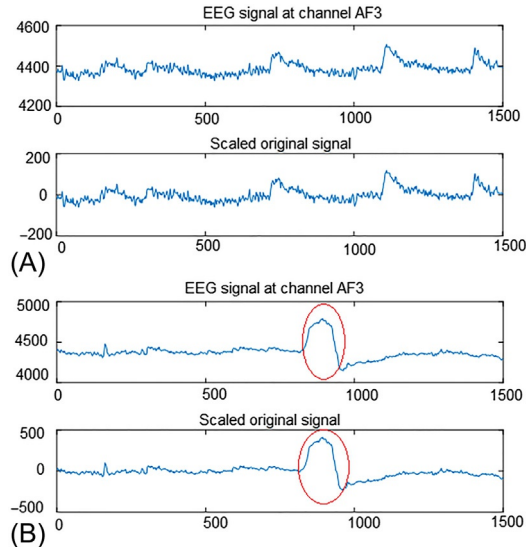


Fig. 6.7 Event-related potential analysis (A) during relaxed state and (B) during forced single eyeblink action.

transmission and reception of this active high signal at interfaced board is indicated by the glowing of transmit/receive LED integrated over Arduino Uno board.

Once a ‘high’ output is received at the LED, it starts glowing as depicted in [Fig. 6.8](#). Once the signal processing algorithm developed in MATLAB workspace got verified by

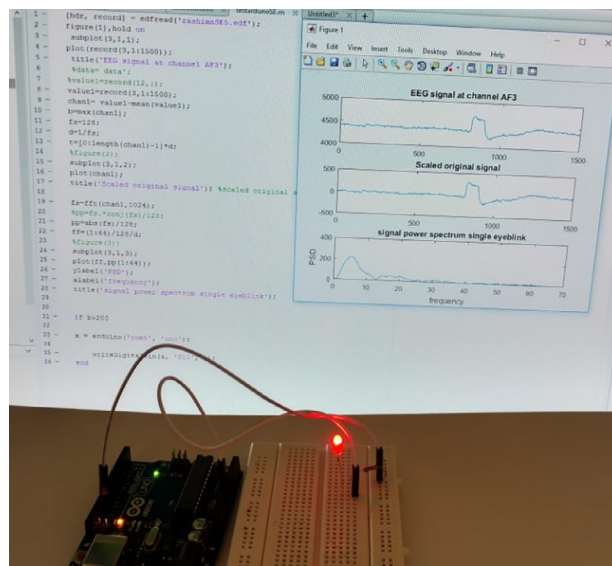


Fig. 6.8 LED control through voluntary single eyeblink EEG data.

monitoring glowing instances of LED, a model is reciprocated in Simulink by introducing “Simin Source Block” to import workspace data in Simulink. Output obtained is connected to pin 11 of “Arduino Output Block.” The model designed is finally deployed on the Arduino microcontroller board and gives a stand-alone application.

6.3 POSSIBLE OTHER CONTROL APPLICATIONS USING EEG-BASED BCI

Brain power is being harnessed in amazingly surprising ways and with the advent of promising trends in computing technologies, BCI systems thus developed enable real-time solutions to complex needs. BCIs have conceivably varied clinical and nonclinical applications as is briefed in [Chapter 2, Section 2.7](#). Major contributions in medical fields range from preventive to diagnostic to rehabilitative for patients suffering from locked-in syndrome (LIS), completely locked-in syndrome (CLIS), or even in healthy individuals ([Berger et al., 2008; Neuper et al., 2003](#)) as highlighted in [Chapter 2](#). Other major real-world applications that assist mutual understanding between human brain and the neighboring systems include neuro-ergonomics, smart home and environment, neuro-marketing, advertisement, education, games, entertainment, security, authentication, defense, and aerospace ([Abdulkader et al., 2015; Mak and Wolpaw, 2009](#)). [Luzheng et al. \(2013\)](#) surveyed the possibility of EEG-based BCI to control mobile robots to assist voluntary movement of disabled people in their daily life. Thus, as is obvious, the BCI technology is swiftly shifting from laboratory environments to everyday life useful products.

Of all the ways of capturing brain signals for control application, EEG-based BCIs are the most convenient and find plethora of applications that have been developed using various software platforms. The sections further detail prototypes developed in MATLAB/Simulink and LabVIEW environment.

6.3.1 National Instruments’ (NI) LabVIEW-Enabled Control Using BCI

LabVIEW, a NI product provides a graphical programming setting consisting of a “BD” and a “front panel (FP)” and the programs developed are called virtual instruments (VIs). Codes are easy to generate graphically in BD window and the FP allows user-friendly approach to interact with the VI (www.ni.com/NI_LabVIEW/). “C” programming language is text based and follows a control-flow execution protocol, whereas in LabVIEW, a data-flow execution model is followed. This helps in visualizing each phase of development which includes integration of hardware from different vendors, measurement, data analysis, debugging, and control interfaces. Researchers find programming in LabVIEW much simpler than other languages. It uses G programming which allows rapid development in automation. Easy drop and wire concept helps in assembling GUI from predefined FP controls. LabVIEW easily integrates with Emotiv EEG headset using *LabVIEW Emotiv Toolkit created by Eric Beutlich* and allows raw EEG data to be saved as .csv files.

An engineering graduate *Michael Callahan and his team mate Thomas Coleman from the University of Illinois* made an outstanding contribution way back in 2005 in the field of

brain-computer interfacing by developing a device “Audeo” which converts thoughts into speech/command to control a wheelchair using NI’s application software LabVIEW (Callahan, 2013). This NI LabVIEW-enabled innovation has the potential to intensely support patients suffering from neurological disorders like ALS/Lou Gherig’s disease, spinal cord injury, etc. Patients suffering from ALS may be able to somehow make mouth movements, but are unable to exercise their lungs sufficiently to make audible speech. Since the speech is originated by brain, so although they are not audible, the signal can be intercepted and speech can be created says Coleman. This motivated him to develop “The Audeo.” The “Audeo” device acquires neurological signals from a sensor put across the subject’s neck and interprets the brain signal that manages vocal chords/vocal tract. The signal is transferred to a computer for noise removal using signal processing algorithms and to generate control commands for wheelchair navigation using LabVIEW-based algorithm designed. The arrangement thus permits thought-based control of a wheelchair enabling a person who could not speak or move to communicate with the external world. Callahan and his team in a continuous endeavor are improving the system, not just for speech production but also to assist control of various other devices. They believe that LabVIEW is a graphical programming environment that simplifies development and promotes creativity and innovation.

There are certain open-source BCI developed in LabVIEW environment like OpenBCI toolkit (<http://openbci.com/>) and “MuSAE Lab EEG Server,” MuLES (<https://github.com/MuSAELab/MuLES>) available that provide versatile and affordable bio-signal acquisition and analysis platform. Thus, enabling researchers and hobbyists across the world with easy framework to understand and develop BCIs for various applications. The hardware board of OpenBCI is available both for 8 bits (based on ATmega328P) and 32 bits (based on PIC32MX250F128B) design applications. OpenBCI communication protocol developed in LabVIEW is utilized to write and read from the OpenBCI hardware board. MuLES provides a user-friendly GUI and compatible interfacing for various EEG acquisition set ups available commercially, thus allowing quick prototyping and total inter-changeability between the devices (Cassani et al., 2015). It also assists data streaming with other software programmed in any language that support basic TCP/IP network. MuLES can be easily installed using “*MuLES_installer.zip*.” John W. Kelly from Carnegie Mellon University and his research team developed a modular framework named “Craniux” based on LabVIEW for real-time processing and analysis of brain signals and its utilization for control signal generation. Craniux utilizes the LabVIEW system design environment and helps researchers in rapid development of novel algorithms for neural data visualization and control rather than worrying on basic development of BCI unit. It is featured in *Computational Intelligence and Neuroscience* journal and is available as an open source. This can be used by novice and assists them in understanding tools of LabVIEW and the integration with acquisition hardware needed for BCI. One hardware unit used for EEG acquisition and which is compatible with LabVIEW is developed by NeuroSky.

NeuroSky Company is into developing user-friendly and economical wireless headsets for acquiring EEG brain waves using “ThinkGear chip” employing dry sensor electrode which enables quick data acquisition. *Andy K.* documented about “LabVIEW–NeuroSky Driver” which allows bio-signal acquisition and other associated functionalities in 2011 and published modification in 2017. LabVIEW–NeuroSky Driver provides a dynamic-linked library (dll) to call virtual com port connected to the headset using a set of functions written in C. The driver module provides examples for basic data acquisition and certain advanced functionalities as well. The support required to set up this driver includes LabVIEW 2010 or above version, VI Package Manager developed by JKI and NeuroSky driver included with the headset. The only hardware tested with “LabVIEW–NeuroSky Driver” is the MindWave headset. MindWave EEG headset is the conclusion of years of research in EEG biosensor technology culminating into one easy to manage, affordable, and wearable unit which can transform science fiction into reality.

NeuroSky MindWave is a single channel simple and affordable EEG acquisition unit that permits easy-to-perceive brain signals. The EEG biosensor technology used provides crisp inputs for distinct applications that give health and wellness, educational, and research inputs for varied control applications. It can be categorized as a high-performance physiological signal acquisition and analysis solution via single chip for precise brain signal acquisition and subsequent processing. Detailed features are presented in [Chapter 3](#), Section 3.2.2.5. Some control applications developed in LabVIEW are given in the sections further.

6.3.1.1 EEG-Based Prosthetic Hand Control Designed Using LabVIEW

Mohamad Amlie Abu Kasim et al. designed a cost-effective prosthetic hand controlled by artifact data embedded in EEG data using LabVIEW in 2017. Advancements in BCI and robotic technology have enabled improved functionality in healthcare domain especially for those who suffer from severe motor impairments. The prosthetic hand developed in this project allows amputee to do routine task in a simple and effective manner. Set up for the development is depicted in [Fig. 6.9](#).

The work flow development process is detailed below:

- Real-time EEG data is acquired using Emotiv EEG headset.
- EEG data is transferred wirelessly over Bluetooth.

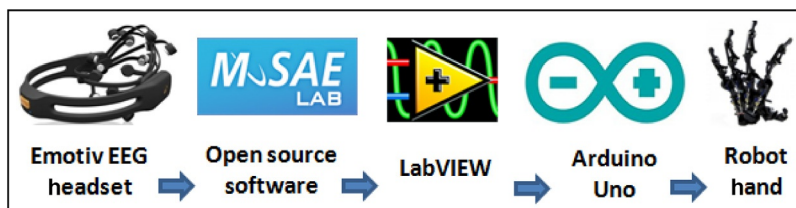


Fig. 6.9 Set up for BCI-based prosthetic hand control using LabVIEW.

- Open-source software MuSAE Lab is used to reduce the complexity and time involved in signal processing tasks.
- Subject is trained to use the prosthetic hand using LabVIEW GUI. Once trained, the need of GUI is eliminated.
- VI created in LabVIEW is used to connect with the Arduino Uno board.
- A MechaTE Robot Left Hand made of anodized aircraft aluminum is used as the prosthetic device for the amputee in this project. This robotic hand gives optimal movement through 14 joints of motion and 5 degrees of freedom. It is controlled by PWM (pulse width modulation) servo controller.

6.3.1.2 EEG-Based Eyeblink Controlled Robot Developed in LabVIEW

A Master Mind Project developed by [Vjvarada \(2012\)](#) using LabVIEW claim to have combined voluntary eyeblink data and attention level information extracted from EEG signal along with advanced signal processing algorithms and neurofeedback system to control robot.

The brain-computer interfacing unit used is the NeuroSky MindWave headset which consists of an ear clip with reference electrodes, and a sensor arm with EEG electrodes which use dry sensors. The sensor placed on “FP1” site above the left eyebrow enables a high degree of freedom and is capable of assessing various mental conditions concurrently. Proximity to eye helps in acquiring muscle movement in ocular region [electro-oculography (EOG)] and so the eyeblink data are captured better. Data are sent serially over Bluetooth communication protocol. A device driver called “Think Gear Communications Driver (TGCD)” allows communication between the LabVIEW software on the computer and the ASIC (application-specific integrated circuit) chip embedded for EEG acquisition inside the headset. BD in [Fig. 6.10](#) shows the data acquisition, analysis, and control process adopted in this project.

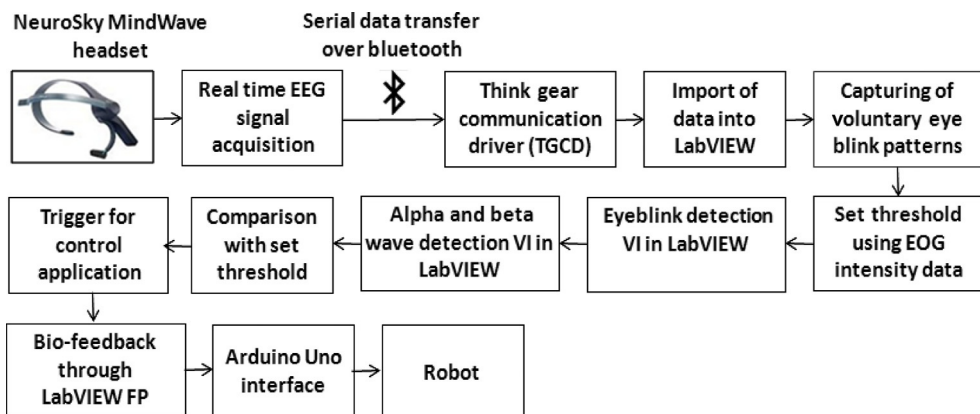


Fig. 6.10 Block diagram of EEG-based eyeblink controlled robots developed in LabVIEW.

The entire work flow process is detailed under:

- Real-time acquisition of EEG data using NeuroSky MindWave headset.
- Serial data transfer over Bluetooth COM port.
- Link set up between LabVIEW and hardware using TGCD.
- Identification of voluntary eyeblink pattern from EOG data.
- Calculation of EOG intensity for setting the threshold. Normally voluntary eyeblink is of the range 400 μ V and above ([Vjvarada, 2012](#)), so natural blinks easily get eliminated.
- Calculation of time difference between consecutive eyeblinks.
- Creation of double and triple eyeblink detection VI in LabVIEW.
- Identification of alpha wave range (3–13 Hz) which is attributed to meditation levels.
- Creation of VI for calculating alpha wave intensity.
- Identification of beta wave range (12–30 Hz) which is an indicator of concentration span.
- VI in LabVIEW for extraction of beta wave intensity.
- Comparison of beta level with set threshold which is more than attention level to send control output.
- Generation of biofeedback through LabVIEW FP.
- Training of subject for improved concentration span and also to ensure relaxed state of mind.
- Generation of control output. Motion in two-dimensional (2D) is controlled by double blink trigger and triple blink is used to stop in this project.
- Serial transmission of data to Arduino Board for controlling the robot wirelessly.

6.3.1.3 EEG-Based Intelligent Stress Buster Developed in LabVIEW

Roy et al. integrated LabVIEW-based VI, Arduino Uno microcontroller board, GSM modem and BCI unit to detect and analyze mental stress and fatigue in real time using a cost effective and portable set up. The entire system can be categorized into three subsystems. The initial task is to have a portable, reliable, and efficient system to acquire, process, and analyze changes in brain signals generated due to mental trauma, anxiety, or exhaustion. Second assignment is the generation of automatic stress releasing mechanism followed by the last task of sending an alert message to the care providers in case of overstressed condition. The entire development of firmware and software for this application has been detailed below:

- EEG and EOG brain wave signal is acquired using NeuroSky MindWave headset having embedded capabilities for noise reduction and signal processing.
- Acquired neurosignal is imported into LabVIEW design platform and is classified into relevant frequency bands.

- Butterworth filters are designed and threshold frequency is set based on beta range (14–30 Hz) to further categorize the brain signal characteristics corresponding to normal, stressed, and overstressed situations.
- VI in LabVIEW is programmed to automatically reduce stress and has soothing effect on an individual by connecting them to applications like music player, game player, and picture viewer when the filter senses a “TRUE” condition of stress.
- When overstressed situation is sensed, GSM module is activated and an alarm is sent to the near and dear ones.
- Arduino Uno microcontroller board is used to control the application. The program may further be sent to FPGA (Field Programmable Gate Array) board “NIMyRio” to create a stand-alone VI to run the application.

6.3.1.4 Read the Smile State and Cognitive Actions Using LabVIEW

Author Beutlich created in 2011 a LabVIEW and Emotiv headset-based example “EmoComposer” that reads SMILES and further enhanced it in 2017. Emotiv BCI API (Application Program Interface) is required to be downloaded from the link “<https://decibel.ni.com/content/docs/DOC-18059>” to read the smiles. This API permits analysis of facial gestures, emotional states, and cognitive activities. The firmware and software required for implementing this example are version 8.6 of LabVIEW or higher, JKI VI Package Manager, Emotiv Toolkit and proprietary software, USB port on the computer, and saline solution.

The VI code created in LabVIEW to read Smiles is executed using the following steps:

- Install EmoComposer and set the path to “edk.dll” file.
- Build a data acquisition task and acquire brain data from Emotiv headset.
- Establish links with the EmoComposer using Emotiv Create Task.vi.
- Acquire and display the Smiling State inside a “For” loop using Emotiv Read.vi.
- End the connection when the task is over.

Beutlich also worked on reading cognitive activities using the above set up during the same years. The VI code created in LabVIEW to assimilate cognitive states is executed using the following steps:

- Install Emotiv EPOC control panel and set the path to “edk.dll” file.
- Load cognitive actions—Control Panel.vi.
- Run the VI and subsequently load Profile.vi.
- Read cognitive states from the acquired signals.

6.3.1.5 Case Studies Related to BCI Developed Using LabVIEW

Certain case studies available on National Instruments’ web page “*Home > Innovations Library > Case Studies*” are presented below.

A Neuropsychology Pilot Study to Examine Mental Fatigue

Mark Ridgley from the Radius Teknologies, LLC (NI Alliance Partner), made use of LabVIEW to deploy a mental rotation task to survey the effects of mental fatigue. Mental rotation task helps in identifying the ability of human brain to manipulate and correlate 2D or three-dimensional (3D) visual stimuli it is subjected to. The visual stimulus is modified in a controlled manner and the subject is required to identify the alteration, which leads to mental rotation. Primary task of mental rotation follows the following procedure:

- A cue image is presented on the screen.
- Subjects are instructed to memorize the image and create a mental image of it.
- Button “Next” is pressed to reach the orientation screen. (The orientation screen indicates the direction and number of degrees needed to rotate the image to zero degree position.)
- Image in this position is memorized now and “Next” button is again pressed. (A test image appears on the screen.)
- Subject is asked to rotate the image mentally till axial orientation permits comparison with the standard image.
- Comparison is done and decision is reported by pressing “Yes” if the image matches else “No” is sent.
- Brain wave variations are recorded throughout the task using EEG as per the International 10–20 setup.

A Therapeutic Game for the Elderly With Notifications for Caregivers

Chee Teck Phua and Boon Chong Gooi representing Nanyang Polytechnic, created a game for the elderly for their well-being, which can be monitored remotely by their caretakers. They combined the functionality of LabVIEW and an economic hardware arrangement embedded with sensors to build a squash game which tracks the motion and brain activities of the elderly person so as to analyze their motor and cognitive abilities. Their motivation came from the aging population of Singapore who needed to be engaged in therapeutic activities through electronic games built for their physical and mental exercise. The users engage with the 2D interface of the bouncing ball squash game using physical movement of arms and can also monitor their physical and mental progress.

This gaming system primarily consists of a sensitive infrared proximity tracking sensor developed by Silicon Labs and NeuroSky MindWave headset that acquires the brain signals. This sensor IC (integrated circuit) has the advantage of being operable remotely and at ultralow power. It allows tracking of lateral arm motion for therapeutic physical monitoring and communicates the output to LabVIEW environment with the help of USB interface. The sensor and the neuroheadset used in this application are effective in recording the neural activities of the elderly while playing and provides 96% accuracy. The researchers plan to further make a trial of the game on Singapore’s elderly community and gather their feedback to improve the system’s popularity.

A Real-Time System to Identify Timely Symptoms of Driver Fatigue to Prevent Accidents

Accidents on roads are on an increase and are a matter of great concern in India. To quote statistics by the Department of Road Transport and Highways in India, accidents have increased by 34% from 1994 to 2004 primarily due to human error. The cause is attributed more to driver inattentiveness, may be distraction or falling asleep during the drive. So, it is important to acquire physiological parameters of the driver in real-time noninvasively and make algorithms and do psychometric tests to identify early signs of fatigue in them. Aurobinda Routray and Sukrit Dhar from the Indian Institute of Technology, Kharagpur, India researched in this area and created an embedded vision system that can monitor a driver's visual attention level in real time and send alarm accordingly. They used the compact vision system hardware and software of NI to create a reliable, non-invasive, and stand-alone system which is capable of ascertaining early onset of driver fatigue to prevent accidents.

It has been researched that measurement of "percentage closure of eyes (PERCLOS)" and the rate of "Eye Saccades (rapid movement of both eyes in same direction simultaneously)" are the most efficient method of estimating fatigue level in a driver. Aurobinda Routray and Sukrit Dhar developed a novel and less complex real-time eye tracking algorithm based on principal component analysis (PCA) and PERCLOS and Saccade measurement method. The NI compact vision system device used in this application is a user friendly, real-time imaging system that acquires, processes, and displays images for image processing. NI-IMAQ (image acquisition) provides the interface with LabVIEW application software. The algorithm runs with an accuracy of more than 90% as claimed by the developers.

Assessment of Motor Cognitive Skills in School Children

Earle Jamieson et al. (ReSolve Research Engineering Ltd.) took up the challenge of creating a precise, transportable, and computerized tool to examine the manual dexterity and cognitive skills of schoolchildren. They developed a software platform Kinelab, which permits children to undertake cognitive activities, and made use of LabVIEW functionality to implement an application that captures movements, does analysis, and generates feedback so as to understand the influences that shape health and well-being of a child.

In 2009, Dr. Peter Culmer and Dr. Mark Mon-Williams from the University of Leeds used LabVIEW to develop the first version of Kinelab, which combines the convenience of customary methods with the speed and accuracy of modern technology. Kinelab provides an easily configurable, rugged, and convenient set up to gather kinematic measurements quickly during the visual stimulus action done by the children. Here, the child is made to use a stylus to interact with 2D objects that appear on the screen and this input is further captured and analyzed to measure its cognitive abilities.

6.3.2 Mathworks' MATLAB/Simulink-Enabled Control Using BCI

MATLAB has become a very influential numerical computing programming environment over the years and is widely accepted and appreciated by researchers, academicians, and industry personnel. MATLAB toolboxes like EEGLAB, BCILAB, ERPLAB, and FieldTrip are a few creations primarily for understanding EEG signals and developing BCIs. These toolboxes have provided a user friendly set up to OpenBCI users for the design, prototyping, testing, and experimentation of BCIs. The GUI also provides effective signal processing, visualization, and analysis tools as also been mentioned in [Chapter 3, Section 3.4.1](#).

Günter Edlinger and Christoph Guger, from g.tec Medical Engineering GmbH, Austria, have developed a futuristic tool “g.tec BCI, called g.BCIsys” for real-time bio-signal acquisition and processing by utilizing versatile data processing functionality of MATLAB and the potential of Simulink for system development. The system includes a digital signal processing (DSP)-based bio-signal acquisition arrangement “g.USBamp” that amplifies, filters, and digitizes the raw data. Additional modules carry out real-time signal analysis and can generate control signals for rehabilitation purposes. Data Acquisition Toolbox in MATLAB or S-function block of Simulink is used to communicate with the amplifier section of g.USBamp. Soft-scopes are then used to analyze real-time EEG data. The firmware and the software designed in g.BCIsys are flexible, customizable, and meet stringent R&D requirements and are used for various applications. Automatic cursor control using EEG data and musical brain cap developed using g.BCIsys has been explained in the sections below. Control of a mini drone, robotic claw, and a biometric authentication system based on EEG-BCI designed in MATLAB environment is also presented.

6.3.2.1 EEG-Based BCI Developed in MATLAB for Cognitive Biometrics

Cognitive biometrics supported by EEG-based BCI system provides an automatic and authentic solution to correctly identify an individual. The scientific reason to deploy bio-signals for authenticating a person is primarily derived from the unique subtle features embedded in them ([Revett and de Magalhães, 2010](#); [Gupta et al., 2012](#)). The theta power band in EEG spectrum has a highly genetic trait and reflects differences in an individual and their intellectual level. A BCI user may be exposed to a sequence of alphabets/colors/images to form a brain word which may further be utilized to authenticate this user in high security environments. [Gupta et al. \(2012\)](#) examined the P300 BCI and rapid serial visual paradigm (RSVP) to present a proof of concept in MATLAB for cognitive biometrics based on EEG. Details of the prototype developed are presented as follows:

- An appropriate paradigm was chosen for cognitive biometrics by examining regular odd ball, RSVP, and spatially varying odd ball.

- Random stimuli alphabets A, B, C, and D representing a block were used for all these paradigms and the time to flash was set to 100 ms and ISI (intersymbol interference) was made 750 ms. Target cue was shown for 2 s and the user was told to count it mentally.
- The background was set to light gray in all cases and the default color during “OFF” state was white whereas black was set as the stimuli for “ON” state.
- The subjects were to report the target cues and flash counts after the experiment.
- The signal processing methods and classifiers used were same for all paradigms. In every assessment, a “Forward Reverse Butterworth Band-pass Filter” with cut-off frequencies set between 1 and 12 Hz was used.
- Data were normalized and validated using Bayesian linear discriminant analysis (LDA) to get accurate classification.
- Of all the examined paradigms, RSVP had the least gaze effect and is recommended for high security authentication.

6.3.2.2 EEG-Based Cursor Movement Control Developed in MATLAB/Simulink

One extension of g.BCIsys is a stimulation set up named g.STIMunit which assists in training the user for assimilating the neural signals and using it as control commands. It has been a proven fact that imagery of limb movements causes subtle variations identified by spectral analysis in EEG signal at sensorimotor regions of the cerebral cortex. An attempt was made to control a cursor represented by a horizontal bar by imagining limb movements using g.STIMunit. A right-hand movement affects the left brain hemisphere at C3 sensor position and if the left hand is imagined to be moved, it alters the right hemisphere at C4 electrode position and accordingly controls the horizontal bar. Signal processing is done to calculate power distribution of EEG signals in specified frequency spectrums (alpha: 8–13 Hz and beta: 16–24 Hz). Simulink’s “Band-Power Block” is used for spectral analysis to classify the EEG data into “right” and “left” classes.

6.3.2.3 Musical Brain Cap Developed in MATLAB/Simulink

Musicians have been exploring signals extracted from brain regions to compose and play automated musical instruments by developing brain-computer music interface (BCMI). g.tec BCI has enabled development of a brain cap by extracting EEG features from different frequency bands to compose music. The Simulink Hjorth block has been exploited in this project to extract meaningful data from EEG signal to control the musical rhythm. The music is finally sent through a MIDI (musical instrument digital interface) interfacing unit to a piano that plays the digital piece of music controlled by brain signals.

6.3.2.4 MATLAB/Simulink-Based Control of Mini Drone Using BCI

Rosca et al. did mathematical modeling and simulation of a drone and BCI using Matlab/Simulink environment in 2018. A mini drone called Parrot and Emotiv Insight BCI

headset is used in this application to prove the concept of controlling a quadcopter through neural signals. The drone used is “Parrot Rolling Spider” which is compact and exhibits significant speed and stability. It is equipped with an autopilot arrangement based on three axis gyroscope and accelerometer both, a pressure sensor for altitude control, ultrasonic Sensor for precision flying, and a upright camera with adequate frame rate to capture real-time images. Proprietary application “Emotiv 3d Brain Visualizer” of Emotiv Insight BCI unit helps in acquiring the neural signals frequency subbands through EEG. The biosensors are placed on the user’s head as per 10–20 international system standard to control the mini drone through brain signals. A quadcopter model is developed in Matlab/Simulink environment using estimation and control module designed by the Massachusetts Institute of Technology. Finally, an embedded C Code is generated and loaded on the drone to make it work in real time.

6.3.2.5 MATLAB-Based Robotic Claw Control Using BCI

Angelakis et al. used BCI to control a Robotic Claw in 2017. Emotiv Epoc + EEG headset equipped with 14 EEG channels and 2 reference channels is used to capture the brain signals in this project, which transfers data to the MATLAB application software on a computer through bluetooth protocol. Output from the computer is transferred to Arduino Uno board which further sends trigger to control two servo motors that handle the motion of robotic claw. One servo motor is programmed to open and close the claw and the other motor takes care of rotation to left or right side. A rigorous training session is required before the user is able to adeptly handle the directional movements and the rotations of the claw. The trainee imagines an action and tries to manipulate the movement of a virtual object, a cube on a computer screen. Physical movement of head or otherwise is restricted during the action as it may hugely distort the brain signal. A personalized cognitive signatures’ database is created for each user. A distinct application software “Mind your OSCs” is made use of to set up communication with the Emotiv control panel and the brain data is encoded into a series of open-source control (OSC) for transmission. These OSCs are decoded for sending control signals to Arduino board and thus controlling the claw. BD in Fig. 6.11 gives the work flow diagram for this project.

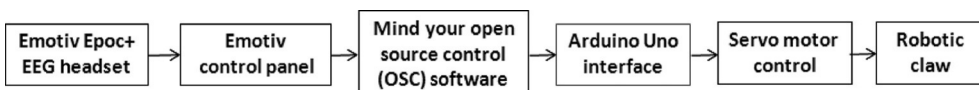


Fig. 6.11 Block diagram of EEG-based robotic claw control.

6.4 CONCLUSION

We represent an era where we can augment the capabilities of a computer to assist mankind in communicating and sharing their thoughts and achieving the impossible. Human brain interfacing has acquired a level of doing tasks and achieving functional targets that were unimaginable at some point of time. Application software like MATLAB/Simulink and LabVIEW is being explored extensively to survey the possibility of developing BCI prototypes. Stand-alone open-source-ware solutions are available that assist a novice in understanding a BCI unit, its functionality and applications. Research in this domain is expanding in every dimension, be it the vast breadth of EEG-based BCI control applications, depth of technology involved, and the usability it presents to disabled and general mass. This chapter gives a comprehensive step-by-step summary of control applications developed by various researchers primarily in MATLAB/Simulink and LabVIEW environment.

REFERENCES

- Abdulkader, S.N., Mostafa-Sami, A.A., Mostafa, M., 2015. Brain computer interfacing: applications and challenges. *Egypt. Informat. J.* 16 (2), 213–230.
- Andy, K., 2011. NeuroSky LabVIEW Driver. edited in 2017.
- Angelakis, D., Zoumis, S., Asvestas, P., 2017. Design and implementation of a brain computer interface system for controlling a robotic claw. *J. Phys.* 931, 012001.
- Bansal, D., Mahajan, R., Singh, S., Rathee, D., Roy, S., 2014. Real time acquisition and analysis of neural response for rehabilitative control. *Int. J. Electr. Robot. Electron. Commun. Eng.* 8 (5), 697–701.
- Bell, C., Shenoy, P., Chalodhorn, R., Rao, R., 2008. Control of a humanoid robot by a non invasive brain computer interface in humans. *J. Neural Eng.* 5, 214.
- Berger, T.W., Chapin, J.K., Gerhardt, G.A., McFarland, D.J., Principe, J.C., Soussou, W.V., Taylor, D.M., Tresco, P.A., 2008. *Brain-Computer Interfaces: An International Assessment of Research and Development Trends*. Springer, the Netherlands. eBook ISBN 978-1-4020-8705-9, Hardcover ISBN 978-1-4020-8704-2, Pages 281.
- Bryan, M., Green, J., Chung, M., Chang, L., Scherer, R., Smith, J., Rao, R.P.N., 2011. In: *An adaptive brain-computer interface for humanoid robot control*. 11th IEEE RAS International Conference on Humanoid Robots, Bled, Slovenia, pp. 199–204.
- Callahan, M., 2013. UIUC Innovators Develop Mind-Computer Interface with NI LabVIEW. <http://www.ni.com/white-paper/6130/en>.
- Cassani, R., Banville, H., Falk, T., 2015. In: MuLES: an open source eeg acquisition and streaming server for quick and simple prototyping and recording. 20th ACM Conference on Intelligent User Interfaces.
- Chae, Y., Jo, S., Jeong, J., 2011. In: *Brain actuated humanoid robot navigation control using asynchronous brain computer interface in neural engineering*. 5th International IEEE/EMBS Conference on NER'11.
- Delorme, A., Kothe, C., Vankov, A., Bigdely-Shamlo, N., Oostenveld, R., Zander, T., Makeig, S., 2010. MATLAB-based tools for BCI research, In: *(B + H)CI: The Human in Brain Computer Interfaces and the Brain in Human Computer Interaction*. In: Tan, Desney S, Nijholt, Anton (Eds.), Springer Publishing (Chapter 10).
- Gerson, A.D., Parra, L.C., Sajda, P., 2006. Cortically coupled computer vision for rapid image search. *IEEE Trans. Neural Syst. Rehabil. Eng.* 14 (2), 174–179.
- Gupta, C.N., Palaniappan, R., Paramesran, R., 2012. Exploiting the P300 paradigm for cognitive biometrics. *Int. J. Cognit. Biomet.* 1 (1), 26–38.

- He B., Gao S., Yuan H., Wlpaw J.R., Springer: (Chapter 2), Brain-Computer Interface. <https://www.springer.com/cda/content/document/cda.../9781461452263-c>.
- Jackson, M.M., Mappus, R., 2010. Neural control interfaces. In: Springer: Brain Computer Interfaces—Applying Our Minds to Human-Computer Interaction. Springer-Verlag Limited, London. ISBN 978-1-84996-271-1 (Chapter 2).
- Kasim Mohamad, A.A., Low, C.Y., Ayub Muhammad, A., Zakaria Noor, A.C., Mohd, S.M.H., Johar, K., Hamli, H., 2017. User-friendly LabVIEW GUI for prosthetic hand control using Emotiv EEG headset. Procedia Comput. Sci. 105, 276–281. Elsevier.
- Luzheng, B., Fan, X.-A., Liu, Y., 2013. EEG-Based Brain-Controlled Mobile Robots: A Survey. IEEE Trans. Human Mach. Syst. 43 (2), 161–176.
- Mak, J.N., Wolpaw, J.R., 2009. Clinical applications of brain-computer interfaces: current state and future prospects. IEEE Rev. Biomed. Eng. 2, 187–199.
- Millan, J., Renkens, F., Mourino, J., Gerstner, W., 2004. Noninvasive brain actuated control of a mobile robot by human EEG. IEEE Trans. Biomed. Eng. 51 (6), 1026–1033.
- Neuper, C., Muller, G.R., Kubler, A., Birbaumer, N., Pfurtscheller, G., 2003. Clinical application of an EEG-based brain-computer interface: a case study in a patient with severe motor impairment. Clin. Neurophysiol. 114 (3), 399–409.
- Pohlmeier, E.A., Wang, J., Jangraw, D.C., Lou, B., Chang, S.F., Sajda, P., 2011. Closing the loop in cortically-coupled computer vision: a brain-computer interface for searching image databases. J. Neural Eng. 8(3). 036025. <https://doi.org/10.1088/1741-2560/8/3/036025>.
- Quigley, M., Gerkey, B., Conley, K., Faust, J., Foote, T., Leibs, J., Berger, E., Wheeler, R., Ng, A., 2009. In: ROS: an open source robot operating system. ICRA Workshop on Open Source Software.
- Revett, K., de Magalhães, S.T., 2010. Cognitive biometrics: challenges for the future. In: Tenreiro de Magalhães, S., Jahankhani, H., Hessami, A.G. (Eds.), Global Security, Safety, and Sustainability. ICGS3 2010. Communications in Computer and Information Science. In: vol. 92. Springer, Berlin, Heidelberg.
- Richardson, M., 2007. Hold That Thought. New Electronics. www.newelectronics.co.uk. pp. 14–16.
- Rosca, S., Leba, M., Ionica, A., Gamulescu, O., 2018. Quadcopter control using a BCI. Mater. Sci. Eng. 294, 012048.
- Springer, 2013. In: He, B. (Ed.), In: He, B. (Ed.), Springer Science+Business Media, New York. https://doi.org/10.1007/978-1-4614-5227-0_2.
- Vjvarada, 2012. The Mastermind Project—Mind Controlled Robots Using EEG. <https://forums.ni.com/t5/Academics-Documents/The-Mastermind-Project-MIND-CONTROLLED-ROBOTS-USING-EEG/ta-p/3524582>.

FURTHER READING

- Beutlich, 2011a. Emotiv EmoComposer Read Smile Example. edited in 2017a.
- Beutlich, 2011b. Emotiv Example for Reading EEG Commands. edited in 2017b.
- Edlinger, G., Guger, C., The Brain-Computer Interface: Using MATLAB and Simulink for Biosignal Acquisition and Processing. <https://www.mathworks.com/company/newsletters/articles/the-brain-computer-interface-using-matlab-and-simulink-for-biosignal-acquisition-and-processing.html>.
- <http://jki.net/vipm>.
- <http://www.neurosky.com>.
- Jamieson E., Chandle J., Mushtaq F., Mason D., Barratt A., Hill L., Waterman A., Allen R., Wright J., Culmer P., Mon-Williams M., n.d. Kinelab: Assessing the Motor-Cognitive Skills of School Children With LabVIEW. National Instruments' Web Page 'Home > Innovations Library > Case Studies
- Kelly J. W., Degenhart A. D., Ashmore R. C., Wang W., n.d. Craniux: A Modular Software Framework for Brain-Computer Interface Research Based on LabVIEW Software, <http://sine.ni.com/cs/app/doc/p/id/cs-13832>.
- MuSAELab, <https://github.com/MuSAELab/MuLES>.
- OpenBCI, <http://openbci.com>.

- Rebsamen, B., Teo, C.L., Zeng, Q., Marcelo Jr., H.A., Burdet, E., Guan, C., Zhang, H., Laugier, C., 2007. Controlling a wheelchair indoors using thought. *IEEE Intell. Syst.* 1541–1672 (07), 18–24. IEEE Computer Society.
- Ridgley M., n.d. Radius Technologies, LLC Uses LabVIEW to Aid Mental Rotation Research Study. National Instruments' Web Page‘Home > Innovations Library > Case Studies.
- Routray A. and Dhar S., Creating a Real-Time Embedded Vision System to Monitor Driver's Visual Attention. National Instruments' web page‘Home > Innovations Library > Case Studies. Indian Institute of Technology, Kharagpur.
- Roy, J.K., Das, A., Dutta, D., Sengupta, A., Ghosh, J., Paul, S., 2014. Intelligent Stress- Buster-A Labview Based Real-Time Embedded System For Thought Control Using Brain Computer Interface.
- Teck Phua C. and Chong Gooi B., Creating a Therapeutic Game for the Elderly With Remote Monitoring for Caregivers Using NI LabVIEW. National Instruments' web page‘Home > Innovations Library > Case Studies, Nanyang Polytechnic.
www.ni.com/NI_LabVIEW.

CHAPTER 7

Conclusion

Dipali Bansal, Rashima Mahajan

Faculty of Engineering and Technology, Manav Rachna International Institute of Research and Studies, Faridabad, India

Contents

7.1 Major Contributions	195
7.1.1 Time-Domain Analysis	197
7.1.2 Frequency-Domain Analysis	198
7.1.3 In-House Development of Eyeblink-Based BCI for Control	198
7.2 Future Directions and Conclusion	199

7.1 MAJOR CONTRIBUTIONS

This chapter summarizes the major contributions and concluding remarks of overall work carried out in this book. The details have been provided in the area of EEG-based brain-computer interfacing for cognitive analysis and control. The major contributions made to acquire the instant of deliberate single eyeblink using EEG-based neural responses and subsequent analysis to use the identified instant as a control signal for development of interactive Brain-computer interfaces (BCIs), are highlighted in detail. This work focused to investigate whether relaxed state event-related potential concentration, spectral power concentration, and EEG coherence are different from those obtained during a thoughtful single eyeblink activity. It also explores the potential directions for future research related to development of more robust BCIs for subjects with severe motor disorders.

A rationale behind requirement of interactive BCIs for control applications has been discussed in detail in this book. The major innovations in neuroscience have motivated neuroscientists to utilize the human neural responses as a trigger to control external set of devices. Yes, this facilitates interactive applications of BCI and possesses the ability to help people with even acute disabilities to lead an independent life. These BCI systems have been evolved to provide tremendous applications including neuro-prosthetics (robotic arms/hands), hands-free mind controlling applications without any muscle-interventions through interpretation of thoughts/feelings. These applications are not only developed to provide aid to medically challenged people, but may also provide assistance to healthy users too in their routine and occupational work. There is a huge market demand for interactive BCIs in present scenario as per the “Allied Market Research” in 2015 followed by “Transparency Market Research” in 2016. The primary reason is the increase in number of patients diagnosed with neurological disorders such as

stroke, depression, Alzheimer's, and Parkinson's disease. Looking at the vast potential applications of BCI technology, an attempt has been made to explain the detailed framework of brain-computer interfacing systems. It consists of signal acquisition unit, control interface, and application processing machine. Human neural activity can be acquired using various techniques and acquisition units. Currently, development of EEG-based noninvasive, portable, and user-friendly BCIs is a very dynamic and curious neuroscience research field. These BCIs possess the capability to be used in real-time applications outside the laboratory environment too. Technological advancements in EEG-based BCIs reveal that EEG-BCIs possess the potential to be established as a neuro-scientific tool for developing real time, portable, and fast BCIs for neuro rehabilitation. Assistive external devices and robotics designed using interactive man-machine interfaces (MMI) for medically challenged subjects are the major application outcomes in the field of rehabilitation.

Conventional EEG-based BCIs were more aimed toward medical applications only. This emerging BCI research and availability of user-friendly and easily wearable EEG headsets have made possible to expand the BCI application areas toward gaming, entertainment, emotion recognition, e-learning, cyber world, automation, etc. This book provides a detailed framework to design and understand the real-time acquisition of voluntary single eye blink-specific brain patterns using EEG. It has been highlighted that rather than considering eyeblink as an artifact, customization of the system could be possible to utilize eyeblink as a trigger to develop interactive BCIs for control applications. This could facilitate the automation of external devices by merely using the neural responses of the subject. The resultant system of brain assistive devices would definitely possess the potential to assist physically challenged subjects having severe motor disabilities.

The analysis of neuro headsets to capture real-time EEG signals from human subjects has been detailed. A 14-channel Emotive EEG neuro headset is selected to acquire real-time raw EEG recordings due to its high resolution and nominal price. The experiment protocol to capture a thoughtful eyeblink-specific cerebral activity of a subject has been designed for subsequent neuro assistive control applications. Multiple recordings were attained from five subjects to prepare a robust database of single eyeblink-specific EEG responses with each record of 20-s duration. These records were saved in .edf file for further analysis in time, frequency and spatial domain to understand the associated EEG dynamics and extract the discriminative feature set. The primary event-related potential and spectral analysis has been performed using an open-source toolbox: EEGLAB. It provides an interactive platform with a rich set of functions to import, preprocess and to analyze acquired EEG responses. The MATLAB platform has been used to analyze the acquired multichannel single eyeblink-specific EEG data and develop a control application. MATLAB has shown its potential in numerical computing programming environment over the years and has been widely accepted and appreciated by researchers, academicians, and industry personnel. MATLAB toolboxes like

EEGLAB, BCILAB, ERPLAB, and FieldTrip are a few creations primarily for understanding EEG signals and developing BCIs. These toolboxes have provided a user-friendly set up to OpenBCI users for the design, prototyping, testing, and experimentation of BCIs. The major contributions in this book are detailed in the following sections.

7.1.1 Time-Domain Analysis

The time-domain features of EEG are frequently used for BCI development. This work details about the implementation of a simple and robust BCI based on exploring event-related potentials (in time domain) as a discriminative feature. It has been found that identified ERP amplitudes can be utilized as a trigger to develop control applications driven by deliberate eyeblink-specific neural responses. The channel event-related potential distributions along with topographic scalp maps have been analyzed to identify the activated scalp channels and correlated neural activity during voluntary eyeblink. The event-related potential analysis primarily determines averaged ERPs of all EEG epochs acquired across 14 scalp electrodes of EMOTIV EEG neuro headset.

- The eyeblink activity-related maximum temporally and spatially independent distinct neural components have been identified by exploring a fourth order spectra-based independent component analysis. It has been found to be an efficient technique to reject distinct artifacts in acquired EEG signals.
- The topographic scalp map analysis indicates that left frontal regions of cerebral cortex are found to possess maximum potential concentration during voluntary eyeblink.
- It reflects that the neural activity correlated to deliberate single eyeblink action can be captured prominently at left frontal channels of EMOTIV neural head set unit. The left frontal regions include AF3 and F7 scalp channels of EMOTIV headset unit.
- The performed thoughtful action has been found to possess a substantial increase in the corresponding event-related potential from 0 to $339.6\mu\text{V}$ at channel AF3 and from 0 to $652\mu\text{V}$ at channel F7, respectively for subject 1. Extracted EEG signal epochs at left frontal scalp channels represent the index of neuronal activity during performed action. This indicates the high level of cognition and neural processing involved in a thoughtful eyeblink action. Similar incidences of results have been observed for rest of the EEG dataset acquired from other subjects.
- This reflects that the intentional eyeblink-specific EEG activated components have the potential to be used as a trigger to develop rehabilitative BCIs.

Event-related potential-based BCIs possess high throughput due to their short latency period. However, due to their low amplitude (microvolts) and dominant background activity, it is sometimes difficult to classify the correlated neural states. Therefore, acquired neural patterns have been invoked for spectral analysis in frequency domain to understand the morphological variations associated with a deliberate single eyeblink activity.

7.1.2 Frequency-Domain Analysis

The frequency-domain analysis of recorded EEG signals involves the application of Fourier transform to estimate the respective spectral details. The fast Fourier transform is applied to track amplitude modulations at a specific frequency by plotting the frequency spectrum of acquired EEG responses. This work has implemented a BCI by exploring subband power spectral and EEG coherence related features to identify deliberate eyeblink-specific instants in acquired neural responses. EEG coherence analysis between neural activities of selected electrode pairs has been accomplished by computing their Fourier transform-based spectrograms. The channel activity analysis comprising of respective ERP image plots, averaged event-related potential traces, and activity power spectra has been performed across all left frontal (AF3 and F7), occipital (O1 and O2), parietal (P7 and P8), and temporal (T7 and T8) channel EEG data. The left frontal channels show increase in event-related potentials in response to a deliberate single eyeblink activity. Major observations listed below:

- The power distribution across left frontal scalp regions is found to be high across delta (2 Hz) to alpha (9 Hz) frequency subband of EEG during a deliberate single eyeblink activity.
- It depicts the activation of these low-frequency EEG subbands across left frontal regions of scalp during deliberate single eyeblink actions.
- Channel activity results obtained at occipital (O1 and O2), temporal (T7 and T8), and parietal (P7 and P8) channels do not show any prominent increase in ERP amplitudes and spectral power amplitudes as observed across frontal channels AF3 and F7.
- The spatial-domain analysis to determine EEG coherence between either pair of left frontal channels (frontal-frontal): AF3 (channel number 3)-F7 (channel number 4) or frontal channels with respect to reference electrodes (frontal-reference) have been performed. The EEG coherence results for single eyeblink activity have been computed using FFT-based spectrogram method. A high level of coherence or synchronization between activated frontal regions of cerebral cortex has been witnessed.

These cognitive analysis findings in time, frequency, and spatial domain have further been utilized to develop BCIs to control assistive devices.

7.1.3 In-House Development of Eyeblink-Based BCI for Control

A set of in house control applications has been developed to translate attained neural event-related potential component activation into action. The high variation captured in event-related potentials on the onset of deliberate eyeblink action has been utilized as a control signal to design an algorithm and framework to implement neural control applications of interest, viz., to play a “handel.mat” audio file in MATLAB environment and to control the glowing instances of a light-emitting diode (LED). The identified high ERP component variations from MATLAB workspace have been translated into control

commands to drive the interfaced device (LED here) via Arduino board. Major contributions are as below:

- The BCI developed in-house has been used to trigger a musical output using software control in MATLAB. In this application, an audio file “*handel.mat*” is played when an “active high” output is generated. Thus, using single eyeblink information captured in human EEG data, the BCI developed is able to play music using software.
- Furthermore, high ERP component variations identified from acquired EEG signals (in MATLAB platform) have been translated into control signals to control the glowing instances of interfaced device through Arduino microcontroller unit. The output instances of interfaced microcontroller can be used for specific controlling action. The peak ERP amplitudes are found to be more than set threshold values during performed single eyeblink activity. At this instance, the ‘high’ output received at the interfaced LED enables it to glow.
- An interfacing between Arduino Uno board and Simulink has also been established, so that the model could be used independently for other control applications. The model designed is finally deployed on the Arduino microcontroller board and gives a stand-alone application.

Therefore, control application-based BCIs possess the potential to be developed as a real-time assistive tool for rehabilitation of differently abled subjects suffering from certain motor disorders. The related research and development in EEG-based brain mapping opens up the perspectives to offer an alternative means of interaction with external environment for subjects with serious motor disabilities. Of all the ways of capturing brain signals for control application, EEG-based BCIs are the most convenient and find plethora of applications that have been developed using various software platforms. This is an era of utilizing the capabilities of a computer to assist humans in communicating with the outside world. Apart from MATLAB, application softwares like Simulink and LabVIEW are being explored extensively to survey the possibility of developing BCI prototypes. Research in BCI has a focused approach toward improving quality of life for everyone. The potential clinical application of this work shall be to develop interactive platforms to control devices by merely using the eyeblink-specific neural signals.

7.2 FUTURE DIRECTIONS AND CONCLUSION

Neuro technologists are tirelessly working on ways and means to merge minds with machines and to understand the underlying causes on the difference in computational limits of human brains. Advancements in neuro technologies are being done both deploying noninvasive and invasive technologies. The idea is to mitigate the injuries sustained due to unforeseen circumstances, provide resolution of diseases around auditory and visual systems, treatment of neurodegenerative disorders and even brain-train to enhance intelligent behaviors or execute repeated and challenging cognitive activities.

While the noninvasive research finds easy takers, but it is quite clear that development of invasive BCI, deep brain simulation channels and study of neural electrochemical coding is unavoidable. Let us remind ourselves these techniques are not new and the first reported deep brain stimulation (DBS) to treat Parkinson Disease was published in 1993 although the first such operation was performed in 1987 in Professor Benabid's clinic. It is also a fact that similar attempts were being made for decades before that.

Human brain has evolved over a period. Our consciousness has diversified as the species have diversified. Like our physical stamina, the computational limits of a biological brain constrain our thinking and feeling capacities. Exponential neurotechnology is an attempt to understand the higher consciousness state beyond the current fathomable limits of the default state. So, to expand and challenge the boundaries, neuro technology would need to Transend us to a state of higher consciousness as reported in "The Future Evolution of Consciousness," by Thomas Lombardo.

Commonly used techniques to enhance consciousness by "consciousness hackers" are EEG, good nutritional methods, virtual reality and to create heightened experiences, and awareness by fashioning ecstatic experiences. The altered states of mind are productive, help heighten our inner potential, and take us to an elated self. Such erratic and debatable states of our consciousness make us perform under intense competition and tide over enormous challenges as say Steven Kotler and Jamie Wheal in Stealing Fire. Scientists are also working on the hypothesis that humans with higher cognition abilities like learning and memory have better connected brains. Nearly 200 regions across the brain are understood to be functionally distinct from each other. fMRI data are extensively used to measure the amount of nerve signaling in between these parts of brain. In contrast, significantly lower connectivity is observed in people scoring high in ordinary traits like anger, poor sleep, drug abuse, and rule-breaking etc. Larger set of data subjects and better resolution fMRI data has given confidence to the scientists to take the research to higher levels. This recognition of the fact that brains with higher cognition are better connected based on the objective measurement of nerve signaling across regions in brain and can lead to the ideas of training people to improve brain connectivity and to hence push them up the scale as report Steve Connor, a Science Editor in September 2015. fMRI studies have revealed commonly understood fact that smart individuals have enhanced connectivity in brains. One may argue that the biological genetic superiority could be the plausible reason for this occurrence. Such individuals perform cognitive tasks relatively easier than many others and show intelligent traits in the way they approach problems. Although it cannot be totally ignored that repeated use of one's ability for cognitively stimulating exercises could positively impact network development in brains. It is quite reasonable to conclude that based on this knowledge about intelligence, both genetic evolution and frequent usage of brain for addressing challenges, enhance connectivity in the brain as per research conducted in the Goethe University (Frankfurt/Sciedaily.com).

The basic sense of touch and feel are simplest examples of how the signal is transmitted from our skin to the brain and the resultant reactions. Our intention to consume a cup of tea or coffee lying on the table is transmitted through the eyes to the brain resulting in the physical movement of hands and fingers based on the response received from the brain. The actual weight, temperature, and the size/shape of the contact finalizes the next response of our limbs again exchanged between the brain and point of contact. While these are the simplest actions and reactions, our body performs a host of auditory and sensory functions with the least of efforts. People with damaged limbs or spinal cords are equipped with advanced prostheses which enable them to perform. The sense of touch and sensory exchange with the brain is however missing. Intracortical microstimulation (ICMS) technique is being tried in a tetraplegic patient who received a metal electrode implant in somatosensory cortex. ICMS normally consists of repeated application of electrical pulses ($6\text{--}12\mu\text{A}$) for short durations ($200\mu\text{s}$) at high frequency (about 300 Hz). A small relevant area $50\text{--}100\mu\text{m}$ in the somatosensory cortex was energized to activate the neurons. The recent ICMS on a tetraplegic patient has revealed that the sensations generated gave a near natural feel like those before injury. The patient reported sensations associated with hand and arm movement. ICMS hence could be interpreted as a capable therapeutic way forward to restore proprioception and touch in tetraplegics.

The microsimulation techniques originated with experiments on Rhesus monkeys in 1990 to human trials very recently. But for an effective therapy to be developed, the interface between the somatosensory cortex and the electrode should be viable for longer periods. One identified thought process is replacement of metallic electrodes with alternate materials to provide a longer interface. The material selected also should get accepted and embodied by the plastic nature of brain to allow the interface with artificial micro signals. Further advancements necessitate the implants to become a source of permanent and seamless integration between brain and external devices.

Microglial cells found in the central nervous system (CNS) represent a cluster of macrophages which digest unwanted proteins or debris in our body. In all, 10%–15% brain cells consist of microglia and maintain the health of CNS. Alzheimer's disease affects millions of people around the globe and such patients typically develop beta amyloid proteins which are not cleared by microglia in the brain. The microglial cells in the disease show inflammatory tendency secreting toxins affecting other brain cells also. Gamma oscillations at 40 Hz induced in the hippocampus regions of brain have led to 40%–50% reduction in beta amyloid plaque. The studies were initially carried on mice which were genetically programmed or chemically treated to show impaired gamma oscillations. These mice could not however develop beta amyloid plaques as desired. Some reasons which are in the horizon include a thought that it is a slow process and humans take a long time to exhibit the signs of Alzheimer's after the onset of the disease. Research needs to look at animals beyond rats and mice to look for

animal species which can be successfully genetically modified. Development of such animals and subsequent tests and trials will cost time and money.

Initial techniques to induce gamma oscillations used optogenetics in which genetically modified neurons were controlled by shining light on brain cells called interneurons. Less invasive techniques were built consisting of simple device having LED's capable of flickering at varying frequencies. However, the results are not long lasting even in mice. All the same it has given a clear direction that gamma oscillations can clean up unwanted deposits in brain which have been known to be linked with the cognitive function. Preliminary investigations and data suggest that light can drive gamma oscillations beyond visual cortex in human brain regions. More work is being planned to further these studies. Messenger RNA from brain of mice has also exhibited under or over expressed genes which also is a research direction in study of Alzheimer's.

Attempts have also been made to make human brain into a read **and** write device rather than only a read-only memory. Memory-encoded electrical signals were extracted from a group of volunteers and fed back during recall. The cognitive performance showed an improvement in the range of 35%–37%—a very large change. This could become important even for people who have suffered some damage to the brain due to an accident or a disease. This situation is common in military personnel in war zones. The experiments were conducted on rats and rapidly tried on monkeys and human beings later. Rats were drugged to block the natural memory. Hippocampus was connected at input and output node to observe the electrical connectivity. Memory signals or the brain activity patterns were however found to be nonlinear, noisy, and overlapping. The memory was reduced into a mathematical equation and put into a computational model. The correct and recorded signal is sent back to stimulate the hippocampus through minute electric shocks. The drugged rats magically regained the memory. The test was repeated on 22 human beings waiting for epilepsy surgery. Such patients already had implants to pin point source of seizures. These patients were shown some images and after a variable delay were made to recognize the image from a set of images. A model was created using the electrical patterns associated with the correct response which when fed back into the participants during recall gave 37% better results over normal baseline.

The current system developed requires major improvements before it can be substituted as a working prosthesis. One glaring limitation is recording of very few parameters from each memory owing to the limitation of the number of electrodes implanted. Space limitation and the fact that there are lacs of hippocampal pyramidal cells vs the recording sites is a hindrance. Assuming even if the issue of number of recording sites is addressed, computational methods to be used need to be modeled using newer techniques like machine learning, etc. Similarly, space-time distribution of neurons is an unknown factor. Issues around neural coding and respective cognitive functions remain as another frontier for neuro science. Elon Musk is working on BCI techniques which allow us to read other's thoughts and enhance our learnings. His team is working on development of advanced neural implants to connect brain to computers like

“Neural Lace” which is injectable, and would complement human brain by creating another layer around the cortex which communicates with the computer. The idea is to create “cyborgs” like mechanism, finally aiming at creating an updatable and upgradable interface. US Defense Advances Research Projects (DARPA) and Neural Engineering System Design (NSED) programs are being designed to mitigate the injuries sustained during combat or otherwise for providing resolution of diseases around auditory and visual systems. The research harbors being challenged include low-power photonics and electronics, neuro science medical device manufacturing, clinical testing, and systems engineering. The ultimate aim is to realize precise signal resolution, volume and speed of data exchange between brain and external devices. This link has to translate electrochemical coding of the neurons into the language understood by computers. The program is funding many projects including vision restoration using LED’s and speech decoding using “neurogram” sensors. Digital holographic microscopes, capable of recording information on the light wave front, originating from the object as holograms would be used to study neural activity. This digital hologram or a computer algorithm thus obtained may help replace lost vision or lost neural connectivity for limbs or to manage artificial limb.

Future advancements in neurosciences would have definite effects on the society. The technology tomorrow may peep into the thought process and identify guilty, gullible, and extraordinary. Similarly, the task-oriented BCI techniques controlling prosthetics, etc., applications which could substitute taste buds or assist “wine tasters” and even use brain signals to predict driving vulnerabilities in case of obstacles or potential threats warranting autocorrections, would never lose relevance. In fact, sustained and constant research efforts would be consumed in improving the quality of life impaired by diseases and accidents. Advanced analytics is just the beginning of a new dimension and approach which could merge brain with the environmental information. Developments in sensor technologies, artificial intelligence, and capacities to handle complex algorithms coupled with BCI techniques would provide a huge potential to benefit social, education, and medical applications. Many advancements in science and technology were possible only because a few dreamt and toiled to peep into the future. The futurists like Ray Kurzweil are setting the sights on to an entirely new thought process of human-brain interface with computers using cloud technology with free exchange of messaging and ideas through nanobots in our RNA strands. Tapping unused brain or downloading memories from brains of dead people may become a possibility. Some others have coined the term “Cloudminds” or even “Crowdmind” based on multiple brains and machines joined together to achieve a collaborative goal. On the simplest side futurists are looking to off-load routine tasks to human clones and evolved tasks or value adds and developed to evolving brains. The future world would not even be a world where humans coexist with AI across avenues, but we may look at AI overtaking human minds all together. Can evolution be driven by unnatural selection and engineered mutation, well it is a journey and not a destination.

Index

Note: Page numbers followed by *f* indicate figures and *t* indicate tables.

A

- Acquisition units
 - actiCHamp, 86, 87*t*
 - ADC bits, 77
 - Ant Neuro, 79*f*, 85
 - Emotiv EPOC, 78*f*, 79–81
 - Emotiv Insight, 78*f*, 81–82
 - LiveAmp, 86, 87*t*
 - montage, 77
 - Muse, 78*f*, 82
 - Neuroelectrics, 79*f*, 85
 - Neurosky Mindwave, 78*f*, 83–84
 - OpenBCI, 78*f*, 83
 - sampling skew, 76–77
 - wearable sensing EEG headset, 79*f*, 84–85
- ActiCHamp, 86, 87*t*
- Adaptive spatial filters, 41*f*, 45–46
- Adhesive wet electrodes, 36
- Alzheimer’s disease, 5–6, 61, 201–202
- Ambulatory EEGs, 37
- Analog-to-digital conversion, 37–38
- Analog-to-digital converter (ADC) bits, 77
- Ant Neuro, 79*f*, 85
- Arduino Digital Block, 177
- Arduino Uno board, 133–135, 199
- Arduino Uno hardware interfacing, 176–180
- Artifacts
 - definition, 38
 - nonphysiological, 39*f*, 40
 - physiological, 38–39, 39*f*
- Artificial neural networks (ANNs), 55*f*, 56
- The Audeo, 167–168, 180–181
- Autonomic nervous system, 8–9
- Autoregressive modeling (AR), 140–141
- Autoregressive moving average (ARMA) model, 140–141

B

- BackHome, 62
- Band-Power Block, 189
- Band power features, 51–52
- BCILAB, 95, 96–97*t*
- BioSig, 95, 96–97*t*
- Bipolar measurement, 35
- Bipolar spatial filter, 44
- Blinking artifacts, 38
- Blood oxygen level-dependent (BOLD), 27, 30–31
- Brain
 - cerebellum, 10
 - cerebral cortex, 9, 9*f*
 - to computer, 11–15
 - lobes, 9–10
 - visual information processing and control action, 10–11, 11*f*
- Brain Composer, 4
- Brain-computer interface (BCI), 2
 - applications, 22, 195–196
 - clinical applications, 58*f*
 - cognitive state analysis, 60–61
 - communication, 58–59
 - locomotion and movement, 59–60
 - medical diagnostics, 61
 - neurorehabilitation, 60
 - cognitive monitoring, 167
 - design, 14, 14*f*
 - electrophysiological responses, 22–23
 - future aspects, 199–203
 - invasive and partially-invasive signal acquisition, 28
 - electrocorticography, 28–29
 - intracortical neuron recording, 29
 - market analysis, 5–6, 7*f*
 - nonclinical applications
 - games and entertainment, 63
 - neuroergonomics, 62
 - neuromarketing and advertising, 62–63
 - security and validation, 63
 - smart home, 62
 - noninvasive signal acquisition, 29
 - electroencephalography, 31–33, 34*f*
 - functional magnetic resonance imaging, 30–31
 - functional near-infrared spectroscopy, 31
 - magnetoencephalography, 29–30
 - types, 12, 12*f*
 - voluntary eyeblink, 15–16
 - Brain-computer music interface (BCMI), 189
 - Butterworth filters, 185

C

Central nervous system (CNS), 6–8, 22–23, 201–202

Cerebellum, 10

Cerebral cortex, 9, 9*f*

Channel ERP analysis, 116–117

Channel spectral analysis, 140, 142–143, 147, 148–154*f*, 156*f*, 158–159*f*

Classification rate, 56

Classifiers

linear, 55, 55*f*

nonlinear, 55*f*, 56

Cognitive analysis. *See* Frequency domain analysis; Time domain analysis

Cognitive biometrics, 186

Coherence analysis, 144–147, 160–164*f*

Common spatial pattern (CSP) algorithms, 46–47

Completely locked-in syndrome (CLIS), 57, 180

Computer, 1

Control applications

EEG based BCI

cursor movement control, 189

mathworks' MATLAB/simulink-enabled control, 188–190

MATLAB for cognitive biometrics, 188–189 musical brain cap, 189

Parrot Rolling Spider, 189–190

robotic claw control, 190

eyeblink-based BCI

Arduino board, 176–180

MATLAB, 173–175

neural activity, 172, 172*f*

LabVIEW

The Audeo, 180–181

C programming, 180

EmoComposer, 185

eyeblink controlled robot, 183–184

fatigue level estimation in driver, 187

intelligent stress buster, 184–185

motor cognitive skills analysis, 187

MuLES, 181

neuropsychology pilot study, 186

NeuroSky Driver, 182

prosthetic hand, 182–183

therapeutic game, 186

Cortically coupled computer vision (C3-Vision), 170

“C” programming, 180

Cranial nerves, 8–9

Crowdmind, 203

Cup-shaped electrodes, 36

D

Delta rhythms, 37

Digital filtering, 111

Discrete Fourier transform (DFT), 42, 43*f*, 143

Discrete-time Fourier transform (DTFT), 111–112

Disposable electrodes, 36

Dry electrodes, 36, 64

Dyslexia, 61

E

eConnectome, 95, 96–97*t*

Edfread, 98, 101

EEG-based BCI, 196

EEG-based brain-computer interface

architecture, 23–24, 25*f*

artifacts

definition, 38

nonphysiological, 39*f*, 40

physiological, 38–39, 39*f*

classification/pattern recognition stage, 26, 54–55

linear classifiers, 55, 55*f*

nonlinear classifiers, 55*f*, 56

data acquisition, 24

analog-to-digital conversion, 37–38

bio-signal amplification, 37–38

electrode positioning, 35–36

electrode types, 36

filtration, 37–38

neuroelectric potential, 33–35

signals and rhythms, 37

feature extraction, 26, 47–48

band power features, 51–52

domains, 47–48, 48*f*

event-related potentials, 48*f*, 49

evoked potentials, 50

power spectrum, 52–53

short-time Fourier transform, 53

slow cortical potentials, 51

spatial domain, 54

wavelet transform, 53–54

feature translation, 26–27

performance, 56–57

preprocessing filters, 41, 41*f*

spatial filtering, 42

- temporal filtering, 42, 43*f*
 signal processing, 24
 EEG epoching, 41
EEGLAB, 95, 96–97*t*, 196–197
 frequency-domain analysis, 142–143
 time-domain analysis, 110–111
EEGNET, 95, 96–97*t*
Eegomylab, 79*f*, 85
Electrocorticography (ECoG), 12, 28–29
Electroencephalography (EEG), 3–4, 23, 31–33
Electrooculographic (EOG) activity, 38–40
EmoComposer, 185
Emotiv, 171–172
Emotiv 3d Brain Visualizer, 189–190
Emotiv EPOC, 78*f*, 79–81
Emotiv Insight, 78*f*, 81–82
Emotiv neuroheadset, 14–15, 74–76, 88–89, 196–197
 frequency domain analysis, 142, 146
 time domain analysis, 119, 122*f*
Enobio 32, 85, 86*t*
EPOC+ headset, 80–81
Error rate, 56–57
European data format (.edf), 91
Event-related desynchronization (ERD), 13
Event-related potentials (ERPs), 13, 28–29, 48–49, 48*f*, 108, 117
 vs. channel activity, 148–149, 149*f*
 eyeblink action, 179*f*
Evoked potentials, 50, 108
Eyeblink acquisition
 brain mapping toolboxes
 import data to EEGLAB toolbox, 95–98, 99*f*
 import data to MATLAB workspace, 98–101, 102*t*
 EEG signal processing, 87–88, 88*f*
 EMOTIV neuroheadset, 88–89
 EMOTIV test bench, 89–90
 European data format, 91
experiment design
 EMOTIV test bench, 91–93
 MATLAB, 91, 93–95
 Simulink, 102–103
Eyeblink-based BCI, 15–16, 198–199
Eyeblink controlled robot, 183–184
Eye Saccades, 187
- F**
Fading memory, 3
Fast Fourier transform (FFT), 140, 169, 198
Feature extraction, 26, 47–48
 band power features, 51–52
 domains, 47–48, 48*f*
 event-related potentials, 48*f*, 49
 evoked potentials, 50
 power spectrum, 52–53
 short-time Fourier transform, 53
 slow cortical potentials, 51
 spatial domain, 54
 wavelet transform, 53–54
Features, 26
FieldTrip, 95, 96–97*t*, 196–197
filtfilt(), 111
The Final Frontier of Science, 2
FIR band-pass filter, 111, 112*f*
Fixed spatial filters, 41*f*, 44
Forward-backward filtering operation, 112, 112*f*
Fourth order statistics, 113–114
Frequency domain analysis, 198
 channel spectral analysis, 140, 142–143, 147, 148–154*f*, 156*f*, 158–159*f*
 EEG coherence analysis, 144–147, 160–164*f*
 neural state classification, 141–142
 subband power analysis, 143–144
 during voluntary eyeblink, 142, 142*f*
Frontal lobe, 9–10, 9*f*
Functional magnetic resonance imaging (fMRI), 4, 12–13, 30–31
Functional near-infrared spectroscopy (fNIRS), 12, 31
- G**
Gamma rhythms, 37
Graphical user interface (GUI), 88–89
g.tec BCI, 188
g.USBamp, 188
- H**
Handel.mat, 133–135
Hanning windowing technique, 143
Hawking, Stephen, 2
Hierarchical BCI (HBCI), 168–169
Hold that Thought, 167–168
Humanoid robotics, 168
Hyperplane, 55

I

- Independent component analysis (ICA), 46, 109–110, 113–115, 116*f*
 Information transfer rate (ITR), 27, 57
 Information Tsunami, 170
 Inion, 35–36
 Instrument Control Toolbox, 170
 Interneurons, 202
 Intracortical microstimulation (ICMS), 201
 Intracortical neuron recording, 29

K

- Kinelab, 187
 k -nearest neighbor (k NN), 15–16, 55*f*, 56
 Kurtosis, 15–16, 113–114

L

- LabVIEW, 108, 180–187, 199
 The Audeo, 180–181
 C programming, 180
 EmoComposer, 185
 eyeblink controlled robot, 183–184
 fatigue level estimation in driver, 187
 intelligent stress buster, 184–185
 motor cognitive skills analysis, 187
 MuLES, 181
 neuropsychology pilot study, 186
 NeuroSky Driver, 182
 prosthetic hand, 182–183
 therapeutic game, 186
 Laplacian filters, 41*f*, 44, 45*f*
 LED control, 179–180, 179*f*
 Light-emitting diode (LED), 133–135, 168, 198–199
 LIMO EEG, 95, 96–97*t*
 Linear classifiers, 55, 55*f*
 Linear discriminant analysis (LDA), 55, 55*f*
 LiveAmp, 86, 87*t*
 Locked-in syndrome (LIS), 57, 180

M

- Magnetoencephalography (MEG), 12–13, 29–30
 Man-machine interfaces (MMIs), 107–108, 195–196
 MATLAB, 196–197
 channel spectral analysis, 142–143
 EEG based BCI, 188–190
 eyeblink-based BCI, 173–175

eyeblink EEG signal acquisition, 91, 93–95

MATLAB-Based Tools for BCI Research, 170

Memory-encoded electrical signals, 202

Memory loss. *See* Fading memory

Menu system, 169

Microsimulation techniques, 201

Mind your OSCs, 190

Mobile brain-computer interfaces, 75–76

Montage, 77

Motor neurons, 10–11

Motor prosthetic control applications, 75

Movement-related cortical potentials

(MRCP), 109

MuLES, 181

Multilayer perceptrons (MLPs), 56

Mu rhythm, 37, 170–171

MuSAE Lab, 183

Muscle movement artifacts, 39

Muse, 76, 78*f*, 82

Musical brain cap, 189

MyEmotiv, 82

N

- Nasion, 35–36
 Needle electrodes, 36
 Nervous system, 6–8, 8*f*
 Neural Lace, 202–203
 Neuroelectrics, 79*f*, 85
 Neuro-engagement factor, 4–5
 Neuroergonomics, 62
NeuroImage, 4
 Neuromarketing, 62–63
 Neurons, 6–8
 Neuropsychology pilot study, 186
 Neurorehabilitation, 60
 NeuroSky brainwave, 14–15
 NeuroSky Driver, 182
 NeuroSky MindWave, 78*f*, 83–84, 182
 Noninvasive signal acquisition, 29
 Nonlinear classifiers, 55*f*, 56
 Non parametric spectral analysis, 141–142, 141*f*
 Nonphysiological artifacts, 39*f*, 40

O

- OpenBCI, 78*f*, 83, 181
 Open source control (OSC), 190
 OpenVibe, 74–75, 95, 96–97*t*

P

- Parametric spectral analysis, 141–142, 141*f*
 Parietal lobe, 9–10, 9*f*
 Parrot Rolling Spider, 189–190
 Partially invasive BCI, 28
 Percentage closure of eyes (PERCLOS), 187
 Periodogram approach, 52*f*, 53
 Peripheral nervous system (PNS), 6–8, 10
 P300 evoked potentials, 50, 59
 Physiological artifacts, 38–39, 39*f*
 Positron emission tomography (PET), 12
 Posterior lobe, 9–10, 9*f*
 Power spectral analysis, 143–144.
 See also Channel spectral analysis
 Power spectral density (PSD), 51–52, 140–143
 Principal component analysis (PCA), 46, 114
 Principle of maximum non-Gaussianity, 115
 Principle of nonlinear decorrelation, 115
 Prosthetic hand control, 182–183
 Pulse artifacts, 38–40
 PyEEG, 95, 96–97*t*

R

- Rapid serial visual paradigm (RSVP), 188–189
 Reference-point measurement, 35
 Retinal prosthesis, 3–4
 Robotic claw control, 190
 Routine EEGs, 37

S

- Sampling skew, 76–77
 Scalp map, 114–115
Science Daily, 3–4
 Sensitive superconducting quantum interference device (SQUID), 30
 Sensitivity, 57
 Sensorimotor rhythms (SMRs), 49, 59
 Short-time Fourier transforms (STFTs), 53, 145
 Signal acquisition, 12, 14
 Simin-Block, 177, 179–180
 Simulink, 177, 199
 Arduino board, 178*f*
 drone and BCI, 189–190
 eyeblink acquisition, 102–103
 Single-photon emission computed tomography (SPECT), 12
 Skewness, 113–114
 Skin and sweat artifacts, 39

Sleep EEGs, 37

- Slow cortical potentials (SCPs), 13, 49, 51, 59, 170–171
 Software development kit (SDK), 88–89
 Somatic nervous system, 8–9
 Spatial domain analysis, 117–118, 160–161, 198
 Spatial filtering, 42–44
 adaptive, 41*f*, 45–46
 CSP algorithms, 46–47
 fixed, 41*f*, 44
 Specificity, 57
 Spectral power, 149–150, 162–165
 Spinal nerves, 8–9
 Steady-state evoked potentials (SSEPs), 13, 50
 Steady-state visual evoked potentials (SSVEPs), 13, 50
 Subband power analysis, 143–144
 Support vector machines (SVMs), 55, 55*f*

T

- Temporal filtering, 42, 43*f*
 Temporal lobe, 9–10, 9*f*
 Think Gear Communications Driver (TGCD), 183
 Third-order statistics, 113–114
 Time domain analysis, 109, 110*f*, 197
 channel ERP analysis, 116–135
 preprocessing, 110–111
 filtration, 111–113
 independent component analysis, 113–115
 scalp map analysis, 117–118
 topographic analysis, 118–135
 Time-frequency representation, 145
 Topographic scalp map analysis, 117–118, 197
 Touch-sensitive robotic limbs, 3–4

V

- Virtual instruments (VIs), 180, 184–185
 Visual evoked potentials (VEPs), 50, 85

W

- Wavelet transform, 53–54
 Wearable sensing EEG headset, 79*f*, 84–85
 Wernicke-Korsakoff disorder, 61
 Willow Garage PR2 humanoid robot, 169

Z

- Zero-phase FIR band-pass filter, 111, 118

EEG-Based Brain-Computer Interfaces

Cognitive Analysis and Control Applications

Dipali Bansal and Rashima Mahajan

In recent years control applications based on brain-computer interfaces (BCIs) have become a crucial area of interest for researchers. Due to long-term usability, easy implementation, and low costs, EEG has become the most acceptable neural signal for practical execution of BCIs.

Brain-Computer Interface: Cognitive Analysis and Control Applications provides a technical approach to using brain signals for control applications, as well as the EEG-related advances in BCI. The research and techniques in this book discuss time and frequency domain analysis on deliberate eye-blinking data as the basis for EEG-triggering control applications. In addition, the book provides experimental scenarios and features algorithms for acquiring real-time EEG signals using commercially available units that interface with MATLAB software for acquisition and control.

- Details the techniques for multiple types of analysis (including ERP, scalp map, sub-band power, and independent component) to acquire data from deliberate eye blinking
- Demonstrates how to use EEGs to develop more intuitive BCIs in real-time scenarios
- Includes algorithms and scenarios that interface with MATLAB software for interactive use

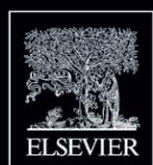
Related titles

Guger / Brain-Computer Interface Research / 9783642547065

Hassanien / Brain-Computer Interfaces: Current Trends and Applications / 9783319109770

Siuly / EEG Signal Analysis and Classification: Techniques and Applications / 9783319476520

Science/Biotechnology



ACADEMIC PRESS

An imprint of Elsevier
elsevier.com/books-and-journals

ISBN 978-0-12-814687-3

